Glacial geology and glaciology of the Younger Dryas ice cap in Scotland

Nicholas Robert Golledge

Submitted for the degree of Ph.D
The University of Edinburgh
November 2008

British Geological Survey
NATURAL ENVIRONMENT RESEARCH COUNCIL

Declaration

This thesis has been entirely written by myself, and is composed of work that has been undertaken by me, unless otherwise specified. Much of the content has been submitted for external publication in academic journals; however, the work has not been submitted for any other degree or professional qualification.

Signature .....

Date .....

Acknowledgements

British Geological Survey:

I am indebted to friends and colleagues at BGS for their considerable and wide-ranging assistance with all aspects of this research over the last four years:
Clive Auton, Tom Bradwell, Mike Browne, Jez Everest, Andrew Finlayson, Siobhan Gilliland, Gail Gray, Graham Leslie, Allan McKay, Andrew McMillan, Jon Merritt, Alison Monaghan, Aoife O' Monghain, Nicola Owensen, Emrys Phillips, Elizabeth Pickett, John Powell, Jane Robertson, Susanne Sargeant, Martin Smith, Chris Thomas, BGS Training

Particular thanks are extended to Tom, since it was his initial encouragement that persuaded me to start this. He has subsequently provided endless advice and comment on all aspects of this work, and taken a considerable amount of time in reading various drafts of papers and chapters of this thesis, for which I am most grateful.

Journal editors and referees:

Sincere thanks are also due to the numerous editors and referees (including those who remained anonymous) who have helped improve the clarity of the papers presented here with their insightful comments:
Colin Ballantyne, Doug Benn, Matthew Bennett, Dave Evans, Chris Fielding, Pirjo-Leena Forsström, Neil Glasser, Ralf Greve, Per Möller, Jan Piotrowski, Vincent Rinterknecht, Jim Rose, Christian Schoof

Supervisors and advisors:

Clearly this work could never have progressed without the constant support, guidance, and above all, patience of my supervisors:
Alun Hubbard, David Sugden, Chris Thomas

I am especially grateful to David, since it was he who initially enabled this Ph.D to happen, and subsequently it has been his solid guidance, inspirational outlook, and genuine enthusiasm that has kept me motivated throughout its duration.

Collaborators:

The following are thanked for their assistance in sample processing and for discussions in the field:
Steve Binnie, Derek Fabel, Stewart Freeman, Ruth Robinson

Other:

Many other individuals have greatly contributed to this work, in various manners; the following are very gratefully acknowledged for their help:

British Antarctic Survey and the crew of HMS Endurance, Chalmers Clapperton, Tibor Dunai, Chris Fogwill, Delia Gheorghiu, Phillip Hughes, Ann Mennim, Maria Miguens-Rodriguez, Wishart Mitchell, Open University Dept. of Earth Science, Charlotte Vye

Final, and very special, thanks to my family for their support and forbearance over the last four years.

Abstract

This thesis uses geological field data and numerical ice sheet modelling to study the Younger Dryas ice cap in Scotland. The Younger Dryas stadial is important because it represents the most recent period of high-magnitude global climate change, and was marked by the expansion of ice sheets in North America and Scandinavia, and the regrowth of glaciers in the British Isles. An integrated methodology linking field results and modelling is developed and applied here, specifically focussing on the deposits, landforms, and palaeoglaciology of Younger Dryas glaciers in western Scotland. This combined approach enables data of different scales to be compared, and connected, from local sedimentological investigations and empirically derived reconstructions, to regional ice-sheet simulations from a high-resolution numerical model. Previous geological mapping in western Scotland resulted in contradictory views of the thickness and extent of ice during the Younger Dryas, consequently leading to uncertainty about the dynamics of the former ice cap. By using a 'landsystem' method to characterise the terrain, it is argued here that geological evidence in the study area implies a relatively thick central ice cap that fed steep outlet glaciers around its margins. These glaciers oscillated throughout the stadial, and during deglaciation produced suites of moraines that marked successive positions of glacier retreat. Widespread preservation of superimposed landforms, and of sediment sequences pre-dating the Younger Dryas, suggest that, despite being active, the Younger Dryas ice cap was not particularly erosive in its central area and only subtly modified its bed. These geological interpretations are supported by high-resolution numerical modelling of the ice cap, which reveals clear spatial variability in the velocity structure, thermal regime, and flow mechanism of the ice cap; patterns that led to local contrasts in basal processes and diversity in the geological imprint. These model experiments also highlight the non-linear relationship between climate forcing and glacier response, identifying evidence of ice sheet hysteresis and climatically decoupled glacier oscillations – concepts as relevant to geological investigations of former ice masses as they are to the prediction of glacier response under future climate changes.

Contents

List of Figures

List of Tables

Chapter 1

Introduction and aims

1.1 Rationale

Establishing the extent of former Younger Dryas – or Loch Lomond – Stadial glaciers in Scotland has been the subject of a considerable volume of research over the last century, partly due to the abundance and clarity of glacial landforms, and perhaps more recently because of the recognition that palaeoglaciological reconstructions can provide information that is relevant to our increasing awareness of modern climate change. Predicting how contemporary glaciers and ice sheets will respond to current environmental forcings is, however, hampered by an incomplete knowledge of the processes involved, their thresholds, lags and feedbacks. By contrast, the empirical record of previous such scenarios mainly reflects the integrated signal of these complex processes, and thus presents a distillation of cause-effect relationships. Although considerable uncertainties still remain, the geological archive can nonetheless be extremely useful in providing basic insights into the way in which glaciers respond to external forcings. By combining geological mapping with numerical ice sheet modelling, the nature and influence of internal (dynamic) forcings can also be established, together offering a powerful means of reconstructing both the total volume of individual ice masses, and the way in which they evolved under particular environmental conditions. Additionally, model simulations can provide information on glacier dynamics that are pertinent to geological investigations, such as the relative likely proportion of sliding or the relative focus of erosion at the glacier bed, thereby aiding the way in which empirical data are interpreted. Geological mapping and numerical ice sheet modelling are thus highly complementary, and when combined effectively, can potentially provide more accurate and insightful results than either technique alone.

The Younger Dryas stadial was abrupt, and short-lived, and most probably resulted from a single catastrophic event that was unique to this glacial termination (Broecker, 2006). Consequently it is more-or-less 'self-contained', and thus makes a suitable case study for understanding rapid climate change and the likely terrestrial and cryospheric responses. Despite the Younger Dryas glaciation of the western Scottish Highlands having been the focus of considerable geological research, controversy still surrounds the pattern and style of glacier inception, the maximum ice-surface altitude that the thickest ice masses achieved, how they flowed, and the manner in which the main ice cap and its outlet glaciers decayed. Previous ideas that Younger Dryas glaciers grew from completely ice-free conditions have now been thrown into doubt by new ^{10}Be exposure ages from northwest Scotland, which indicate that ice may have survived, and remained active, throughout the interstadial that preceded the Younger Dryas (Bradwell *et al.*, 2008). In interpreting its maximum extent, some workers favoured an extensive Younger Dryas glaciation (e.g. Charlesworth, 1955; Horsfield, 1983), whereas other syntheses prefer more restricted ice growth (Sissons, 1979b, 1980; Clark *et al.*, 2004). Likewise with regard to the maximum thickness of ice that built up, Thorp (1984, 1986) reconstructed a low aspect-ratio (thin) *icefield* flowing over widespread deforming beds, whereas Horsfield (1983) envisaged a thicker ice *cap*, and suggested that certain landforms in the area may actually pre-date the Younger Dryas. Final decay of Younger Dryas glaciers was initially thought to have resulted from *in situ* ice stagnation (Sissons, 1965), but more recent work has shown that deglaciation proceeded actively, with dynamic glaciers oscillating during their retreat (e.g. Benn *et al.*, 1992; Bennett & Boulton, 1993a; Phillips *et al.*, 2002; Lukas, 2005a). Related studies have used the abundance of 'hummocky moraine' to suggest that the

climate of the Younger Dryas was somewhat wetter than present, resulting in glaciers with a relatively high mass-turnover that transported large volumes of debris to their margins (Benn & Lukas, 2006).

Empirical investigations such as these are highly informative, but are commonly restricted in their scope because of the amount of time that is required to undertake detailed field mapping. Remotely sensed datasets go some way towards speeding up geomorphological mapping, but lack the ability to provide sedimentological information. Numerical modelling greatly accelerates the process of glacier reconstruction, but may lack validity without an empirical grounding. A requirement therefore exists for an integrated approach, in which field mapping is informed by interpretations of remotely sensed data in order to derive empirical guidelines for numerical modelling experiments. Model predictions can then also be used iteratively to evaluate geologically based interpretations.

1.2 Aims of thesis

This thesis aims to evaluate some of the specific controversies outlined above - namely:

1. Did Younger Dryas glaciers grow from ice-free conditions, and did they achieve their maximum extent and thickness early or late in the stadial?

2. Was the Younger Dryas glaciation extensive or restricted in its extent, and was it characterised by thick or thin ice masses?

3. Did glaciers rely on pervasive deforming beds for motion, or was ice deformation ('creep') instrumental in their flow?

4. Were advance and retreat patterns governed entirely by climatic variability, and did glaciers stagnate during deglaciation, or retreat actively?

5. What was the dominant climate like in Scotland during the Younger Dryas?

More broadly, the thesis sets out to establish whether:

1. The glacial landforms and sediments of the western Scottish Highlands can be used to reconstruct the form, extent, and dynamics of the Younger Dryas ice cap.

2. The ice cap can be numerically simulated in a way that honours geological interpretations not just in this area, but also in a wider Scottish context.

3. These palaeoglaciological reconstructions and ice sheet models can make a contribution to the understanding of broader issues, such as the sensitivity of modern glaciers to changes in North Atlantic climate.

1.3 Geographic & climatological context

1.3.1 The Younger Dryas

The Younger Dryas was defined as a chronozone by Mangerud *et al.* (1974), spanning the period 10 - 11 ^{14}C ka BP. The episode is identified in Greenland ice core records as a period of renewed cooling – 'Greenland Stadial 1' (GS 1) (Björck *et al.*, 1998; Rasmussen *et al.*, 2006; Lowe *et al.*, 2008) – which, (according to the GICC05 age model), started soon after 12.9 ka BP and terminated at around 11.7 ka BP (Fig. 1.1). Recent insights into the uncertainties associated with ^{14}C calibration and correlation to ice core records, however, have led some authors to suggest that the onset and termination of the Younger Dryas may have occurred up to 300 years later than this (Muscheler *et al.*, 2008). These controversies aside, δ^{18}O records from ice cores and sea bed sediments indicate that during this period, despite increasing insolation in the northern hemisphere (Imbrie *et al.*, 1984), air and sea temperatures, as well as sea surface salinity, all underwent a marked decline throughout much of the world (e.g. Maslin *et al.*, 1995; Kroon *et al.*, 1997; Broecker, 2003). Although relatively short in duration, the amount of atmospheric cooling in the northern hemisphere during the Younger Dryas was almost equal to that reached during the coldest parts of the Late Devensian (Weichselian) (Stuiver *et al.*, 1995). Southern hemisphere ice core records suggest that climatic patterns at low southern latitudes were similar to those of the northern hemisphere (Fig. 1.1)(Thompson *et al.*, 1998), whilst higher southern latitude areas, such as Antarctica, appear to have warmed slightly during the Younger Dryas, following the Antarctic Cold Reversal (ACR, c. 14.5 - 12.5 ka BP, EPICA Community Members, 2006). Climatic extremes were accentuated around North Atlantic margins (Lowe *et al.*, 1994; Lie & Paasche, 2006), leading to cooler summers but much more severe winters than the preceding warm period, Greenland Interstadial 1 (GI 1, Denton *et al.*, 2005; Lowe *et al.*, 2008). Exising ice sheets and glaciers readvanced, such as those covering North America, Iceland, and Scandinavia, whereas other areas, such as Britain, experienced a regrowth of glaciers from much reduced, if not entirely ice-free conditions. Whether or not expansion of southern hemisphere glaciers was coincident with those in the northern hemisphere has long been debated (cf. Clapperton, 1993; Denton & Hendy, 1994; Broecker, 2003; Sugden *et al.*, 2005). Recent cosmogenic exposure ages, however, appear to demonstrate that glacier advances both in South America and the sub-Antarctic culminated prior to, or during the early stages of the Younger Dryas (Fogwill & Kubik, 2005; Bentley *et al.*, 2007). In non-glaciated areas, the climatic changes during the Younger Dryas produced considerably drier and windier conditions, leading to widespread periglaciation throughout much of northwest Europe, increased storminess in Asia, and a global reduction in the extent of tropical wetlands (Broecker, 2003).

The methane drop seen in ice core records that span the Younger Dryas is not seen in longer ice cores covering earlier glacial terminations, a factor presumed to indicate that the Younger Dryas was a unique event, and not typical of deglacial transitions (Broecker, 2006). Since the Younger Dryas stadial was too short to have been forced by Milankovitch-style orbital variability, and since it abruptly interrupted a prior warm period (Greenland Interstadial 1), it is likely that the widespread cooling was brought about by disruption of terrestrial systems, such as oceanic or atmospheric circulation. Several possibilities have been proposed, including catastrophic outburst floods, melting of vast armadas of icebergs, and shifts in wind patterns

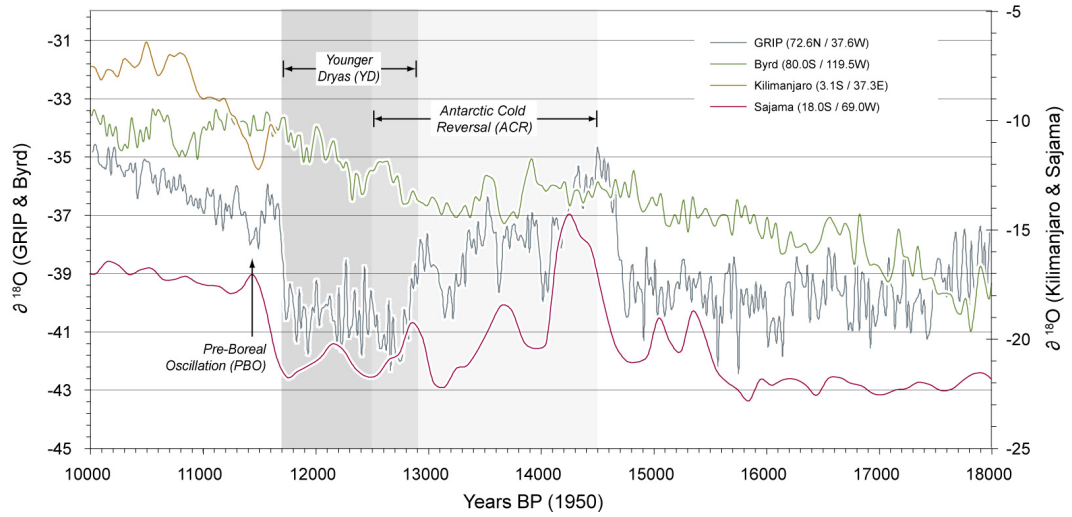

Figure 1.1: Global ice core records showing climate variability during the period 18 - 10 ka BP, based on records from Greenland (GRIP), Kenya (Kilimanjaro), Bolivia (Sajama), and Antarctica (Byrd). Note the close similarity during the Younger Dryas between the pattern of fluctuation in Sajama and GRIP, and the mismatch of both with Byrd. Data from Thompson *et al.* (1998); Blunier & Brook (2001); Thompson *et al.* (2002); Rasmussen *et al.* (2006). GRIP data is presented according to the age model of Rasmussen *et al.* (2006), as employed by Lowe *et al.* (2008) and Rasmussen *et al.* (2008).

that gave rise to greater sea ice formation in the northern hemisphere (Seager & Battisti, 2005). The general concensus is that the hemispheric, if not global, cooling most likely occurred in response to a freshening of the North Atlantic by the rapid input of a large volume of freshwater. This temporarily disrupted North Atlantic oceanic circulation, particularly the formation of North Atlantic Deep Water (NADW). Under modern (interstadial) conditions, North Atlantic Deep Water forms when surface waters of the North Atlantic cool and sink in the seas over the Greenland - Scotland ridge (Fig. 1.2 A). This overturning generates a deeper current that returns southward, and in doing so both draws more tropical water northward, and also limits the incursion into northern seas of cold, Antarctic Bottom Water (ABW) currents. The NADW is therefore critical in maintaining the 'heat pump' that redistributes heat from tropical areas to the northern seas (Fig. 1.2 B), which in turn heats the air masses that influence the North Atlantic seaboard, especially northwest Europe. Modelling experiments demonstrate that any reduction in the efficiency of overturning currents in the North Atlantic significantly reduces regional air temperatures and can perturb large sectors of the global climate (Fig. 1.2 C) (Rahmstorf, 2002). A decrease in the amount of NADW formation is thought to have given rise to a markedly different 'glacial' ocean circulation system many times in the past, in which only shallow overturning occurred, less warm water was drawn northward, and ABW had greater influence. This state probably existed throughout much of the last (Late Devensian / Late Weichselian) glacial cycle, when mean air temperatures were significantly reduced during both summer and winter. If NADW is further curtailed to the extent that little or no overturning occurs, ABW dominates and severe cooling of neighbouring areas ensues. Such a scenario probably dominated 'Heinrich Events' of the last glacial episode (Fig. 1.2 D), which were also characterised not just by a drop in mean annual temperatures, but also by an associated increase in the intra-annual range of temperatures, leading to extremely cold

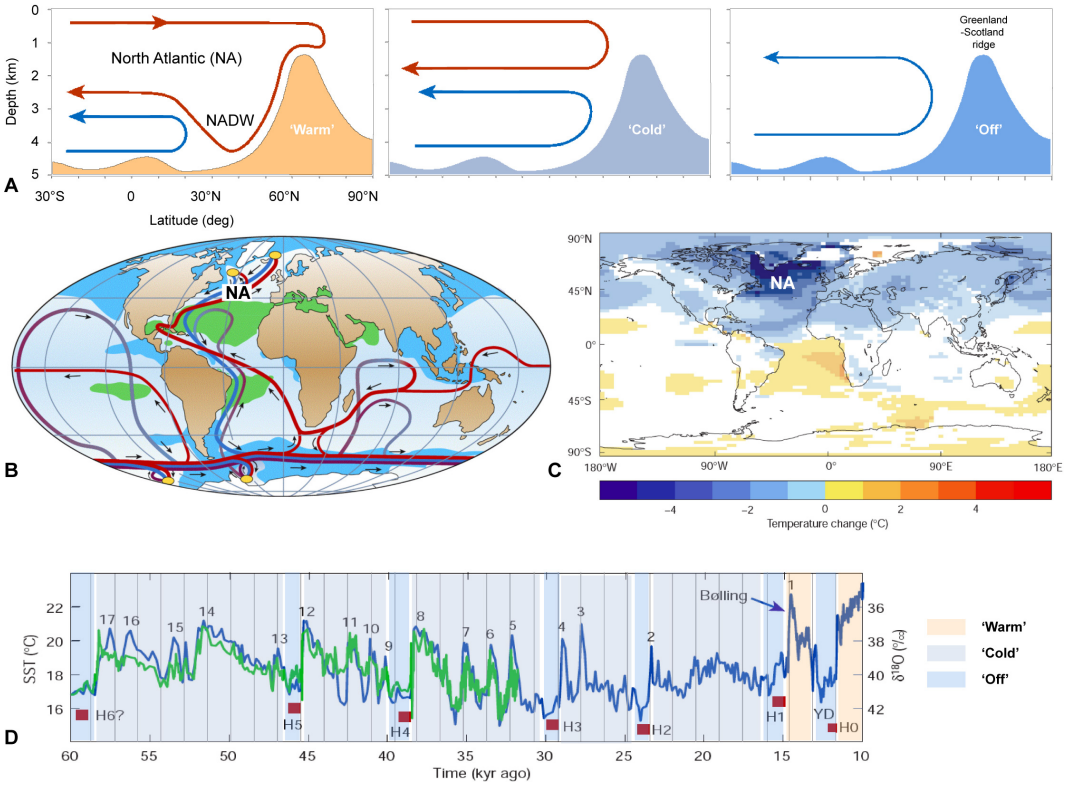

Figure 1.2: North Atlantic oceanic circulation, showing A: overturning in the vicinity of the Greenland - Scotland ridge and formation of North Atlantic Deep Water (NADW), B: global ocean circulation pattern distributing heat from the tropics to higher latitudes, C: modelled temperature changes resulting from NADW collapse, D: GRIP ice core data showing episodes when different ocean states shown in (A) may have prevailed. H0-H6 - Heinrich Events, YD - Younger Dryas. All redrawn or modified from Rahmstorf (2002).

winters (Isarin & Renssen, 1999; Denton *et al.*, 2005; Lie & Paasche, 2006).

The oceanic forcing mechanism for the Younger Dryas climatic shift is relatively well-established, but the primary cause of the oceanic freshening is still widely debated. The abrupt onset of the stadial and its rapid termination may suggest that it resulted from temporary disruption of the oceanic circulatory system that involved a significant reduction in the formation of NADW, perhaps in response to a distinct and perhaps catastrophic event. The North Atlantic thermohaline circulation (THC) relies on effective overturning of the layered water masses of high latitude seas; large perturbations in the salinity or temperature of surface waters can therefore be highly disruptive to this process and, if sustained, may result in switching between the different modes of ocean circulation described above. Such disruption requires the input of considerable volumes of freshwater into the North Atlantic, and in the places where it will most strongly affect the THC (Manabe & Stouffer, 2000). Evidence for the former existence of extensive ice-dammed lakes at the margins of the retreating Laurentide Ice Sheet (LIS) at the end of the last glacial (Fig. 1.3) led to proposals that their catastrophic drainage may have released sufficient freshwater into the North Atlantic to shutdown the THC and to thereby instigate the Younger Dryas cooling (Broecker *et al.*, 1989; Teller, 1990; Teller *et al.*, 2002). Considerable uncertainty still surrounds the chronology and routing of outburst

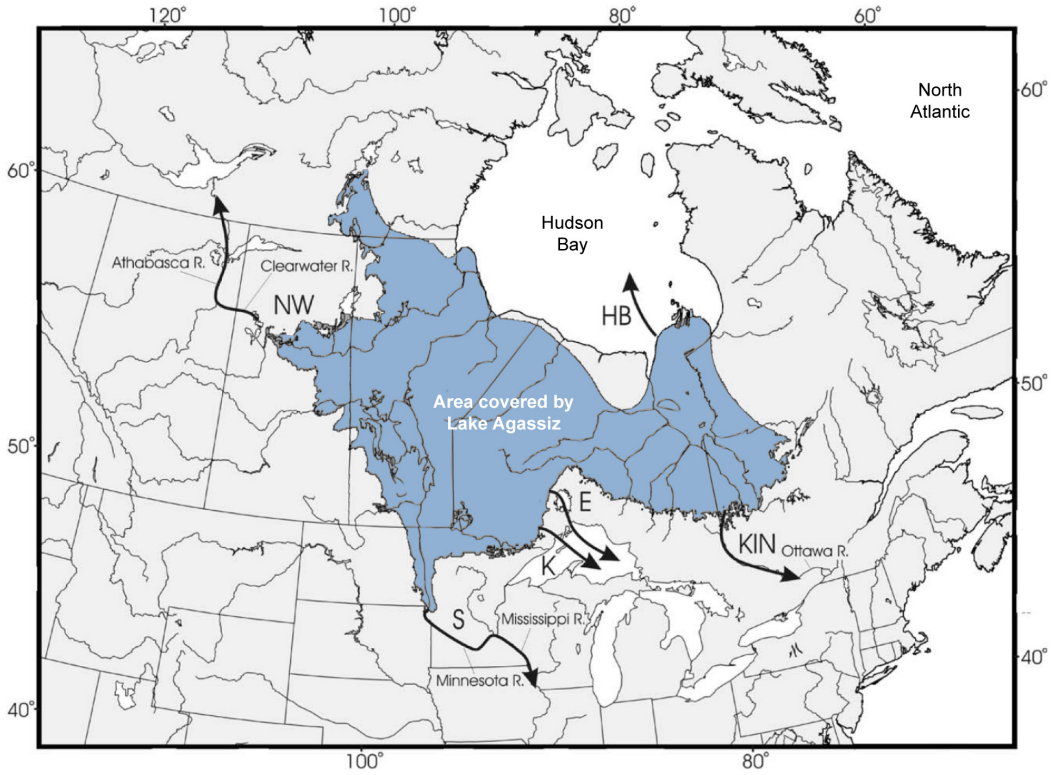

Figure 1.3: Location and total area covered through the 5000-year lifetime of glacial Lake Agassiz, North America, showing principal outlets: NW - Northwestern outlet, S - Southern outlet, K - eastern outlets through Thunder Bay area, E - Eastern outlets through Nipigon basin, KIN - Kinojévis outlet, HB - Hudson Bay route of final drainage. Modified from Teller *et al.* (2005).

floods from Lake Agassiz, with much recent work suggesting that although outbursts occurred through southern, eastern and northern routes throughout the Lateglacial and early Holocene, none coincided with the precise timing of onset of the Younger Dryas cooling (Fisher & Smith, 1994; deVernal *et al.*, 1996; Teller *et al.*, 2002; Lowell *et al.*, 2005; Teller *et al.*, 2005). The exact location of freshwater input has similarly been the source of considerable debate, with some authors suggesting that the influx took place along the Arctic fringes of the LIS, rather than from its eastern margins (e.g. Tarasov & Peltier, 2005).

Regardless of the location of flooding, the scenario invisaged above is one of a continual build-up of meltwater in terrestrial ice-dammed lakes, and episodic release when ice dams were breached or when outlets opened as a result of steady deglaciation. Recently, however, suggestions have been made for a more catastrophic triggering of meltwater influx to the North Atlantic (Firestone *et al.*, 2007). In this novel proposal, extensive and wide-ranging field data across north-eastern USA is cited as evidence for an extraterrestrial impact event that took place at around 12.9 ka BP. The suggestion is based on dating of a thick, widespread, carbon layer marking the apparent demise of the North American Clovis culture, and its stratigraphic association with deposits exhibiting enhanced iridium levels, magnetic microspherules, carbon, soot, nanodiamonds, and fullerenes with extraterrestrial helium. The event is thought to have been characterised by the explosion of a large meteorite above the LIS, which led to

devastating terrestrial wildfires, significant melting of parts of the ice sheet, and impact explosions of meteorite fragments that may have led to the break-up and destabilisation of the LIS sufficient to release dammed meltwater. If correct, this theory explains both the timing of onset of the Younger Dryas as well as its abruptness and uniqueness. After catastrophically perturbing the oceanic circulation in the North Atlantic, the THC recovered and resumed the non-glacial state that had begun in the previous interstadial (Fig. 1.2 D).

1.3.2 The Younger Dryas in Scotland

Mean annual temperatures in Scotland declined by around 8 - 10°C during the Younger Dryas (Hubbard, 1999; Isarin & Renssen, 1999), which was instrumental in the rapid regrowth of ice in much of Scotland and parts of northern England (Clapperton, 1997; Hubbard, 1999). A coeval southerly shift in the location of the oceanic polar front (Ruddiman & McIntyre, 1981; Bard *et al.*, 1987; Isarin & Renssen, 1999) possibly produced more vigorous atmospheric circulation that may also have given rise to increased precipitation in western Scotland (Ballantyne, 2002). Palaeoglaciological reconstructions by Sissons (1979c, 1980) suggested that the dominant snow-bearing winds were southerlies whilst the snow-blowing winds were west- or south-westerlies. The high mountains flanking Rannoch Moor most probably acted as 'snow-fences' (cf Andrews *et al.*, 1970), accumulating large volumes of snow that initially enabled ice build up in corries and on plateaux, and ultimately led to the growth of a substantial ice cap that fed interconnected outlet glaciers (Golledge & Hubbard, 2005). North-south and east-west precipitation gradients limited effective accumulation beyond the central area (Sissons & Sutherland, 1976; Clapperton, 1997; Hubbard, 1999), so that around the ice cap margins, extensive icefields developed (e.g. Bennett & Boulton, 1993a; Benn & Ballantyne, 2005; Lukas, 2005b), but the considerably reduced precipitation further east was only sufficient to nourish corrie glaciers (Brazier *et al.*, 1996a,b). Widespread periglacial activity occurred throughout northern Britain. This glacial state persisted for approximately 1.2 kyr (Alley, 2000; Rasmussen *et al.*, 2006), towards the end of which the Younger Dryas ice masses began to decay - at first slowly, triggered by reduced precipitation that led to active recession involving numerous stillstands and minor readvances, and subsequently more quickly as a result of rapid climate warming (Dansgaard *et al.*, 1989; Benn *et al.*, 1992; Dix & Duck, 2000). Localised ice stagnation only occurred where topographic barriers cut-off ice tongues from their accumulation areas (Benn, 1992).

1.3.3 Previous work in the study area

The magnitude and spatial variability of palaeoclimatic forcing during the Loch Lomond Stadial had a significant impact on the extent, geometry and dynamics of the resulting glaciers (Sissons, 1980; Bennett & Boulton, 1993a; Benn & Ballantyne, 2005; Golledge *et al.*, in press). Topography played an equally important role in controlling ice build up and its pattern of flow. The western Highlands are dissected by deep valleys such as glens Orchy, Lochy and Fyne (governing ice flow to the west), and glens Lyon and Lochay in the east (Fig. 1.4). Glen Falloch and Glen Dochart drain the southern extent of the study area, southward and eastward respectively. The extent to which this pattern of topography controlled the southward dispersal

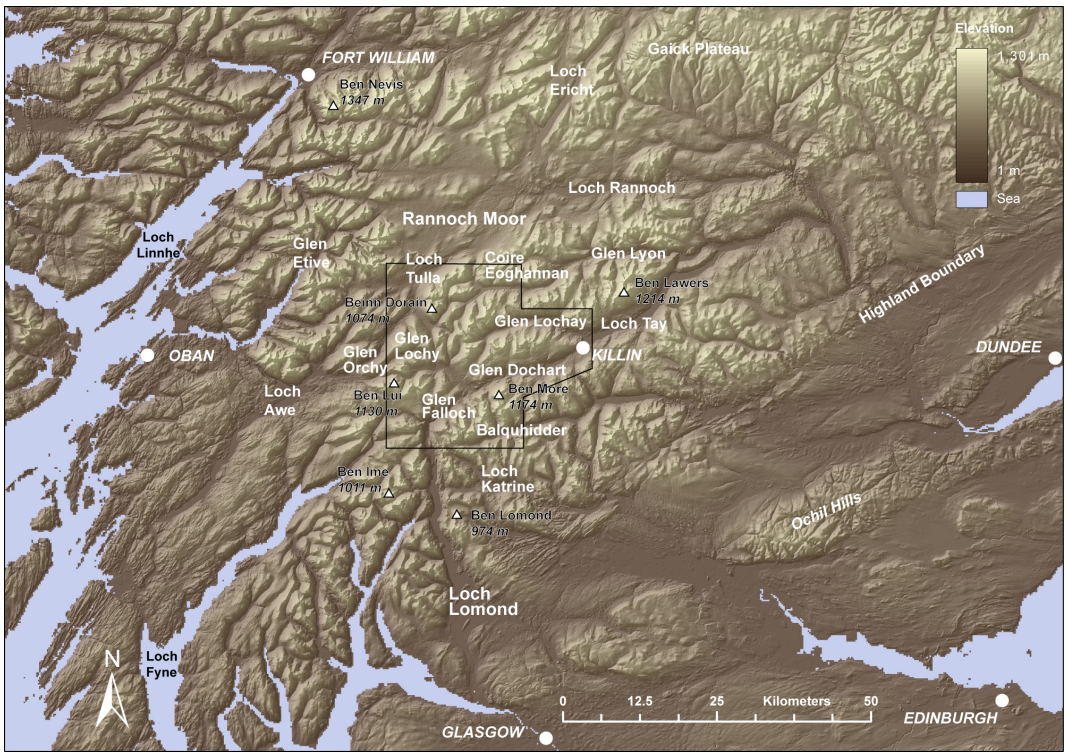

Figure 1.4: Digital terrain model (DTM) of part of the western Scottish Highlands, showing principal valleys, mountain summits, lochs and settlements. Box shows approximate area of field mapping described in this thesis.

of ice from the main ice cap accumulation zone has long been debated. Geomorphological mapping by Thompson (1972), Horsfield (1983) and Thorp (1984, 1986, 1987, 1991a) identified many of the landforms and landform-sediment assemblages present, which allowed each to make inferences about the size and dynamics of the former Loch Lomond Stadial ice cap in this area.

Taking the early Geological Survey Memoirs as starting points, Thompson (1972) added his own field observations and suggested that Glen Lyon was formerly occupied by a dynamic eastward-flowing valley glacier that may have been sourced at altitudes of >900 m a.s.l. He proposed that the numerous corries and high valleys surrounding Glen Lyon acted as the main accumulation areas for the snow (and ultimately ice) that fed the Glen Lyon glacier. The ice descending from these accumulation areas is suggested to have bifurcated and also fed the Glen Lochay glacier to the south. Thompson identified that high-level cols had been streamlined, and suggested that the ice that had flowed across them moved westwards and north-westwards away from Glen Lyon towards Loch Tulla. It was also argued that the considerable thickness of local ice in Glen Lyon prevented Rannoch ice from flowing south (Thompson, 1972, : p 143). The absence of Rannoch granite erratics in the Glen Lyon area, noted earlier by Hinxman *et al.* (1923) was used to support this reconstruction, and mounds identified in Coire Eoghannan at 760 m a.s.l. were taken as evidence for a minimum ice thickness in that area.

Subsequently, Horsfield (1983) set out to test two other deglaciation scenarios in the area against geomorphological evidence mapped from aerial photographs. The first tested was

that of Charlesworth (1955), who proposed that the moraines and other ice-marginal features represented the last glaciers in this area, following his 'Highland Readvance'. The second scenario was that of Sissons (1965), who instead argued that the hummocky moraine seen throughout the area was a result of in situ stagnation of glaciers that developed in the western Highlands after the Main Late Devensian ice sheet had disappeared. Horsfield (1983) used ice-marginal features interpreted from air photos to constrain the size and extent of the ice cap, and used palaeo-iceflow indicators to reconstruct its dynamics. Horsfield concluded that during the Loch Lomond Stadial, the ice cap that overwhelmed this part of the western Highlands was centred on the Etive and Nevis mountains west and northwest of Rannoch Moor, and had a maximum surface altitude of >1000 m a.s.l. Importantly, Horsfield was one of the first to suggest that the ice then retreated actively back to these centres, rather than decaying in situ. Whilst accepting many of Charlesworth's (1955) maximum limits, Horsfield disagreed with his 'valley glaciation' interpretation.

Working generally in the mountainous area north and west of Rannoch Moor, Thorp (1984, 1986) mapped moraines, thick drift, fluvioglacial landforms, erratics, ice-smoothed bedrock, striae, friction cracks and relict periglacial forms in order to determine the upper limits (trimlines) of Loch Lomond Stadial ice masses. After extensive mapping, Thorp reconstructed the extent of the Loch Lomond Stadial icefield in the western Highlands and described its morphology and dynamics, including calculations of basal-shear stresses for the main outlet glaciers (Thorp, 1991b). Thorp envisaged a low-aspect ratio Loch Lomond Stadial icefield, drained by numerous fast flowing valley glaciers, significantly thinner than previous reconstructions with ice-shed altitudes of approximately 750 m a.s.l., a maximum width of 80 km and an area of 2000 km^2.

Compared to this relative wealth of geomorphological research, very little work has been published on the sedimentology and stratigraphy of the study area. Sutherland (1993) stated that deposits pre-dating the Loch Lomond Stadial were 'not known' in this area (p 307), but new data presented in this thesis provides evidence to the contrary (Golledge, 2007a,b). In fact, the Loch Lomond Stadial ice cap in the study area appears to have 'recycled' subglacial material, and remoulded existing landforms, rather than completely removed them. Preservation of pre-existing deposits was determined by their location within the ice cap, with the thickest sequences of older sediments coinciding with zones of low basal velocity (Golledge *et al.*, in press). Formation of the present landscape was therefore glaciologically conditioned, and now incorporates elements pertaining not only to the preceding Main Late Devensian glaciation, but in some instances also to even earlier glacial deposition.

1.4 Methods

1.4.1 Field mapping

Field mapping was carried out by walkover survey, during which as many observable geomorphological features and geological boundaries as possible were recorded, together with descriptive notes and detailed logs of sedimentary exposures. Description of landforms and

sediments, and their depiction on field maps, followed standards defined by the British Geological Survey 1:10 000 scale Map Specifications (Ambrose, 2000). Pencilled linework was inked-in and coloured-up prior to creation of digital 'clean copies'. Section logs were recorded using British Geological Survey 'GN' record cards, including key header data such as date, geologist identifier code, and National Grid Reference of locality. Ordnance Survey map bases of 1:10 000 and 1:25 000 scale were used to record spatial data, with 5 m or 10 m contour intervals. Surveys in 2004 - 2006 used traditional paper map bases, whereas digital mapping was undertaken in 2007 using a ruggedised Tablet PC and ArcGIS 9.1 software. The mapping techniques employed were largely the same, regardless of the means of data recording.

Stereographic 1:24 000 scale monochrome aerial photographs were used for a large part of the study area, for the identification and mapping of geomorphological features and geological boundaries. Wherever possible, an inital interpretation of the imagery was made prior to field survey, with further iterative use in field accomodation during field work, and in the office subsequent to field survey, to amend or extend linework where appropriate. In some areas, where digital imagery was available, this was done within the ArcGIS environment to ensure geospatial accuracy. Considerable use was made of the NextMAP Digital Terrain Model (DTM), both for mapping landforms and geological boundaries where possible. The dataset has a vertical accuracy of 1.2 m and a horizontal resolution of 5 m, equivalent to 0.5 mm on a 1:10 000 scale map, or 0.2 mm at 1:25 000 scale. Artificially illuminating the dataset from different angles produces different results, and so features mapped from these DTMs were carefully checked against other data sources, such as aerial photographs or field observations, before final interpretations were made. Use of this dataset on the Tablet PC in the field enabled the rapid identification of areas of complex geomorphology, and allowed strong geological boundaries (such as fluvial terraces) to be mapped quickly and accurately. Field data captured on paper maps was finalised, inked-in and edge-coloured either during or subsequent to the field mapping period. Finished linework was then digitised either by myself or by BGS Cartography, using ArcGIS. Data recorded digitally in the field was finalised on-screen before transfer to BGS Cartography for archiving in corporate databases.
Additional field data, in the form of notecards, photographs and samples, were recorded and databased according to BGS corporate policy.

1.4.2 Analytical techniques

Laboratory analysis techniques were used for a small part of the thesis work. For particle size analysis of subglacial till units in the study area, samples were disaggregated using sodium hexametaphosphate and agitated in a sonic bath, sieved to isolate sediment <900 μm, then repeatedly flushed through a Coulter LS100 Laser Diffractometer to derive size frequency data. X-Ray diffraction was undertaken in order to shed light on the likely chemical compounds present in the till matrix of each subglacial unit. For this, samples were freeze-dried, ground to a fine powder, mounted in metal discs and analysed in a Phillips PW 1800 X-Ray Diffractometer to produce diffractograms. The presence of particular compounds was judged by comparison of diffractogram peaks with standard spectra. All stages of these analyses were carried out under the supervision of Ann Mennim at the Grant Institute, Edinburgh University.

A small amount of preparatory work was also required for the cosmogenic dating samples. This involved crushing and milling of rocks in the Grant Institute rock crushing laboratory, followed by 'cleaning' of the quartz in the cosmogenic preparation laboratory of the Geography Department, University of Edinburgh. This latter stage was undertaken by Dr. Steve Binnie.

1.4.3 Digital data manipulation and interpretation

Increasing availability of digital data sets and improving computing performance have enabled considerably greater geospatial data processing capabilities than previously feasible. Commonly, a standard Geographic Information Systems (GIS) interface is used to collate disparate data sets within a single environment. For this thesis I have used ArcGIS, including ArcMap (ArcInfo interface), ArcCatalog, ArcToolbox, and ArcGlobe. Geological field data was captured from georectified traditional paper maps by digitising attributed lines, points and polygons using the ArcGIS-based BGS Geological Spatial Database (GSD). This application includes a variety of customised tools and settings developed by BGS specifically for digital geological data capture, and is increasingly closely linked to the field-based digital data capture system, MIDAS (Mobile Integrated Data Acquisition System). Field data recorded both on paper maps and digitally using MIDAS were integrated into a single GSD project for ease of interpretation and map compilation.

ArcGIS also lends itself to data manipulation and to geoprocessing tasks. I used ArcGIS, for example, to digitise ice surface contours for the palaeoglaciological reconstruction in Paper III (Golledge, 2007a). From these contours a gridded surface was computed, enabling pseudo-3D visualisation of the reconstructed ice cap and thus facilitating comparison with primary field data and numerical model output. Grid data also allow raster calculations to be performed, such as calculating ice thicknesses or driving stresses from ice surface and bed topography data. Spatial analysis techniques enable surface slope angles and azimuths to be generated, from which former ice flow can be inferred.

The numerical modelling component of this thesis relied heavily on ArcGIS for the interpretation and assessment of model output. Floating-point grid data produced by model runs were converted to ESRI grid format and displayed in a GIS project that also held digitised empirical data, such as reconstructed glacier limits from the Britice compilation (Clark *et al.*, 2004), from other published surveys (e.g. Bradwell, 2006; Finlayson & Bradwell, 2007), and from my own mapping. Raster calculations between grid layers enabled derivatives of the model outputs to be calculated, such as meltwater flow accumulation from hydrologic potential and bed topography, or erosion potential from basal velocity and ice thickness (Golledge *et al.*, in press). Functionality implemented in ArcGIS 9.2 allowed batch geoprocessing for the first time within the ArcMap interface, enabling the rapid import, export or conversion of multiple grid files.

1.4.4 Numerical ice sheet modelling

The ice sheet model used for the simulations described here (Papers VI and VII, Golledge *et al.*, 2008a, in press) is one modified by Dr. Alun Hubbard from that which was used in the first high-resolution model of the Scottish Younger Dryas ice cap (Hubbard, 1999). This three-dimensional thermomechanical model allows the accumulation and flow of ice to be simulated using input data of topography, temperature depression from present, and the precipitation distribution. Variables within the model parameter file allow aspects such as the amount of sliding, or rate of calving, to be adjusted. I used the model to predict the likely spatial pattern of ice build-up during the Younger Dryas by assuming initially ice-free conditions, and by imposing climatic changes that included stepped temperature depressions, as well as more variable scaled GRIP-pattern temperature changes. Precipitation is controlled by linearly reducing present precipitation between start and end point coordinates. Sensitivity tests were used to establish the approximate degree of influence exerted by each of the key variables (temperature, precipitation, and sliding), with specific experiments designed to identify the combination of variables and their ranges ('parameter space') that most realistically reproduce empirical reconstructions.

Model output data was imported into ArcGIS for visualisation, interpretation, and for derivative calculations, as described above. Use of the ArcMap platform in this manner greatly facilitated the iterative nature of the empirical–numerical comparisons. Model outputs imported into an ArcGIS MIDAS project for field mapping in 2007 allowed direct evaluation of model predictions in the field, and comparison against the empirical evidence. Using the modelling in this way lends greater credence to spatial relationships that were previously simply intuitive, for example, the correlation between low velocity zones and the occurrence of thick, preserved sediment sequences. Consequently, greater confidence can be placed on inferences drawn from model predictions, which is of considerable benefit in areas where field data are lacking.

1.5 Thesis format

This thesis is constructed as a series of seven integrated papers, each addressing one of the four broad chapter themes. There are two reasons for using this format: firstly, the research aimed to cover widely ranging studies, from the very detailed study of sedimentary sequences in individual valleys, to regional ice surface reconstructions from geomorphological evidence, to the very widest scale of modelling the Younger Dryas ice build-up throughout mainland Scotland and proximal islands. Secondly, the research was undertaken on a part-time basis, tightly integrated with the BGS mapping programme and the remit of the 'Geology of the Grampian Highlands' project. Consequently, there was a need to produce output throughout the lifetime of the project, rather than compile all the research at the end of the research period.

The geological work on which the papers are based was conducted concurrently as field mapping progressed from one area to the next, however, the detail of their interpretation is presented separately in order to do justice to each theme rather than each geographical area. Thus sedimentology is largely separated from geomorphology, and both are treated

in isolation from the modelling. Naturally, some degree of overlap exists, since sediments cannot be entirely divorced from the landforms that they compose, and vise versa. Later papers attempt to build on and develop ideas of earlier papers, add new interpretations, and if necessary address previous shortcomings. The papers were, however, written in a different order to their presentation here. This is because each paper reports findings and ideas as they occurred during the research, aware that they formed part of a larger investigation but isolated in the sense that further work was required on other aspects of the thesis. Here the articles are presented in an order that aims to show an increasing scale of interpretation, starting with a local sedimentological investigation in a single valley and culminating in more generic glaciological inferences concerning the Younger Dryas ice cap as a whole. Whilst this perhaps obscures the linearity of research evolution, conceptually it makes far greater sense and is intended to draw attention to the notion that local studies can be of great value to much larger scale interpretations, if intermediate stages are able to interpret and extend them correctly.

The main aims, methods and principal conclusions of each paper are summarised at the beginning of each chapter, in order to give an overview of the chapter as a whole and its role, or context, in the thesis. These summaries also explain the level of input to each paper by any co-authors, and in one instance, the way in which the content has been modified from the published version. All of the papers have either been published, or are currently in press. With the exception of Paper IV (Golledge, 2006), all the articles were submitted to international journals.

Chapter 2

Sedimentology and glacier dynamics

2.1 Summary

Previous geological investigations in the study area have focussed largely on the geomorphological aspects of the landscape, and have paid less attention to the sedimentary archive. The detailed mapping carried out for this research involved considerable sedimentological logging and analysis, in order that,

1. typical facies types could be identified,

2. the spatial distribution of facies may be deduced, and

3. a local stratigraphy might be constructed.

By recording the above, landform composition may be established, and inferences can be made with regard to the glaciodynamic conditions under which the sediments were deposited, and, in some cases, subsequently disturbed. In this way, the geological record can be considered in a more complete way than when landforms are interpreted in isolation, enabling more solid conclusions to be drawn.

The first paper describes a series of exposures in a single valley in the south of the study area, each section revealing sediments typical of deposition in an aqueous environment. The facies types and their inter-relationships suggest that much of the sediment was laid-down in an ice-marginal lake in this valley, Glen Chaorach, when the Younger Dryas glacier still filled the much larger Glen Dochart, to the north. Significantly, glaciotectonic structures in several of the sediment sequences demonstrate that the ice margin embayed in Glen Chaorach periodically readvanced into the lake and deformed the sediment pile accumulating at and beyond the glacier grounding line. The landforms produced by these oscillations are interpreted as De Geer moraines, which are more commonly associated with marine margins of larger ice sheets. The conclusions drawn in this article emphasise the importance of detailed and geographically focussed sedimentological investigations in interpreting former glacier dynamics at a local scale. Emrys Phillips assisted through discussions concerning the nature and interpretation of the sedimentary sequences and their tectonic structures. All the text was written, and all figures drafted, by myself.

The second of the following two papers reports sedimentological investigations of a larger scale, describing, categorising, and interpreting 53 sedimentary sequences in the wider study area. By identifying eight facies types according to factors such as grain size, sorting, and lithology, sediments recorded in disparate areas are correlated or contrasted with one another. The order of superposition of the sediments, when thus correlated, enables a local stratigraphy to be defined for the first time in this area. Relationships between the sediment units, in terms of the nature of their upper and lower bounding contacts, provides further information on the mode of deposition or emplacement of each unit. On the basis of these investigations, this paper assigns a tentative age to each of the eight facies, concluding that only the uppermost sediments are attributable to the Younger Dryas glaciation. Other sediments lower in the overall stratigraphic sequence are thought to represent Late Devensian glaciation, and the very lowest facies are likely much older. These findings provide the first sedimentological and stratigraphic evidence in this area for partial preservation of pre-existing sediments through

subsequent glaciations, and enable inferences to be made with respect to the basal conditions of these later glaciers. [NB: In its published form (Quat. Res., 68, 79-95), this paper included an incorrect version of Table 1; the correct version was subsequently published as a 'Corrigendum' (Quat. Res., 68, 456-457). In this thesis, only the correct version has been reproduced.]

PAPER I

Sedimentology and architecture of De Geer moraines in the western Scottish Highlands, and implications for grounding-line glacier dynamics

Nicholas R. Golledge[1,2], Emrys R. Phillips[1]
[1]British Geological Survey, West Mains Road, Edinburgh, EH9 3LA, UK
and [2]School of Geosciences, University of Edinburgh, West Mains Road, Edinburgh, EH9 3JW, UK.
ph: +44 131 667 1000, fx: +44 131 668 1535, email: n.golledge@bgs.ac.uk

Abstract

Sedimentary exposures in moraines in a Scottish Highland valley (Glen Chaorach), reveal stacked sequences of bedded and laminated silt, sand and gravel, interspersed or capped with diamicton units. In four examples, faults and folds indicate deformation by glaciotectonism and syndepositional loading. We propose that these sediments were laid down in an ice-dammed lake, close to the last ice margin to occupy this glen. Individual units within cross-valley De Geer moraine ridges are interpreted by comparison with examples from similar environments elsewhere: stratified diamictons containing laminated or bedded lenses are interpreted as subaqueous ice-marginal debris flows; massive fine-grained deposits as hyperconcentrated flows, and massive gravel units as high-density debris flows. Using an allostratigraphic approach we argue that glaciotectonically deformed coarsening-upward sand and gravel sequences that culminate in deposition of subglacial diamicton represent glacier advances into the ice-marginal lake, whereas undisturbed cross-bedded sand and gravel reflects channel or fan deposits laid down during glacier retreat. A flat terrace of bedded sand and gravel at the northern end of Glen Chaorach is interpreted as subaerial glaciofluvial outwash. On the basis of these inferences we propose the following three stage deglacial event chronology for Glen Chaorach. During glacier recession, ice separation and intra-lobe ponding first led to subaquaeous deposition of sorted and unsorted facies. Subsequent glacier stabilisation and ice-marginal oscillation produced glaciotectonic structures in the ice-marginal sediment pile and formed De Geer moraines. Finally, drainage of the ice-dammed lake allowed a subaerial ice-marginal drainage system to become established. Throughout deglaciation, deposition within the lake was characterized by abrupt changes in grain size and in the architecture of individual sediment bodies, reflecting changing delivery paths and sediment supply, and by dynamic margin oscillations typical of water-terminating glaciers.

KEYWORDS: De Geer moraines; Scotland; grounding-line; palaeoglaciology; Younger Dryas.

2.2 Introduction

'Water-terminating glaciers' are those whose margins are at least partially floating, either in a marine setting or in an ice-marginal lake. They play a key role in ice sheet mass balance by facilitating episodic calving of potentially large volumes of ice – a process evident at the periphery of modern polar ice sheets (Rignot & Kanagaratnam, 2006) – and may be responsible for greater mass loss from the glacier system than terrestrial margins (Reeh, 1968; Paterson, 1994). Consequently there is a clear need for effective recognition of their signature in the geological record if we are to fully appreciate the behavioural dynamics of former ice masses, and any connection these may have to the climatic or internal forcings that gave rise to them (e.g. Peck *et al.*, 2007).

Glaciers terminating in water become buoyant where the depth of water is sufficient to counter the thickness-dependent normal stress of the ice margin, according to the difference in their relative densities. Extensional flow towards the margin, due to reduced basal drag, as well as flexuring induced by water-level fluctuation, leads to the development of both basal and surface crevasses. Calving occurs when surface crevasse depths equal the height of the ice cliff above water level, and it is the pattern of these major crevasses – or rifts – that controls the location of slab or block detachment (Benn *et al.*, 2007a,b). As a consequence of these specific conditions, floating margins are susceptible to rapid and cyclical fluctuations in the location of their grounding line, giving rise to distinctive landform suites known as De Geer moraines, the form and composition of which reflect the dynamics of the glacier under which they formed. Accurate identification of these diagnostic landforms and sediments therefore plays an important role in identifying water-terminating glacier margins in all previously glaciated terrains, regardless of whether the water body is marine or lacustrine.

Terrestrial De Geer moraines within the limits of the last British Ice Sheet have more-or-less escaped attention until now, especially those formed by Younger Dryas age glaciers. Dix & Duck (2000) present the only description of such landforms from Scotland, based on seismic stratigraphic data from a sea loch on the Isle of Skye. They conclude that at least one of the marine-terminating glaciers draining the Younger Dryas Skye ice cap reworked earlier deposits and formed push moraines at its grounding line during a period of oscillatory retreat early in deglaciation. As yet, however, no published studies specifically describe De Geer moraines from mountainous areas of Scotland, despite the very likely occurence of such landforms in areas of high relief where separating or retreating ice margins flowed against reverse slopes and impounded meltwater (e.g. Borgström, 1979; Benn *et al.*, 2003; Heyman & Hättestrand, 2006).

Whilst some workers differ in their interpretations of De Geer moraine genesis, most are agreed on the general scale, context and morphology of these landforms (Table 2.1). Typically these moraines are less than 10 m high, a few tens of metres in width, and several hundreds of metres long. They form subaqueously at or near ice margins, and are aligned transverse to iceflow. Originally described by De Geer (1889), and named after him by Hoppe (1959), these features are also known as 'minor moraines' (Lee, 1959; Smith, 1982), 'washboard moraines' (Mawdsley, 1936), 'transverse eskers' (Virkkala, 1963) and 'cross-valley moraines' (Andrews & Smithson, 1966; Heyman & Hättestrand, 2006). Although the origin of De Geer moraines is widely debated, two main interpretations are favoured. One explanation for these

Study site	Orientation	Scale Height	Width	Length	Spacing	Slope	Facies & architecture	Interpretation	Reference
Glen Chaorach, western Scottish Highlands	Broadly perpendicular to valley axis and presumed ice flow	<10m	20-35m	50-100m	30-400m	Asymmetric, steeper distal slope	Diamicton, silt, sand and gravel; intercalated, stratified, folded, thrust	Ice-marginal subaqeous debris flows, lake floor deposits, deformation by oscillating ice margin	This study
Raudvassdalen, Northern Norway	Perpendicular to ice flow; oblique to valley slope	0.5-5m	1-30m	<300m	25-240m, av. 86m	Symmetrical, 20deg, some slightly steeper down-ice	Till, glaciofluvial sediments, marine sediments; folded, stacked, deformed	Overridden grounding line deposits	Blake (2000)
Norrbotten, Northern Sweden	Transverse to iceflow, upflow concave in topographic lows, convex on elevated ground	1-3m	av. 30m	100m-3km	50-200m	Asymmetric, steeper distal slope	Diamictons, silt, sand, gravel and cobbles; stratified, interfingered, stacked, folded, thrust	Intercalated deforming bed diamictons and glaciofluvial canal-infill sediments, syn- and post-depositional deformation, distal slope prograding sediment gravity flows	Linden & Moller (2005)
Loch Ainort, western Scotland	Perpendicular to valley axis and presumed ice flow	0.2-12m	<30m	40-470m	<70m	Asymmetric, steeper proximal slope (18deg vs 11deg distal)	Poorly-sorted sandy muddy gravel interpreted as glacigenic diamicton	Subaqueous grounding line moraines	Dix & Duck (2000)
More, western Norway	Perpendicular to ice flow, slightly convex or concave	3-6m	20-30m	250m-10km	50-1200m	N/A	Sandy diamicton, sorted sediments, isolated clasts; stacked, sheared, faulted, liquified, diapir structures	Formation at a retreating glacier grounding line	Larsen et al. (1991)
Swedish mountains	Cross-valley, straight or slightly convex downvalley	1-10m	N/A	10's-1000's m	N/A	N/A	N/A	Formed at terminus of water-terminating glaciers flowing up-valley	Heyman & Hattestrand (2006)
Quebec, Canada	Perpendicular to ice flow, some chevron shaped	1-10m	N/A	N/A	60-400m	Symmetrical or asymmetrical	Predominantly glaciofluvial sediments, often glaciotectonised	Deposition from meltwater flowing through transverse subglacial cavities	Beaudry & Prichonnet (1991)
Swedish mountains	Transverse to iceflow, straight or slightly concave up-valley	<4m	1-20m	<200m	30-50m	Symmetrical or asymmetrical	Mainly firm, sandy till, rare glaciofluvial material	Subaqueous moraines formed at or near the ice margin	Borgstrom (1979)
Pasvik, north Norway	Transverse to iceflow	<10m	50m	1km	10's-100's m	Steeper distal side	Proximal side – homogeneous sandy material, distal side – interbedded till and sorted sediments	Subaqueous glaciofluvial deposition along ice margin, from debouching central conduit	Sollid (1989)
Finland	Straight, transverse to iceflow	1-3m	10-20m	100m-2km	60-180m	Symmetric or steeper distal side	Sandy and poorly-sorted till	Squeezing of subglacial till up into subglacial crevasses following surge advance	Zilliacus (1989)

Table 2.1: Characteristics of De Geer moraines from published examples, as well as data from the features described in this study.

linear, closely spaced moraines is that they formed subglacially in crevasses at the glacier bed, some distance behind a calving margin (Zilliacus, 1989). Surge advance of a glacier margin produces stresses parallel to the ice front, leading to the development of basal crevasses. Where the advanced margin is initially floating, subsequent settling of the crevassed glacier sole into unconsolidated sediment leads to bi-directional squeezing and infilling of the cavity. A variation on this interpretation is favoured by Sollid (1989) and Beaudry & Prichonnet (1991), who invoke subglacial deposition from meltwater within the basal crevasses in preference to sediment squeezing to explain the glaciofluvial sediment within De Geer moraines in northern Norway and southeast Canada, respectively. Both mechanisms necessitate rapid lift-off and almost instanteous recession of the glacier in order to preserve these landforms and avoid any reworking during subsequent marginal oscillations.

Others have suggested a quite different mode of formation. This alternative model

requires deposition of sorted sediments beyond the grounding line of a water-terminating glacier, and subsequent deformation of these sediments into transverse ridges by ice-marginal advance (Larsen *et al.*, 1991; Blake, 2000; Dix & Duck, 2000; Lindén & Möller, 2005). In this scenario, stacked sequences of fine-grained sediments are common, and diamicton units are interpreted as redeposited (water-lain) till, lodgement till, or subaqueous debris-flow deposits. Characteristically, De Geer moraines are seen to form at the grounding line of a glacier, whether the margin is a floating tongue, an overhanging cliff, or is completely grounded and only calving above the waterline. Few workers claim chronological inferences from De Geer moraines, as originally proposed (De Geer, 1889), but many accept that the accurate genetic interpretation of their sedimentary and geomorphological characteristics can be highly instructive with respect to understanding former glacier dynamics at retreating margins.

Here we describe a series of sedimentary exposures in the De Geer moraines of Glen Chaorach in the western Scottish Highlands, in order to better understand sedimentological processes and glacier dynamics at water-terminating margins. Exposed sections at nine localities are interpreted by comparing their constituent facies with those from other deglaciated environments. By coupling the sedimentology with architectures suggestive of glaciotectonic deformation, we present an allostratigraphic interpretation in which we make inferences with respect to the dynamics of the former outlet glacier during overall ice-cap recession. The resulting event chronology identifies three key stages of deglaciation – glacier separation, intra-lobe lake development with ice-margin fluctuation, and final lake drainage associated with deglaciation.

2.2.1 Study area

In the western Scottish Highlands climatic deterioration during the latter stages of the Windermere (Allerød) Interstadial (c. 14.5-12.9 ka BP) instigated the regrowth of an ice cap that extended 150 km from north to south and around 50 km from east to west (Sissons, 1980; Thorp, 1986; Ballantyne, 1997) (Fig. 2.1). The ice cap consisted of a major dome over Rannoch Moor feeding outlet glaciers south to Loch Lomond, west to Loch Awe, Loch Etive, and Glen Coe, north through Loch Ericht, and eastwards via Loch Rannoch, Glen Lyon and Glen Dochart (Thompson, 1972; Sissons, 1979b; Horsfield, 1983; Thorp, 1986; Golledge, 2006, 2007a). Separate icefields accumulated around the fringes of the main ice mass, and fed topographically constrained valley glaciers that deposited suites of 'hummocky moraine' and other ice-marginal landforms during their retreat (Bennett & Boulton, 1993a; Lukas, 2005a; Benn & Ballantyne, 2005; Bradwell, 2006; Finlayson, 2006).

During the Younger Dryas glaciation a major eastward-flowing outlet glacier – the Dochart Glacier – drained a significant part of the main ice cap by connecting Strath Fillan to Loch Tay, where the glacier is thought to have terminated (Thompson, 1972; Sissons, 1979b). Glen Chaorach is a south-trending tributary valley of Glen Dochart (Fig. 2.2), and during deglaciation it hosted an embayed marginal lobe of the Dochart Glacier. At its northern end, the valley is characterised by abundant morainic landforms, valley-side till cover, and spreads of glaciofluvial sand and gravel. Higher ground to the south has a somewhat sparser distribution of moraines, with thinner, less extensive till cover and with more widespread

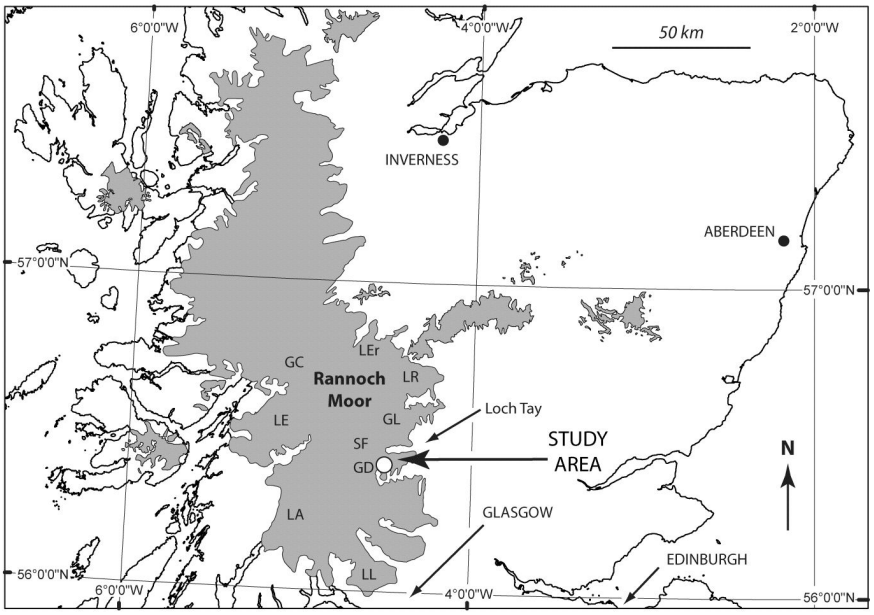

Figure 2.1: The location of the study area in a Scottish context, and in relation to the extent of Younger Dryas glaciation (shaded area) in the western Highlands (from various sources). Note the position of the site at the margin of a key eastward-draining outlet glacier. Abbreviations: GD - Glen Dochart, LL - Loch Lomond, LA - Loch Awe, LE - Loch Etive, GC - Glen Coe, LEr - Loch Ericht, LR - Loch Rannoch, GL - Glen Lyon, SF - Strath Fillan.

evidence of bedrock at or near surface.

2.2.2 Geomorphology and context of exposures

The landforms of Glen Chaorach are predominantly elongate ridges that trend obliquely across the axis of the valley from approximately southwest to northeast (Fig. 2.2). The ridges are linear or weakly curvilinear and are convex either up- or down-valley. They are typically less than 10 m high, 20 to 35 m wide, and up to 100 m in length. Inter-ridge spacing varies between 30 and 400 m, and individual ridges are typically asymmetric with a steeper southern side (Table 2.1). In Glen Dochart, rounded mounds up to 20 m high and 150 m long rise above the present valley floor. These typically larger features are less elongate than those in Glen Chaorach. Between these two groups of mounds are terraces, the flat surfaces of which are locally punctuated with discrete rounded mounds up to 5 m high. Several large channels up to 500 m long incise the terraces, in many cases originating above the terraces on till or bedrock slopes, and in all cases descending to the northeast. Many of the higher slopes flanking Glen Chaorach are free of superficial deposits, and largely consist of approximately flat-lying metasedimentary bedrock. The rock is ice-scoured at elevations up to c. 550 m, and hosts perched boulders in some areas (Fig. 2.2). At these higher levels, glacial meltwater has exploited structural weaknesses in the bedrock and incised northeast-trending channels up to c. 5 m deep.

The sedimentary sequences described here are all located in the lower, northern part of

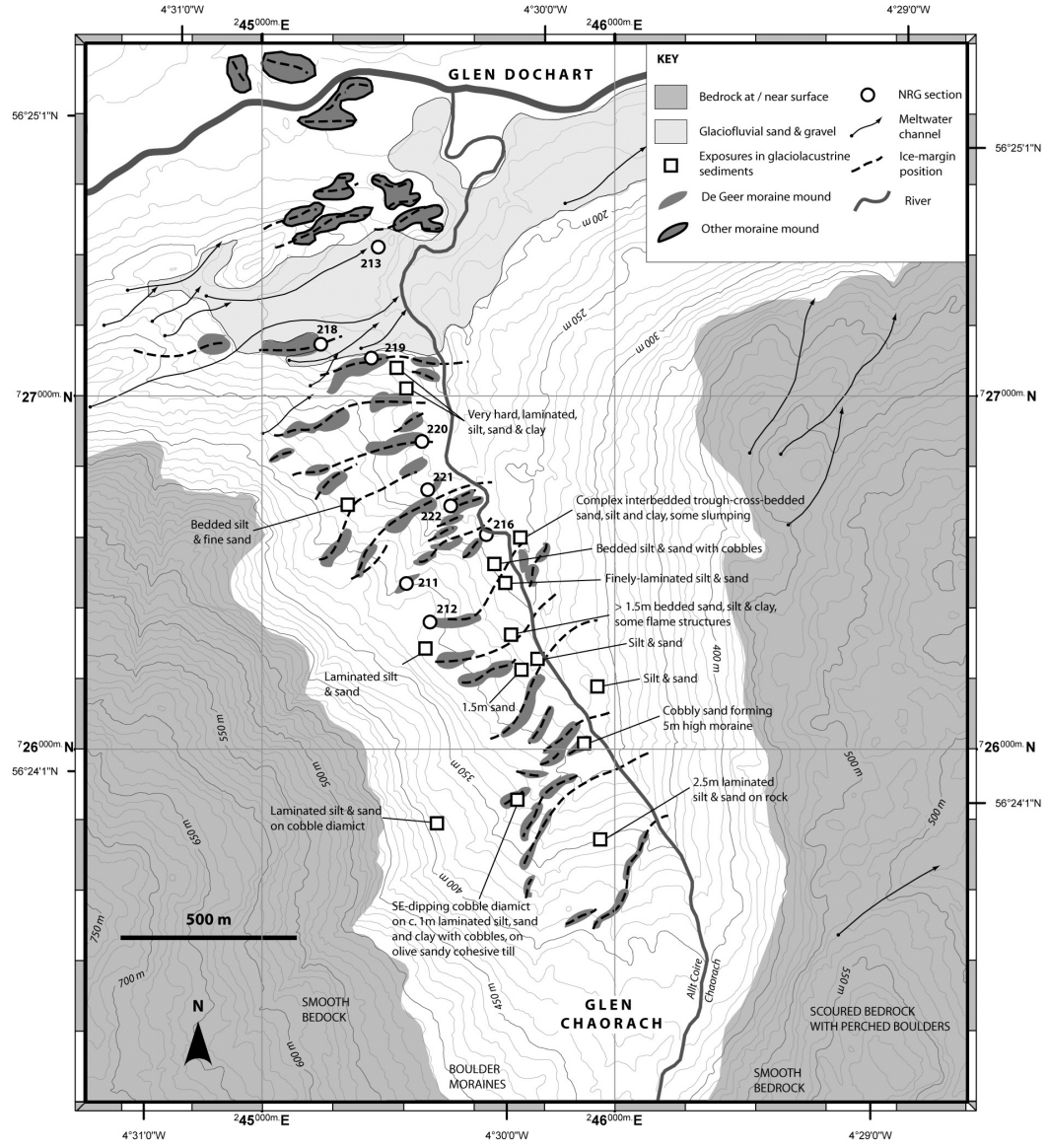

Figure 2.2: The physiography and simplified geology of Glen Chaorach and its confluence with Glen Dochart, showing the positions of numbered locations described in the text and other localities where sediments were observed. Topographic contours are at 10 m vertical interval, derived from Ordnance Survey Profile data, © Crown Copyright.

Composition	Character	Facies	Description and Code	Interpretation	Environment	References
Diamicton	Massive	1	Diamicton, matrix or clast-supported, massive (Dmm/Dcm)	Debris flow or submarginal	Subglacial deposition /emplacement directly from the glacier sole	Zielinski et al (1996); Brazier et al (1998); Blake (2000)
	Stratified	2	Diamicton, matrix or clast-supported, stratified (Dms/Dcs)	Debris flow	Ice-marginal, high energy, episodic	
Gravel	Massive, sorted	3	Gravel, massive, sorted (Gms)	Debris flow	Ice-proximal, high energy, episodic. Subaerial or subaqueous. Iceberg overturning	Lowe (1982); Lonne(1993, 1995); Nemec et al (1999); Blake (2000); Winsemann et al (2004)
	Massive, unsorted or openwork	4	Gravel, massive or openwork (Gm/Go)	High-density debris flow, or subaerial glaciofluvial		
	Normally graded	5	Gravel, fining-upwards (Gfu)	Low-density debris flow		
	Reverse graded	6	Gravel, coarsening-upwards (Gcu)	Debris flow		
Sand	Massive	7	Sand, massive (Sm)	Hyperconcentrated flow	Relatively high velocity, turbulent flow; ice-proximal fan lobes or aprons, possibly with channelised surface	Blake (2000); Fard (2001); Bennett et al., (2002); Etienne et al., (2006)
	Planar cross-bedded	8	Sand, planar, horizontal, or cross bedded, upwards-fining, or laminated (Sp/Sh/Sc/Suf/Sl)	Apron or fan deposits (overbank)		
	Trough cross-bedded	9	Sand, trough-cross bedded or upward-coarsening (St/Su)	Channel sediments		
Silt & clay	Massive	10	Fines, massive (Fm)	Hyperconcentrated flow	Distal runout from ice-proximal source	Lonne (1993); Bennett et al. (2002); Thomas and Chiverrell (2006)
	Laminated	11	Fines, laminated or varved (Fl/Flv)	Basin muds	Suspension settling distal to ice margin basin muds; proximal sedimentation in quiet water, low sedimentation rate	

Table 2.2: Facies interpretation for the range of sediments recorded in Glen Chaorach, based on examples from both presently and formerly glaciated areas. Facies codes from Eyles & Miall (1984); Eyles *et al.* (1984).

Glen Chaorach. The nine sections described were identified and logged during resurvey of the area by the British Geological Survey in 2006. All of the sections except NRG 216 and 213 occur within the cross-valley ridges described above. NRG 216 is cut into a terrace contiguous with one of these ridges, while NRG213 incises a considerably more extensive terrace at the confluence of Glen Chaorach and Glen Dochart. In addition to these key sections, a number of smaller or less well-exposed sections in stratified sediments were also noted (Fig. 2.2). Table 2.2 summarises the facies present and the basis for their interpretation, drawing on examples from both relict and active glaciofluvial, glaciolacustrine and glaciomarine environments. Figure 2.3 shows the stratigraphic relationships of these facies types at each of the nine key localities, in an approximately south to north sequence. An allostratigraphic approach, based on the recognition of distinct 'events' within a depositional sequence (Walker, 1990; Lønne, 1995), is used to infer the glaciodynamic episodes shown in Figure 2.3. These include periods of ice-margin advance or recession when variability in sediment input is likely to be at its greatest (Teller, 2003).

2.3 Sedimentological interpretation

2.3.1 Section NRG 212

This exposure occurs on the side of the valley rather than the valley floor, at an elevation of approximately 310 m. The massive to weakly laminated silt and sand (Facies 10/11) at the base of the exposed sequence (Fig. 2.3 A) was probably deposited relatively rapidly, perhaps from repeated hyperconcentrated flows that partially liquified previous flow deposits and dropped isolated 'floating' clasts. This requires subaqueous rather than subaerial deposition and suggests a minimum water level at the altitude of deposition (c. 310 m a.s.l. (above sea level)). The fine grain-size of the material may indicate a long transport path and deposition

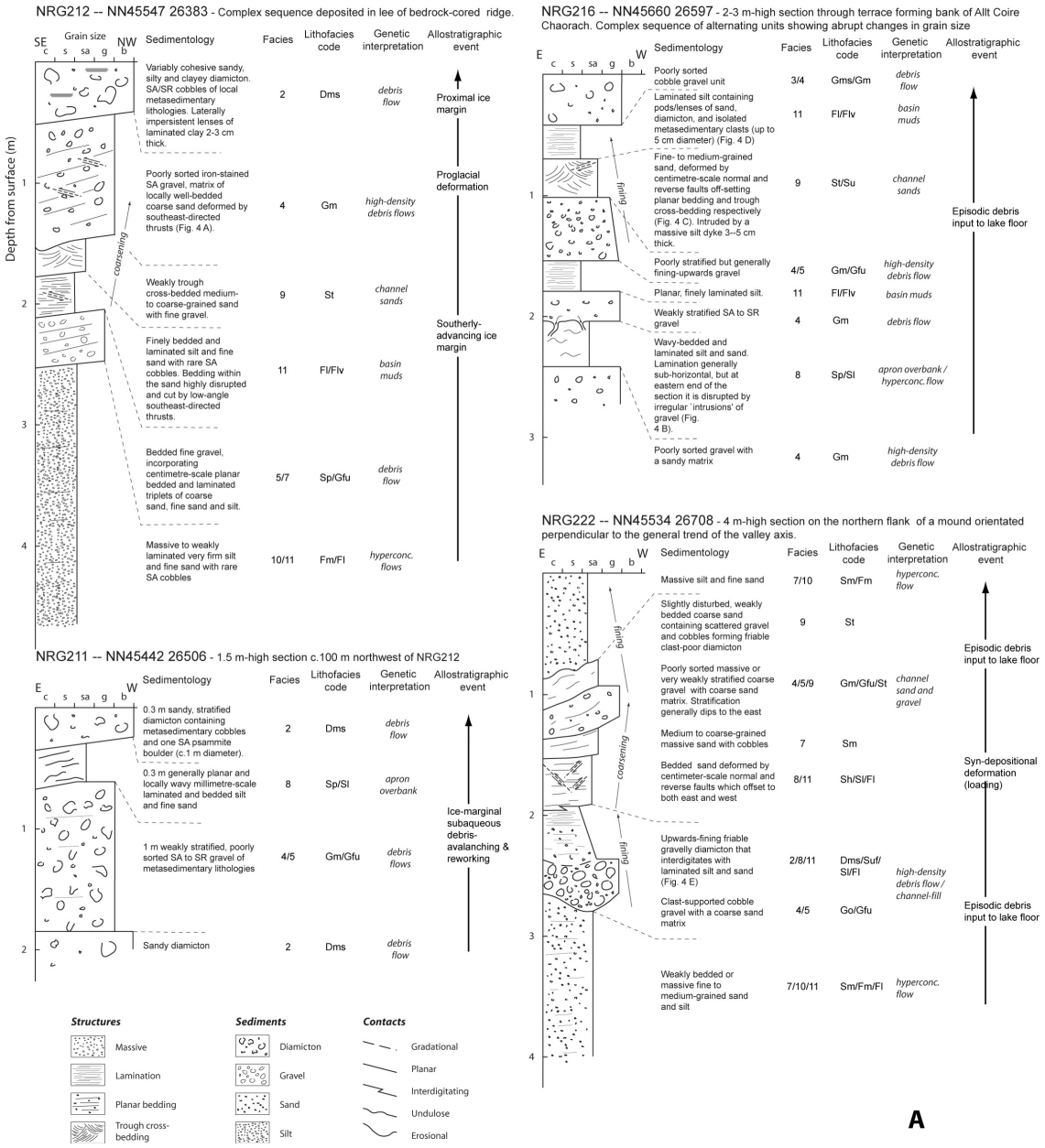

Figure 2.3: A & B (overleaf): Scaled sedimentological logs illustrating vertical sections through the nine exposures described in this study, presented in order as described in the text. The logs show key facies types and the nature of bounding contacts, and are only generalised where units exhibit high lateral variability in thickness and / or character. The composition of each unit, their stratigraphic relationships, and the nature of their upper and lower contacts provide the basis of the genetic interpretations and allostratigraphic significance. Facies codes from Eyles & Miall (1984) and Eyles *et al.* (1984).

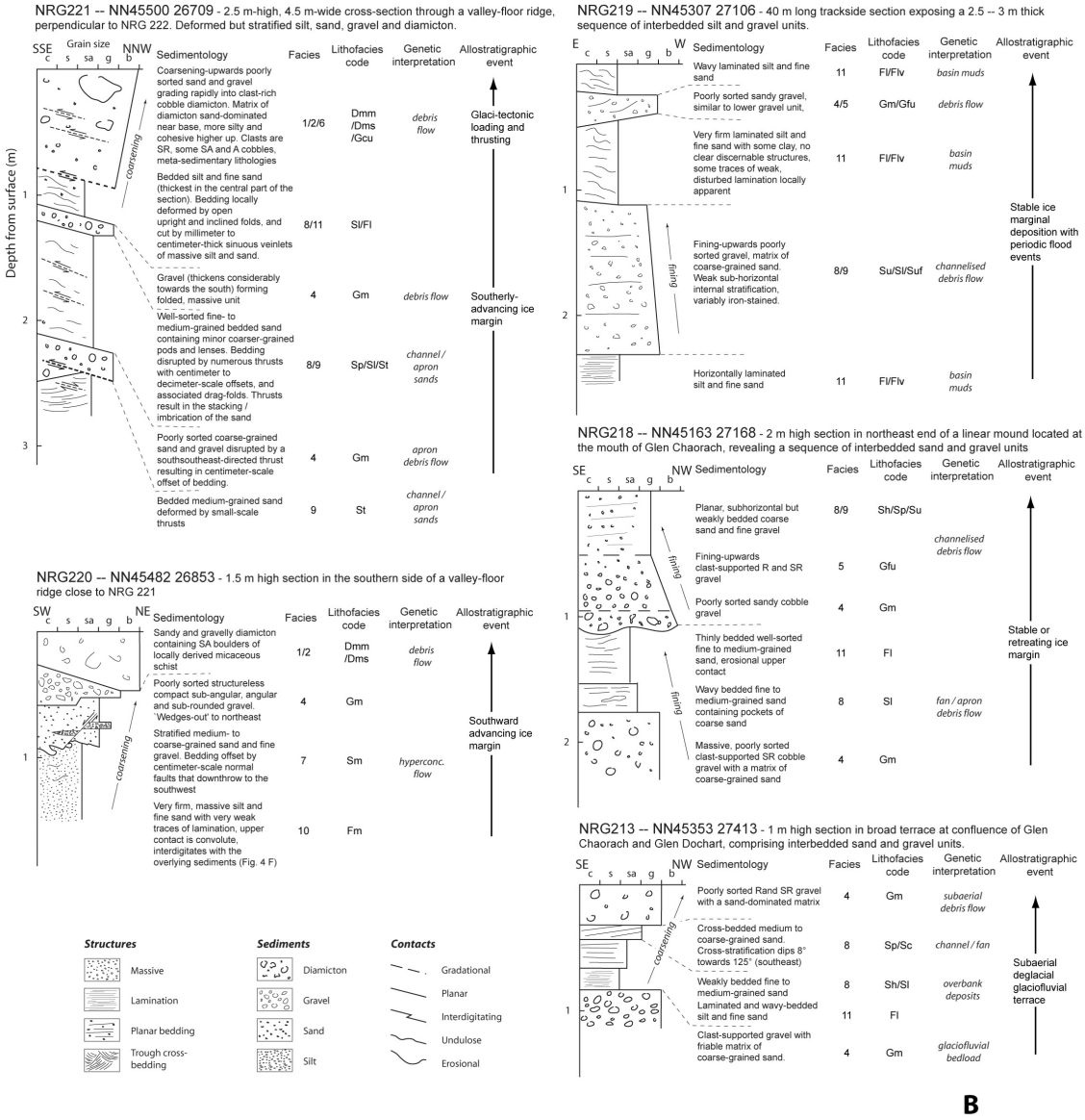

Figure 2.3: B: (see previous page for caption details).

some distance from the glacier margin, or may simply be a function of sediment availability. Rhythmic deposition of overlying sorted gravel (Facies 5) represents a shift to a more episodic depositional environment (or at least a less turbulent water column), whilst the coarser grain size could reflect either more proximal deposition, or a switch in sediment supply. Basin muds (Facies 11) are succeeded by coarse-grained trough cross-bedded sand (Facies 9) and subsequently gravel (Facies 4); the sand was a product of higher-energy, channelised, transport, and the gravel was probably laid down by medium to high-density turbidity currents perhaps sourced from a subglacial meltwater conduit. Development on a fan surface of channels, such as indicated by the sediments described above, indicates (at least temporary) stabilisation of the fan / apron system.

Upward-coarsening throughout the section culminates in the diamicton that caps the sequence (Facies 2). The subangular and subrounded clasts in the deposit suggest derivation from subglacial sources (Benn & Ballantyne, 1994), but the high variability of matrix composition and consolidation argues against it having been deposited subglacially, since such deposits are likely to be more-or-less homogeneous. Instead, this diamicton is interpreted as subglacial substrate that has been redeposited as a subaqueous debris flow. This inference is supported by the presence of lenses of laminated clay within the otherwise variable matrix, suggesting settling-out of suspended material between flow events. That the deposition of this diamicton was associated with an advance of the ice margin is further supported by the compressional deformation (thrusting) observed in the underlying sediments (Fig. 2.4A). Section NRG 212 therefore appears to preserve evidence of subaqueous deposition that initially occurred some distance from the glacier front, but was succeeded by more proximal sedimentation and ultimately by ice-contact glaciotectonism. There is no evidence (such as overconsolidation) that the sequence was overridden by the advancing ice, however.

2.3.2 Section NRG 211

The sequence at NRG 211 is shorter and shows more restricted facies variability (Fig. 2.3 A). The lowest diamicton (Facies 2) lacks the degree of cohesion typical of subglacial tills and its friable sandy matrix is more consistent with emplacement by debris-flow processes, although no reverse-grading typical of debris-flow deposition is apparent. That it is overlain by poorly sorted gravel (Facies 4/5) suggests the later presence of meltwater, but it remains uncertain whether the diamicton was deposited subaerially or subaqueously. The weakly stratified gravel unit is indicative of a flow regime with sufficiently high-energy to entrain material of a coarse grade, and if deposited subaqueously, may have been emplaced by episodic high-density turbidity currents. The laminated silt and fine sand that overlie it (Facies 8) reflect subsequent non-turbulent conditions in which settling-out of suspended sediment occurred, probably in a subaqueous overbank environment beyond the margins of the main debris-flow channel. The degree of sorting of the sediments is consistent with transport to the ice margin as suspended load via subglacial meltwater conduits. The uppermost stratified diamicton (Facies 2) and the single large boulder at the top of the section probably relate to ice-proximal debris avalanches. In summary, NRG 211 can be interpreted as recording ice-marginal sedimentation most probably in a subaqueous environment dominated by input from emerging subglacial

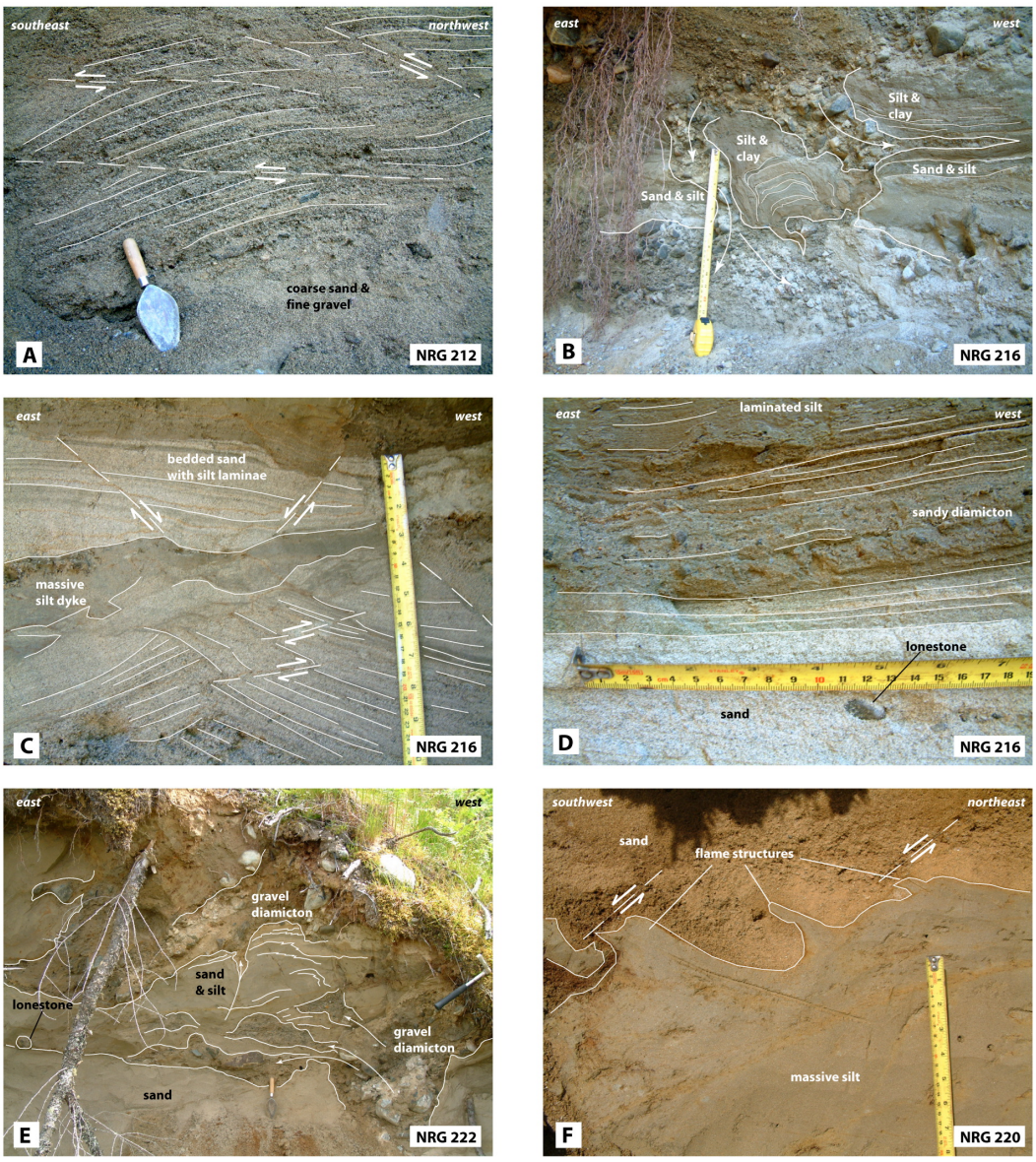

Figure 2.4: Examples of facies types from some of the sections described. A: Bedded sand and gravel exhibiting southeasterly directed thrusts and minor folding, NRG 212. B: Laminated and bedded silt and sand unit disrupted by hydrofracturing, NRG 216. C: Faulted trough-cross-bedded and planar-bedded sand intruded by a massive silt dyke, NRG 216. D: Conformable planar sequence of massive sand overlain by thin diamicton and laminated silt, NRG 216. E: Complex intercalation of sorted and bedded sediments with unsorted gravel diamicton units, NRG 222. F: Flame structures in silt intruding into overlying sand, NRG 220.

streams, and punctuated by periodic avalanching of unsorted sediments from the glacier margin.

2.3.3 Section NRG 216

This section is characterised by facies bounded by conformable planar contacts with numerous abrupt changes in grain size (Fig. 2.3 A). The poorly sorted gravel (Facies 4) at the base of the section was probably deposited from high-density turbidity currents forming a subaqueous fan or apron (Table 2.2). That it does not grade into the overlying silt and sand (Facies 8), however, suggests that the two units represent separate depositional events, and not different stages of a single event. The higher energy flow required to transport the gravel may have arisen during periods of seasonal melt when subglacial water volume and glaciohydrostatic pressure was high. The abrupt switch to rhythmic sedimentation of silt and sand suggests a period of lower-energy flow, perhaps as a result of decreased melt or, given the likely fan or apron-type environment, as a result of channel-switching that directed the dominant meltwater input elsewhere. Similar stratigraphic relationships are evident throughout the sequence, and together give an impression of a highly variable sedimentation regime perhaps controlled by meltwater and sediment supply routes and by their seasonal fluctuations. The trough cross-bedded sand unit (Facies 9) indicates that at least some of this sediment and meltwater input took place in migrating channels, which is consistent with a palaeo-fan / apron environment.

Localised deformation occurs in discrete horizons within the section. Near the base of the exposure the silt and sand (Facies 8) is cut by gravel-filled fractures (Facies 4). Large blocks of silt and sand within the gravel are plastically deformed, with the geometry of the deformation structures being consistent with the downward injection of the fluidised gravel (van der Meer *et al.*, 1999) (Fig. 2.4 B). This is interpreted to have occurred as a result of loading (either by increasing water depth or rapidly accumulating sediment) and increasing pore-water pressure in the overlying gravel. Higher in the section a bedded sand unit (Facies 9) at approximately 0.8 m depth is intruded by a dyke of massive silt, also interpreted as indicative of high pore-water pressure that in this case led to sediment liquefaction, fluidisation and hydrofracturing. Normal and reverse faults in the sand unit, in some instances forming conjugate pairs, provide further evidence of loading-induced deformation (Fig. 2.4C). Thus the overall sequence seems to reflect variable sedimentation, under abruptly changing conditions, that was accompanied by loading-induced synsedimentary deformation, the latter perhaps reflecting high sedimentation rates. The location of this section in the valley bottom (Fig. 2.2) is consistent with these sediments having been laid down on the floor of a former lake.

2.3.4 Section NRG 222

Massive silt and sand (Facies 7/10) at the base of NRG 222 (Fig. 2.3 A) suggests rapid deposition from hyperconcentrated flows, probably as underflow turbidity currents (Table 2.2). A high-density turbidity current carrying gravel and coarse sand (Facies 4/5) eroded into the massive sand unit, suggesting that the gravel was transported by channelised rather than sheet flow. The graded diamicton (Facies 2/8/11) above this unit fines upwards and reflects the gradual settling out of suspended sediment following initial input of a poorly sorted

sediment mass. This may have occurred in a channel under waning flow conditions. Continued input of silt and sand (Facies 8/11) which settled in non-turbulent or distal water produced the laminated unit in the middle of the section, and was initially followed by periodic input of variably well-sorted coarser-grained sediments (Facies 4/5/7/9) and later by renewed hyperconcentrated flows that laid down the uppermost massive silt and sand unit (Facies 7/9/10).

The section exhibits lateral variability in the sedimentary sequence, with greatest facies variation occuring at the western end (Fig. 2.4 E). The complex architecture of the units in this part of the section, and the orientation of the exposure perpendicular to the valley axis, presents difficulties in genetic interpretation, but a few possibilities may be proposed. The interdigitating relationship of the silt and sand (Facies 8/11) with gravel and diamicton (Facies 2) may be the result of liquefaction and intrusion of the latter into the finer-grained substrate. This could have occurred under self-weight and hydrostatic stresses (static loading) or as a result of glacier advance and the propagation of stress through proximal sediments. Normal and reverse faulting of bedded sand (Facies 8) in the section may lend some support to these proposals. Alternatively, the irregular contacts between facies may be the result of glacier-induced shearing along a plane normal to the face, brought about by compression of the sediment as the ice margin advanced. A third possibility is that this part of the section slumped at some stage, and the interfingering facies are the result of post-depositional deformation. This may have taken place following recession of the ice margin when support for the sediment pile was removed. The final consideration is that the architecture could reflect primary sedimentation variabilities, that is, localised and abrupt switching in sediment supply and deposition. Whilst all four may have played a role to some extent, the interpretation favoured here involves a combination of loading, liquification and slumping, on the basis that the contacts between facies do not appear to be either primary sedimentary features or the result of compressional glaciotectonism. These uncertainties aside, it is clear that the sediments represented in section NRG 222 reflect glaciolacustrine deposition of sediments sourced from both glaciofluvial and ice marginal environments.

2.3.5 Section NRG 221

The section NRG 221 lies close to, and perpendicular to, NRG 222, but occurs within a different cross-valley ridge. The majority of the section is dominated by bedded sand units (Facies 8), with minor laminated silt (Facies 11) and beds of massive gravel (Facies 4) (Fig. 2.3 B). The reverse-graded diamicton (Facies 1/2/5) that caps the sequence is silty and cohesive near the top, and resembles a submarginal till possibly originating as a debris flow deposit but subsequently compacted. The most striking features of the exposure, however, are the deformation structures in the sediments (Fig. 2.5). The gross structure is a broad southward-verging asymmetric open or overturned fold, cut by south-directed thrusts indicating that folding preceded thrusting (but not necessarily in a separate event). Folded bedding is clearly visible in the sand (Facies 8/9), and to a lesser extent in the laminated silt (Facies 11). This ductile deformation occurs in close association with brittle deformation in the form of thrusts and minor reverse faults. The largest thrust can be traced laterally for approximately 3.5 m and offsets the bedding within the sands and silts by up to 0.25 m (Fig.

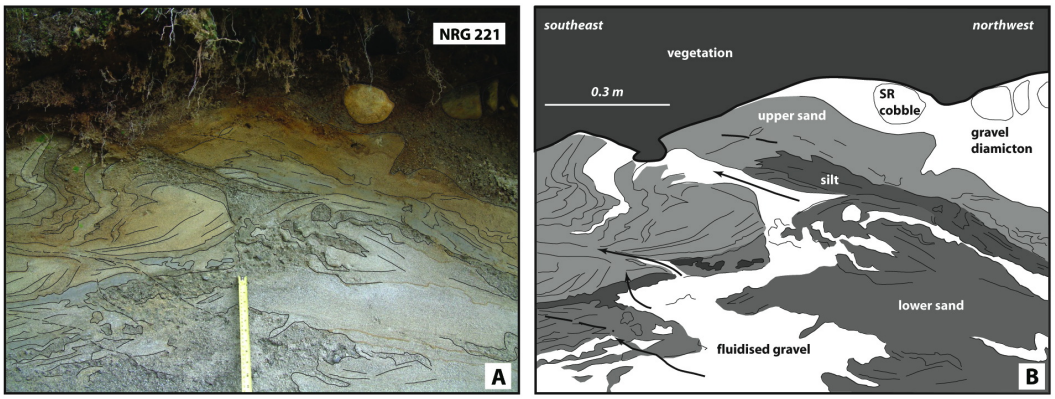

Figure 2.5: Field photograph of the folded, sorted sediments described at NRG 221, and tracing of principal facies and their structures. Note 1) the close association of ductile deformation (folding), with brittle deformation (fractures and thrusts), and 2) bed-thickening in the lower limb of the folded and fluidised gravel unit.

2.5). Gravel (Facies 4) infills this discontinuity, and thickens in the central part of the section and towards the south. Smaller structures are present in the section, notably disruptions to bedding in the sand and silt units. The silt and sand dykes that punctuate, but do not offset the bedding, are interpreted as water-escape features, in which sediments with high water content were fluidised and remobilised. Their high pore pressures first led to hydrofracturing of the surrounding substrate, and subsequently to infilling of the discontinuities when pore-water pressures subsided. This evidence of saturated sediments lends further support to their being deposited subaqueously. That the water-escape features cross-cut the folded beds suggests that they formed after the episode of compressional deformation.

On the basis of the deformation architecture exhibited by the sediments exposed in this section, the following scenario can be proposed. Initial glaciolacustrine and/or glaciofluvial sedimentation that deposited the interbedded silt, sand and gravel sequence (Facies 4/8/9/11) was succeeded by a period of lateral compression that produced the open folding seen in the sediments. Continued lateral stress led to the development of thrusts and an increase in pore-water pressure in the gravel unit. Hydrofracturing of the confining strata then occurred and water-escape took place, remobilising sediment and subsequently infilling the discontinuities (thrusts). The most likely mechanism to produce this sequence of events is the steady advance of the Dochart Glacier, from which avalanching debris (Facies 6) and deposition of submarginal till (Facies 1/2) produced the uppermost diamicton (Fig. 2.6).

2.3.6 Section NRG 220

NRG 220 exposes an overall coarsening-upward succession of silt, sand, gravel and diamicton in a cross-valley ridge (Fig. 2.3 B). The silt at the base of the exposure is massive and very firm (Facies 10) and has a convolute contact with the overlying sand (Facies 7) (Fig. 2.4F). The lack of lamination or bedding in the silt suggests that it may have been deposited rapidly, perhaps from a hyperconcentrated flow (Table 2.2), and was subsequently loaded prior to dewatering to produce partial liquefaction and convolutions interpreted as flame structures

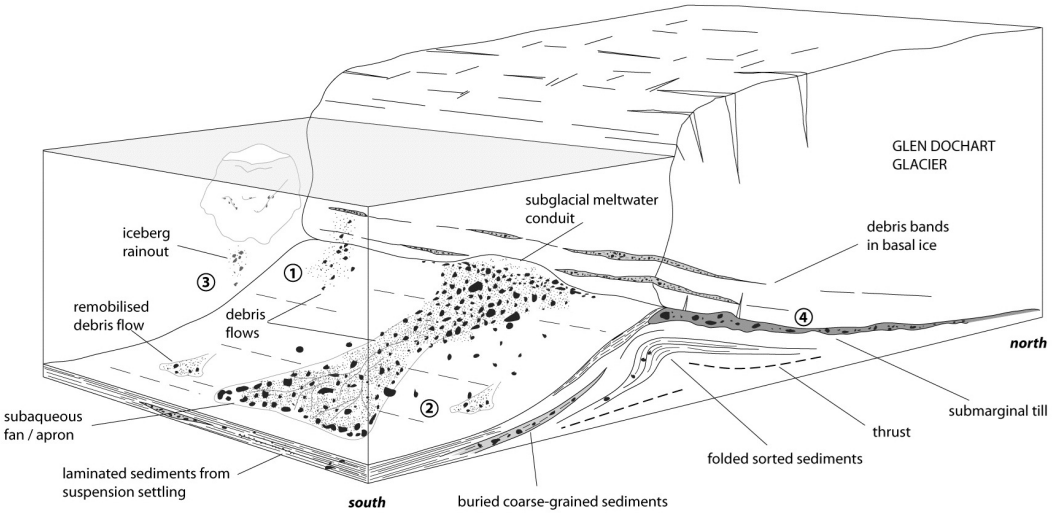

Figure 2.6: Schematic illustration of the ice-marginal environment thought to have existed in Glen Chaorach during Younger Dryas deglaciation. Sediment input to the ice-dammed lake occurred 1) through debris flows from emerging englacial debris bands, 2) via subglacial meltwater conduits, 3) from iceberg rainout, and 4) as submarginal till. Oscillation of the glacier at the grounding line tectonised the adjacent sediment pile and generated the transverse ridges interpreted as De Geer moraines. Not to scale.

that intrude the overlying sediments. As with NRG 221, the evidence of liquefaction suggests high porewater contents consistent with subaquaeous conditions. The gravel unit (Facies 4) suggests higher energy meltwater deposition, perhaps in the form of turbidity currents, and is succeeded by a sandy diamicton (Facies 1/2) at the top of the sequence. It is likely that this sequence represents the encroachment of an ice margin into a glaciolacustrine sediment pile, producing stresses sufficient to engender liquefaction and bringing unsorted ice-marginal debris into the sequence. Normal faulting in the sand unit may have resulted from slumping on the ice-distal side of the moraine.

2.3.7 Section NRG 219

Near the confluence of Glen Chaorach with Glen Dochart, the tributary valley widens and section NRG 219 exposes sediments in a cross-valley ridge. Laminated silt (Facies 11) at the base of the sequence reflects suspension settling in non-turbulent water, which was followed by episodic but sustained input of gravel (Facies 8/9), possibly via debris flows from an emerging subglacial stream. This sequence of gravel overlying laminated silt is repeated throughout the rest of the section, indicative of abrupt changes in sedimentation style (Fig. 2.3 B). This may have been the result of possibly seasonal fluctuations in meltwater flux, or may reflect channel switching within the glaciofluvial / glaciolacustrine system. None of the sediments show evidence of deformation, although the upper silt units are very firm and may have been subjected to high overburden pressures. Overall, the sedimentary sequence at this locality represents a relatively stable ice-marginal glaciolacustrine setting in which periodic high-discharge events punctuated background sedimentation.

2.3.8 Section NRG 218

Alternating units of sand (Facies 8/9/11) and gravel (Facies 4/5) in NRG 218 attest to variations in transport capacity of the glaciofluvial or glaciolacustrine system that deposited them. An overall sense of normal grading dominates the sequence, and only where coarser sediments overlie finer-grained material do erosional contacts occur (Fig. 2.3 B). The poor sorting of each sediment unit suggests a turbulent or short transport path, and may be reflective of a debris-flow origin from emerging subglacial streams. Despite the sediments forming an elongate cross-valley ridge, suggesting ice-contact formation, no evidence of glaciotectonism is apparent. The sequence is therefore best interpreted as reflecting ice-marginal sedimentation at a stable or receding margin.

2.3.9 Section NRG 213

The short section exposed at NRG 213 is composed of well-sorted, bedded sediments (Fig. 2.3 B) that form a flat extensive terrace at the mouth of Glen Chaorach. The basal gravel (Facies 4) is well-sorted and has little sand in its matrix, consistent with prolonged, relatively high-energy fluvial transport. Suspension settling in a glaciolacustrine environment laid down the overlying silt (Facies 11), which is succeeded by coarsening units of sand (Facies 8). One of these sand units is cross-bedded and reflects flow to the southeast, probably in a fan or channel environment. The uppermost unit is poorly sorted gravel (Facies 4) that may have been deposited in a highly turbulent fluvial environment, or as a high-density turbidity current in a glaciolacustrine setting. That the sequence composes part of an extensive terrace suggests that the sediments may best be interpreted as products of glaciofluvial deposition, probably laid down in a sub-aerial ice-proximal environment.

2.4 Discussion

Sediment is supplied to glacier margins predominantly by two key mechanisms – subglacial deformation of unconsolidated unsorted material (till), and meltwater transport either through or on the ice that delivers sorted sediments in suspension and as traction bed-loads (Edwards, 1986; Lønne, 1995; Benn & Evans, 1998). The dominance of sorted and bedded or laminated sediments over unsorted diamictons in all of the Glen Chaorach sections provides convincing evidence that deposition from glacial meltwater was particularly important, probably in a glaciolacustrine or glaciofluvial setting. This was brought about by separation of a major outlet lobe of the Younger Dryas ice cap that drained eastward along Glen Dochart (Golledge, 2007a) from a mountain icefield to the south. Sedimentary evidence at NRG 212 suggests a former water level at around 310 m a.s.l., and since the valley floor below this site lies at 250 m a.s.l. it is likely that, at its maximum, the depth of the former lake was c. 50 - 60 m. The lake most probably drained and refilled throughout its life, as is known to have occurred in former glacial lakes elsewhere in Scotland (Ballantyne, 1979; Brazier *et al.*, 1998), possibly as ice-marginal crevasses and subglacial conduits either opened or closed.

The exposed sediments commonly exhibit abrupt, but not necessarily erosional contacts, and reflect a highly variable sedimentary environment. Laminated sediments indicative of suspension settling under non-turbulent conditions are often juxtaposed with poorly sorted coarse gravel units typical of high-density turbidity currents or unsorted diamictons more commonly associated with ice-proximal avalanching of sub- and supraglacial material (Fig. 2.6). Blake (2000) suggests that compositional variation within De Geer moraines may be related to the location of outlets of subglacial streams, a notion that echoes earlier sedimentary investigations of ice-contact submarine fans (Lønne, 1995). Others suggest that advection of subglacial sediments towards the ice margin, and their intercalation with glaciofluvial canal-infill sediments, forms the proximal part of subaqueous moraines, and that more distal sediments are deposited by prograding sediment gravity-flows that interfinger with glaciolacustrine deposits (Benn, 1996; Lindén & Möller, 2005). Since clastic sedimentary sections are thought to be reliable archives of 'short-lived internally controlled events' (Fard, 2001, : p145), whether climatically induced or not, both scenarios may help to explain the localised nature of the sedimentary record produced in such environments, and the facies variability seen in the Glen Chaorach examples described here.

Where glaciotectonic deformation occurs in these examples, it is always uni-directional (south-vergent) and provides evidence of ice-marginal oscillations after accumulation of the sediment pile. The presence of both brittle and ductile deformation features is common in sediments found at ice margins (Benn & Evans, 1998; Menzies, 2000; Golledge, 2002; Phillips *et al.*, 2002), and results from the propagation of glacier-induced stresses through the glacier bed. The glacier advances associated with sediment deformation and deposition of diamictons appear to have been the final events. This may indicate that whilst marginal advance was relatively slow, its recession was probably more rapid. This is typical of water-terminating margins that lose the majority of their mass through calving (Paterson, 1994), particularly where glacier thinning occurs (van der Veen, 1996). Since none of the recorded sedimentary sequences is capped by drapes of glaciolacustrine silt and clay commonly associated with widespread suspension settling, it may be speculated that the majority of sediment delivery into the glacial lake was as focussed underflows rather than as diffuse plumes, probably governed by the locations of emerging subglacial meltwater conduits.

2.4.1 Event chronology

During the Younger Dryas glacial episode, Glen Chaorach was occupied by ice from two confluent glaciers (Fig. 2.7, A). Northward ice flow from the Ben More glacier contributed to the much larger, eastward-flowing Dochart glacier, which acted as one of the principal southern outlets of the ice cap centred over Rannoch Moor (Fig. 2.1). Thinning of these glaciers during the initial stages of deglaciation led to the creation of an intralobe lake, and deposition of laminated and bedded fine-grained sediments. Continued separation of the glaciers was accompanied by an increase in the area and depth of the ice-dammed lake, and by changes in the flow pattern of the two ice masses (Fig. 2.7, B). Southward-directed deformation structures preserved in the lake sediments indicate that during this phase, minor oscillations of the Dochart Glacier formed De Geer moraines by tectonising glaciolacustrine sediments at

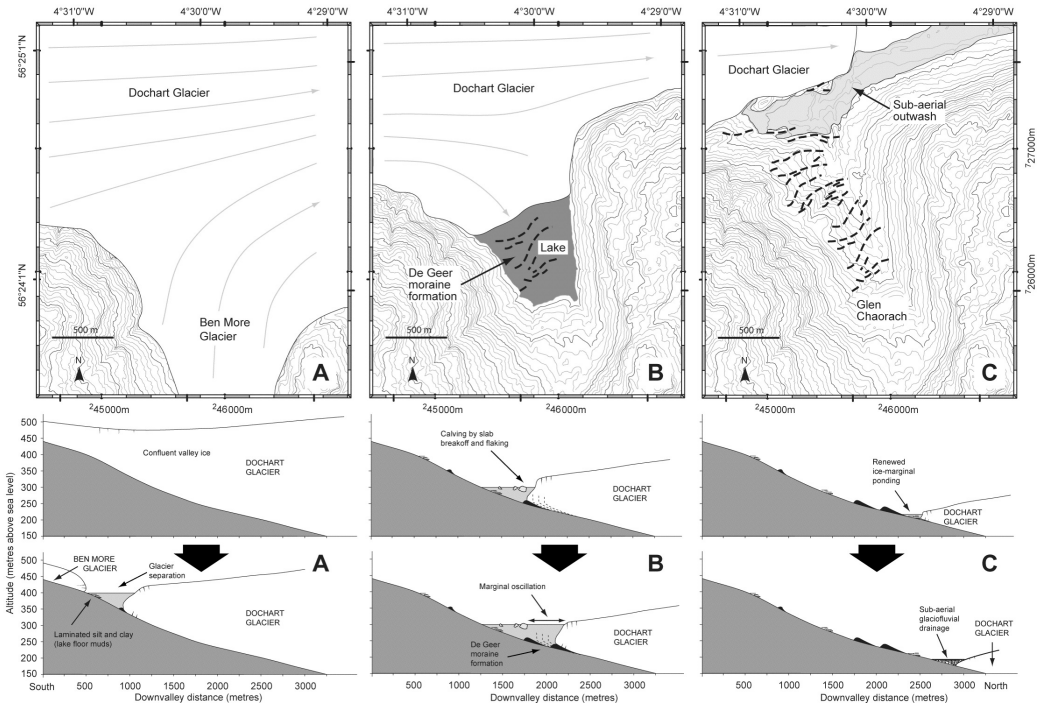

Figure 2.7: Key stages in ice-margin evolution during deglaciation of the study area. A: Glen Chaorach is filled by confluent ice of the Dochart and Ben More glaciers. Thinning leads to separation of the ice masses which leads to early development of an ice-dammed lake and deposition of fine-grained sediments. B: continued recession produces a lake deep enough to enable calving of the grounded glacier, and the margin is stable enough to oscillate at its grounding line and thereby form De Geer moraines. C: During the final stages of ice-marginal ponding, the confining glacier no longer oscillates or tectonises the sediments, and ultimately thins to the mouth of Glen Chaorach enabling free marginal drainage that gives rise to sub-aerial glaciofluvial deposition. Topographic contours are at 10 m vertical intervals, derived from Ordnance Survey Profile data, © Crown Copyright.

successive grounding lines (Fig. 2.7, B). The locations of such grounding lines were probably governed by high points on the valley floor, such as bedrock knolls, that acted as 'pinning points'. Further deglaciation following this period of stability led to recession of the ice margin towards Glen Dochart until Glen Chaorach became ice free, eventually removing the dam that had previously impounded supraglacial and subglacial meltwater. Consequently, an ice-marginal, subaerial glaciofluvial environment was established in which the extensive, channelled terraces composed of bedded, well-sorted sediments were formed (Fig. 2.7, C). Subsequent retreat of the glacier front formed the large morainic mounds in Glen Dochart (Fig. 2.2), prior to final disappearance of the ice sometime after 11.6 ka ± 1.0 ka BP (Golledge *et al.*, 2007).

2.5 Conclusions

Geological and geomorphological mapping has identified a population of elongate linear cross-valley ridges in Glen Chaorach, a tributary valley of the much larger Glen Dochart. During the Younger Dryas, Glen Dochart accomodated a major outlet glacier of the west Highland ice cap, formerly centred over Rannoch Moor, and Glen Chaorach was filled with confluent

ice sourced on the east side of Ben More. After initially feeding ice into the main glacier, the tributary valley glacier thinned and the two ice masses separated. Moraines formed in Glen Chaorach as the glaciers retreated, and meltwaters accumulated to form an ice-dammed lake. Sedimentary characteristics of the moraines, together with their geomorphology and context, strongly suggest that they formed at the grounding line of a water-terminating glacier margin that occupied a quasi-stable position in the valley during intial deglaciation. Sediments were deposited in the ice-marginal lake primarily through focussed delivery in subglacial conduits and from ice-front debris-flows. Oscillations of the glacier margin led to deformation of the sediment pile but were followed by rapid recession to pinning points lower in the valley. When glacier thinning had proceeded to the extent where an ice dam could no longer confine meltwater in Glen Chaorach, ice-marginal glaciofluvial sedimentation ensued, followed by frontal retreat of the Dochart Glacier.

PAPER II

Sedimentology, stratigraphy, and glacier dynamics, western Scottish Highlands

Nicholas R. Golledge
British Geological Survey, West Mains Road, Edinburgh, EH9 3LA, UK
and School of Geosciences, University of Edinburgh, West Mains Road, Edinburgh, EH9 3JW, UK.
ph: +44 131 667 1000, fx: +44 131 668 1535, email: n.golledge@bgs.ac.uk

Abstract

Glacial sediments of the western Scottish Highlands are comprehensively described and characterized here for the first time, enabling the first glacial stratigraphy for the area to be proposed. This classification is based on the results of extensive geological mapping and field investigation of sedimentary sequences and their structures, X-Ray Diffraction and Particle Size Distribution analyses, and comparison with deposits formed in contemporary glaciated environments. These new data are subsequently appraised in terms of their implications for late Pleistocene glacier evolution and dynamics. Together, the data suggest that much of the landscape is palimpsest, and can be attributed to the Weichselian (Late Devensian) glaciation. Subsequent glacier advance during the Younger Dryas did little to modify the area, suggesting that ice flow was dominated by sliding on a meltwater-lubricated rigid bed, with deformation of basal sediments playing a more limited role. Final deglaciation was marked by a significant increase in basal meltwater flux, reflecting the warming climate and increasing precipitation. These new palaeoglaciological and palaeoenvironmental insights advance our understanding of former glacier dynamics in the western Scottish Highlands, improve our knowledge of Pleistocene landscape evolution of this area, and enable comparisons to be made with sedimentary sequences elsewhere.

KEYWORDS: Late Weichselian; Younger Dryas; British Ice Sheet; stratigraphy; glacier dynamics; palaeoglaciology; Scotland.

2.6 Introduction

The growth and decay of ice caps and ice sheets is intimately related to global climate change, hydrological storage, land-ocean sediment flux and long-term landscape evolution (Alley & MacAyeal, 1994; Krüger, 1996; Hodgkins, 1997; Alley, 2000; Jansson *et al.*, 2003; Barnard *et al.*, 2006). The study of former ice-mass behaviour may therefore be useful in understanding how these Earth-systems operated in the geological past. Perhaps the most direct evidence available for the study of former glacier dynamics is the sedimentary record left by the ice. Indeed, geological and geomorphological mapping of deglaciated terrains is often used to determine the size and extent, (i.e. the geometry), of both ancient ice masses as well as those that were formerly more extensive (e.g. Sugden, 1977; Thorp, 1986; Van Tatenhove *et al.*, 1996; Clark, 1997; Anderson *et al.*, 2002; Evans *et al.*, 2005). In Britain this approach has been employed since the earliest recognition of glacial features (Agassiz, 1841; Geikie, 1863; Hinxman *et al.*, 1923; Charlesworth, 1955) and has enabled significant advances to be made in our understanding of Earth-system processes. More recent developments, in both geological and glaciological sciences, have allowed far more detailed interpretations to be made now than ever before, particularly when founded on empirical data from field mapping (Benn, 1994; Mitchell, 1994; Merritt *et al.*, 1995; Lowe & Anderson, 2003; Clark *et al.*, 2004; Glasser & Bennett, 2004). Additionally, field-based reconstructions are often used to inform, test or constrain numerical models (e.g. Van Tatenhove *et al.*, 1996; Jones, 1998; Golledge & Hubbard, 2005; Hubbard *et al.*, 2005).

Oxygen isotope data obtained from Greenland ice cores show that the climate of the northern hemisphere oscillated between cold and warm phases throughout the late Pleistocene, giving rise to particularly long-lasting cold periods from c. 70–57 ka BP (Oxygen Isotope Stage 4) and from c. 25–15 ka BP (Oxygen Isotope Stage 2) (Dansgaard *et al.*, 1993). Interstadials punctuated these colder spells, most notably prior to c. 90 ka BP and from c. 35–28 ka BP, during which temperatures ameliorated slightly, but were still sufficiently low that glaciers would have survived in the Scottish Highlands (Clapperton, 1997). Palaeoclimatic data based on coleopteran and chironomid data from four sites in Britain indicate that even during the Windermere Interstadial, (c. 15–13 ka BP), the climate affecting Scotland was warm for only a short time before renewed cooling and instability led to the onset of the Younger Dryas stadial (Mayle *et al.*, 1999). This period of renewed global cooling was characterized in Scotland by an abrupt c. 8–10°C drop in mean annual temperature at its onset, a subsequent decline in precipitation due to sea ice formation during the Stadial, and final rapid warming that terminated the glacial readvance (Benn *et al.*, 1992; Clapperton, 1997; Hubbard, 1999; Isarin & Renssen, 1999).

This study reports geological and geomorphological field data gathered by the British Geological Survey over the period 2003 – 2006, during the resurvey of part of the western Scottish Highlands (Fig. 2.8), together with the results of sedimentological analyses and palaeoglaciological reconstructions. Facies genesis is established by comparison of sedimentary characteristics with contemporary analogues in Iceland and Svalbard and with descriptions of similar deposits in the literature. Together, these data allow a new stratigraphy to be presented and conclusions to be drawn with respect to the former glacier dynamics of the ice masses that overwhelmed this part of the western Scottish Highlands during both the Main

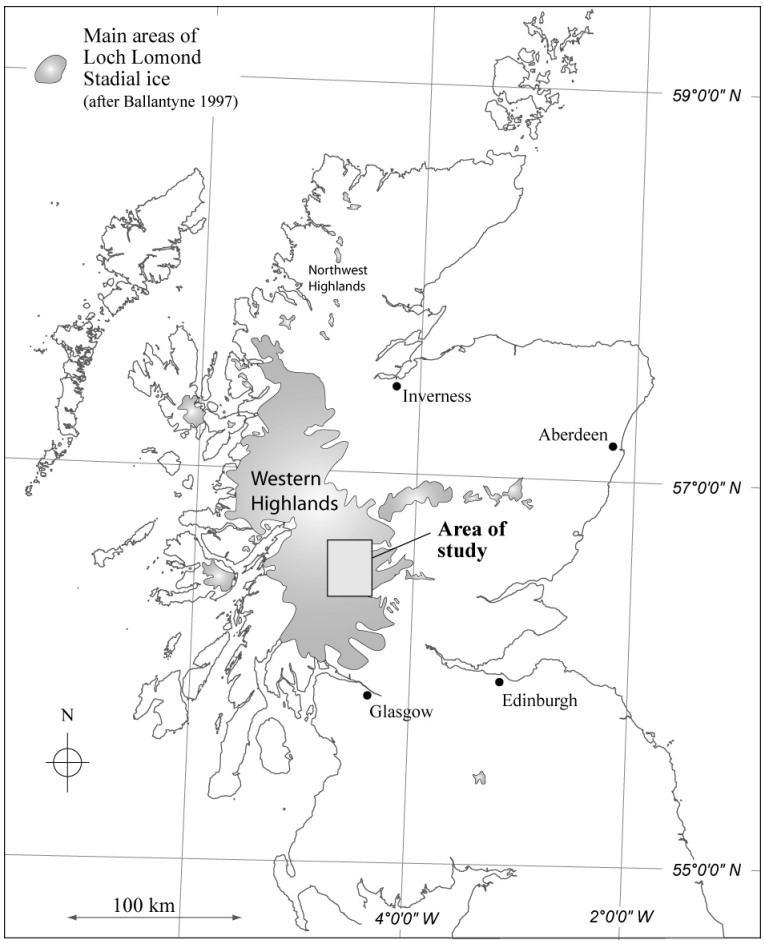

Figure 2.8: Location map showing area of study in Scottish context, and in relation to approximate maximal extent of Younger Dryas ice cover (after Ballantyne, 1997).

Late Devensian (Late Weichselian, c. 25 – 15 ka BP) and the Younger Dryas (12.7–11.3 ka BP).

2.6.1 Field area

The research is focussed on a large area (960 km^2) of the western Scottish Highlands to the south of Rannoch Moor and north of Loch Lomond (Figs. 2.8 & 2.9 A). The study area is one of steep-sided mountains and intervening 'U'-shaped valleys ('glens'), with many mountain tops covered in regolith derived from metasedimentary bedrock. Where the regolith mantle has been affected by frost-heave, saturation by rainfall, and gravity, solifluction terracettes have resulted. Exposed bedrock is particularly common, with talus aprons or cones developed below most crags. Some of the valleys host a covering of till along their flanks and floors, which varies in thickness from 1 – 30 m. In many places the till is overlain by morainic deposits of poorly-sorted sand, gravel and diamicton, which often form elongate boulder-strewn ridges. Glaciofluvial deposits are not extensive, and where present are mainly confined to large fans and sparse ice-contact features. The floors of many valleys reflect fluvial activity since deglaciation, and exhibit rock-cut channels, thin bouldery alluvium, or large and extensive terraces of sand and gravel. Peat overlies much of the ground at both

high and low levels, and although generally thin, attains thicknesses of up to 3 m in some places.

2.6.2 Previous research

Early mapping by the Geological Survey (1890 – 1920) focussed on the bedrock geology of the area, with limited description of the abundant glacial deposits, their inter-relationships, and their association with the wide variety of landforms present. Reconstruction of the glacial history was attempted for adjoining areas by Hinxman *et al.* (1923), who recognised that much of the area had been overwhelmed by ice from Rannoch Moor during the Last Glacial Maximum (LGM). Charlesworth (1955) described the moraines and ice-marginal features of much of the Scottish Highlands; in the field area described here he associated these features with the decay of glaciers after his 'Highland Readvance'. Sissons (1965) later proposed that the 'hummocky moraine' seen in the area resulted from *in situ* stagnation of glaciers at the end of a renewed phase of glaciation after the Main Late Devensian ice sheet had disappeared. Subsequent mapping has been limited to studies that cover smaller parts of the area (Thompson, 1972; Horsfield, 1983; Thorp, 1984, 1986, 1987, 1991b), and which mainly describe geomorphological rather than sedimentological features. Nonetheless, these studies have greatly improved our understanding of the former Younger Dryas ice mass that affected the area most recently. Whilst Thompson (1972) favoured a valley-glacier type reconstruction, Horsfield (1983) concluded that the area had been glaciated by an invasive ice cap centred on the Etive and Nevis mountains to the north-west. Thorp (1984, 1986) based his reconstruction on periglacial 'trimlines', and deduced that the ice cap on Rannoch Moor was relatively thin, restricted in extent, and fed outlet glaciers that together formed a mountain icefield. Recently, Golledge & Hubbard (2005) reassessed the area and found field evidence suggesting a thicker ice cap than proposed by Thorp. The empirical reconstruction based on this data finds good agreement with the numerical model of Hubbard (1999).

Given the differing interpretations and the lingering uncertainty surrounding the style and impact of Younger Dryas glaciation in the western Scottish Highlands, the intention here is to set out a new stratigraphical framework based on sedimentological classification of the glacial deposits of the study area, and to use this to inform interpretations of former local and regional glacier dynamics.

2.7 Methods

2.7.1 Data capture

Geomorphological features and interpreted geological boundaries were added to 1:10 000 or 1:25 000 scale topographic base maps from the interpretation of 1:24 000 scale monochrome aerial photographs, high-resolution digital terrain models (DTMs), and where applicable, Thematic Mapper satellite imagery. This was achieved either digitally in an onscreen GIS environment, or in a more traditional manner using paper map bases. These interpretations were subsequently field-checked by detailed walk-over survey in which lines were modified as appropriate. Sedimentological data was added to the map based on the availability and

accessibility of natural sections. The distribution of 53 logged sections is shown on Fig. 2.9 A, although the many hundreds of minor exposures noted on field maps that informed the geological interpretation are, for clarity, not shown. For deposits with consistent matrix colour a Munsell Soil Color chart was used (Table 1).

2.7.2 PSD and XRD analysis

Samples were collected from four of the key facies described below for X-Ray Diffraction (XRD) and Particle Size Distribution (PSD) analysis. Only deposits possessing a relatively homogeous matrix were deemed meaningful for analysis. Samples for XRD analysis were freeze-dried prior to grinding in a tungsten-carbide gyromill to produce a fine powder. Discs were prepared of each powdered sample using metal mounts, and were analysed using a Philips PW 1800 X-Ray Diffractometer to produce diffractograms. Systematic peak-matching against standard spectra enabled dominant compounds to be identified. Samples for PSD were taken from wet sediment, agitated with sodium hexametaphosphate in an ultrasonic bath to create a suspension of suitable density, seived to remove the $> 900\mu$m fraction and repeatedly flushed through a Coulter LS100 Laser Diffractometer to derive size-frequency data.

2.8 Results

2.8.1 Bedrock

The underlying strata in the field area are polydeformed Neoproterozoic metasedimentary rocks of the Dalradian Supergroup, which comprise mainly metasandstone and metasiltstone, with less abundant interbedded pelitic and calcareous rocks. Deformation of the bedrock has resulted in wide variation in its dip and strike, although the regional strike is approximately W – E in the south and SW – NE further north. Bedrock is easily discernable almost everywhere, due to the mainly thin covering of superficial deposits. In many places the bedrock is highly abraded, smoothed or polished, reflecting the legacy of successive glacial episodes. Particularly clear examples of ice-smoothed bedrock occur in Lairig Arnan, Gleann nan Caorann, Lairig nan Lunn, and Glen Falloch, on cols between Beinn Dorain and Beinn a' Chreachain, also between Ben Lui and Beinn Dubhchraig, and at higher levels on the flanks of mountains south of Glen Falloch such as Beinn Chabhair, Beinn a' Chroin and Cruach Ardrain (Fig. 2.9B). Zones of disaggregated bedrock – where blocks have been detached and moved less than a few 10's of metres from source outcrops – occur on some plateau areas between mountain peaks and valley troughs (Fig. 2.9B). Where the detached blocks form drumlinoid mounds, the former direction of ice flow can be inferred. Erosional landforms such as roches moutonnée, P-forms and striae were recorded in Glen Falloch, Lairig Arnan, Loch Easan, Glen Lochay, Coire Chailein and Mam Lorn.

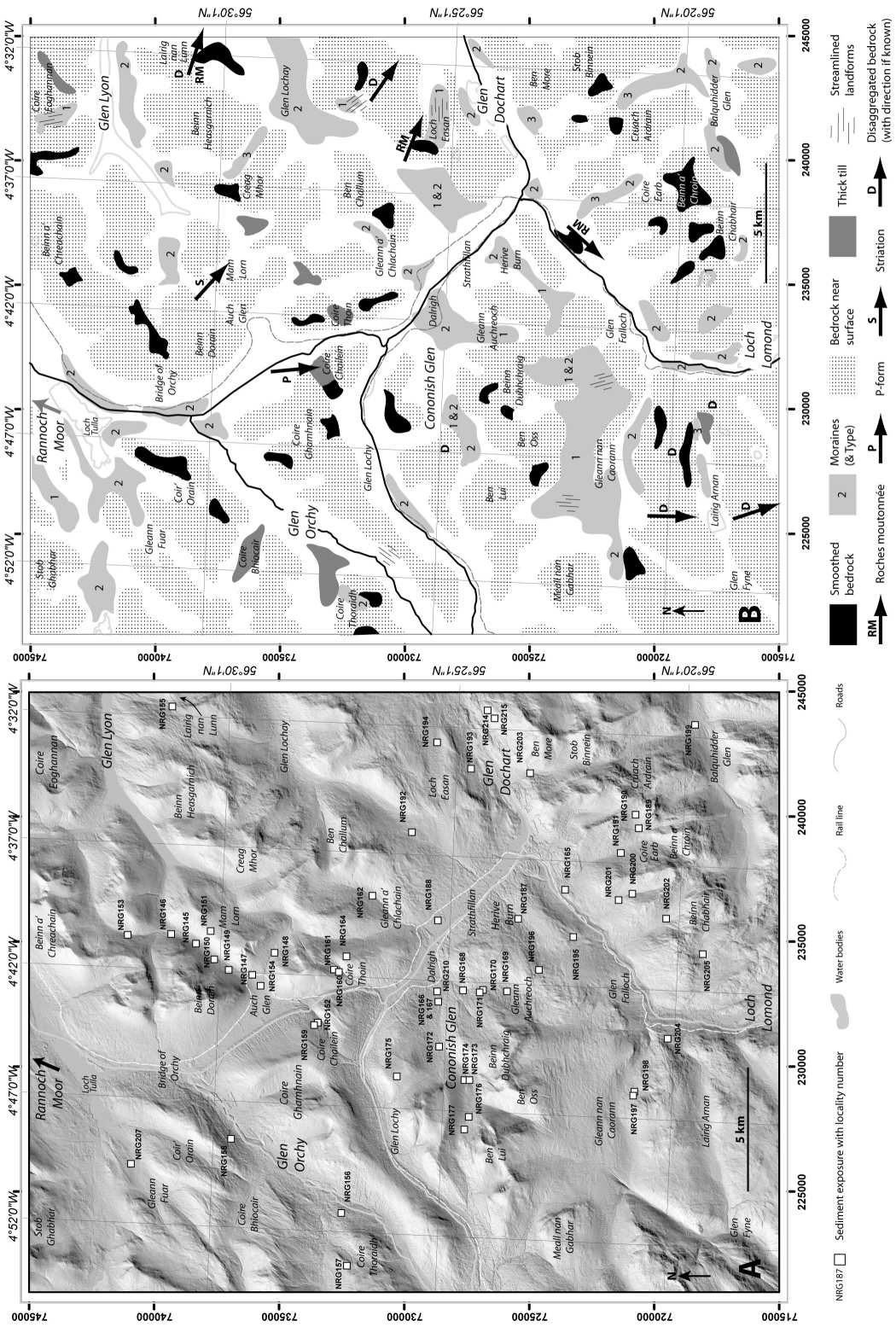

Figure 2.9: A: The study area, showing principal mountains, valleys and water bodies, and the locations of sediment exposures reported here. Digital terrain model built from Intermap Technologies NEXTMap 1.5m resolution topographic data. B: Occurence of key bed-types in the study area, showing areas of bedrock at or near surface, ice-smoothed bedrock, disaggregated bedrock, thick till accumulations, suites and types of moraine. Some generalisation has been necessary and some smaller occurrences are not shown. Erosional landforms such as roches moutonnée, P-forms, and striations are shown with arrows indicating the inferred former ice flow direction. Northern and eastern margins show Lat / Long; southern and western margins show British National Grid references.

2.8.2 Glacial deposits

Sedimentology

A description of each facies type encountered, their expression and occurence in the study area, and their genetic interpretations are presented in Table 2.3. As no formal stratigraphy exists for the study area the facies are differentiated on their colour, texture, composition and internal structure, and are coded here A – H. This simple approach enables identification and classification of deposits in the field and allows units to be confidently correlated between exposures.

Facies A, B, C, and D are all well-consolidated generally massive diamictons composed of sand, silt and clay and containing sub-angular and sub-rounded clasts. Facies A, B and D are locally weakly stratified, however, and host centimeter to decimeter-scale pods or laterally-impersistent partings of silt and fine sand, whereas Facies C is never stratified and has a finer-grained matrix that produces an almost choncoidal cleavage pattern. All of these diamictons are firm or very firm but they differ from one another in their colour and matrix mineralogy. Facies A and B are reddish-brown and yellow-brown respectively, and both contain kaolinite. Facies C is blue-grey or greenish-grey and contains calcite, whilst Facies D is light olive-brown in colour and contains neither calcite or kaolinite. Facies E and F are similarly-coloured diamictons to Facies D but are considerably less consolidated. They are often stratified, with sand beds up to 1 m thick in Facies E and thinner lenses and beds in Facies F. Both diamictons are rich in well-rounded to very angular clasts ranging from gravel and cobbles to boulders.

Facies G comprises a range of grain-sizes but in all instances is characterized by a high degree of size sorting not seen in the other units. Whilst some units are massive, others show primary sedimentary structures such as planar bedding, trough cross-bedding or lamination. Facies H is identifiable by the grade of its constituents (boulders) and lack of sedimentary structures. Deposits of this facies are commonly very localised and cannot be laterally correlated. In most cases, however, the other facies (A – G) show remarkable inter-site uniformity, and can be traced across the study area relatively easily, although the number of exposures of each unit is widely variable. For example, Facies A and B were only seen in Coire Thoin and Coire Chailein respectively, but the remainder are considerably more widespread (Table 2.3). Examples of the main facies types and the typical form of ice-smoothed bedrock are shown in Fig. 2.10A–D, and PSD data for Facies A – D are plotted in Figure 2.11.

Stratigraphy

The sediments described in Table 2.3 are patchily distributed across the study area, but exposed metasedimentary bedrock is widespread. Whilst most valleys have only thin valley-floor till cover, some – such as Coire Chailein, Coire Thoin, Coire Bhiocair, and Glen Auchreoch – host sediment accumulations up to 30 m thick (Fig. 2.9B). These thicker sequences provide the basis for facies correlation between sections, and are described in more detail below.

The section exposed in Coire Chailein is shown in Fig. 2.12. Although some lateral variation occurs, the overall sedimentary sequence can be summarised as follows. The lowest unit, Facies

Facies	A	B	C	D	E	F	G	H
Sediment type	Diamicton	Diamicton	Diamicton	Diamicton	Diamicton	Diamicton	Sorted sediments	Boulders
Structure	Massive to weakly-stratified, some centimeter to decimeter-scale pods, lenses and beds of silt and sand.	Massive to weakly-stratified, some laterally-persistant partings of silt and fine sand.	Massive, never stratified. Matrix has conchoidal cleavage, no apparent fissility	Massive to weakly-stratified	Stratified, containing sand lenses and beds up to 1m thick. These range from planar bedded to highly folded	Stratified, often clast-rich, containing folded and / or faulted sand lenses and beds	Bedded and / or laminated	Clast-supported beds
Facies code (after Eyles & Miall 1984)	Dmm	Dmm	Dmm	Dmm	Dms	Dms	Gfo, Gm, St, Sfo, Sm, Fl	Bcm
Matrix material	Sand	Silt and sand	Silt and clay	Silt and sand	Coarse sand and fine gravel	Coarse sand and fine gravel	Gravel, sand, silt, clay	Sand, gravel
Matrix Particle Size Distribution	Trimodal, main peak in fine sand, secondary peak in fine silt, tertiary peak in clay	Trimodal, main peak in fine sand, secondary peak in fine silt, tertiary peak in clay	Bimodal, main peak in fine-med silt, secondary peak in med sand	Unimodal to bimodal, peak in med-coarse silt, weak secondary peak in med sand	N/A	N/A	N/A	N/A
Consolidation	Firm but friable	Very firm	Firm to very firm	Firm	Often friable but highly variable	Often friable but highly variable	Compact to firm	N/A
Upper contact	Sharp, conformable, planar, marked by SA boulders > 1m diameter	Conformable	Conformable, sharp, planar	Conformable, in places undulose or gradational	Undulose, sometimes erosional	Undulose	Often erosional	Undulose
Lower contact	Not seen	Not seen	Conformable, sharp, planar	Conformable, sharp, planar	Conformable, in places undulose or gradational	Conformable / undulose, sometimes erosional	Conformable and planar, or erosional	Undulose
Colour	Reddish to yellow-brown	Yellowish-brown (2.5Y 6/3)	Blue-grey or greenish-grey (5GY 5/1)	Light olive brown (2.5Y 5/4 - 5/6)	Olive-brown or light olive brown (2.5Y 4/4 -- 5/6)	Olive-brown or light olive brown (2.5Y 4/4 -- 5/6)	Variably grey, brown or yellow	N/A
Matrix mineralogy (XRD)	Contains kaolinite	Possible kaolinite	Contains calcite	Neither kaolinite or calcite present	N/A	N/A	N/A	N/A
Clast lithologies	Metasedimentary rock	Psammite, semi-pelite, rare white granodiorite	Metasedimentary rock and rare granite	Metasedimentary rock, quartzite, rare pegmatite	Metasedimentary rock	Metasedimentary rock	N/A	Psammite, semi-pelite, rare granite
Clast grade	Cobbles & gravel	Cobbles & gravel	Cobbles	Cobbles & gravel	Cobbles, gravel, boulders	Cobbles, gravel, boulders	N/A	Boulders, some cobbles
Clast rounding	SA / SR	SR / SA	R / SR / SA	R / SR / SA	WR -- VA	WR -- VA	N/A	A / SA
Occurrence	Coire Thoin only	Coire Chailein only	Well-distributed but limited	Ubiquitous	Widespread but patchy	Widespread but patchy	Glens Orchy & Cononish, Strathfillan, Coire Earb	Coire Chailein and Glen Orchy only
Maximum thickness	c. 25m	c. 13 m	> 5 m	c. 5 m	< 3 m	c. 10 m	< 5 m	< 2 m
Depositional environment	Subglacial	Subglacial	Subglacial	Subglacial	Submarginal	Ice-marginal, sub-aerial	Sub-aerial, proglacial and ice-marginal	Ice-marginal, sub-aerial
Genetic interpretation	Basal substrate ('till')	Basal substrate ('till')	Basal substrate ('till')	Basal substrate ('till')	Reworked older substrates and melt-out from basal ice	Debris flows and basal melt-out	Glaciofluvial outwash	Debris avalanche
Landform association	None	None	Smooth spreads and Type 1 moraines	Smooth spreads and Type 1 moraines	Hummocky spreads	Type 2 moraine ridges and mounds	Fans, deltas and terraces	None
Comments	Some pervasively weathered pelite clasts present	Poorly-exposed due to slippage from above	Evidence of hydrofracturing in Coire Chailein	Often the only facies seen exposed	Transitional between Facies D & F	Highly variable composition	Wide range of grading, sorting and structure	May reflect very local source
Interpreted age	Pre-Main Late Devensian	Pre-Main Late Devensian	Main Late Devensian	Late Devensian deglaciation	Younger Dryas	MLD & YD	Pre-MLD to YD	Pre-MLD to YD

Table 2.3: Characteristics of the eight facies types described in the text, including postulated genetic interpretations and inferences of depositional environment. Facies codes after Eyles & Miall (1984); Eyles *et al.* (1984).

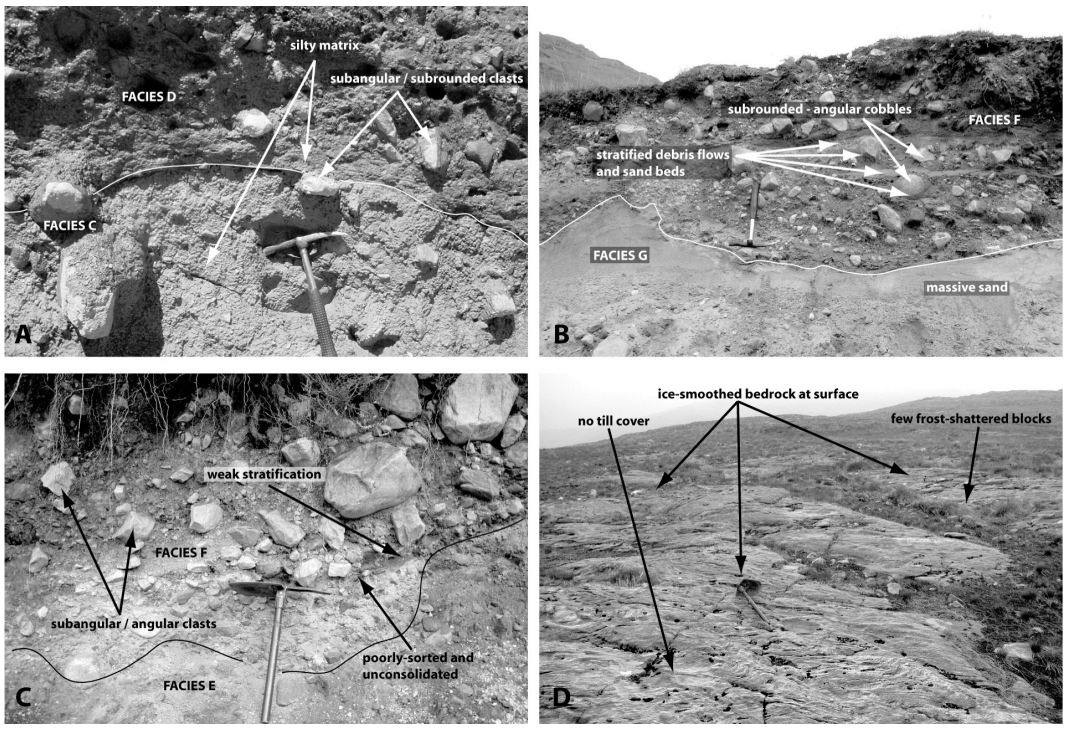

Figure 2.10: Field photographs showing A: Facies C and D, B: Facies F and G, C: Facies E and F, and D: ice-smoothed metasedimentary bedrock at 560m a.s.l, Glen Orchy (former iceflow approximately right to left).

B, is a 12–13m thick, very firm, yellow-brown, sandy diamicton containing subangular and subrounded metasedimentary clasts. This is overlain by a complex sequence of interbedded sand, gravel and diamicton units. These are laterally variable in thickness but include an approximately 1 m thick clast-supported predominantly sub-angular psammite boulder bed, (Facies H), beds of weakly stratified sandy and gravelly diamicton up to 1 m thick (Facies F), and an overlying unit of laminated clay, silt and trough-cross-bedded sand 1–2 m thick (Facies G). In places the bedded sand exhibits centimetre-scale faults and folds. Overlying the sand is weakly stratified gravel that grades upward into gravelly diamicton (Facies F), which is then overlain by 8 m of grey, clayey diamicton (Facies C), and firm, brown, diamicton (Facies D).

The dominant sediment exposed in Coire Thoin is Facies A – a cohesive diamicton that in a weathered section appears uniformly reddened, but when dug becomes increasingly yellow-brown with depth. The diamicton is sandier and more clearly stratified higher up, and is overlain by Facies C diamicton. In Coire Bhiocair the sedimentary infill is poorly-exposed, but appears to consist predominantly of Facies D diamicton. In Glen Auchreoch and Gleann nan Caorann conformable sequences of Facies C and D up to 10 m thick are preserved, the two units separated by abrupt, sub-planar contacts.

Smaller exposures elsewhere are also instructive. In Glen Lochy Facies D is overlain by up to 5 m of stratified sandy, unconsolidated diamicton (Facies E) containing discrete sand beds up to 1 m thick. In Cononish Glen and Gleann Auchreoch, moraines are composed of Facies F stratified diamictons that dip up-valley, host numerous folded and faulted sand and silt

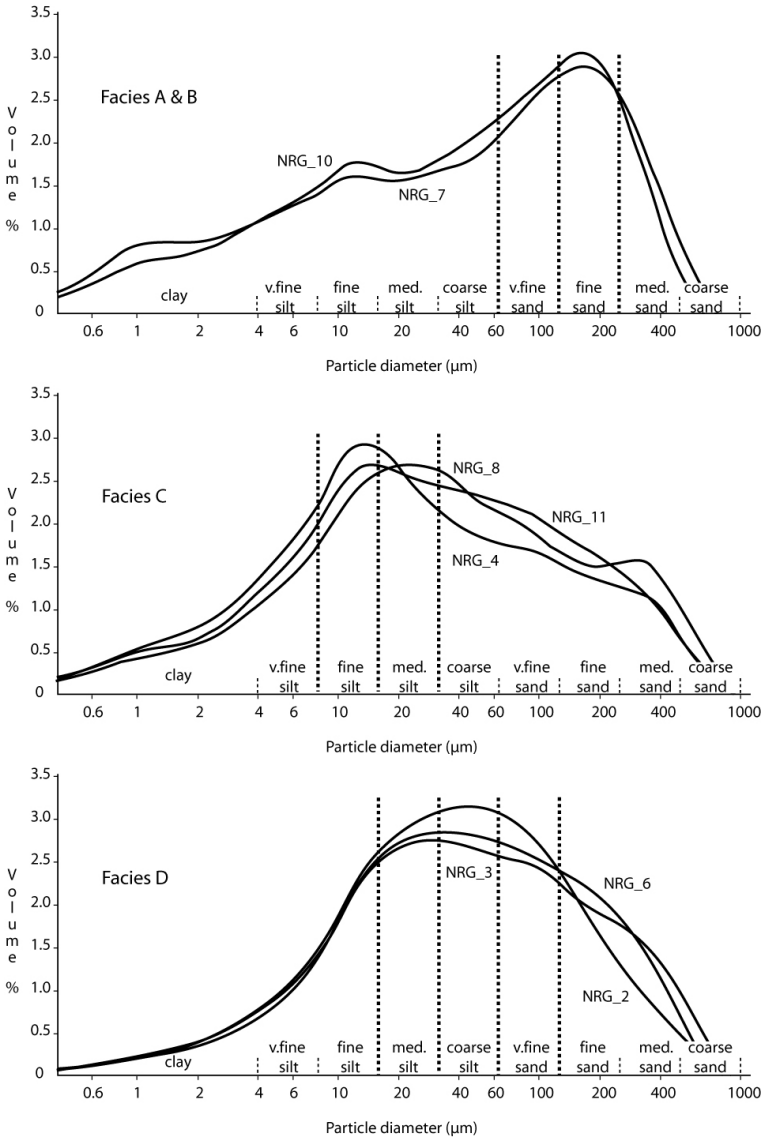

Figure 2.11: Particle size distribution curves for sub-900μm fraction of matrix material from Facies A – D, interpreted as subglacial tills. Note the difference between each plot, and the degree of internal consistency.

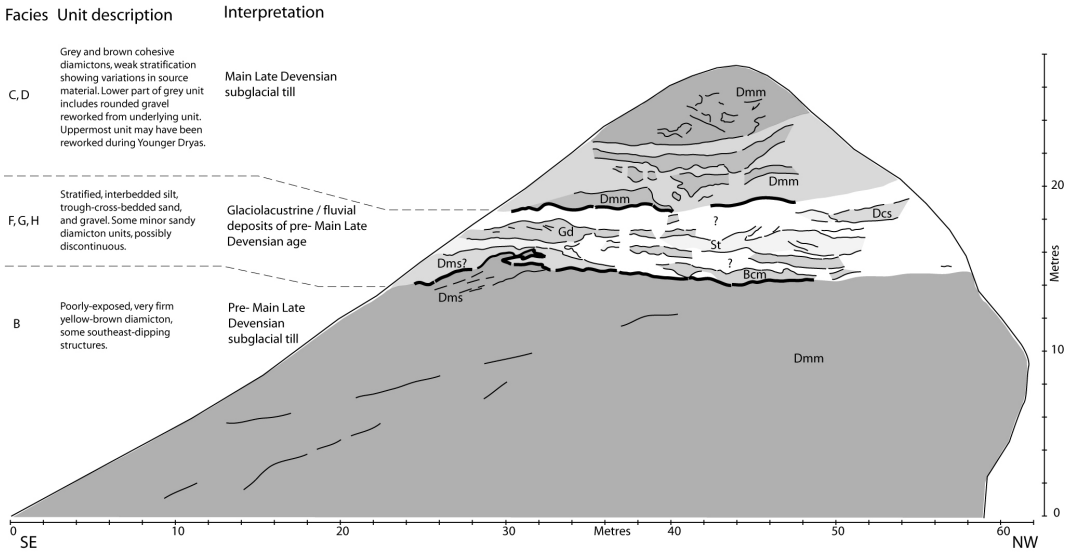

Figure 2.12: Sketch of exposure in Coire Chailein, traced from a photo-montage. Section reveals complex stratigraphy of diamictons (Facies B, C, D, F) interbedded with overridden gravel, sand and silt units (Facies G) and a 1m thick boulder bed (Facies H).

laminae or beds, and in upper Cononish Glen are overlain by Facies G fines. Elsewhere, such as in Balquhidder Glen, Glen Lyon, and Glen Falloch, Facies G is intercalated with laterally impersistent and variably thick diamictons of Facies F.

Facies occurence and spatial distribution

Figures 2.13A–C show, respectively, scaled logs of the principal exposures in the study area, inter-site correlation of units, and, based on these, the first composite glacial stratigraphy for the region. Note that in many cases there may be several units of the same facies present, representing a stratified deposit that records episodic deposition. In Figure 2.13A the logs are grouped according to the facies present at each locality in order to facilitate comparison. The horizontal 'baseline' divides deposits interpreted as Younger Dryas in age from those deemed older (cf. Table 2.3).

From Fig. 2.13A it is apparent that Facies A and B are each only found at one locality, in glens where their preservation suggests that former ice flow was oblique to the valley axis (Golledge, 2007a). In both cases the diamictons occur at the base of the preserved sequences, and are overlain by Facies C. The latter is more widespread than either Facies A or B, but its occurence is nonetheless restricted to isolated 'pockets', such as near Ben Glas, in Gleann nan Caorann, Gleann Auchreoch, Gleann a' Chlachain, Coire Thoin and Coire Chailein. Facies D is ubiquitous and is generally the dominant deposit in most glens.

Landform-sediment assemblages

Neither Facies A or B are associated with any characteristic topographic expression, but Facies C & D commonly form both smooth valley-side veneers and compose large, broad, ridges.

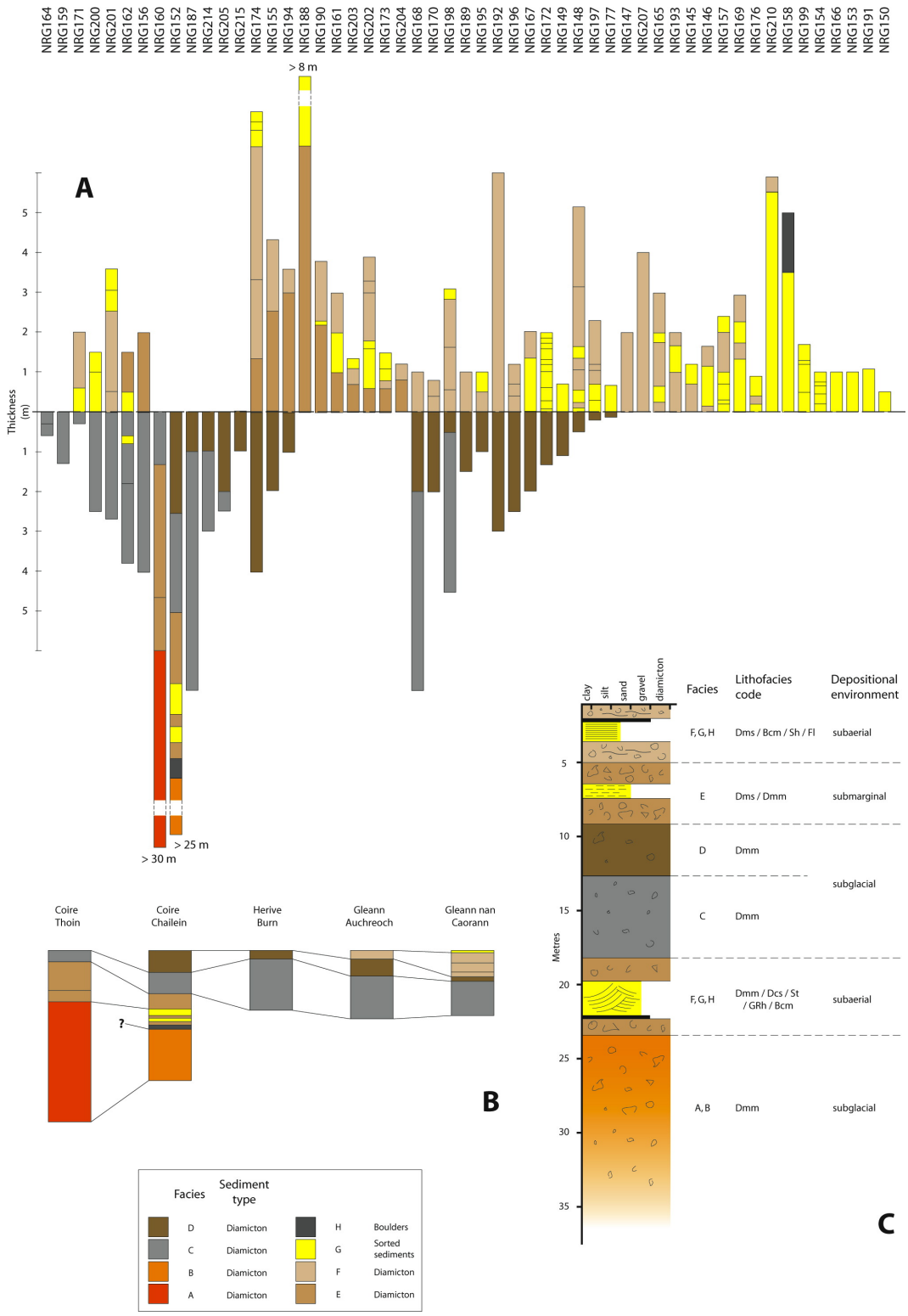

Figure 2.13: A: Compiled logs of sedimentary units at 53 localities in the study area showing the relative thickness of each facies type. B: Correlation of units between sites where the thickest sequences were recorded. C: Composite stratigraphy for the whole study area. Note that in A, sections NRG152, 160 and 188 are truncated to reduce overall length, and that the scale of logs NRG152 and NRG160 is reduced 50% to facilitate display and comparison with others. In C the vertical scale is approximate and intended to show typical unit thicknesses for comparison with each other. Grain-size depictions are intended to summarize key characteristics of the facies present.

Facies E drapes many of these larger ridges, and also composes irregular moundy spreads. The latter are often characterized by abrupt transitions from diamicton to fines, and in many cases exhibit complex faulting and folding. Whilst compositionally similar, Facies F tends to form distinct sharp-crested moraines, and thus the two facies can be differentiated on the basis of their landform-sediment assemblage and mapped separately. Since these moraines have important implications for reconstructing former glacier dynamics, they are considered in more detail below.

Moraines include all ridges interpreted to result from direct formation by glacier ice, whether their origin is primarily subglacial (e.g. ribbed moraine), or subaerial (e.g. latero-frontal moraine). Those in the study area can be classified into three types.

Type 1 moraines are typically broad-crested, relatively smooth features that may be $>$ 10 m high and 10's – 100's metres in length (Fig. 2.14). Some are bedrock-cored, and may show alignments similar to the structural trend of the underlying strata, for example northwest of Loch Tulla (Fig. 2.9B). Many Type 1 features, however, are largely composed of cohesive diamictons of Facies C and D, and may host superficial drapes of more friable Facies E or F diamicton, as well as one or two scattered boulders on their crests. The best examples of these moraines occur in an extensive sub-parallel suite that trends approximately west-east in an arcuate belt 2 – 3 km wide, at a height of 350 – 550m a.s.l. on the undulating plateau area south of Ben Lui and Beinn Dubhchraig (Fig. 2.9B). Landforms within this assemblage, particularly at the western and eastern margins of the plateau, show superimposed lineations that cross-cut or distort their 'parent' ridges. Suites of overridden or streamlined landforms also occur around Loch Easan (Fig. 2.9B) and Coire Eoghannan (Golledge & Hubbard, 2005).

Type 2 moraines are generally $<$ 10 m high and up to a few 10's metres in length, exhibit sharp crests, and are often arcuate across valley floors (Fig. 2.14). They are predominantly composed of stratified or interdigitated units of Facies F (sandy diamicton) and G (bedded or laminated clay, silt and sand). Contacts between units may be either conformable and planar, or erosive and irregular. In a number of cases small faults, thrusts or folds may be seen, reflecting low strain deformation. The most well-developed moraines occur at the east end of Cononish Glen (Fig. 2.9B). The abundant steep-sided mounds are typically concave on their north and northeastern sides, and where exposures exist, often exhibit generally southward-vergent glaciotectonic structures. Further west in Cononish Glen abundant moraines occur on the northern valley side, but not on the southern side. Again, vergence of glaciotectonic structures is to the south or southwest. Many of the valley floor moraines near the western end of the glen are composed of stratified diamictons whose architecture is consistently dominated by westward-dipping very clast-rich subunits. Gleann Auchreoch, a tributary of Glen Cononish, hosts well-developed moraines along much of its valley floor. Many of the other glens mapped host at least some Type 2 morainic landforms - other good examples can be seen in upper Auch Gleann, Coire Thoraidh, and Gleann a' Chlachain.

Type 3 moraines are boulder ridges (Fig. 2.14). These landforms are considerably less abundant than either Type 1 or 2 moraines, and are most prevalent in glens of the Beinn Chabhair – Ben More massif, south of Glen Falloch and Glen Dochart. In lower Coire Earb, for

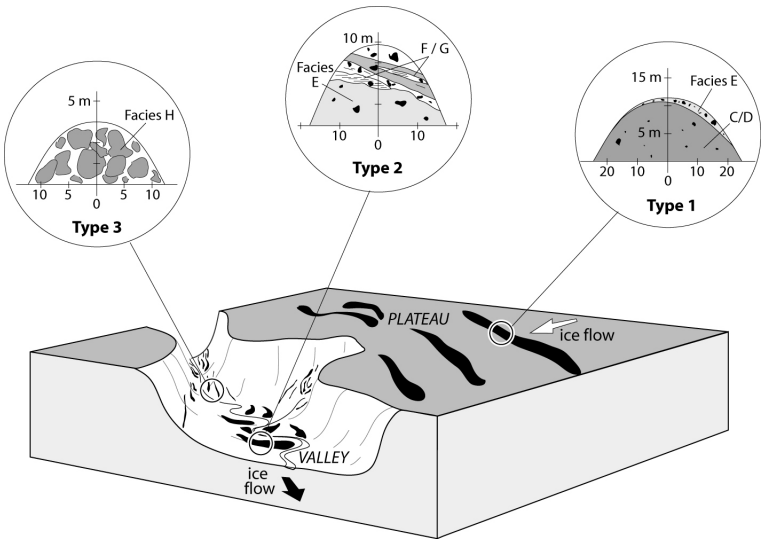

Figure 2.14: Moraine types and their typical geomorphological context in the study area. Annotations show generalised composition and approximate scale of features.

example, low boulder ridges < 5 m high descend the valley sides in arcuate nested groups that can be traced up-valley to the former glacier source area of Beinn a' Chroin. Type 3 moraines are predominantly composed of locally-derived large boulders, but may overlie diamictons of Facies D or incorporate units of Facies F or G.

Glaciofluvial and glaciolacustrine deposits (Facies G) rarely form distinct landforms in the study area, but bedded or laminated fine-grained sediments were often found on-lapping, overlying or intercalated with the morainic deposits. In Coire Chailein, Facies G silt and clay units are buried and have no surface expression. In most other cases, however, these sediments form flat terraces located in either intra-moraine areas, or are contiguous with moraines. For example, in Coire Earb Facies G sand and silt form a flat-topped gently north-sloping glaciolacustrine delta. Bedded sand was noted in two places in upper Glen Cononish: dipping south into the hillside north of Ben Oss, and dipping northwestward (up-valley) below Ben Lui. Glaciofluvial fans and terrace remnants were mapped in Glen Orchy, in Strathfillan, and near the head of Loch Lomond. Exposures in Strathfillan reveal southward-dipping bedded sand, and laminated silt and clay. Ice-contact glaciofluvial mounds were recorded near Bridge of Orchy and amongst the moraines at Dalrigh, distinguished by their well-sorted composition.

2.9 Interpretation: facies genesis

The accuracy of any glacier reconstruction depends to a large extent on the accurate interpretation of sedimentological and stratigraphic evidence in a landform-sediment and process-form context. Many recent studies have reviewed the common nomenclature of glacigenic sediments, and with varying scales of focus, have attempted to refine the theories on which genetic interpretations and facies classifications are based (Menzies, 1989; Benn & Evans, 1996; Krüger & Kjær, 1999; Piotrowski *et al.*, 2004; Menzies *et al.*, 2006; Evans *et al.*, 2006).The sedimentological character, stratigraphic relations and landform context of the bedrock features

and glacial sequences in the western Scottish Highlands are compared below with these studies, and where appropriate, with modern examples.

Although potentially classifiable as *'M' beds* (Menzies, 1989), *'deformation till'* (Benn & Evans, 1996), *'tectomict'* (Menzies *et al.*, 2006), or *'traction till'* (Evans *et al.*, 2006), Facies A – D are simply considered here to be of unspecified subglacial origin, for the following reasons: they contain predominantly subangular and subrounded clasts that are often striated, and have a silt and sand-dominated matrix showing a bimodal grain-size distribution. They are very firm in outcrop and closely resemble subglacial till observed at modern glacier margins (e.g. Fig. 2.15A). Facies E is similar in composition but is very poorly consolidated. On this basis it is interpreted as 'submarginal', that is, largely derived by reworking of underlying substrates by the glacier sole and by the addition of 'new' material melting-out subglacially, in a manner similar to that shown in Figure 2.15B. Although such deposits have relatively poor preservation potential compared to more consolidated substrates (Evans *et al.*, 2006), they are found in a number of locations in the study area (Fig. 2.13A). The presence of planar-bedded sand and silt inclusions within units of Facies E argues against these units having been pervasively deformed either during or after deposition (Piotrowski *et al.*, 2001).

The stratigraphic position of Facies A and B, together with their very limited preservation and, in the case of Facies A, the presence of clay minerals typical of long-term weathering (kaolinite), suggests that these sediments relate to a significantly earlier phase of glaciation than the one that deposited the more widespread units higher in the sequence. Although distinguished by slight colour differences, Facies A and B are likely to be the same unit, since they share many common characterisics (grain size, composition, mineralogy) and are stratigraphically equivalent.

Since Facies C has a silt and clay (rock flour) matrix and is very firm, it is interpreted as the product of bedrock erosion by plucking or micro-fracturing (*sensu* Hutter & Olunloyo, 1981). This process requires intimate ice-bedrock contact and only sufficient basal meltwater to facilitate sliding. Lower effective overburden pressures (whether due to more basal meltwater or thicker unconsolidated basal substrate) would have prevented such effective bedrock erosion. It is thus inferred that this high shear strength, low permeability grey till is the product of a thick, relatively cold-based, and hence slowly-moving ice mass that transported the material englacially (Fig. 2.15C & D).

Facies C and D are almost identical in terms of their structure, clast content, and composition, differing only in their matrix grain size and colour. They are never separated by intervening units and the colour contrast is often abrupt and, for example near Ben Glas (Fig. 2.9A), cross-cuts individual clasts. Metasedimentary bedrock underlies the majority of the field area and thus, even if changes in ice-flow direction and concomitant sediment provenance occurred, they would be unlikely to produce debris of significantly different colour. Since the colour change is seen to cross-cut individual clasts (Golledge, 2006), a plausible explanation may be that the red-brown colour of Facies D reflects a greater concentration of ferrous oxides, produced by post-depositional weathering. Facies C and D can thus be interpreted as pertaining to the same glacial advance, an inference supported by

interpretations of similar grey–brown till sequences in Canada (Hendry *et al.*, 1984), Sweden (Lagerbäck, 1992), Estonia (Rattas & Kalm, 2001), Denmark (Christoffersen & Tulaczyk, 2003) and England (Madgett, 1975; Madgett & Catt, 1978). These diamictons constitute many of the thickest and most widespread exposures in the area, and compose many of the large Type 1 moraines, consistent with deposition beneath a well-established and long-lived ice sheet such as the one known to have existed in Britain during the Main Late Devensian.

Facies E is widespread in its occurence, is spatially variable in its composition, and is generally less well-consolidated than the Facies D diamicton that it overlies. The presence of bedded sand and silt, conformably stratified within units of Facies E, suggest that these sediments were deposited by flowing water. The presence of well-rounded as well as angular cobbles indicates that debris was derived from both subglacial and supraglacial environments, whilst the lack of cohesion of Facies E suggests that effective ice overburden pressures were relatively small. Facies E may therefore have a complex and variable origin. It is likely that subglacial meltwater eroded and reworked the underlying till sheet (where present) (cf. Piotrowski & Tulaczyk, 1999), thus giving rise to conformable, and in some instances, transitional contacts between Facies D and E. This must have occurred subsequent to the emplacement of Facies D, and most likely can be attributed to recycling of the older deposits by the Younger Dryas ice cap. During this readvance, debris melting-out from englacial and subglacial transport (Fig. 2.15B–E) became superimposed on these saturated basal sediments, and were patchily intercalated with well-sorted material deposited from emerging subglacial streams. The high degree of sorting indicates sediment transport as suspended load in water of steady velocity, flowing either in well-defined subglacial channels or through a network of linked cavities. Sheet flow is considered unlikely given the inherent instability of such systems (Fountain & Walder, 1998). Laterally impersistant bedded sand bodies up to 1 m in thickness in Facies E lend support to the notion of low-pressure cavities, canals or lakes at the glacier bed, where decreased flow velocities enabled sediment deposition. Such features have been recorded in ancient till sequences elsewhere, for example in North America (e.g. Clayton *et al.*, 1989). Whilst compositionally similar to Facies F and G that overlie it, Facies E commonly exhibits primary sedimentary bedding and rarely shows convolutions and glaciotectonic deformation, suggesting a relatively passive depositional environment.

Marginal recession accompanying Younger Dryas deglaciation also led to deposition of material from supraglacial sources in the ice-marginal environment, where debris flows from the ice surface augmented deposits of ablated basal ice (Fig. 2.15F). These deposits are distinguished here as Facies F where they form Type 2 moraine mounds and ridges, comparable to those found at contemporary ice margins (Fig. 2.15G). These poorly-consolidated heterogenous deposits are commonly associated with retreat of the Younger Dryas ice cap in Scotland, albeit with interpretations of genesis ranging from melt-out of stagnant debris-rich ice to thrusting at the margins of actively retreating glaciers (see Lukas, 2005a,b, for a comprehensive review). Recent research tends to agree, however, that the abundance and close spacing of such moraine mounds are indicative of actively retreating, high mass-turnover ice that is close to equilibrium (Thorp, 1991a; Benn & Ballantyne, 2005; Benn & Lukas, 2006).

Widespread intercalation of Facies G with Facies F, commonly near the top of the strati-

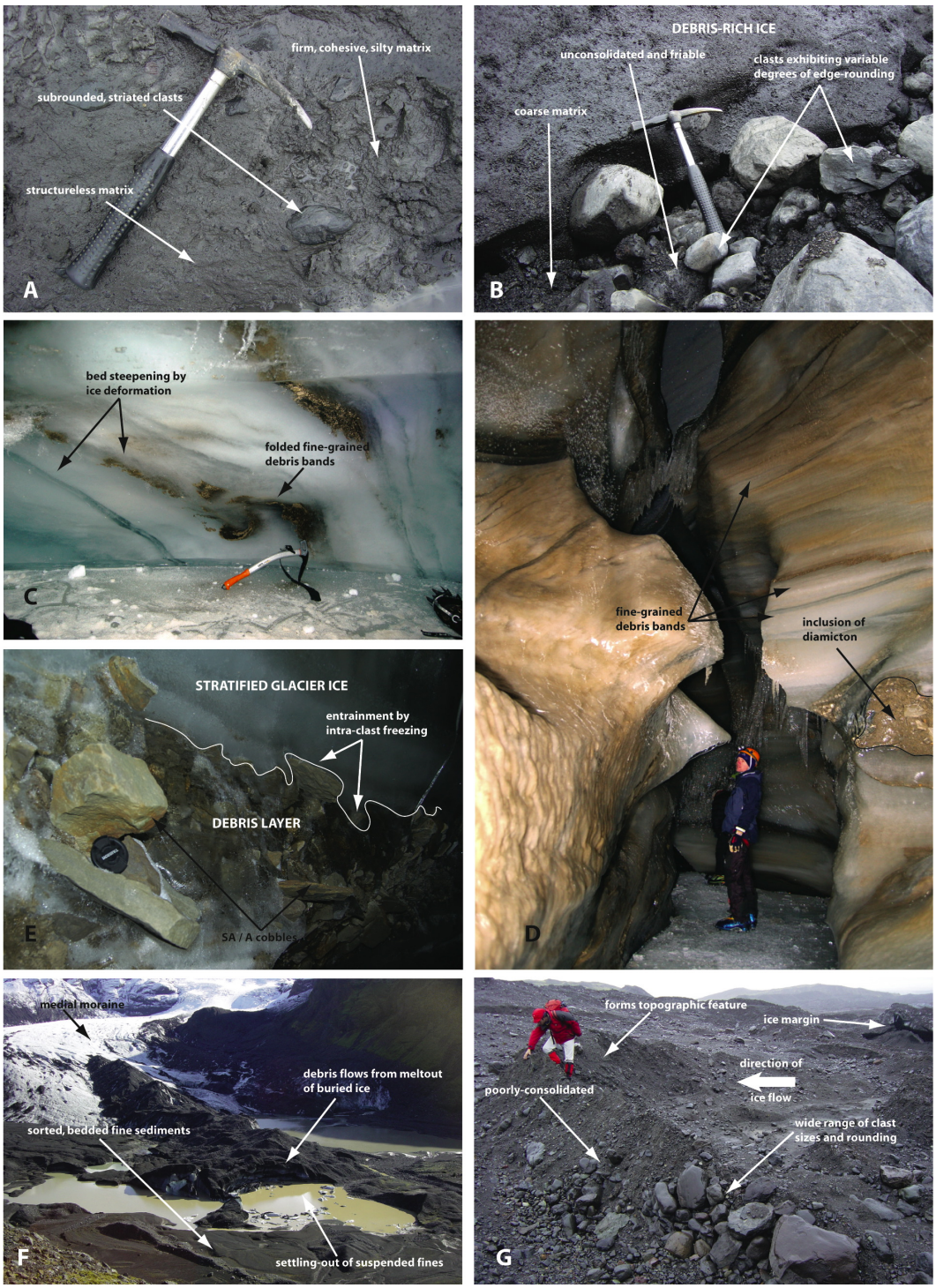

Figure 2.15: Examples of facies types, their various transport pathways and depositional environments at modern glaciers. A: Cohesive subglacial till exposed at the retreating margin of Solheimajökull, Iceland. B: Melt-out of subglacial debris from the sole of a retreating glacier, Solheimajökull, Iceland. Note the poor sorting and surface cobbles. C: Folded and attenuated fine-grained englacial debris bands, Longyearbreen, Svalbard. D: Fine-grained debris bands and pod of matrix-dominated diamicton probably incorporated subglacially, Longyearbreen, Svalbard. E: Angular debris band of coarse clasts and gravelly matrix buried supraglacially and incorporated into glacier ice, Longyearbreen, Svalbard. F: The very wet glacier foreland of Steinholtsjökull, Iceland, showing proglacial lakes, sandur, and debris-covered medial moraine. G: Recently vacated ice-margin position, marked by a moraine of poorly-consolidated diamicton, Svinafellsjökull, Iceland.

graphic sequence, suggests that ice-proximal deposition by glaciofluvial drainage was, at least initially, contemporaneous with ice-marginal debris flows. As sediment supply waned, however, probably as a result of ice margin recession, ice marginal ponds developed and accumulated the uppermost laminated and bedded sediments. Facies G in Coire Chailein, however, intervenes between subglacial till units. For this reason is suggested that it was deposited during an early phase of ice recession that enabled sub-aerial deposition of the trough-cross-bedded sand and stratified gravel unit, probably in a braided fluvial or ice-marginal glaciofluvial system prior to the Main Late Devensian glacial advance. This scenario is corroborated by preliminary results from luminescence dating of the sediments (Golledge & Robinson, 2007).

In summary, it is suggested that Facies A & B pre-date the Main Late Devensian glaciation, that Facies C & D are the subglacial product of the MLD glaciation, and that Facies E and surface occurences of Facies F were deposited by glaciers of the Younger Dryas readvance. Facies G & H occur at different stratigraphic levels within the sedimentary sequence and reflect depositional processes common to each glacial advance.

2.10 Discussion: Glacier dynamics in the western Scottish Highlands

The sediments and their stratigraphic relations described above enable a composite stratigraphy to be constructed for the first time in this area (Fig. 2.13C), and allow the following inferences to be made with respect to the evolution of ice masses and former glacier dynamics in the study area. Areas of scoured bedrock and the isolated cases of sediment preservation represent opposing end members of the erosion–deposition continuum, thus their respective distribution can be used to infer basal conditions beneath the ice.

That scoured or simply bare bedrock surfaces are widespread in the area indicates that, for the most part, the last ice to overwhelm the study area – the Younger Dryas ice cap (Golledge *et al.*, 2007) – was resting on a rigid bed and probably moved through meltwater-lubricated sliding (Hall & Glasser, 2003; Roberts & Long, 2005). The ice mass in these areas therefore did not flow on a thick deformable bed, and deposited relatively little substrate during its subsequent retreat. This is consistent with much of the field area occurring beneath the central portion of the former Younger Dryas ice cap. Ice-flow during this episode was instead accomodated in some areas through ice deformation (creep or shear) and meltwater lubrication at the ice – bed interface. Where ice deformation was the dominant process, flow would have been slow and largely non-erosive, governed mainly by the temperature-dependent creep rate of the ice. The presence of areal bedrock scouring, fluting of both bedrock and unconsolidated deposits, roches moutonnée, P-forms, and striae all indicate more rapid ice flow and at least some erosion of the bed, suggesting that some parts of the ice cap flowed by meltwater-lubricated basal sliding. This is known to have occurred elsewhere where streamlined bedrock features have been preserved (Glasser, 2002; Stoker & Bradwell, 2005; Roberts & Long, 2005).

Whether bedrock smoothing is partially inherited, isochronous, or time-transgressive is difficult to determine without, for example, cross-cutting striae. Thus it is not possible

from this evidence alone to determine the evolution of the basal thermal regime during the lifetime of the Younger Dryas ice cap, only that it must have been at least partially warm-based at some point, and probably most extensively during the warming period that accompanied deglaciation. This inference does not, however, preclude the very likely possibility that flow mechanisms evolved throughout the lifetime of the ice cap. The field evidence is, therefore, a time-transgressive assemblage that superimposes features pertaining to the last phase of glacial activity on a pre-existing, Main Late Devensian, landscape. The juxtaposition of scoured bedrock in some areas with preservation of older sediments in others suggests convincingly that processes operating at the glacier bed were spatially (and so probably also temporally) variable, such as is typical of glacial environments (Piotrowski *et al.*, 2004).

Sutherland (1993) asserted that, 'no deposits older than the Loch Lomond Stadial' are known in this part of the western Scottish Highlands, and thus the recognition of superimposed Main Late Devensian landforms, their constituent sediments, and the discovery of two sequences containing sediments that even pre-date the Main Late Devensian is particularly significant. Since these older deposits have not been removed, later ice flow in these parts of the study area must have been accomodated either through ice deformation, sliding, or by deformation of only a thin zone of the bed.

Deposition of Facies C, a rock-flour dominated subglacial till, reflects intimate ice–bed contact during the build-up of the Main Late Devensian ice sheet (Fig. 2.16A) which may have persisted until glacier sliding was inhibited, perhaps by extreme cold and increased aridity. Without high mass turnover the ice sheet may have become largely immobile in this area and probably frozen to much of its bed. Landscape preservation associated with former frozen bed conditions is widely reported from Scandinavia (e.g. Kleman, 1994; Kleman & Borgstrom, 1994; Kleman & Hättestrand, 1999), and thus may be an equally plausible scenario for this central portion of the former British Ice Sheet.

Deposition of subglacial till continued during deglaciation, but, as a result of higher velocity meltwater flow that preferentially removed silt and clay (Alley *et al.*, 1997), was characterized by a coarser matrix. This subsequently controlled downward migration of the post-depositional weathering front that produced the colour contrast that distinguishes Facies D. Areas of scoured bedock in the study area may partly have been produced by accelerating ice sheet flow and the presence of fast-flowing outlet glaciers during deglaciation, both catalysed by enhanced meltwater-lubricated sliding (Fig. 2.16B). Together with localised deformation of dilatant unconsolidated substrates, this led to dynamic lowering of the ice sheet surface.

Widespread preservation of sediments and the streamlining of Late Devensian landforms in the study area reflects the restricted basal erosion that took place during the Younger Dryas. This last period of glaciation also failed to deposit a distinct subglacial till of it own, instead reworking and remoulding older sediments. Lenses and beds of sand and fine gravel in Facies E record localised, possibly channelised, subglacial meltwater flow, and testify to limited deformation of the substrate following their deposition. The demise of the Younger Dryas ice cap is thought to have resulted from a rapid climatic amelioration that abruptly terminated the steady cooling of the early part of the stadial (Clapperton, 1997; Hubbard, 1999). Non-topographically aligned moraines in many glens provide convincing

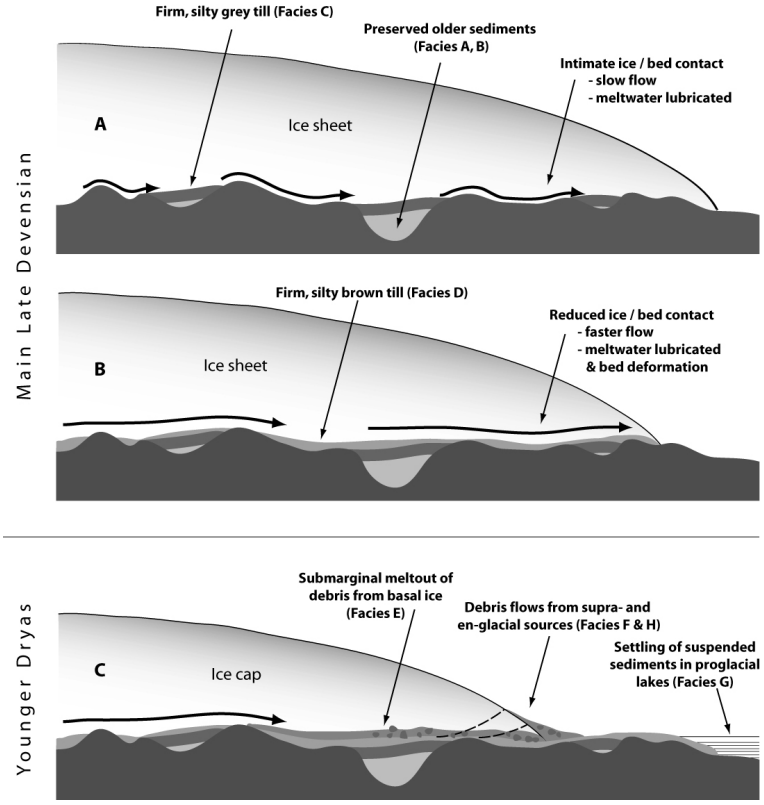

Figure 2.16: Conceptual model of the formation of the stratigraphic sequence described in the text. A: Advance of Main Late Devensian ice overwhelms topography and preserves pre-existing sediments only in topographic hollows. Intimate ice–bed contact produces rock-flour that is deposited as Facies C, grey subglacial till. B: Changes in the meltwater flux at the glacier bed during deglaciation lead to greater ice–bed separation and the deposition of the coarser-grained Facies D subglacial till. C: Younger Dryas glaciation reworks the upper substrate and adds new material via melt-out from the glacier sole (Facies E) and the emplacement of subaerial debris flows (Facies F). Ice-marginal lakes form in the warming climate and allow gradual settling-out of fine-grained suspended sediment (Facies G).

evidence that the ice mass decayed as a coherent ice cap in much of this area, most probably supporting a relatively steep marginal gradient that even during retreat was able to overwhelm topographic barriers (Golledge, 2007a). Glaciotectonic indicators in many of the moraines and intercalated outwash deposits attest to the dynamic nature of the retreating ice margin, even at this close proximity to its main source areas surrounding Rannoch Moor. To enable this, the warming climate must have been accompanied by sufficient precipitation to continually nourish the receding ice mass to a level adequate to significantly abate surface lowering.

That the uppermost units in many of the recorded sedimentary exposures show laminated or bedded fine sediments (Facies G) interdigitated with coarser diamictons (Facies F) may either reflect oscillations of the retreating ice margin, or climatically-controlled changes in meltwater and concomitant sediment flux.

Either way, the abundance of laminated fine-grained sediments in many of the glens indicates that final deglaciation took place in a very wet environment characterized by widespread ephemeral proglacial ponding (Fig. 2.16C). Poor connectivity between glacial and fluvial systems has been documented in Younger Dryas landsystems elsewhere in Scotland (Benn & Lukas, 2006), and may be equally applicable here. This is further supported by the relative paucity of glaciofluvial outwash deposits seen in the study area.

Final disappearance of ice from the study area occurred after 11.6 ± 1.0 ka BP (Golledge *et al.*, 2007), and may well have broadly coincided with the Younger Dryas climatic termination identified in ice cores at c. 11.3 ka (Alley, 2000).

2.11 Conclusions

Geological mapping, section logging and laboratory analysis has allowed a suite of eight distinctive glacial sediment facies to be identified. This has enabled, for the first time, a coherent glacial stratigraphy to be defined for part of the western Scottish Highlands that encompasses deposits spanning three glacial episodes. Widespread preservation of these sediments, and the landforms that they compose, indicates that former ice masses in this area were less erosive than previously envisaged, and that the present landscape constitutes a 'palimpsest' in which features of different ages are superimposed. When considered in their proper context, the landsystem elements indicate that glacier flow over a deformable bed was considerably more prevalent during the Late Devensian than the subsequent Younger Dryas, when instead ice movement may have been governed to a larger extent by meltwater-lubricated basal sliding. These new insights into the former behaviour of ice masses in the area enable better comparison with deglaciated landscapes elsewhere, and provide a testable model for future glaciological modelling experiments.

Chapter 3

Geomorphology and landform-sediment assemblages

3.1 Summary

The complexity of surviving landform-sediment assemblages in the western Scottish Highlands presents difficulties in their interpretation, particularly with regard to their relative age, genesis, and the style of glaciation that they reflect. With a view to accurately reconstructing the vertical extent of the Younger Dryas glaciers in an area north and west of Rannoch Moor, Thorp (1984, 1986) used detailed geomorphological mapping to identify 'trimlines' in the landscape, which were interpreted to reflect maximum former ice surface altitudes during the Younger Dryas. On this basis, Thorp (1984, 1986) reconstructed an extensive 'west Highland icefield' composed of relatively thin, interconnected, valley glaciers. This interpretation contrasted strongly with previous work that had inferred much thicker ice (Thompson, 1972; Horsfield, 1983), and quickly became accepted as the most plausible scenario. Other published work on the area is limited to publications of the Geological Survey for Rannoch and Black Mount (Hinxman *et al.*, 1923), and to overview papers such as those of Sissons (1979b, 1980) and Thorp (1991a). More recent mapping, focussing in particular on Glen Lyon and its surrounding mountains, identified a geological signature more compatible with higher ice surface altitudes than invoked by Thorp (1984, 1986), leading to a local reconstruction that bore close resemblance to previous numerical simulations (Hubbard, 1999; Golledge & Hubbard, 2005).

Differing interpretations of the surviving glacial landscape therefore exist. The following two papers describe new geological mapping aimed at addressing these divergent reconstructions, focussing at a regional scale that covers the entire study area. The first of these articles identifies a set of diagnostic criteria that may be applied to a landscape, in order that the character of its former glaciation may be most accurately defined. The article first describes the likely geological contrasts expected with differing scales of glaciation, from corrie accumulation to complete ice sheet cover. By assessing the relative differences, a 'landsystem' model is developed in which key elements are identified as indicative of relative thick and relatively thin ice cover. This is pertinent, since one of the chief uncertainties in the study area surrounds the former thickness of its glaciers.

By developing a landsystem model and applying it to the study area, the paper concludes that in much of the area, the geological evidence reflects thick ice cover typical of ice cap glaciation that overtopped topographic barriers. Evidence for valley glaciation is found only in the south of the study area, and is interpreted to have comprised numerous radial outlet glaciers fed from a central plateau icefield centred on broad mountain peaks. The reconstruction is important in that it proposes a new interpretation of the style of glaciation in this area, and by inference in the wider area.

The second paper takes many of the landsystem concepts and extends them (for example by sub-dividing different types of moraine), and incorporates sedimentological and stratigraphic data from the study area in order to assess the likely style of former glacier flow and the potential for subglacial erosion. The article describes the altitudinal transitions that occur on many of the mountains, identifying the chief characteristics of particular 'zones', and their significance for intepretations of former ice cover. Bedrock surfaces are widespread in the study

area, and can provide a considerably greater depth of information than simply whether or not they have been glacially smoothed. In some areas, coherent bedrock forms an end-member of a streamlined bedform continuum, within which are partially disaggregated rock outcrops whose drumlinoid form reflects glacial modification, but whose structure indicates only limited subglacial detachment. The alignments of these features reflect former ice flow directions. Ribbed moraine and elongate depositional glacial landforms are also mapped in the study area, principally from high-resolution relief-shaded digital elevation datasets, which, together with the characteristics of the bedrock features, enable inferences to be made concerning the overall surface slope of the glacier, as well as hinting at likely conditions at its bed.

The key findings of this article are that much of the landscape of the study area is 'palimpsest', and reflects the overriding of a Main Late Devensian topography by a Younger Dryas ice mass that was limited in its erosive capacity. The field evidence also helps constrain the altitude of former ice surfaces in this area, and, by identifying the abundance of both bedrock and other non-deforming substrates, indicates that the Younger Dryas ice in this area moved principally by meltwater-lubricated basal sliding, rather than by ice or bed deformation. Zones of greatest flow acceleration are inferred from the locations of streamlined bedforms to have occurred near the heads of topographic troughs.

PAPER III

An ice cap landsystem for palaeoglaciological reconstructions: characterizing the Younger Dryas in western Scotland

Nicholas R. Golledge
British Geological Survey, West Mains Road, Edinburgh, EH9 3LA, UK
and School of Geosciences, University of Edinburgh, West Mains Road, Edinburgh, EH9 3JW, UK.
ph: +44 131 667 1000, fx: +44 131 668 1535, email: n.golledge@bgs.ac.uk

Abstract

This paper reviews the contrasting behaviours of ice caps and icefields, defines a generic landsystem model that can effectively discriminate between them, and applies the model to landform-sediment assemblages in an area of western Scotland. Such a model is necessary, since many palaeoenvironmental inferences from formerly glaciated terrains are based on the geometry, extent and dynamics of reconstructed ice masses. The validity of these glacier reconstructions is dependent on the accurate initial interpretation of relict landforms and sediments, and their inter-relationships. A new landsystems model is presented here, in which individual geological and geomorphological elements are checked against a set of eight theoretical diagnostic criteria that characterize the style of former glaciation. When applied to a 1200 km^2 area of the western Scottish Highlands, the landsystem tool predicts 1) an extensive Younger Dryas ice cap with a maximum surface elevation of 900 m above sea level, implying colder or wetter conditions than previously thought, and 2) the survival of an independent mountain icefield in part of the area during deglaciation. Glaciological theory, proxy palaeoenvironmental data and established glacier-climate-topography relationships support these predictions, thereby giving credibility to the landsystem methodology as a generic tool for palaeoglaciological reconstructions.

KEYWORDS: Ice cap; landsystem; palaeoglaciology; reconstruction; Scotland.

3.2 Introduction

Considerable uncertainty and debate surrounds the nature of the former ice mass that developed on the western Scottish Highlands during the Younger Dryas (12.7 – 11.3 ka Alley, 2000), (cf Thompson, 1972; Horsfield, 1983; Thorp, 1984, 1986; Golledge & Hubbard, 2005). The contention rests on whether the ice formed a coherent, domed ice cap (e.g. Barnes ice cap, Baffin Island; Langjökull, Iceland), or was instead a mountain icefield characterized by interconnected valley glaciers (e.g. Breheimen, Norway; Harding and Juneau icefields, Alaska). Far from being a purely semantic argument, the difference between the two forms is manifest in behavioural contrasts that impact on the palaeoclimatological inferences drawn from postulated glacier reconstructions, and on the geomorphological evolution of formerly glaciated terrain. A requirement therefore exists for a tool that allows accurate appraisal of the style of former glaciation of an area. This tool may be coupled with standard inversion modelling techniques so that the landforms and sediments used in the latter are treated in the correct glaciological context. Where possible, mapped features in a study area should be compared with those typical of different types of glacial landscape, so that the most appropriate style of glaciation may be inferred. This article defines a set of broad criteria that enable differentiation between landscapes glaciated by ice caps and those glaciated by icefields. The methodology is then applied to a study area of 1200 km^2 in the western Scottish Highlands, in an attempt to resolve the existing icefield / ice cap controversy.

In order to identify the geomorphological and sedimentological criteria necessary for such a method it is important to appreciate the differences between the ice masses that produce them. Icefields and ice caps have been variably defined. Andrews *et al.* (1970) cite the definitions established by Ahlmann (1948), the American Geological Institute (1957) and the American Geographical Society (1958), in which icefields and ice caps are distinguished by size and by the relative relief of the ground on which they form. In their scheme an icefield covers less than 10 km^2 and occupies land of high relief, whilst an ice cap is greater than 10 km^2 in area and covers land of 'moderate' relief. Such definitions are rather simplistic, and their only concession to glaciological differentiation is in the assertion that ice caps flow outwards in all directions from a central area. A significantly more useful set of criteria are identified by Sugden & John (1976). They define an icefield as an 'approximately level', non-domed ice mass whose flow is influenced by the underlying topography, and an ice cap as consisting of two components – domes, and outlet glaciers. Outward flow from the central dome by creep or basal sliding is possible even where topographic gradients are low, as a result of the great thickness of ice and high driving stresses. Underlying bedrock rises may produce muted ice-surface bumps depending on their scale. Sugden & John (1976) emphasize that overlap may exist between icefield and ice cap morphology, and that the differences between a mountain icefield and a non-equilibrium ice cap may be hard to distinguish. In summarising many earlier ideas, Benn & Evans (1998) focus on the role of topography in their definitions: an ice cap will (at least in its central area) 'submerge the landscape' and will flow independently of bed topography. In contrast, an icefield does not possess a dome-like surface and its flow is influenced by underlying topography. Again, it is recognised that there are rarely clear distinctions between types of ice mass; instead they all lie along 'spatial and temporal continuums of form'. Given a suitable climatic regime, glaciers will grow from localised corrie glaciers into a single coherent ice sheet through various intermediate

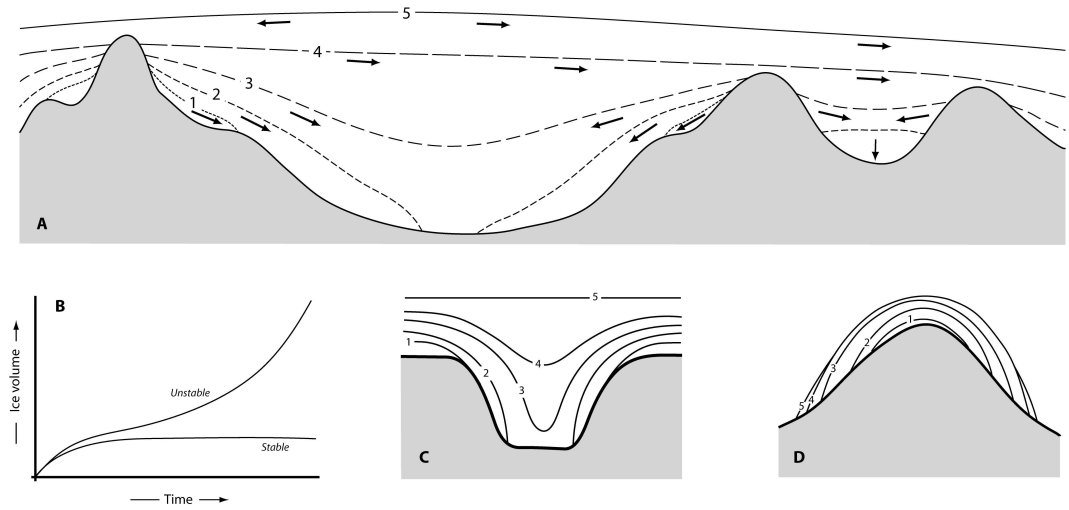

Figure 3.1: A. Schematic representation of glacier evolution from 1) corrie glacier through 2) valley glacier, 3) mountain icefield, 4) ice cap into 5) ice sheet. Note the lateral expansion in addition to vertical thickening, and the changing ice flow directions that may occur as the ice shed becomes increasingly independent of topography. B. The bifurcation in ice-mass evolution that results from large and small temperature depressions, leading to unstable and stable ice sheets respectively (adapted from Payne & Sugden, 1990). C & D. Contrasting growth of ice masses on different topographies (redrawn from Payne & Sugden, 1990).

forms (Fig. 3.1A). Different magnitudes of climate change produce bifurcations in the response of ice which appear to govern whether the ice mass evolves to a stable or unstable state (Fig. 3.1B). Ultimately these bifurcations are tempered by the nature of the underlying topography (Payne & Sugden, 1990) (Figures 3.1C & D).

There are several important glaciological and behavioural differences between thick ice caps and thinner icefields. A mountain icefield is, to a great extent, confined by topography, and will discharge towards lower ground along lines of least topographic resistance. In contrast, flow of an ice cap is governed by its surface slope, largely independent of bed topography (Glasser, 1997) (Fig. 3.1A). The thickness and surface slope of the ice significantly influence driving stresses, which in turn: control the velocity of ice flow (Weertman, 1973; Thorp, 1991b; Mitchell, 1994); influence the thermal regime of basal ice (Glasser, 1995; Glasser & Siegert, 2002); and in combination with the rheology and shear strength of underlying substrate, dictate the resultant mechanism of glacier flow (either internal deformation, meltwater-lubricated basal sliding, deformation of basal substrate, or a combination of all three). Ice geometry therefore significantly affects glacier dynamics, and consequently, different styles of glaciation will produce contrasting glacial landsystems (Benn & Evans, 1998; Evans, 2003c) (Table 3.1). In simple terms, icefield glaciers give rise to landforms that are generally concordant with topography because they tend to flow in the direction of land surface slope, and are constrained by the valleys they occupy. Icecap margins on the other hand are significantly less affected by topography and may therefore also produce landforms whose alignments are discordant with the land surface. When positive or negative mass balance perturbs steady-state conditions, valley glacier margins expand or recede respectively, that is, they are climatically sensitive. Large ice caps may exhibit longer response times, however, partly because their often higher surface altitude and greater ice surface area (and consequent albedo) enable them to modify local climate more effectively. This

may be achieved by creating greater orographic precipitation, lower surface air temperatures, and stronger katabatic winds.

3.3 The ice cap landsystem

In order to assess the style of former glaciation in an area and ensure the most appropriate inversion model reconstruction is produced, field evidence must be compared with geomorphological and sedimentological elements that together constitute idealized icefield and ice cap 'landsystems'. The landsystem concept has been around for almost a century (cf Eyles, 1983; Evans, 2003c) and in recent years has been increasingly applied to both modern and relict glacial environments, and has become widely accepted (e.g. Andrzejewski, 2002; Evans & Twigg, 2002; Kovanen & Slaymaker, 2004; Clark & Stokes, 2003; Colgan *et al.*, 2003; Evans, 2003b; Fitzsimons, 2003; Glasser *et al.*, 2003; Ó Cofaigh *et al.*, 2003; van der Wateren, 2003). In identifying areas of 'common terrain attributes' the glacial landsystem approach enables individual landform elements to be grouped into units, which when collectively linked to process-form models provide a powerful tool in palaeoglaciological reconstruction (e.g. Stokes & Clark, 1999; Evans, 2003c). Fundamental to this method of landscape assessment is the recognition that whilst climate, bed geology and topography largely influence the formation of glacial landforms (Colgan *et al.*, 2003), landsystem elements (and the units they make up) will also reflect both spatial and temporal differences in the behaviour of the ice mass that formed them. Thus, careful analysis of a landsystem can enable inferences to be drawn about the evolution of former ice masses, as well as their steady-state dynamics (Clark, 1997). Whilst Rea *et al.* (1998) and Rea & Evans (2003) provide comprehensive summaries of plateau icefields and their diagnostic landforms, and Evans (2003a) collates detailed descriptions of many other landsystem types, a holistic view of the landform-sediment assemblages typical of ice cap landsystems is lacking. A requirement therefore exists for a set of criteria, or landsystem, that accurately defines the landforms and sediments diagnostic of ice-cap style glaciation.

Given that the most apparent distinction between ice caps and icefields is in the degree of topographic control exerted on the direction of former iceflow, evidence that reflects non-topographic iceflow might be especially useful in identifying areas where ice cap glaciation has previously occurred. Such topographically unconstrained flow may be manifest in the geological record by preservation of any of the following:

1. Topographically discordant ice-marginal landforms, such as retreat moraines aligned across valleys obliquely or with their ice-contact slope on the down-valley side.

2. Areas of thick subglacial till and preservation of pre-existing deposits, particularly where ice has flowed obliquely across a valley or up a reverse slope, or across a col (Thorp, 1991a). In addition, the upper limit of till on steep valley sides where ice has flowed obliquely may be asymmetric, due to a predominance of lee-side cavity infilling on the up-glacier side and increased basal erosion on the down-glacier side.

3. Streamlined high-level cols where ice has overtopped local watersheds as a result of ice flow governed by surface slope rather than underlying topography. The streamlining may be evident in the presence of ice-scoured bedrock or streamlined glacigenic deposits (flutes or drumlinoid forms), or both.

Landsystem elements	Decreasing ice thickness / increasing topographic control →				
	Ice sheet	**Icecap**	**Icefield**	**Valley glacier**	**Corrie glacier**
Scale (approximate order of magnitude only)	>10 000 km^2	>1000 km^2	>100 km^2	>10 km^2	<10 km^2
Geometry	Domed accumulation area, with outlet lobes of variable gradient (particularly where marine terminating).	Mainly domed accumulation area, with relatively steep outlet glaciers.	Non-domed, approximately level accumulation area with low surface-slope outlet glaciers.	Elongate, with variable ice surface slope from accumulation area to margin.	Sub-circular, steep-sided, generally concavo-convex surface profile.
Ice marginal landforms and sediments.	Often offshore, at formerly grounded or calving margins.	Typically terrestrial, often in lowland areas. Deglacial features may be *discordant* with local topographic slope.	Typically terrestrial, often in lowland areas. Deglacial features generally *concordant* with local topographic slope.	Typically terrestrial, often in upland areas or fringes of lowlands.	Terrestrial assemblages in well-defined generally high-altitude topographic hollows.
Subglacial sediment deposition.	Often complete removal of pre-existing sediments in upland areas. Ubiquitous deposition of subglacial till.	Asymmetric deposition of till on valley sides. Accumulation of thick sediment sequences in valley floors, preservation of pre-existing deposits.	Erosion of pre-exisitng valley-floor deposits. Symmetrical valley-side till deposition.	Erosion of pre-existing valley-floor deposits. Symmetrical valley-side till deposition.	Erosion of pre-exisitng sediments, limited subglacial deposition, often bouldery supraglacial and ice-marginal deposits.
High-level cols and interfluves	Generally always overtopped and streamlined.	Often overtopped and streamlined, particularly in central areas.	Only streamlined at low altitudes and in central areas.	Rarely overtopped unless very low, more often act as barriers to flow.	Not applicable.
Pattern of local iceflow shown by kinematic indicators.	Determined by ice surface slope, irrespective of topographic slope.	Determined by ice surface slope, irrespective of topographic slope.	Typically parallel to major valleys and topographic lows. Generally follows slope of underlying land surface.	Always valley-parallel, following topographic slope.	Outward from the cirque backwall along lines of steepest topographic gradient.
Direction of flow of ice-marginal drainage.	Away from ice margins either with or against topography.	Away from ice margins either with or against topography.	Away from ice margins generally following topography.	Away from ice margins always following topography.	Away from ice margins always following topography.
Style of palaeo-iceflow of whole ice mass	Radial from a central dome or iceshed.	Predominantly radial from a central or local dome, or iceshed.	Only radial where unconfined, otherwise generally directed by major topographic features.	Always valley-parallel, following topographic slope.	Outward from the cirque backwall along lines of steepest topographic gradient.

Table 3.1: Summary of generalised physical, geomorphological and sedimentological characteristics – landsystem elements – for a range of ice masses of different scales.

4. Glaciotectonic structures and palaeo-iceflow indicators that attest to former ice flow against the topographic gradient.

5. Ice-marginal drainage where bedding suggests palaeoflow was against the modern topographic gradient, often forming ice-contact fans and resulting in ephemeral ice-marginal lakes or ponds in which laminated clay, silt and sand were deposited.

6. Streamlined and superimposed bedforms, striae, and erratic transport paths indicating predominantly radial outward ice flow from a central dome, irrespective of the trend of major valleys.

Whilst isolated occurences of the above may not be particularly instructive, their widespread presence may be diagnostic. Thus the greater the abundance and wider the distribution of such features, the stronger the case for ice cap glaciation. Where ice cap landsystem elements are either sparse or entirely absent, it can be inferred that topographic control was greater and that perhaps an icefield reconstruction is more appropriate. When a suitable reconstruction has been achieved, the overall size and geometry of the former ice mass should also be considered (Table 3.1).

The ice cap landsystem defined above can be regarded as a tool for palaeoglaciological reconstruction in the same manner as has been achieved elsewhere (cf Stokes & Clark, 1999; Evans, 2003c). Comparison of empirical field evidence with landsystem elements characteristic of particular styles of glaciation enable the most glaciologically plausible explanation for landscape formation to be derived. However, since ice-mass morphologies form continuums rather than distinct and separate entities (Benn & Evans, 1998) a degree of overlap may be expected. Additionally, it is rare for all elements of a landsystem to be present in every case (Stokes & Clark, 1999).

Presented here are the results of detailed geomorphological and sedimentological mapping at 1:10 000 and 1:25 000 scale in an area of the western Scottish Highlands, focusing on the landsystem elements pertinent to the ice cap / icefield debate. These data form the empirical foundation for a palaeoglaciological reconstruction of a 1200 km^2 study area, from the southern margin of Rannoch Moor at Black Mount to the head of Loch Lomond, and from Glen Lyon to Glen Orchy (Fig. 3.2). The area is characterized by dissected mountain ranges with peaks exceeding 1000 m in height rising from deep valleys, the lowest of which lie almost at sea level (e.g. Loch Lomond). The area was last glaciated during the Younger Dryas , or Loch Lomond Stadial (12.7 ka – 11.3 ka, Alley, 2000).

3.4 The Younger Dryas in western Scotland

3.4.1 Palaeoclimate

The rapid, high-magnitude transition to cold conditions that characterized the onset of the Younger Dryas (Dansgaard *et al.*, 1989; Alley, 2000; Brooks & Birks, 2000) depressed mean temperatures by up to 8°C in Scotland, and produced steep west-east and south-north precipitation gradients of 40 and 50% respectively (Clapperton, 1997; Hubbard, 1999). The climate of northwest Europe was highly unstable at this time (Witte *et al.*, 1998), and it is likely that the UK experienced more pronounced and varied effects of this climate transition than anywhere else in the Northern Hemisphere, as a result of its maritime location and the proximity of polar water (Sissons, 1979b). Snow-bearing winds from the south and south-west dominated the more vigorous atmospheric circulation of the stadial (Sissons, 1979b, 1980; Ballantyne, 2002). The combination of global temperature decline with migrating precipitation fronts brought about renewed glacial and periglacial conditions in Britain, possibly rejuvenating mountain icefields that survived the Windermere Interstadial (Clapperton, 1997; Bennett & Glasser, 1991). It is likely that glacier initiation occurred at different times in different places as a result of topographic variation, the 'snow fence effect' of mountain crests (Andrews *et al.*, 1970; Hulton & Sugden, 1997), precipitation differences, and the southward migration of the polar front (Sissons, 1979b). Glaciers were consequently larger in the west of Scotland than in the east (Sissons *et al.*, 1973). Using the dimensions and distribution of Younger Dryas glaciers in Scotland, Sissons (1979b) calculated firn lines, which closely reflect Equilibrium Line Altitudes (ELAs), (Porter, 2001). For the Rannoch Moor area firn line altitude was approximately 600 m a.s.l, declining to 550 m a.s.l over Glen Lyon and c. 470m a.s.l over the Beinn Chabhair - Ben More massif (Fig. 3.2). After reaching a maximal extent in c. 550 years (Hubbard, 1999), the ice mass is thought to have decayed in two phases - the first triggered by reduced precipitation, the second by rapid climatic warming (Dansgaard *et al.*, 1989; Benn *et al.*, 1992). Complete disappearance of the Younger Dryas ice mass by 10.6 – 10.4 ^{14}C ka BP is inferred from dated basal organic sediments on Rannoch Moor (Lowe & Walker, 1976).

3.4.2 Style of Younger Dryas glaciation

Recent work in part of the western Scottish Highlands has identified a mismatch between the widely accepted icefield reconstruction, largely based on the work of Thorp (1981, 1984, 1986, 1991b,a), and model predictions constrained by field evidence that suggest higher maximum

ice-surface altitudes typical of ice cap glaciation (Golledge & Hubbard, 2005). These more recent findings support previous research that similarly referred to the west Highland ice mass as an ice cap (e.g. Sissons, 1979b; Horsfield, 1983; Sutherland, 1984b; Payne & Sugden, 1990; Hubbard, 1999; Purves *et al.*, 1999), but are at odds with the views of other workers who worked further to the north (Thorp, 1984, 1986; Bennett & Boulton, 1993a) or further west (Ballantyne, 2002). For any given set of parameters (such as ice temperature, bed rheology, and glacier extent) that describe (or force numerical models of) the Younger Dryas ice mass in the western Scottish Highlands, a larger volume of ice is required for an ice cap rather than an icefield reconstruction (Golledge & Hubbard, 2005). As a result, the ice thickness in the central dome will be greater and the surface slope of the ice margins correspondingly steeper. The greater shear stress imposed by the thicker ice mass will ultimately give rise to higher strain rates and greater ice velocities (Weertman, 1973; Benn & Evans, 1998) in the ice cap outlet glaciers than in the icefield valley glaciers reconstructed by Thorp (1991b). In order to maintain these higher balance velocities an ice cap must experience correspondingly steeper accumulation – ablation gradients, an implication which may impact significantly on palaeoclimate inferences drawn from such glaciological reconstructions.

The differences in terminology adopted by the various workers may reflect little more than the spatial and temporal variation of the ice mass in each study area, however. Those concerned with the central portion of the ice mass may find evidence typical of ice cap glaciation during its maximal extent, whilst studies focussed nearer the ice margins – on purely deglacial field evidence or on independently glaciated areas away from the main accumulation area (e.g. Benn & Ballantyne, 2005; Benn & Lukas, 2006), – may lean more toward an icefield interpretation. In actuality, the ice mass likely evolved during its life from one form to another, leaving behind a complex geomorphological signature. The focus here is on the identification of geomorphological and sedimentological features that enable any area of a former ice mass to be critically appraised and accurately defined based on its nature at its maximal thickness and extent.

3.5 Study area

3.5.1 Existing model and previous literature

Topography has long been recognised as a major forcing factor in glacierization (e.g. Manley, 1955; Schytt, 1967; Andrews *et al.*, 1970; Ives *et al.*, 1975; Payne & Sugden, 1990; Glasser *et al.*, 2005), and thus the degree to which the topography influences the build up and evolution of an ice mass must be regarded with at least equal import as climate. It has been suggested that the topography of the western Scottish Highlands, where high mountains surround the relatively high-altitude plateau area of Rannoch Moor, significantly influenced the style of ice mass that evolved there during the Younger Dryas (Payne & Sugden, 1990). The study area connected the former accumulation and dispersal centre around Rannoch Moor with the southern glacier margins at Loch Lomond and Menteith, and, consequently, affected both the style and direction of former ice flow. Investigations in this area are therefore crucial to resolving ongoing differences of interpretation with regard to palaeoglaciological reconstructions.

Payne & Sugden (1990) favoured an ice cap scenario, but other studies have been more equivocal. Mapping by Thompson (1972); Horsfield (1983); Thorp (1984, 1986, 1987, 1991a), identified the relict glacial landforms, and to a lesser extent the sediments, of different parts of the western Highlands, and from these drew inferences about the size and dynamics of the former Younger Dryas ice mass. Thompson (1972) proposed a valley glacier reconstruction for the area around Glen Lyon, with individual glaciers sourced at altitudes > 900 m a.s.l. and flowing for the most part along the major valleys of the area. This interpretation was disputed by Horsfield (1983), who instead concluded that an ice cap with a maximum surface altitude of > 1000 m a.s.l. and centred on the Etive and Nevis mountains dominated the area. Working predominantly to the north and west of Rannoch Moor, Thorp (1984, 1986) found no evidence of the thick ice postulated by Horsfield (1983), but instead mapped periglacial trimlines to infer much lower ice surfaces. He reconstructed a low aspect-ratio icefield with icesheds no higher than 750 m a.s.l, drained by numerous fast flowing valley glaciers.

Recent research based on detailed geomorphological and sedimentological field mapping combined with numerical model predictions (Golledge & Hubbard, 2005) produced a reconstruction whose maximum ice surface altitude contrasts significantly with that of Thorp (1984, 1986). This latest interpretation proposed an ice cap with a maximum surface altitude of c. 900 m a.s.l., and with flow in its central area largely determined by its surface slope, rather than the underlying topography. The ice cap dome maintained a relatively steep surface in areas up-ice of its outlet glaciers, suggesting higher basal shear stresses than those proposed by Thorp (1991b).

3.5.2 New data

The timing of glaciation in the study area is bracketed by organic deposits buried beneath subglacial till at Croftamie, southeast of Loch Lomond, suggesting a maximum glacier extent at 10, 560 ± 160 ^{14}C ka BP (Evans & Rose, 2003), and inferred ice-free conditions on Rannoch Moor by 10, 660 ± 240 – 10, 390 ± 200 ^{14}C ka BP (Lowe & Walker, 1976). Although the dates from Rannoch Moor may be 'too old' (Sissons, 1979b), the Croftamie dates nonetheless imply that the Younger Dryas ice reached its maximum southerly extent very late in the Stadial, and that subsequent deglaciation was very rapid indeed.

Landforms and sediments in the northern sector of the study area (Fig. 3.2) have been described elsewhere (Golledge & Hubbard, 2005), and consequently are only summarised here. There is a marked within-valley asymmetry in the distribution of moraines in the northern sector, unrelated to differential rockfall input (*sensu* Benn, 1989), and in many cases the moraines are aligned obliquely across valley floors. Thick accumulations of subglacial till are preserved only in localities where ice flowed against the topographic gradient; within-valley asymmetry of till cover is particularly prominent in e.g. glens Lochy and Lyon. A number of high-level (> 700 m a.s.l) cols show evidence of glacial streamlining indicative of transfluent ice flow, and glaciotectonic structures and sedimentary bedding in glaciofluvial sediments are consistent with radial iceflow from Rannoch Moor. Striae, roches moutonnée and erratic carry also indicate non-topographically constrained iceflow in a broadly radial pattern consistent with a major iceshed to the northwest.

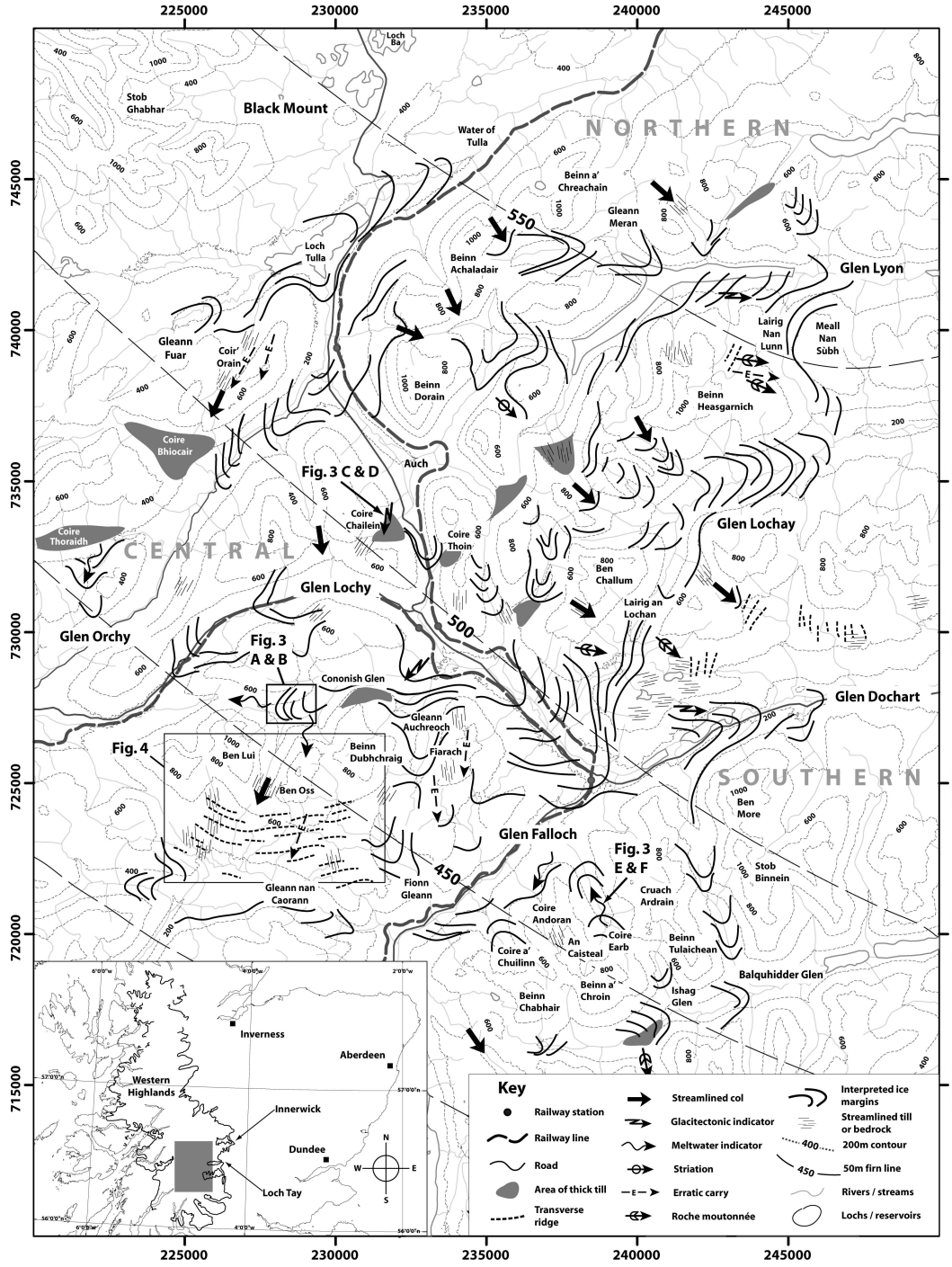

Figure 3.2: The study area in western Scotland, showing generalized distribution of the key landsystem elements, localities described in the text and the approximate locations of detailed examples given in Figures 3.3 & 3.4. Firn lines are interpolated from a grid built from the contours of Sissons (1979b, 1980). Inset shows the location of the study area in Scotland, the extent of Younger Dryas glaciation (Sissons, 1980), and localities mentioned in the text beyond the study area. Scale given by 5 km British National Grid ticks (main map), and Lat / Long lines (inset). OS topography © Crown copyright. All rights reserved.

Recent mapping south and west of this area has identified abundant ice-marginal landforms (predominantly moraines), for example in Cononish Glen where they trend obliquely across the valley sides and valley floor, that is, generally discordant to the local topographic slope. Two large lateral moraines steeply descend the hillsope at the western end of the glen (Fig. 3.3 A, B) and are aligned with valley-floor moraines to form cross-valley ice-marginal assemblages. There is a high density of moraines in much of Cononish Glen, and many of the individual diamicton and sand and gravel-composed mounds are 5 – 10 m in height with complex internal stratification. Some areas of the glen, however, are devoid of moraines. Neighbouring Glen Auchreoch hosts numerous morainic ridges that, although concordant with topography in terms of their cross-valley alignments, display steep ice-contact slopes on their northern (down-valley) sides. Sections in the moraines prove their composition to be stratified ice-contact debris flows and bedded sand and gravel, a characteristic of Younger Dryas moraines elsewhere in Scotland (Lukas, 2005b; Benn & Lukas, 2006). Another high-density area of topographically discordant moraines exists in Lairig an Lochain (Fig. 3.2) where the ice-marginal landforms (moraines and associated meltwater channels) form sub-parallel linear assemblages descending obliquely across the valley floor. The most abundant moraines in the study area, however, occur in the undulating plateau area south of the Ben Lui - Beinn Dubhchraig watershed (Fig. 3.2). Here a sub-parallel assemblage of broad moraine ridges trend approximately west-east in an arcuate belt 2 – 3 km wide at a height of 350 – 550m a.s.l. Many of these ridges are overprinted with approximately north-south aligned lineations, or show evidence of remoulding (Fig. 3.4). The larger, 'parent', moraines undergo a transition up to 700 m a.s.l into bedrock ridges of the same orientation.

Distribution of till in this central area is highly variable both in spatial extent and in terms of its thickness. Many of the valleys (e.g. upper Glen Orchy) have only thin valley-floor till cover, whereas others (e.g. Coire Chailein, Coire Thoin, Coire Bhiocair, Glen Auchreoch) host till accumulations up to 35 m thick. In Coire Chailein, Coire Thoin and Gleann nan Caorann a distinct cross-valley asymmetry of infill is apparent. In these valleys, till occurs significantly higher on one side of the valley than the other. Complex stratigraphies are present in the Coire Chailein and Coire Thoin valley infills, representing more than one period of sediment deposition. In Coire Chailein c. 6 m disturbed but bedded gravel, sand, silt and clay separates a 13 m thick lower sand-dominated yellow-brown till from an upper 8 m thick silt- and clay-dominated grey and brown till. In Coire Thoin the grey till abruptly overlies a reddish sandy diamicton that when subjected to X-Ray Diffraction (XRD) analysis yielded a strong peak consistent with the presence of kaolinite, a clay mineral weathering product whose abundance in a deposit increases with age.

Streamlined high-level cols in this central area attest to the prevalence of transfluent ice in many areas. Transfluent flow is indicated by ice-smoothed cols south of Ben Challum (650m), and between Ben Lui and Ben Oss (690m), (Fig. 3.2). In these cases glacial streamlining is manifest as ice-smoothed bedrock with few loose frost-shattered surface blocks. Elsewhere, streamlined cols host drumlinoid ridges or flutes (e.g. around Coir' Orain and above Coire Chailein). These ridges are variably composed of diamicton, boulders, and / or disaggregated bedrock, and in most cases range in height from 2 – 5 m. Deformed sedimentary structures

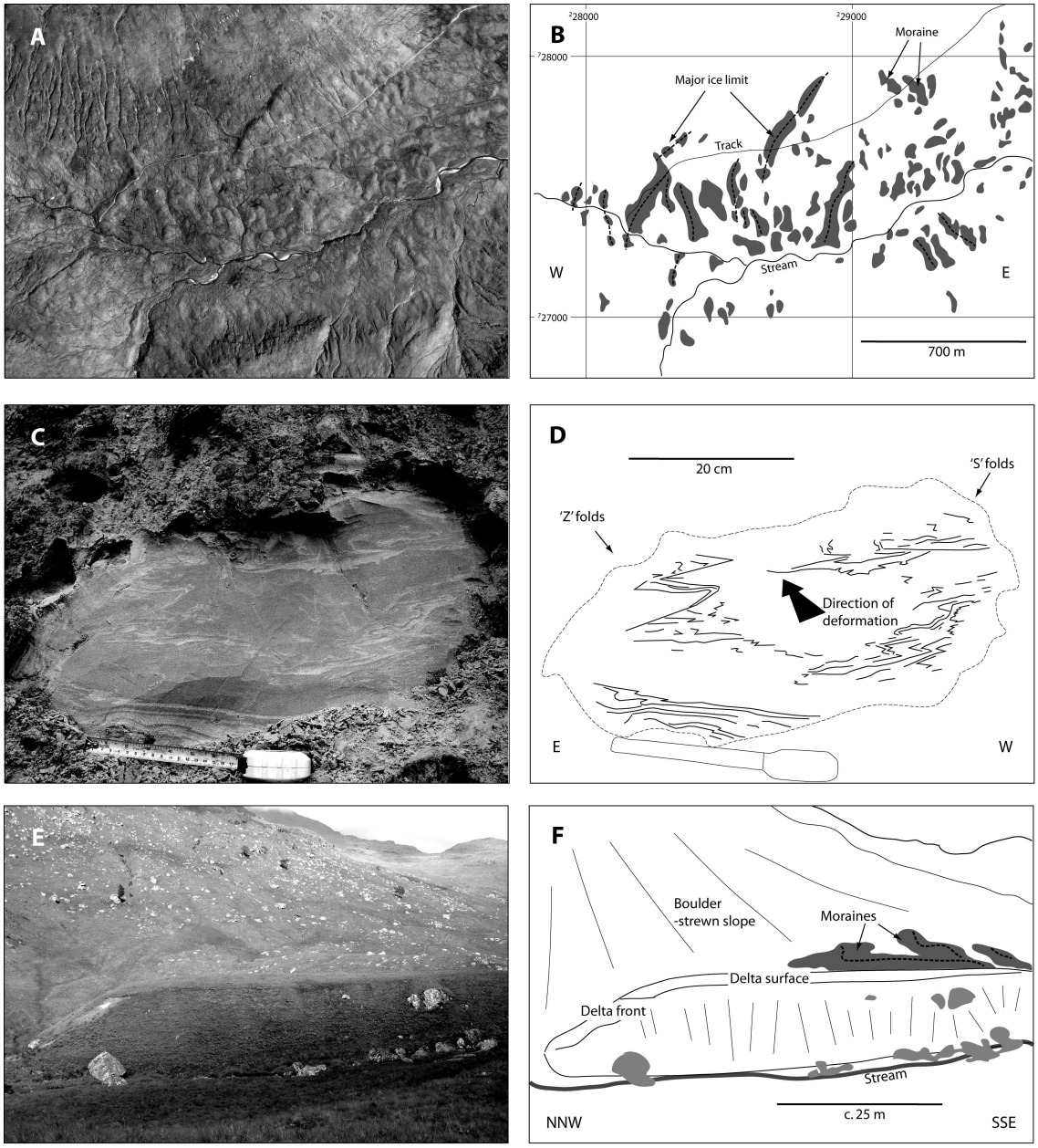

Figure 3.3: Examples of geomorphological and sedimentological elements of the ice cap landsystem: A & B, topographically discordant moraines in Cononish Glen showing still-stand positions and intervening, more chaotic, recessional moraines; C & D, bedded sand exhibiting sheath fold with southerly vergence, Coire Chailein; E & F, glaciolacustrine delta concordant with topographic slope, Coire Earb. Note the gently sloping surface and steeper delta front. Orthorectified aerial photograph in (A) © NERC, 2006, from original image © Royal Commission on the Ancient and Historical Monuments of Scotland (RCAHMS). Photos (C) & (E) BGS registered photographs, © NERC, 2006.

preserved in a 1 m thick sand, silt and clay unit in Coire Chailein resemble a sheath fold, which, when carefully dug out, showed southerly vergence (Fig. 3.3 C, D). Elsewhere, minor silt and sand units within or associated with moraines often show glaciotectonic folding or faulting. Exposures in Cononish Glen and Gleann Auchreoch reveal abundant evidence of post-depositional sediment deformation (folding and faulting) typical of actively oscillating ice margins. The vergence of these deformation structures is shown in Fig. 3.2. Evidence of non-topographically directed sub-aerial deposition of bedded sand and gravel at former ice margins is preserved in the central sector of the study area in e.g. Coire Thoraidh and Cononish Glen. Exposures on the lee side of a moraine in Coire Thoraidh proved steeply southwestward-dipping foreset-type beds of alternating sand, gravel and diamicton. In Glen Cononish, well-sorted sand beds flanking a low moraine exhibited an approximately 10° west-northwestwards dip; counter to the local topographic slope. Also in Glen Cononish proglacial sand and gravel outwash was recorded dipping southward into the hillslope below Ben Oss.

Patterns of former high-level iceflow can be inferred from erratic transport paths. Southerly iceflow across a NW-SE aligned mafic dyke crossing the summit ridge of Fiarach (Fig. 3.2) produced long erratic trains (> 1km) along the wide summit ridge to the south-southwest. Sub-rounded boulders of coarse-grained granite up to 2 m diameter were recorded on moraines south of Fiarach, below Cruachan Cruinn col (492m). Granite is found in situ only to the north, underlying Rannoch Moor, and to the southwest from the head of Glen Fyne to Garabal Hill. Metalimestone erratics from the southern flanks of Ben Oss also show generally southerly transport across the wide plateau.

South of Glens Dochart and Falloch, the Ben More - Ben Chabhair massif hosts a landform-sediment assemblage that contrasts distinctly with those described above. Moraines in this area are numerous but generally restricted to valley floors and lower hillslopes. At the northern end of Coire a' Chuilinn (Fig. 3.2) latero-frontal moraine ridges arc across the valley, indicating that ice lay to their southeast. The ridges are typically < 10 m high and fragmentary. At the northwest end of Coire Andoran is a > 10 m high morainic bank composed of stratified debris-flow diamictons and capped with southwest-dipping cross-bedded sand and gravel (> 1 m thick). Few other features were observed further south. Topographically concordant, low, arcuate, bouldery spreads and cross-valley moraines also occur along the length of Coire Earb, indicative of active south-southeastward ice margin recession. Many of the moraine crests are strewn with angular blocks of local metasedimentary lithologies 2 – 5 m diameter. On the southern side of the massif, topographically-concordant cross-valley moraines occur in Balquhidder Glen and Ishag Glen (Fig. 3.2). Thick till was mapped in limited parts of Balquhidder Glen but in none of the tributary valleys, and no asymmetry in valley-side till cover was observed. Rather, many of the glens showed a notable absence of till on all but the lowest slopes (e.g. Coire a' Chuilinn and Coire Andoran). The floors of these glens, particularly in their upper reaches, are dominated instead by ice-scoured bedrock and ubiquitous locally derived, angular, rockfall boulders.

Ice-smoothed bedrock is abundant at higher altitudes across the massif, but can be misidentified due to the naturally smooth mica-rich sub-horizontal metasedimentary bedding planes. Distinction can be based instead on the relative abundance of frost-shattered surface debris, or where smoothing contrasts can be identified within the same lithology over small

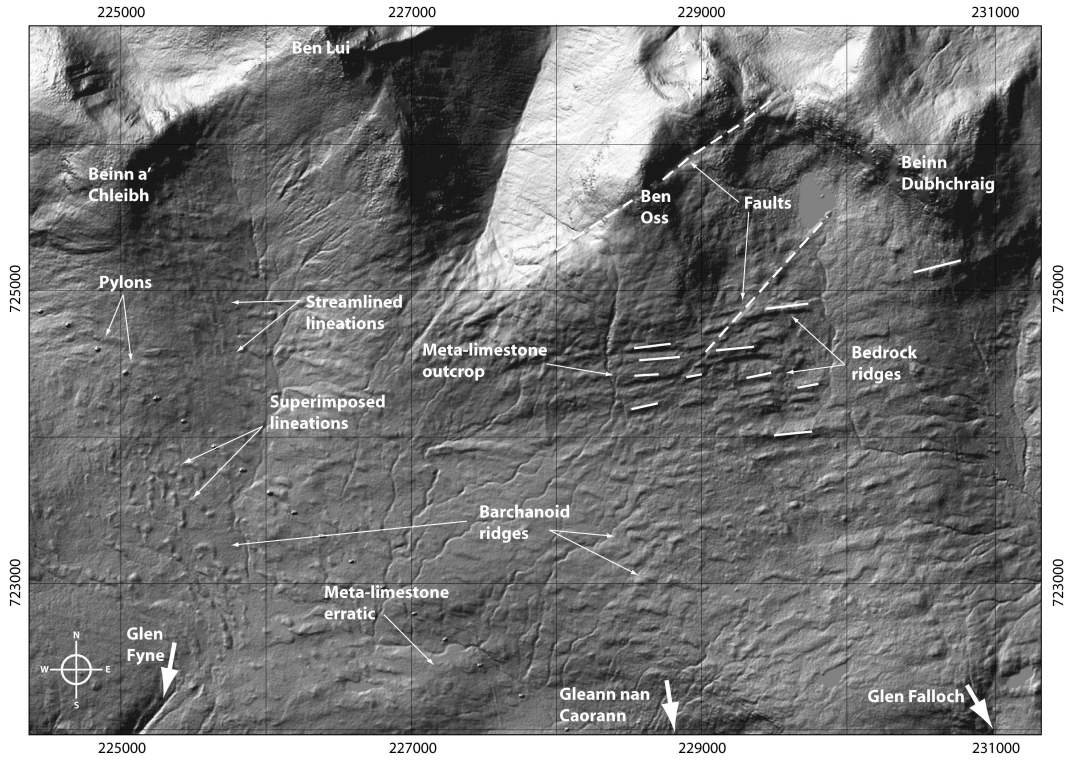

Figure 3.4: Relief-shaded digital terrain model (DTM) of the plateau area south of the Ben Lui – Beinn Dubhchraig massif, showing streamlined bedrock, remoulded (barchanoid) ridges, and superimposed bedforms composed of subglacial diamicton. Thick arrows indicate direction of former ice flow via outlet valleys, based on the orientation of the bedforms and the direction of local erratic carry. DTM built from Intermap Technologies NEXTMap 1.5 m resolution topographic data. Scale given by 5 km British National Grid lines at 1 km intervals.

Landsystem element(s)	Northern Sector	Central sector	Southern sector
Scale (approximate order of magnitude only)	>1000 KM^2	>1000 KM^2	>10 KM^2
Geometry	CENTRAL DOME & OUTLET GLACIERS	CENTRAL DOME & OUTLET GLACIERS	VALLEY GLACIERS SOURCED FROM SUMMITS
Topographically discordant ice-marginal landforms	YES	YES	NO
Localised thick till accumulations, preserved sequences, asymmetric valley-side till cover	YES	YES	NO
Streamlined high-level cols	YES	YES	YES
Counter-topographic palaeo-iceflow indicators	YES	YES	NO
Counter-topographic flow of ice-contact fan sediments	YES	YES	NO
Collective evidence of radial ice-flow	REGIONAL	REGIONAL	LOCAL

Table 3.2: Character, presence or absence of each of the eight key landsystem elements in the study area.

areas. Northeast of Cruach Ardrain for example, ice-smoothed rock occurs up to 930 m but no higher. The north flank of Ben More exhibits a vertical transition to fractured, frost-shattered rock around 860 m; the 862 m col and rock surfaces up to 930 m between Ben More and Stob Binnein are similarly smoothed, but their summits at 1174 m and 1165 m, respectively, exhibit thin regolith mantles over frost-shattered bedrock. No glaciotectonic deformation was observed in sediments in the southern area. However, clear evidence of topographically concordant ice-marginal drainage exists in Coire Earb where a flat-topped, gently northwest-dipping (down-valley) terrace is preserved (Fig. 3.3 E, F). The up-valley margin of the terrace is contiguous with a well-developed cross-valley moraine, and a section in the distal end proved it to be composed of bedded sand and laminated silt. Its location in the middle of the valley floor, but significantly higher than any fluvial terraces in the glen, suggests that the terrace may have a glaciodeltaic origin.

In summary, the landsystem elements in the northern and central sectors of the study area comprise moraines aligned obliquely across valleys; preservation of older deposits and localised thick accumulations of till; streamlined high-level cols; and glaciotectonic and ice-marginal sedimentary structures indicative of non-topographically controlled ice and meltwater flow. By contrast, landsystem elements in the southern area indicate topographically concordant moraines; limited till deposition; bedrock smoothing at variable altitudes and ice-marginal meltwater flow that was governed primarily by topographic slope.

3.6 Testing the landsystem model

The above examples illustrate that a variety of landform-sediment assemblages are present in the study area of the western Scottish Highlands. By comparing the distribution and abundance of individual landsystem elements with the theoretical criteria defined above an assessment of dominant glaciation style can be made for each sector of the study area (Table 3.2).

It is apparent that whilst the northern and central areas exhibit key similarities, the southern sector is markedly different. The maximum altitude of widespread streamlined bedrock decreases southward and southeastward from Rannoch Moor but rises abruptly south of Glen Falloch. Thick till accumulations and preserved sedimentary sequences are

present north of Glen Falloch but absent further south. Deglacial landsystem elements such as moraines and ice-marginal glaciofluvial sediments reflect non-topographic large-scale radial ice flow in the northern and central sectors of the study area, whilst those in the southern sector are topographically-concordant and show only small-scale radial ice flow. On the basis of the landsystem evidence it is therefore proposed that the northern and central sectors were overwhelmed during the Younger Dryas by an ice cap flowing radially from Rannoch Moor and the surrounding mountains. During deglaciation the ice cap thinned and retreated actively back to its source area, maintaining margins steep enough in some areas to form topographically discordant landsystem elements. By contrast, the mountains in the southern sector may have acted as a subsidiary accumulation centre of the ice cap at maximum extent, which separated from the main ice cap during deglaciation and survived as a mountain icefield feeding topographically constrained outlet glaciers. This hypothesis can be tested by theoretical reconstruction of the former ice surface.

Field mapping has already enabled accurate constraint to be placed on the upper limit of ice in the northern sector of the study area (Golledge & Hubbard, 2005). The same methodology is adopted for the central and southern sectors, enabling ice surface contours to be constructed along flowlines based on the empirical data and constrained by equations for theoretical parabolic profiles (Nye, 1952; Paterson, 2000). The overall geometry of the ice mass between flowlines is then approximated and guided by previous reconstructions (e.g. Horsfield, 1983) (Fig. 3.5). Digitised ice-surface contours were used to generate a triangulated ice cap surface using ArcGIS 9.0, from which a 3D surface grid was interpolated. Raster subtraction of the topographic surface from the ice cap grid allowed ice thicknesses and the location of nunataks to be checked quickly and accurately. These methods also allow basal shear stresses to be calculated, using:

$$\tau = \rho g h \sin \alpha \tag{3.1}$$

where ρ is the ice density (900 kg m^{-3}), g is gravitational acceleration (9.81 m sec^{-2}), h represents ice thickness (m), and α is the ice surface slope (Paterson, 2000). Applying Equation (3.1) to centre points of Glen Orchy, Glen Falloch / Loch Lomond, and Glen Lyon yields, respectively, values of τ = 30 – 50 kPa; 45 – 60 kPa; 50 – 80 kPa.

Importantly, the feasibility of the local ice centre in the southern sector can be tested using the summit breadth vs height relationship defined by Manley (1955). The curve defines the non-linear inverse relationship between mountain or plateau summit breadth and the height above the firn line (or ELA) at which snow can be expected to accumulate. When the breadths of major summits in the Beinn Chabhair - Ben More massif are plotted against height relative to the local ELA (435-505m a.s.l., Sissons, 1979b), five of the seven summits could theoretically support snow accumulation during the Younger Dryas (Figure 3.6). Geomorphological evidence indicates, however, that whilst many of the summits may have accumulated snow, their ice-cover was probably thin, cold-based and non-erosive (cf Kleman, 1994; Rea *et al.*, 1998; Rea & Evans, 2003). Nonetheless, the concordant moraines and glaciodeltaic sediments suggest that accumulation on these summits was at least sufficient to nourish a local mountain icefield which remained active following recession of the Rannoch Moor ice cap.

The sensitivity of this mountain icefield to climatic changes typical of a warming deglacial

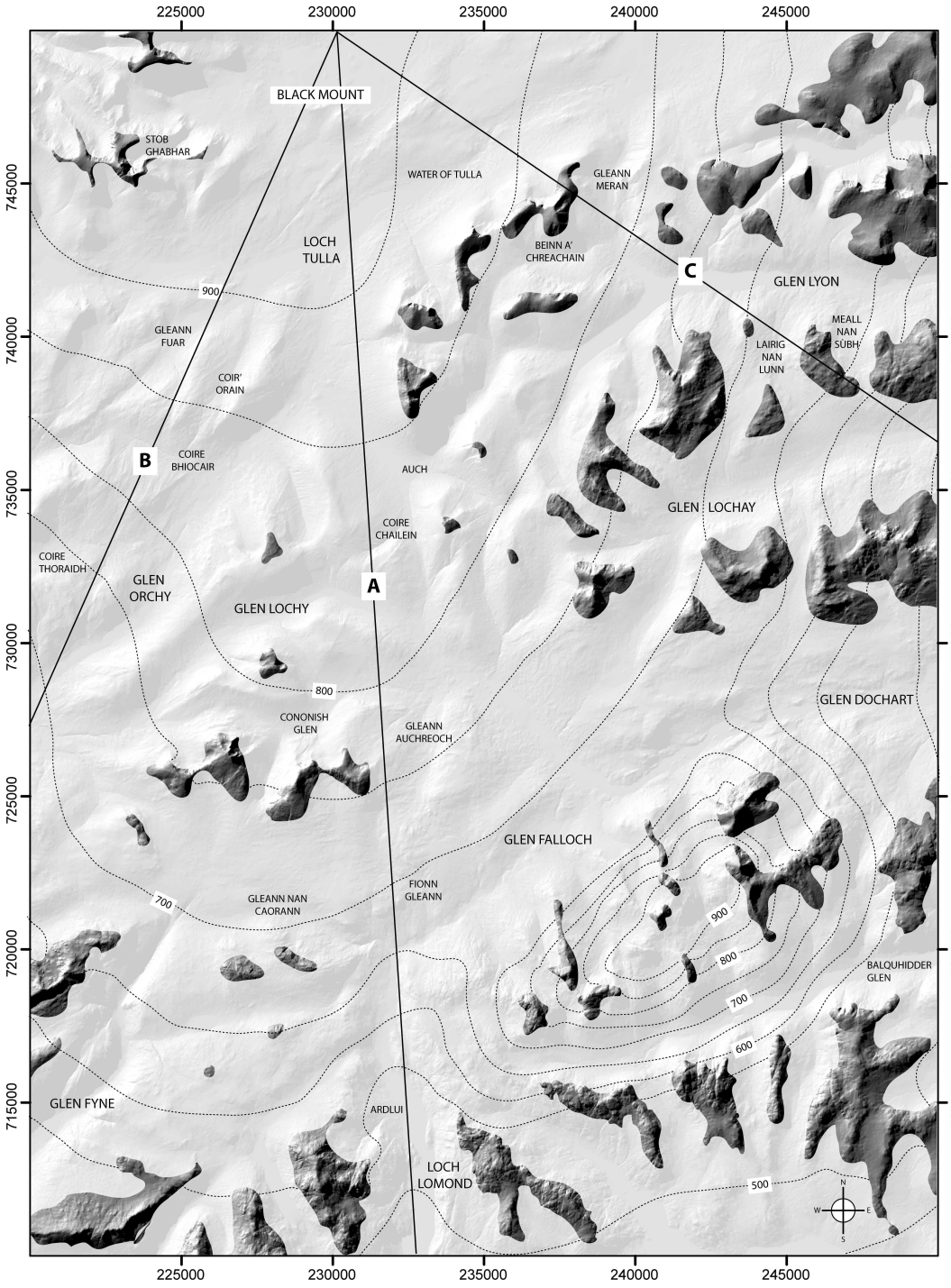

Figure 3.5: Palaeoglaciological reconstruction of the Younger Dryas ice cap in the study area, based on the field data summarized in Fig. 3.2. The hillshaded digital terrain model illustrating bed topography and nunataks was built from Intermap Technologies NEXTMap 1.5 m resolution topographic data. Lines A, B, and C locate the cross-sections shown in Fig. 3.7. Nunataks probably supported snow cover and may have hosted thin, immobile ice not represented here. Scale given by 5 km British National Grid ticks.

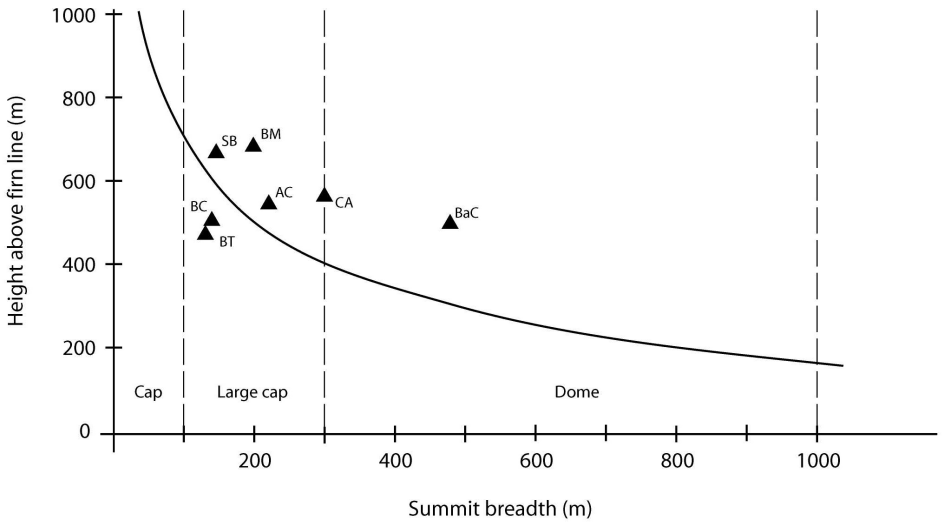

Figure 3.6: Curve describing the inverse relationship between summit breadth and height above ELA required for snow accumulation proposed by Manley (1955), showing the characteristics of Ben More (BM), Stob Binnein (SB), Cruach Ardrain (CA), Beinn Tulaichean (BT), An Caisteal (AC), Beinn a' Chroin (BaC) and Beinn Chabhair (BC). The summits of all except BT and BC could theoretically support snow accumulation. Dashed lines indicate the broad classification of summit accumulation types inferred by Manley for different summit breadths.

environment can be tested by using a number of palaeoclimatic parameters and proxies. Air temperatures in Scotland during the Late-glacial have been inferred from palaeoecological data c. 170 km southeast of the study area (Brooks & Birks, 2000), which, when corrected for sea-level, indicate a mean summer air temperature of 8.5°C during the Younger Dryas. Use of this proxy seems appropriate, given that present sea-level mean summer temperatures in the two areas are almost identical (c. 14°C). Palaeo-precipitation values can be calculated from this using the global ELA temperature and accumulation data presented by Ohmura *et al.* (1992), which yield the following linear regression equation ($R^2 = 0.81$):

$$a = (t + 0.9419)/0.0024 \tag{3.2}$$

in which a is the total annual accumulation, and t is the mean summer air temperature, at the ELA. Using an altitudinal lapse rate of 0.68°C / 100 m to derive t from the sea-level temperature above, Equation (3.2) predicts a likely accumulation at the ELA of 2364 mm a^{-1}, implying former mean annual precipitation (MAP) of 3547 mm a^{-1} (Ballantyne, 2002). Deglaciation would only begin to affect accumulation on this massif after a rise in local ELA of approximately 65 m, which equates to a rise in mean annual ELA air temperature of 0.44°C or a drop in annual precipitation of approximately 130 mm a^{-1}. A temperature rise of 1.15°C and 1.31°C at the ELAs of the highest and broadest summits (Ben More and Beinn a' Chroin), or net decreases in annual precipitation of 331 and 403 mm a^{-1} respectively, would suppress effective accumulation.

3.7 Discussion

Landform-sediment assemblages diagnostic of ice cap glaciation have been defined above (Table 3.1). By using the alignment of former moraines, the distribution of thick till sequences, the altitudes of streamlined cols, kinematic indicators such as glaciotectonic structures, and the direction of flow of ice-marginal outwash, it has been possible to reconstruct the style of Younger Dryas palaeo-iceflow in part of the western Scottish Highlands (Fig. 3.5). This empirical reconstruction is constrained by published maximal limits and overall ice-mass geometries (Sissons, 1979b; Horsfield, 1983; Thorp, 1984, 1986; Hubbard, 1999) and is supported by theoretical ice surface profile calculations (Nye, 1952; Paterson, 2000) and established accumulation area / altitude relationships (Manley, 1955; Rea *et al.*, 1998). The reconstruction shows that ice flowing radially from Rannoch Moor overwhelmed many of the high-level cols between mountains to the southeast, and many of the hills to the south and southwest (Fig. 3.5). Transects from south of the Rannoch Moor source area to 3 main outlet glaciers are shown in Fig. 3.7. These cross-sections demonstrate the variable degree of topographic control exerted on the ice cap in this study area. Significantly, ice surfaces projected from the maximal ice height of c. 700 m a.s.l. proposed by Thorp (1984, 1986) show that the ice would have been constrained by bed topography to a much greater degree, consequently giving rise to a very different style of glaciation and landsystem. In the new reconstruction, flow is concordant with the underlying topography in areas where bed slope and ice surface slope were similar, but discordant where the two differed. Where the latter is true, former ice flow was governed primarily by the direction of ice cap surface slope.

Where soft-bedded outlet glaciers drained the central dome, such as in Loch Lomond and Glen Dochart, decreased basal drag enabled lowering of the ice surface. Steeper ice surface gradients at the heads of these outlets no doubt propagated greater strain heating of the drawn-down ice, and enabled faster flow through a combination of bed deformation and basal sliding. The coincidence of these drawdown zones with areas of streamlined, remoulded or superimposed bedforms (Figures 3.2 & 3.4) suggests that formation of such features was largely controlled by the occurence of these particular glaciological conditions.

South of Glen Falloch and Glen Dochart a local dome in the main ice cap is inferred; one that thinned during deglaciation to a climatically sensitive mountain icefield whose outlet glaciers were confluent with the retreating ice cap margin in Glen Falloch. Independent centres such as this are known to have existed elsewhere in Scotland during the Younger Dryas (Sissons *et al.*, 1973; Lukas, 2005b; Benn & Ballantyne, 2005). The local dome on the Beinn Chabhair – Ben More massif deflected south-flowing ice southwestward through Glen Falloch, and contributed to eastward iceflow through Balquhidder Glen. Much of the ice forming the Loch Lomond glacier was probably sourced in the high plateau area south of Ben Lui and Ben Oss, a factor that no doubt enabled greater southerly extension of the ice cap than could otherwise have been achieved. The new reconstruction may also call into question the eastern limit of ice in Glen Lyon, proposed by Thompson (1972) to lie at Innerwick (Fig. 3.2 inset). For this to be the case the ice-surface gradient in this area would have had to have been especially steep, falling c. 600 m in less than 10 km. Instead it is preferable to invoke a staged recession of the ice cap (Fig. 3.8), perhaps as windward migration of the ice divide led to overall thinning and early retreat of eastern margins, as seen, for example, in Patagonia (e.g.

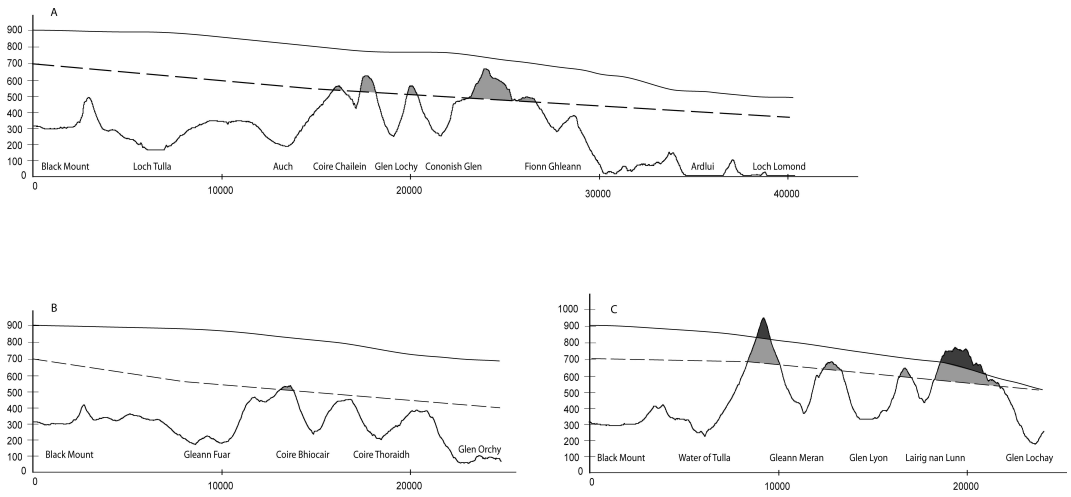

Figure 3.7: Cross-sections showing topography and reconstructed ice surfaces from A., the southern margin of Rannoch Moor at Black Mount to Loch Lomond; B., Black Mount to Glen Orchy; and C., Black Mount to Glen Lochay. Surfaces are interpolated from grids of ice surface and topography using ArcGIS 9.0. Dashed lines indicate ice surfaces extrapolated from the prescribed maximum ice heights of Thorp (1984, 1986) in the north of the area. Light shading denotes nunataks under the Thorp model; dark shading represents nunataks under the new model proposed here. Note the difference in the degree of topographic control in each transect.

Sugden *et al.*, 2002).

The patchy and generally thin subglacial till in the study area shows that, in general, bed deformation played only a limited role in glacier motion. Instead, ice flow in the central area of the ice cap was probably accomodated through a combination of basal sliding and internal deformation. Basal shear stresses in the Loch Lomond and Glen Lyon outlet glaciers were of the order 45 – 60 kPa and 50 – 80 kPa respectively – slightly higher than the values of 40 kPa and 53 kPa calculated by Thorp (1991b). Higher stresses are consistent with the steeper ice cap profile predicted here. The new reconstruction implies greater net accumulation than necessary in Thorp's (1984, 1986) model, suggesting either greater palaeo-precipitation, lower summer palaeo-temperatures, or both. Many Scottish studies have attempted to link palaeoglaciological reconstructions of individual glaciers or icefields with climate (e.g. Sissons, 1979b; Ballantyne, 1989; Benn *et al.*, 1992; Ballantyne, 2002), but significant problems are known to exist in applying such an approach to larger areas, due to the complex and non-linear response of ice masses to climate fluctuations (Kerr, 1993; Purves & Hulton, 2000a; Sugden *et al.*, 2002). The link between ELA and climate is well established (Sutherland, 1984b; Benn & Lehmkuhl, 2000), but misinterpretation of the style of glaciation is a key source of error in the determination of ELAs and the palaeoclimatic inferences drawn from them (Rea *et al.*, 1998). Additionally, any reconstruction, including that presented here, can only offer a 'snapshot' of the ice cap during its dynamic evolution. It may be postulated therefore that the periglacial trimlines used to determine former ice-surface altitudes (e.g. Thorp, 1981, 1984) represent later 'snapshots' in the time-transgressive fluctuations of the ice cap's lateral margins. A possible reconciliation of the differing interpretations might thus rest on the exact chronology of formation of each landsystem element. Early growth of a thick, relatively immobile, ice cap that overwhelmed much of the

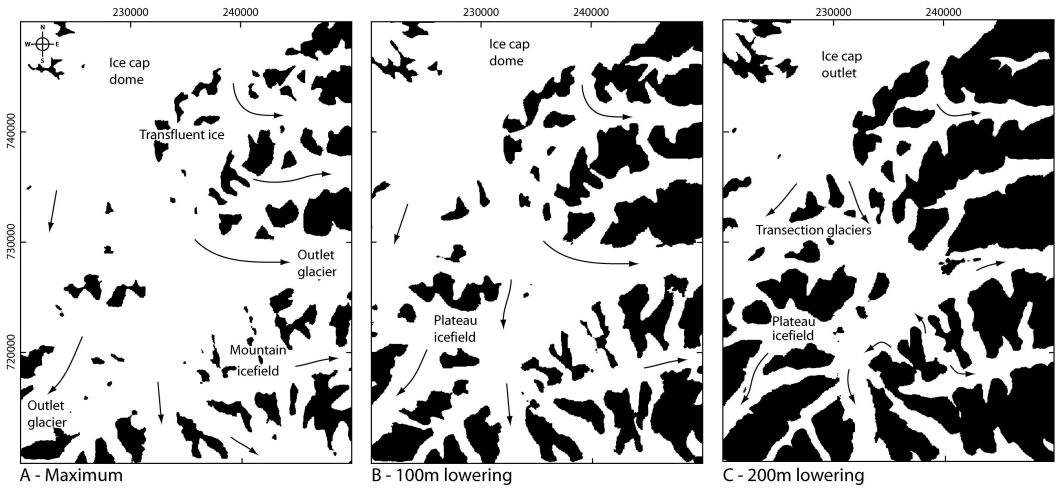

Figure 3.8: Calculated ice extent in the study area (white areas), based on grid subtraction of topography from the reconstructed ice surface grid in Fig. 3.5. Panels show, A: ice extent at Younger Dryas maximum, B: the impact of 100 m ice thinning and C: the impact of 200 m ice thinning. Note the result of increasing topographic control on ice flow directions, and the more rapid recession of eastern margins than those in the west. This simple decay scenario does not, however, account for local ice surface variability and does not differentiate between active and stagnant ice. Scale given by British National Grid ticks at 10 km intervals.

area south and southeast of Rannoch Moor may have been followed by a period of dynamic drawdown that led to thinning and ice surface lowering. Greater temperature fluctuations in this period of unstable climate may have promoted aggressive freeze-thaw processes that shattered newly exposed, glacially-weakened rock surfaces. Lithological contrasts governing bedrock strength controlled the efficacy of these processes, thus giving rise to spatial variability in the development of trimlines. Accelerating flow of outlet glaciers at this time may have enabled their maximal southerly limits to be reached late in the Stadial, before irreversible negative mass balance led to rapid recession of ice margins and widespread deglaciation.

3.8 Conclusions

This article defines a set of eight physical, geomorphological and sedimentological criteria for the identification of non-topographically confined ice flow, allowing landform-sediment assemblages to be treated as elements of a larger landsystem. This ice cap landsystem, characterized here for the first time, sets forth diagnostic criteria that can be used together as a generic tool in determining the nature of a former ice mass in any relict glacial landscape.

In this study of part of the western Scottish Highlands, the field evidence in much of the area satisfies the eight key criteria indicative of ice cap-style glaciation: a reconstructed ice cap greater than 1000 km^2, a low domed centre feeding outlet glaciers, topographically discordant moraine alignments, preservation of thick valley-floor sediment infills, streamlined high-level cols, counter-topographic iceflow indicators and ice-marginal drainage, and collective wider evidence of radial outflow from the central dome. Only in the south of the study area does the field evidence indicate topographically confined ice flow. The former presence of a subsidiary

but coalescent ice cap dome is inferred, which downwasted to a climatically sensitive mountain icefield feeding discrete outlet glaciers.

Together, these elements strongly suggest that the ice-mass in the western Scottish Highlands was largely unconstrained by topography during Younger Dryas maximum but became progressively more so during deglaciation. This interpretation is supported by good agreement with numerical reconstructions (Hubbard, 1999) and is based on physical glaciological principles (Nye, 1952; Paterson, 2000), palaeoecological climate-proxy data (Brooks & Birks, 2000) and established glacier – climate (Ohmura *et al.*, 1992) and glacier – topography (Manley, 1955) relationships. This new reconstruction implies greater accumulation than previously envisaged, perhaps reflecting a wetter or colder Younger Dryas climate.

PAPER IV

The Loch Lomond Stadial glaciation south of Rannoch Moor: new evidence and palaeoglaciological insights

Nicholas R. Golledge[1,2]
British Geological Survey, West Mains Road, Edinburgh, EH9 3LA, UK
and School of Geosciences, University of Edinburgh, West Mains Road, Edinburgh, EH9 3JW, UK.
ph: +44 131 667 1000, fx: +44 131 668 1535, email: n.golledge@bgs.ac.uk

Abstract

The mountains and valleys south of Rannoch Moor were of key importance in governing both the style and direction of ice flow during the Loch Lomond Stadial (LLS), and yet have, until now, received limited attention from glacial researchers. New evidence, based on recent geological mapping of the area, shows that a landform – sediment assemblage exists that, at least in part, pre-dates the Loch Lomond Stadial. This last glacial episode was therefore characterised by very limited glacial erosion in this area, and in fact favoured landscape preservation. Geological and geomorphological data suggest that the former LLS ice cap flowed largely by meltwater-lubricated sliding on rigid beds, with deformation of unconsolidated basal substrate occurring only where pre-existing sediments were overridden.

KEYWORDS: Loch Lomond Stadial; glacial geology; glacier dynamics; palaeoglaciology; Scotland.

3.9 Introduction

Abrupt global cooling took place around 12.7 ka BP (Alley, 2000), which, in the northern Hemisphere, led to the expansion of extant glaciers and the regrowth of ice masses in areas that had been deglaciated during the Lateglacial (Windermere) Interstadial. In Scotland, the 8 - 10°C depression of mean annual temperature (Hubbard, 1999; Isarin & Renssen, 1999), combined with increased precipitation resulting from the southward migration of the oceanic polar front, resulted in rapid glacierization in the western Highlands but more limited ice build-up in central and eastern areas (Clapperton, 1997; Hubbard, 1999).

The high mountains surrounding Rannoch Moor received high volumes of snow, probably through 'snow-fence' mechanisms (cf Andrews *et al.*, 1970), leading to ice accumulations in corries and on plateaux that quickly coalesced to form a central ice cap with interconnected outlet glaciers (Golledge & Hubbard, 2005). Steep north-south and east-west precipitation gradients controlled glaciation away from this central area (Hubbard, 1999), permitting extensive icefields to develop around the ice cap margins (e.g. Bennett & Boulton, 1993a; Benn & Ballantyne, 2005; Lukas, 2005b), but only corrie glaciers farther inland (Brazier *et al.*, 1996a,b). Whilst this approximate distribution and configuration of Loch Lomond Stadial glaciers is widely accepted, many uncertainties still exist with regard to glacier behaviour (and hence landform genesis), and the palaeoglaciological and palaeoclimatic inferences that may be made from the surviving landform-sediment assemblages.

3.9.1 Study area

The area south of Rannoch Moor acted as an important routeway for ice dispersing from the main ice cap accumulation zone, and consequently was instrumental in controlling the style, rate, and direction of former ice flow (Golledge & Hubbard, 2005). The western Highlands massif is dissected by numerous valleys; in this area the largest being glens Orchy and Lochy (feeding into Loch Awe) and Glen Fyne in the west, and glens Lyon and Lochay in the east (Fig. 3.9). The major distributaries in the south of the area are Glen Falloch (connecting to Loch Lomond) and Glen Dochart, both remnants of a preglacial drainage route that supplied the Tay basin to the east (Linton & Moisley, 1960). Thus despite the numerous and high mountains, the area is heavily dissected and offered a range of environments to each successive glaciation of the Quaternary period.

In summarising the glacial history of the area, Sutherland (1993) declared that deposits older than the Loch Lomond Stadial were 'not known' from this area (p307). However, new geological and geomorphological data collected in this part of Scotland as part of ongoing mapping by the British Geological Survey provide compelling evidence to the contrary. Instead of removing older sediments and landforms, the Loch Lomond Stadial ice cap in this area appears to have 'recycled' subglacial material, and remoulded existing landforms. Thus the landsystem fingerprint that remains is in part a palimpsest landscape characterised by overprinting or superimposition of landform-sediment assemblages. Most significantly, the glacial legacy preserved in the current landscape reflects not only the preceding glaciation, the Main Late Devensian, but perhaps also sediments from an even earlier glacial phase.

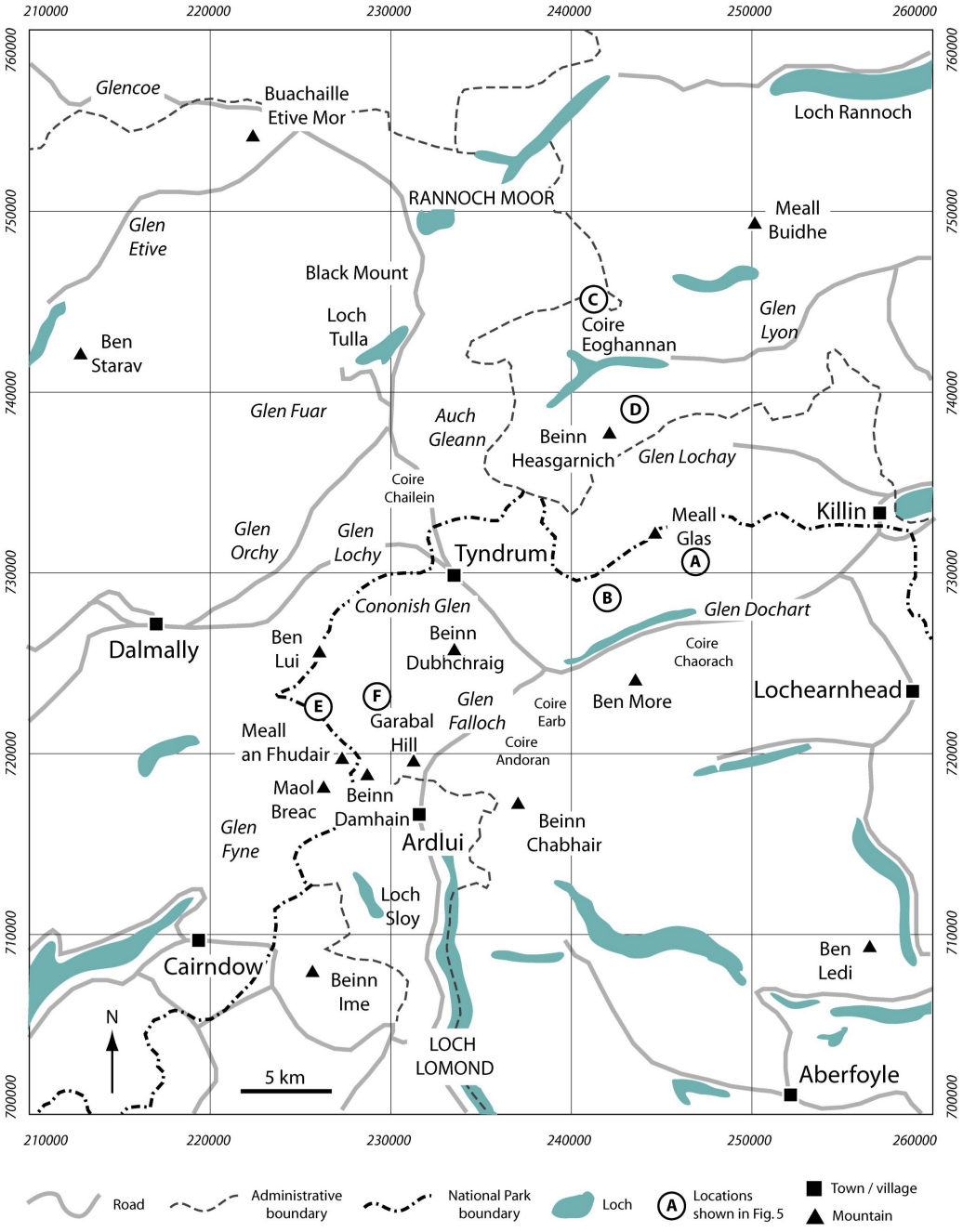

Figure 3.9: The field area south of Rannoch Moor, showing principal features and locations mentioned in the text. National Park and other administrative boundaries are approximate and shown for context only.

3.10 Previous research in the study area

The study area, bounded to the north by Loch Tulla and Black Mount, and to the south by the head of Loch Lomond at Ardlui (Fig. 3.9), has been the focus of relatively little published research. Thompson (1972) conducted field mapping around Glen Lyon and neighbouring glens in the east of the area, and, on the basis of mainly geomorphological observations, reconstructed a number of valley glaciers that drained eastward along the main glens, with flow governed by the underlying topographic slope. The reconstruction was based on evidence of former ice flow at altitudes up to c. 900 m above sea level (a.s.l.), and thus Thompson (1972) argued that the glaciers were sourced primarily from local snow accumulation in the corries around Glen Lyon. This work was encompassed in a wider review by Sissons *et al.* (1973), and no doubt informed subsequent papers (c.f. Sissons, 1979b, 1980).

The interpretation of stereo aerial photographs as a tool for palaeoglaciological reconstruction was becoming more common at this time, and was used extensively by Horsfield (1983) to map the deglaciation pattern of a large area of the 'western Grampians'. Focussing on ice-directed landforms, such as moraines and flutes, Horsfield was able to reconstruct ice margins, as well as flow patterns, at a scale that was impractial by field survey alone. By correlating marginal landforms across large areas, Horsfield (1983) presented a comprehensive picture of an ice cap whose maximum surface altitude achieved $>$ 1000 m a.s.l. over Rannoch Moor, and which decayed actively and coherently back to the high mountains of this source area.

In contrast, concurrent research undertaken largely by field survey of high peaks, cols and ridges in an area centred on the Etive and Nevis mountain ranges led Thorp (1984) to propose a very different scenario for the Loch Lomond Stadial. Using a 'trimline' method, Thorp (1981) equated the height of periglacial weathering limits – the zone between occurences of frost-shattered bedrock and glacial abrasion forms such as friction cracks and striae – with former glacier surfaces. Based on this approach, Thorp (1984) found evidence to suggest that the Loch Lomond Stadial ice mass had formed a relatively small ice cap centred on the low ground of Rannoch Moor, but which nonetheless fed numerous outlet glaciers that occupied the surrounding glens. These glaciers were sourced no higher than 750 m a.s.l. and consequently had lower surface gradients than the ice masses envisaged by either Thompson (1972) or Horsfield (1983). In order that these glaciers could still reach accepted Loch Lomond Stadial terminal moraines, for example at Menteith or Loch Etive, Thorp (1991a) invoked the presence of widespread deformable beds that would facilitate glacier flow despite the low driving stresses implied by the thin ice masses.

Despite their differences, each of the above interpretations makes the assumption that the majority of landforms and sediments of the field area relate to the Loch Lomond Stadial glacial phase, and that older deposits were largely removed. New research in the study area, however, has identified features more compatible with landscape *preservation* than with erosion, a concept that has gained widespread acceptance in Scandinavia with respect to the former presence of cold-based, non-erosive ice (c.f. Kleman, 1994; Hättestrand, 1997; Fabel *et al.*, 2002; Hättestrand & Stroeven, 2002). Described below are the results of detailed field-mapping, aided by air photo interpretation and analysis of high-resolution digital terrain models (DTMs), and sedimentological investigations involving X-Ray Diffraction and automated grain size analysis. These data provide valuable new insights into the style and pattern of flow of the Loch Lomond Stadial ice cap in the western Highlands, raising important questions with respect to the nature

of the extant landscape and the way in which it must be interpreted.

3.11 Landform – sediment assemblages

A glacial stratigraphy for the area has recently been compiled (Golledge, 2007b), based on 53 sedimentary logs of natural exposures in the study area, as well as many hundred point observations. Particle size analysis and X-Ray Diffraction have also been used to characterise the deposits, whilst cosmogenic exposure age and luminescence dating techniques are currently being used to constrain the chronology of the stratigraphic sequence. Described below is a summary of the underlying bedrock of the study area, and the regional glacial stratigraphy, based on logged exposures recorded throughout the area.

3.11.1 Bedrock

The area is underlain by polydeformed Dalradian metasedimentary rocks of Neoproterozoic age, whose regional strike is generally southwest – northeast. These metasedimentary rocks are locally intruded by mafic to felsic rocks, most extensively in the south of the area from the head of Loch Fyne to Garabal Hill. Mineralised quartz veins and minor dykes (both mafic and felsic) are also common. Thus whilst the majority of rock is metasedimentary, there are a number of local intrusions that provide valuable point sources for erratic dispersal, from which palaeo-iceflow may be approximated. Exposed bedrock is more widespread in the study area than is at first apparent – the prolific vegetation cover on many of the hills more directly reflecting the high annual precipitation than the presence of thick 'soils'.

Where exposed, the bedrock may exhibit a variety of characteristics (Fig. 3.10). Near valley floors bedrock is often smooth and may exhibit plucked faces on the lee side of roche moutonnée. At higher levels on valley sides these plucked faces are less common, but bedrock surfaces are still commonly ice-smoothed and more comparable with whaleback forms. On plateau areas and cols between mountains, ice-smoothed bedrock surfaces often host perched boulders – sub-angular or sub-rounded erratics of either local or 'foreign' lithologies (Fig. 3.11A). Where slope gradients increase above these plateaux, the surface debris initially becomes dominated by smaller but nonetheless similarly edge-rounded clasts. At yet higher altitudes, however, ice-smoothed bedrock is commonly strewn with more angular debris, and may show signs of surface weathering. Where significant weathering has taken place, metasedimentary bedrock may be partially buried by a thin layer of regolith composed of highly fractured, frost-shattered, angular debris of solely local lithologies. Igneous lithologies at similar altitudes tend to form 'tors' (Fig. 3.11B).

In many cases, whether metasedimentary or igneous, the bedrock underlying cols or wide bealachs and plateaux is disaggregated and forms extensive areas of bouldery mounds. These mounds are largely composed of loose blocks, commonly have cores of coherent bedrock, and in rare cases may also host pockets or discontinuous veneers of glacigenic diamicton. Mound morphology does not always reflect the strike orientation of the parent strata, and in some instances, for example on the plateau west of Beinn Damhain (Fig. 3.9), there may be a continuum from more-or-less in situ rock to ice-directed, almost drumlin-like forms. Boulders of single rock types are widespread and numerous in areas underlain by their parent lithology, but are virtually absent beyond a few tens of metres from lithological boundaries.

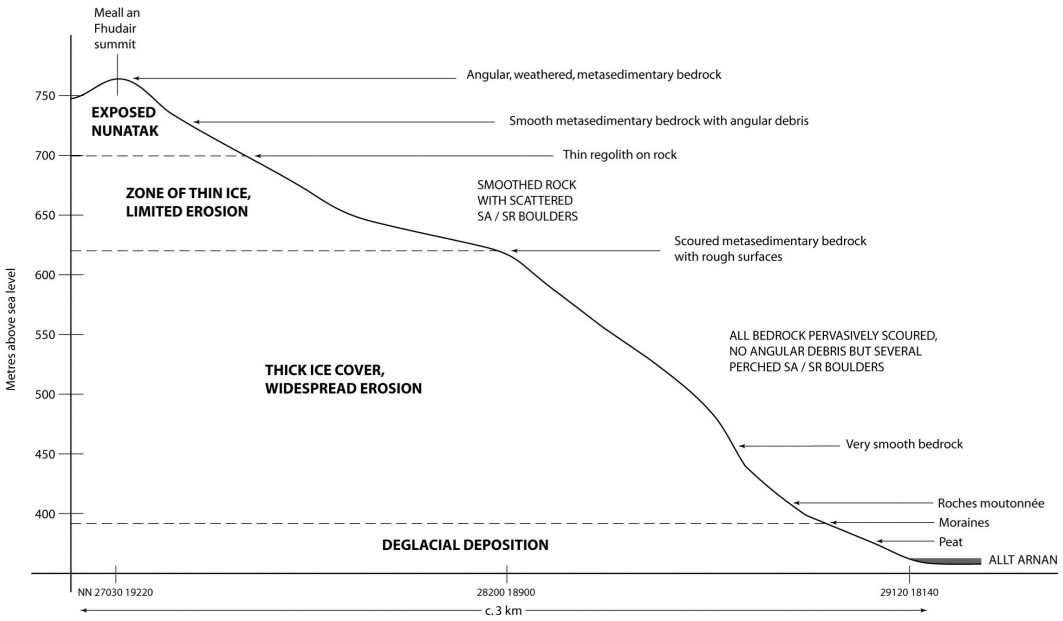

Figure 3.10: Vertical transect from Lairig Arnan to summit of Meall an Fhudair, showing altitudinal zones of bedrock erosion and debris deposition. See Fig. 3.9 for location.

3.11.2 Glacial deposits

In some areas, bedrock is buried beneath a variety of unconsolidated glacial deposits. The lowest, and presumably oldest, facies is a very firm, sandy, yellow-brown to reddish-brown diamicton containing sub-rounded and sub-angular clasts of varied lithologies. This facies has only been observed in two glens, where it appears to form deposits up to 25m thick. XRD analysis revealed the presence of weathered clay minerals, particularly kaolinite, at one of the sites. In Coire Chailein, this diamicton facies is overlain by trough-cross-bedded sand and silt that exhibits post-depositional deformation (thrusts, faults and folds) (Fig. 3.11C). The unit grades conformably upward into gravel that in turn appears to grade into the overlying grey diamicton, which is very firm, silt-dominated, and contains predominantly sub-rounded and sub-angular clasts of a wide range of lithologies.

This grey diamicton is found throughout the study area, but rarely exceeds 5m in thicknesses. It is invariably directly and conformably overlain by a reddish or yellowish-brown diamicton of similar composition and compaction, but with a slightly more sand-dominated matrix. The abrupt change from grey to brown mostly occurs sub-horizontally, but, in some instances, is sub-vertical and cross-cuts individual clasts (Fig. 3.11D), indicating that the colour results from post-depositional weathering within a single till unit. The grey and brown diamictons form smooth veneers on slopes, in some cases thick valley-floor infills, and in a number of areas compose low, broad ridges (see 'Moraines' below).

Conformably overlying the firm, brownish, diamicton, is commonly a sandy, stratified, yellow-brown diamicton containing predominantly sub-angular clasts of mixed lithologies. Stratification ranges from decimeter to metre-scale, is both laterally and vertically variable, but generally intercalates sand-dominated strata with gravel units or diamictons. The contact between this unit and underlying cohesive brownish diamictons is generally transitional, marked predominantly by an upward-increasing proportion of sand in the matrix and a more friable,

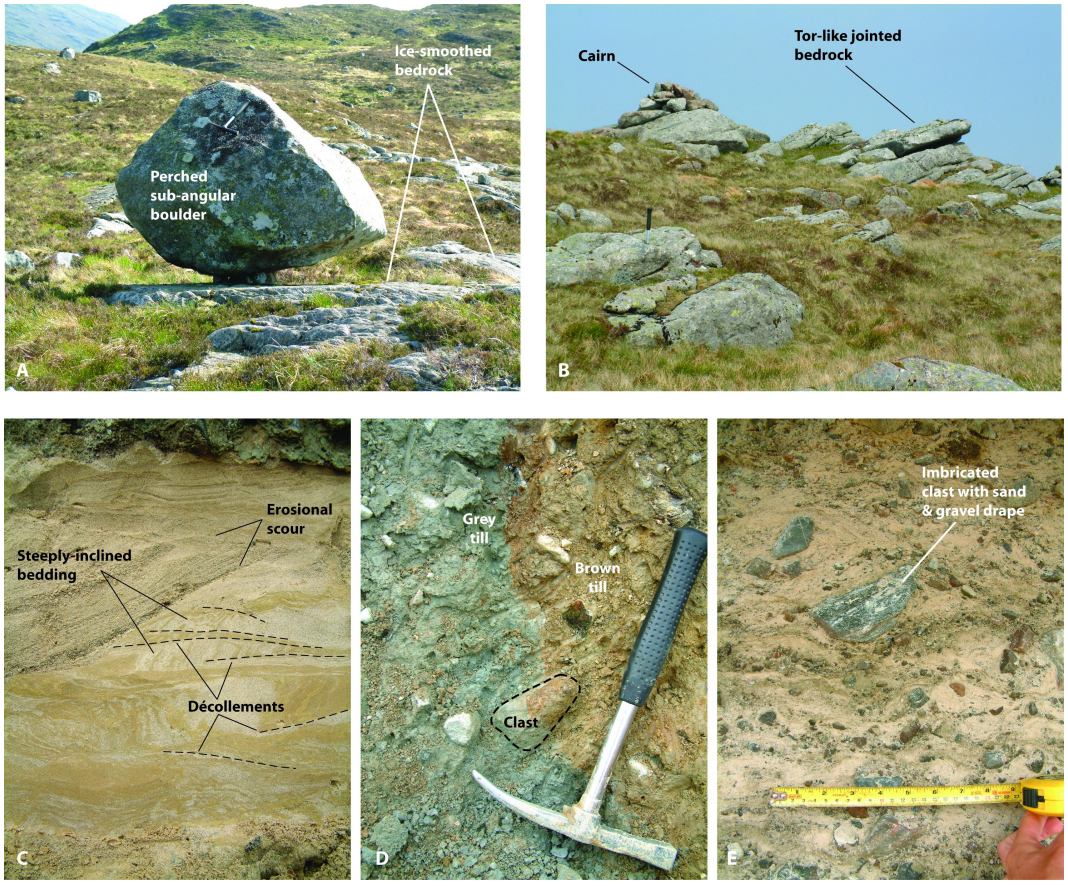

Figure 3.11: Field photographs showing A: perched subangular metasedimentary boulder resting on ice-smoothed metasedimentary bedrock, Garabal Hill; B: Jointed granitic bedrock forming low tor, Maol Breac summit; C: Trough-cross-bedding and post-depositional deformation in buried sand layer, Coire Chailein; D: Weathering front cross-cutting clast in subglacial till, Ben Glas; E: Stratified sandy diamicton forming Type 2 moraine, Glen Fuar.

less consolidated, texture.

This facies of diamicton forms hummocky spreads as well as distinct moraines. In the latter, the diamicton tends to exhibit a coarser-grained, loose matrix, and a greater concentration of cobbles and boulders (Fig. 3.11E). Stratification in these moraines is typically inclined in the direction of former ice flow. In ice-marginal areas, where moraines are common, bedded or laminated clay, silt, sand and gravel is also often seen. These sediments may intercalate with, partially overlie, or be entirely overlain by the sandy, stratified, diamictons described above. In some instances, isolated clasts are seen within the finer sediments.

Moraines

Three types of moraine are present in the study area, distinguished by their size, morphology, and composition (Fig. 3.12). Type 1 moraines form extensive spreads of elongate, linear ridges, each up to 10 m high and 10 - 100's m long, and occur most prominently on the plateau south of the Ben Lui – Beinn Dubhchraig massif, on the plateau south of Meall Glas, at the head of Coire Eoghannan, along the southern flanks of Glen Dochart, and across the slopes of Black Mount north of Loch Tulla (Fig. 3.9).

In most cases these mounds are broad and smooth-topped, and are commonly composed of cohesive diamicton overlying a bedrock core. Some examples exhibit a superficial drape of friable sandy diamicton and boulders, whilst others are entirely devoid of loose debris. Their crests may be aligned perpendicular to former ice flow, or at oblique angles. In a number of cases these ridges have been moulded to form ribbed moraine or lunate, barchan-type mounds (*sensu* Dunlop & Clark, 2006), whilst others exhibit a distinct secondary, superimposed, lineation that is often aligned parallel to former ice flow (Figs. 3.13 & 3.14). These superimposed lineations are shorter and less well-developed than the large ridges on which they are formed, and appear to be best developed on relatively high ground that, in the direction of inferred former ice flow, immediately precedes deep troughs.

The second form of moraine, Type 2, is characterised by short ridges with steep crests, (< 10 m high and 10's of metres in length), and which occur on valley floors such as in Gleann Fuar, Auch Glen, Coire Chaorach, and Cononish Glen. These moraines are composed of clast-rich stratified sandy diamictons, and may include bedded sand units. They are often strewn with sub-angular boulders and have crestlines that tend to arc across the valleys. In some instances the moraines show signs of low-strain glaciotectonism (faults and folds).

Type 3 moraines are largely restricted to the corries and valleys of the southern mountains, particularly the Ben More – Ben Chabhair massif. In upper Coire Chaorach, Coire Earb and Coire Andoran, low, arcuate, ridges occur. Some exposures of diamicton are seen in these landforms, but they are primarily composed of large boulders of local bedrock lithologies. Often the low ridges are hard to discern from the surrounding boulder-strewn slopes and abundant outcrops of bedrock, but once identified are nonetheless arcuate in plan form and occur in nested groups.

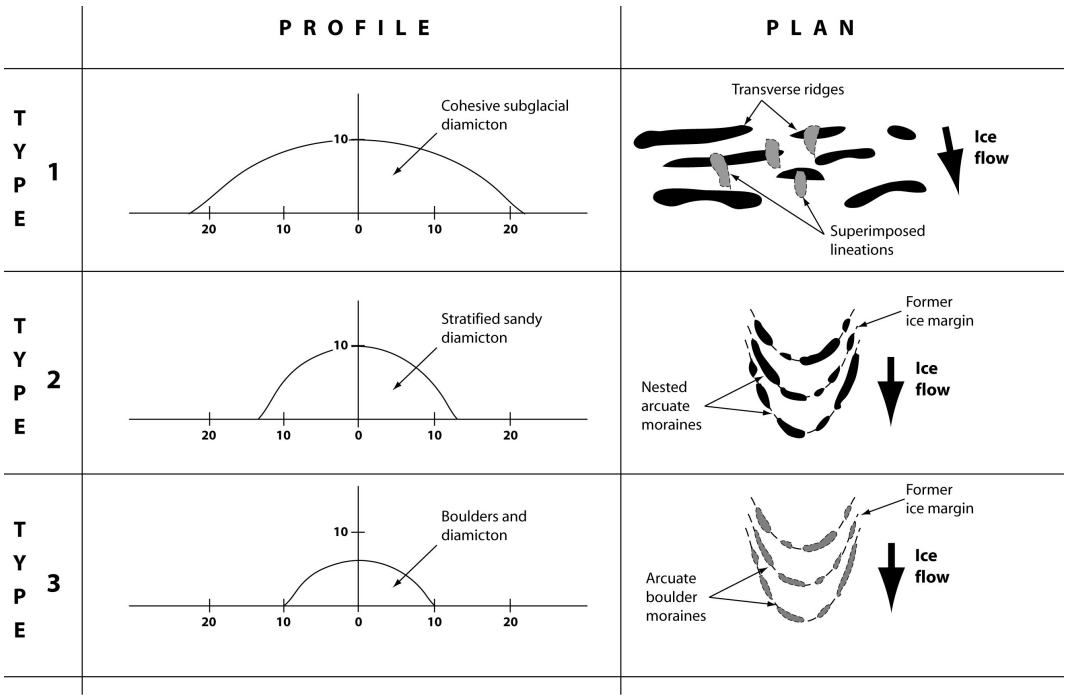

Figure 3.12: Schematic representation of the three types of moraine present in the study area, showing generalised profile and plan views, and typical composition.

3.12 Interpretation and Discussion

3.12.1 The Loch Lomond Stadial landsystem

The nature of ice-smoothed bedrock in the area is one of transition and superimposed debris cover; bedrock surfaces are variably well-scoured across a range of altitudes, and the debris lag that they support varies accordingly. Although Fig. 3.10 illustrates these altitudinal 'zones' based on one mountain transect, the pattern has been identified throughout the field area, and across various lithologies.

It therefore seems possible that the 'periglacial trimline' approach of Thorp (1981) could be modified to include a more critical appraisal of debris lag and its relation to underlying parent rock surfaces, with the aim of more accurately appreciating the occurence of *inherited* surfaces. Often the superficial veneer of debris on rock surfaces forms a thin lag of sub-rounded or sub-angular boulders. These edge-rounded clasts are more instructive of their origin (mainly subglacial) than more angular material, since the latter could be derived from either *in situ* frost-shatter or from supraglacial sources during ice recession. Thus, where angular material is present, the nature of the underlying rock surface should be examined for signs of frost-shatter, especially if a 'trimline' is to be invoked.

The altitudinal transition in the degree of ice-smoothing of bedrock, reaching a maximum towards the valley floors, suggests increasingly warm-based, wet, ice in the valleys, and implies glacier movement through meltwater-lubricated sliding (Roberts & Long, 2005). On wide plateaux and bealachs in the study area, bedrock outcrops are commonly disaggregated and strewn with large, locally-derived, boulders. That the bedrock is not pervasively scoured suggests that ice flow in these areas was relatively slow, and the abrupt transitions in lithological predominance of particular rock types across bedrock boundaries show that dislocated blocks

were not transported very far from their source. However, ice-directed boulder mounds, especially those that are drumlinoid, indicate that the disaggregated bedrock has, nonetheless, been shaped by the passage of ice.

These findings are consistent with observations on Rannoch Moor, where it was recognised that, 'the large granite blocks ... seem to be almost entirely of local origin, ... derived by plucking from the underlying granite floor' (Hinxman *et al.*, 1923, p84). The granitic and granodioritic bealachs of the study area particularly lend themselves to subglacial disaggregation by plucking, due to their well-developed orthogonal joint-sets, but limited dispersal of detached blocks indicates that entrainment of debris (either by thrusting to englacial positions or by basal freeze-on) was very restricted.

Unconsolidated deposits overlying the bedrock have been described above, and are discussed in more detail elsewhere (Golledge, 2007b). Considering the assertion of Sutherland (1993) that pre-Loch Lomond Stadial deposits were unknown in this region, the evidence of a long glacial stratigraphy in the study area is particularly important. The lowest diamictons are very restricted in occurence, but nonetheless represent an early glacial episode. Most importantly, their subsequent preservation indicates that successive ice masses in this area have been insufficiently erosive to remove them. Given that these sediments are only preserved in short, deep, glens oblique to regional ice flow, their survival is most likely a function of the local topography. Whilst these sediments exhibit no surface expression, units higher in the stratigraphic sequence show preferred landform associations that can be used to deduce a relative chronology of their deposition.

Ribbed moraine in the study area (Fig. 3.13A & B), and other Type 1 moraines (low, broad ridges of >100 m length composed predominantly of cohesive subglacial diamicton), appear both morphologically and sedimentologically more similar to subglacially-modified forms (e.g. Dunlop & Clark, 2006) than to undisturbed, ice-marginal forms typical of Loch Lomond Stadial glaciers (Lukas, 2005b). Natural exposures in mounds that exhibit superimposed lineations (Fig. 3.14B) show that the parent landforms are composed of diamicton, which must, therefore, predate formation of the secondary flutings.

Such superimposition of features is common in glaciated terrains (e.g. Rose & Letzer, 1977; Clark, 1993; Salt & Evans, 2004) and may be attributed to ice-divide migration, lobate margin retreat, or to separate glacial events (Clark, 1997). The majority of features described here occur far from reconstructed ice divides in the area (Golledge, 2007a) and where other ice-marginal landforms (e.g. terminal moraines) are lacking. Thus it seems likely that their formation reflects a two-stage process involving more than one episode of glaciation. This inference accords with evidence reported from northwest Scotland that also identifies the role of '...pre-existing till' that has been overprinted by '...subglacially-formed streamlined features' (Wilson & Evans, 2000, p154-155). The authors attributed deposition of the former to the Devensian ice sheet, and the latter to Loch Lomond Stadial ice advance.

Type 2 and Type 3 moraines differ considerably from Type 1 features. Despite compositional differences, Types 2 & 3 are similar to each other in that they are both always smaller than Type 1 moraines, are more clearly arcuate in plan form, and constitute landform assemblages similar to those formed at contemporary glacier margins (Evans, 2003b). Type 2 moraines are commonly composed of stratified, friable, sand and cobble diamicton, often forming units that dip away from the former ice margin, suggesting that the material was deposited primarily by ice-frontal debris flows – a mechanism favoured for Younger Dryas-age moraine formation in

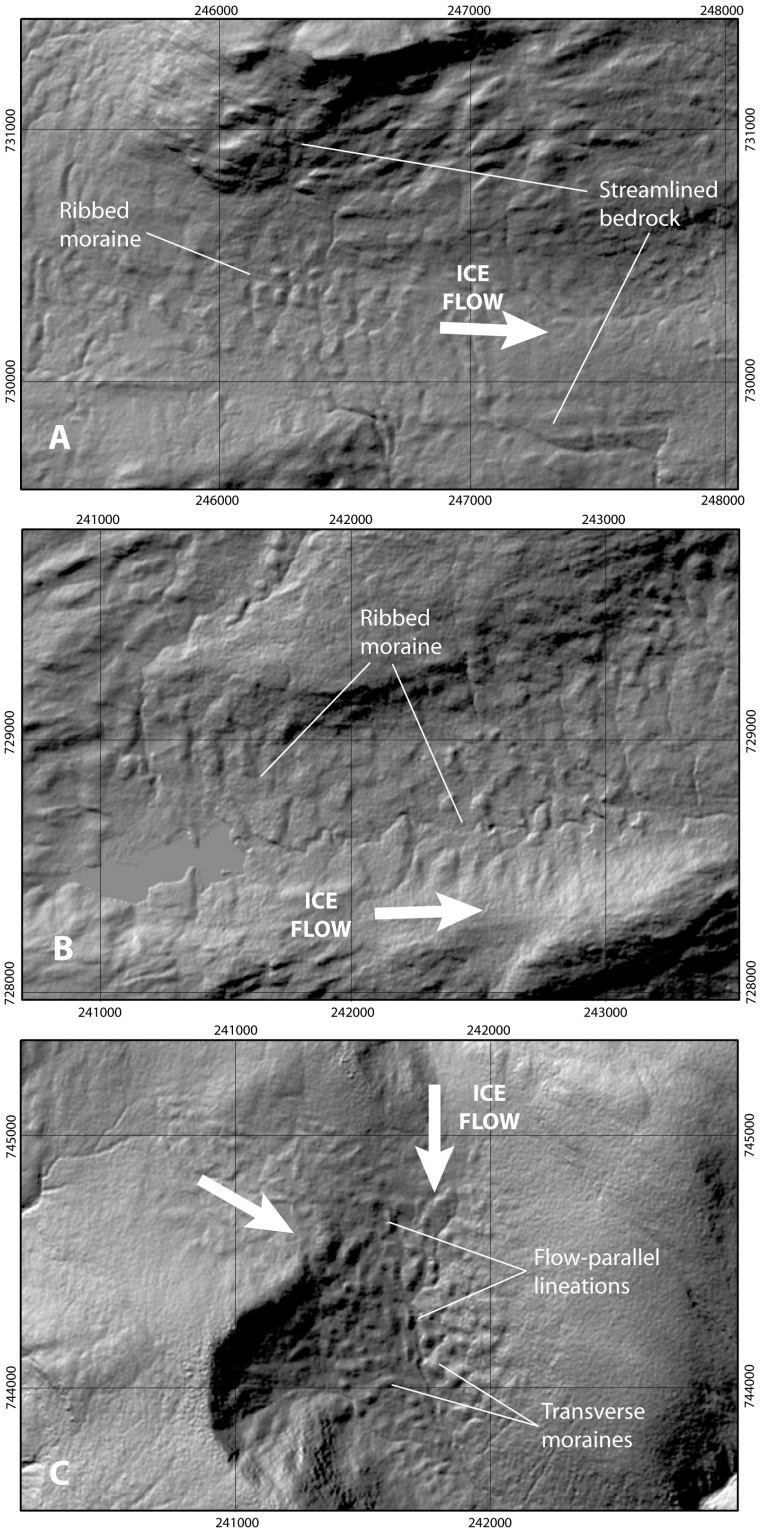

Figure 3.13: Extracts of relief-shaded digital terrain models built from Intermap Technologies high-resolution Nextmap data, showing A: Ribbed moraine near Meall Glas; B: Ribbed moraine at Loch Easan; C: Superimposed landforms in Coire Eoghannan.

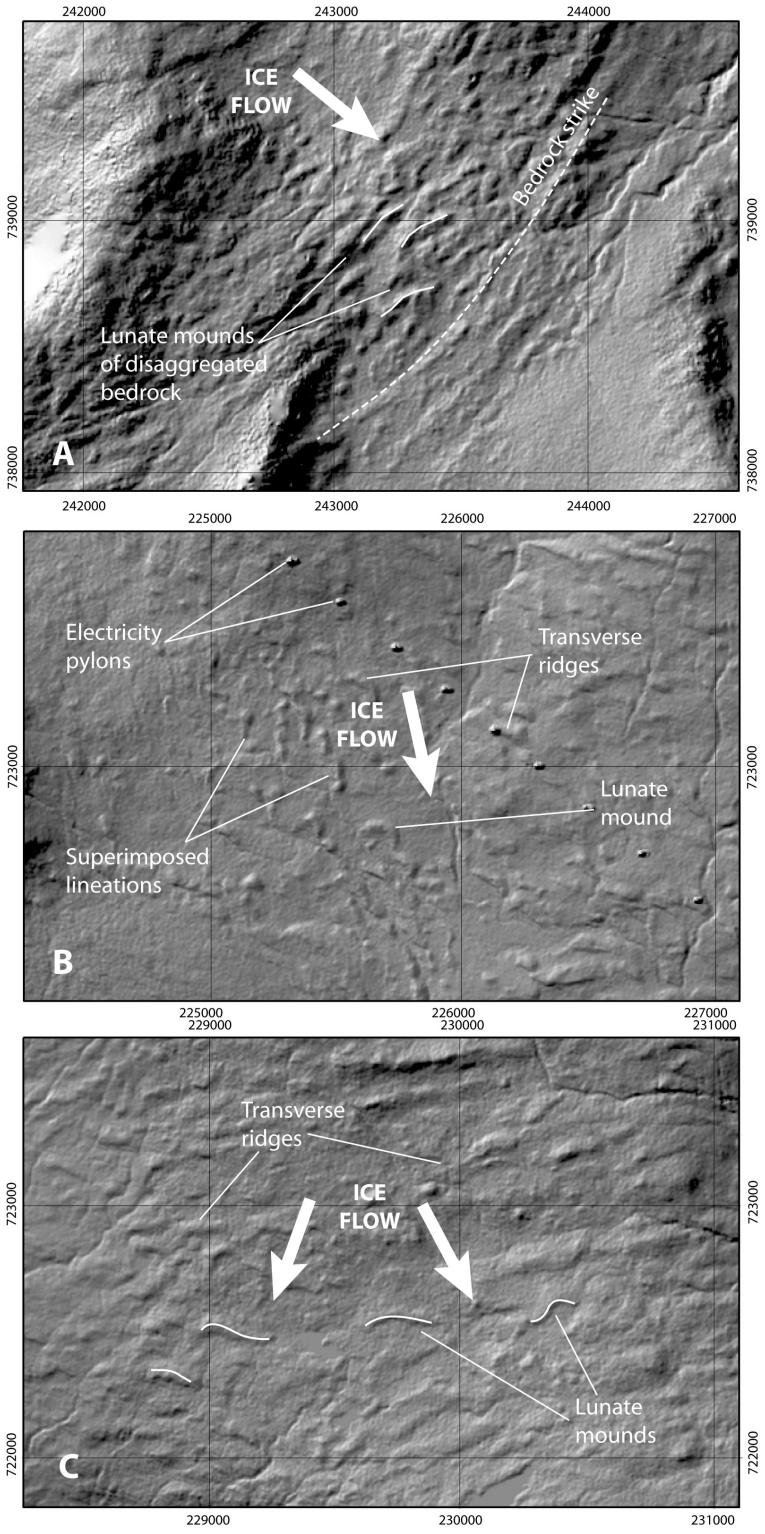

Figure 3.14: Extracts of relief-shaded digital terrain models built from Intermap Technologies high-resolution Nextmap data, showing A: Subglacially disaggregated bedrock ridges near Beinn Heasgarnich; B: Superimposed landforms south of Ben Lui; C: Barchanoid (lunate) moraines southwest of Beinn Dubhchraig.

northwest Scotland (Lukas, 2005b).

Similar material forms a surface drape over some Type 1 moraines, and may also occur as hummocky spreads across large areas of valley sides. The conformable and transitional contacts this facies shows with respect to underlying diamictons may indicate either that the upper unit formed during the same glacial episode as the lower, but under different basal conditions, or that the lower unit has been partially reworked into the upper. Since the geomorphological evidence appears to refute the former, and that it also attests to moulding of the lower diamictons into secondary lineations, the second hypothesis seems the more plausible explanation of the stratigraphic relationships observed.

The composition, form, and geomorphological context of Type 2 moraines demonstrate that these features were produced during the last retreat of ice from the study area at the termination of the Loch Lomond Stadial, and therefore post-date Type 1 moraines. Type 3 moraines may be contemporaneous with Type 2 features, and probably reflect formation by local ice masses where fine-grained substrate was lacking, and where rockfall onto the ice became the dominant source of debris. Such moraines are common elsewhere in Scotland, for example in the Cairngorm Mountains of the central Highlands, where steep precipitation gradients during the Loch Lomond Stadial allowed only very limited ice accumulation, and consequently the formation of restricted corrie glaciers, rock glaciers, and protalus ramparts (Hubbard, 1999; Everest, 2003; Golledge, 2004).

3.12.2 Relative chronology

The sedimentological and geomorphological evidence in the study area allows the following inferences to be made with respect to the glacial history of the area. An early glacial advance deposited a thick subglacial till that has been preserved in two localities. At one of these sites subsequent fluvial deposition occurred – suggesting ice-free conditions – laying down bedded sand and gravel. Renewed glaciation reworked the gravel in this glen into the grey subglacial till that was deposited over much of the study area, forming its thickest accumulations in topographic hollows and at the bases of reverse slopes.

This subglacial diamicton accreted around bedrock obstacles in some localities, forming pronounced bedforms aligned either transverse or oblique to former ice flow. Elsewhere it was deposited as a smooth veneer on valley sides, particularly where ice flow was parallel to valley axes. During a subsequent period of ice flow across the area, this diamicton was partially reworked into a stratified, sandy diamicton (perhaps by winnowing of fines by basal meltwater), and was elsewhere moulded into ice-directed lineations superimposed on their parent landforms. Similarity with landform-sediment assemblages elsewhere in Scotland suggest that the superimposed landforms date to the Loch Lomond Stadial, whilst the parent substrate reflects earlier deposition, possibly during the Main Late Devensian (Wilson & Evans, 2000).

Where the Loch Lomond Stadial ice encountered bedrock outcrops, its influence was governed by the structural competence of the rock. In lithologies that possessed structural weaknesses (fractures or joints for example), blocks were detached by the ice and entrained subglacially, albeit for only short distances. More competent strata, perhaps exhibiting some degree of inherited ice-scour, were abraded and polished, and during deglaciation were overlain by a thin lag of edge-rounded subglacial debris.

Along valley floors at this time, receding ice margins built sharp-crested moraines composed

of sand and cobble-rich stratified diamictons, emplaced primarily by debris-flow processes. Investigations elsewhere in Scotland have shown that, in an analogous manner to the superimposed landforms described above, much of the sediment composing Younger Dryas moraines may be inherited from pre-existing deposits (Lukas *et al.*, 2007). Widespread and abundant deposition of laminated and bedded sand, silt and clay show that Loch Lomond Stadial deglaciation was associated with numerous small ice-marginal ponds.

3.12.3 Palaeoglaciology

The above interpretation of geological and geomorphological evidence in the field area illustrates several key aspects of glacier behaviour during the Loch Lomond Stadial. The presence of extensive areas of bedrock at, or near, the surface suggests that ice flow can not have been entirely accounted for by deformation of a 'soft' bed, but rather, a large proportion of movement must have resulted from meltwater-lubricated sliding on a rigid, or 'hard', bed. Detachment, but only local transport, of boulders from bedrock outcrops shows that the sliding ice in these areas did not actively entrain its debris for distances greater than a few tens or hundreds of metres. The production of subglacial till, by comminution of entrained debris and abrasion of underlying rock surfaces, was consequently limited.

Such an interpretation is borne out by the apparent lack of any Loch Lomond Stadial subglacial diamicton that is distinct from older deposits. Rather than form its own deformable bed, the ice moulded and reworked existing material and preferentially laid down a sandy, often stratified, deposit only where fine-grained material was already present. Thus movement by the deforming bed mechanism (*sensu* Boulton, 1986; Boulton & Hindmarsh, 1987; Boulton, 1996), was actually rather limited in this area.

Where bed deformation did occur, it was instrumental in the formation of superimposed subglacial bedforms. Many of these streamlined landforms occur in areas that lie immediately up-ice of topographic troughs – for example, superimposed landforms are present on the Type 1 moraines south of Ben Lui and Beinn Dubhcraig, but only in the west where ice descended rapidly into Glen Fyne (topographic gradient approximately 8.5%), and in the east where ice flowed steeply into Loch Lomond (topographic gradient approximately 14%). In between these areas, the parent landforms appear largely unmodified. This topographic relationship is also evident in the boulder drumlins above Loch Sloy, the fluted moraines above Glen Lyon, and the ribbed moraine above Glen Dochart. It seems likely that ice in these locations (where bed slopes were greatest) would have experienced the greatest degree of accelerating, extensional, flow that engendered greater strain heating (and therefore faster ice deformation) as well as enhanced basal melting through frictional effects.

Deglaciation began as a result of increasing aridity (Benn *et al.*, 1992), but by the time ice margins had receded to the study area, close to glacier source areas west of Rannoch Moor, retreat was being forced by rapid climatic warming (Hubbard, 1999; Alley, 2000). Warmer air temperatures and a greater proportion of rain (instead of snow) in lower areas led to rapid retreat in glacier ablation zones. Elsewhere, the decaying ice cap remained sufficiently active to build recessional moraines, mainly through debris flow processes where subglacial material was elevated to the ice front by thrusting in a narrow band of cold-based marginal ice (Benn & Lukas, 2006).

3.13 Conclusions

Five key conclusions may be drawn from the research summarised here:

1. In the study area south of Rannoch Moor, the Loch Lomond Stadial ice cap flowed largely by meltwater-lubricated sliding on a rigid bed, removing loose surface material from inheritied ice-smoothed bedrock surfaces and depositing only a veneer of debris during deglaciation.

2. Where structurally-weakened bedrock outcrops occurred, the ice prised them apart and detached large blocks, but transported the debris only short distances from their source.

3. The ice cap was not particularly erosive in the study area and did not generate significant basal till, rather it reworked pre-existing sediment and moulded older landforms.

4. During deglaciation of the ice cap, new moraines were formed on valley floors, composed predominantly of cobble-rich diamictons emplaced by debris flows from active ice-margins, which were intimately associated with ephemeral ice-marginal ponds.

5. The present landscape of this part of the western Scottish Highlands constitutes a glacial 'palimpsest', in which landforms and sediments representing up to three distinct periods of glaciation have been preserved.

These conclusions are based solely on evidence in the field area described above, but may nonetheless be pertinent to other areas of Scotland and perhaps further afield. Recognition of inherited elements in the present landscape, and their correct interpretation, is key to the accurate reconstruction of former ice masses and the derivation of associated palaeoclimatological inferences.

Chapter 4

Chronology

4.1 Summary

Glacier reconstructions based on the kinds of information presented in the preceding papers are only relatively temporally constrained, that is, the age of various landforms and sediments is inferred primarily by their geological context, both spatially and stratigraphically. A key question, therefore, is the *absolute* age of the suites of features identified in the study area. This is important for several reasons. Firstly, the timing of glacial episodes is commonly inferred from ice core records depicting changes in atmospheric composition through time, which are dated and calibrated using either a layer-counting method or an ice-flow modelling technique. Key marker horizons (e.g. known tephra layers) enable absolute constraint to be placed at particular intervals, and allow an age model for the ice core to be reasonably accurately defined.

Whether or not ice sheets and glaciers waxed and waned in synchrony with the changes seen in ice core records is less clear, however. This uncertainty arises from the fact that glacier advance is influenced not just by fluctuations in temperature, but also by precipitation volumes, survival of older ice, internal glacier dynamics, and the non-linearity of growth-decay hysteresis. Previous work in the region surrounding the study area has identified organic horizons within glacigenic sequences, whose radiocarbon ages are used to bracket the deposition of the intervening glacial sediments (and by inference the glacier oscillations that laid them down) (e.g. Rose *et al.*, 1988). Whilst these dates are considered reliable, the application of other dating methods provides an important independent comparison. In the following paper cosmogenic surface exposure dating techniques were used to derive ages of exposure for both bedrock and erratics. The site, Beinn Inverveigh, was chosen for the following reasons:

1. Granodiorite erratics were identified during field survey, at altitudes between 550-600m above sea level on the mountain summit, resting on metasedimentary bedrock.

2. The site lies only 20 km to the south of Rannoch Moor, the principal accumulation and dispersal area for the Younger Dryas ice cap.

3. The altitude at which the erratics occur is above the height predicted by Thorp (1986) as the maximum glacier surface altitude.

With the above in mind, this site was considered an ideal location both to establish the age of glacier overriding of the area in general, and also to test the hypothesis that the Younger Dryas ice mass in this region was thicker than previous thought. From the exposure age determinations, it was concluded that the area was most likely glaciated during the Younger Dryas to an altitude somewhat greater than the summit of the mountain, thereby refuting the interpretation of Thorp (1986).

The samples were collected by myself, Jez Everest and Chris Fogwill. I crushed and milled the samples, which Steve Binnie subsequently cleaned to pure quartz. Further preparation and processing was undertaken by Stewart Freeman and Derek Fabel. I interpreted the ages and wrote the paper.

PAPER V

First cosmogenic ^{10}Be age constraint on the timing of Younger Dryas glaciation and ice cap thickness, western Scottish Highlands

Nicholas R. Golledge[1,2], Derek Fabel[3], Jeremy D. Everest[1], Stewart Freeman[4], Steven Binnie[2]
[1]British Geological Survey, Murchison House, West Mains Road, Edinburgh, EH9 3LA*
[2]Institute of Geography, University of Edinburgh, Drummond Street, Edinburgh, EH8 9XP
[3]Dept. of Geographical & Earth Sciences, University of Glasgow, Glasgow, G12 8QQ
[4]Scottish Universities Environmental Research Centre, East Kilbride, G75 0QF
ph: +44 131 667 1000, fx: +44 131 668 1535, email: n.golledge@bgs.ac.uk

Abstract

We use cosmogenic ^{10}Be surface exposure age techniques at a locality close to Rannoch Moor, western Scottish Highlands, in order to establish the age and chronology of its most recent glaciation. Glacial erratics and an in situ bedrock quartz vein sampled from this site – the summit of Beinn Inverveigh – have yielded zero-erosion exposure ages of 12.9 ± 1.5 ka to 11.6 ± 1.0 ka, implying complete ice cover of the mountain during the Younger Dryas, or Loch Lomond Stadial. These results fit closely with published ^{14}C dates that bracket the maximum (lateral) extent of ice cap outlet glaciers, and are the first internally-consistent ages to specifically address this period of glaciation in Scotland. Furthermore, the dates imply that previous palaeoglaciological reconstructions for this area may have underestimated both the thickness of the former ice cap and, by implication, its volume.

KEYWORDS: Cosmogenic; Younger Dryas; chronology; palaeoglaciological reconstruction; Scotland

4.2 Introduction

Surface exposure dating using cosmogenic ^{10}Be is being increasingly widely used to address problems relating to former glacier configurations during the Scottish Main Late Devensian glaciation (Stone *et al.*, 1998; Everest, 2003; Everest *et al.*, 2006; Everest & Kubik, 2006; Phillips *et al.*, 2006; Stone & Ballantyne, 2006), as well as studies of postglacial (Flandrian) landscape readjustment (Ballantyne & Stone, 2004). However, no cosmogenic dates relating specifically to the intervening Younger Dryas cold spell – broadly equivalent to the Loch Lomond Stadial – have yet been published. During this short-lived episode, renewed glacial conditions led to the regrowth of an ice cap in the western Scottish Highlands (Fig. 4.1), known as the Loch Lomond Readvance (Sissons, 1979b; Thorp, 1986; Golledge, 2007a). Currently, the growth and subsequent demise of the Younger Dryas ice cap in western Scotland are constrained by ^{14}C dates of overridden deposits at former glacier margins (e.g. Rose *et al.*, 1988) and by basal dates from postglacial organic accumulations (Lowe & Walker, 1976; Lowe, 1978). Despite a degree of overlap, these dates suggest that Younger Dryas glaciers in the western Scottish Highlands reached their maximal extents after c. 12.8 ka (Table 4.1).

Whilst these terminal positions are unlikely to have been reached contemporaneously, the overall extent of Younger Dryas ice cover is now fairly well established, due for the most part to extensive geomorphological mapping of the moraines of former outlet glaciers (e.g. Sissons, 1980; Bennett, 1993; Bennett & Boulton, 1993a; Jones, 1998; Graham, 1999). Combined with the ^{14}C chronology, this geomorphological framework underpins and provides essential constraint on numerical models of the ice cap (e.g. Hubbard 1999).

The upper (vertical) limit of the ice cap is less well constrained however, and has been variously interpreted over the last 30 years (Thompson, 1972; Horsfield, 1983; Thorp, 1984; Hubbard, 1999; Golledge & Hubbard, 2005). Thorp (1981, 1984, 1986) advocated the use of geomorphological contrasts, or 'trimlines' that could be equated with the upper limit (and thus the thickness) of the former ice mass. This approach rapidly gained widespread acceptance, but recent mapping in an area south of Rannoch Moor has identified geological and geomorphological evidence that, when treated as a complete landsystem, indicates an ice surface somewhat higher than that predicted by the trimline model (Golledge & Hubbard, 2005; Golledge, 2007a). These differences in surface height have significant bearing on the total volume of the ice cap, with consequent ramifications for palaeo-precipitation and palaeo-temperature estimates.

Additionally, the difference in reconstructed ice heights fundamentally changes the way in which the ice mass would have behaved; with ice sheds no higher than 750 m above sea level (a.s.l.) (Thorp, 1984, 1986), palaeo ice-flow would have been directed by the underlying topography, and so the ice mass would have behaved as an icefield of interconnected glaciers. In contrast, with an upper surface at 900 m a.s.l. (Golledge & Hubbard, 2005; Golledge, 2007a) the ice would have formed a much more extensive icecap whose flow, at least in central areas, was largely unconstrained by the underlying topography.

In this paper we report the initial results of a cosmogenic exposure age dating programme

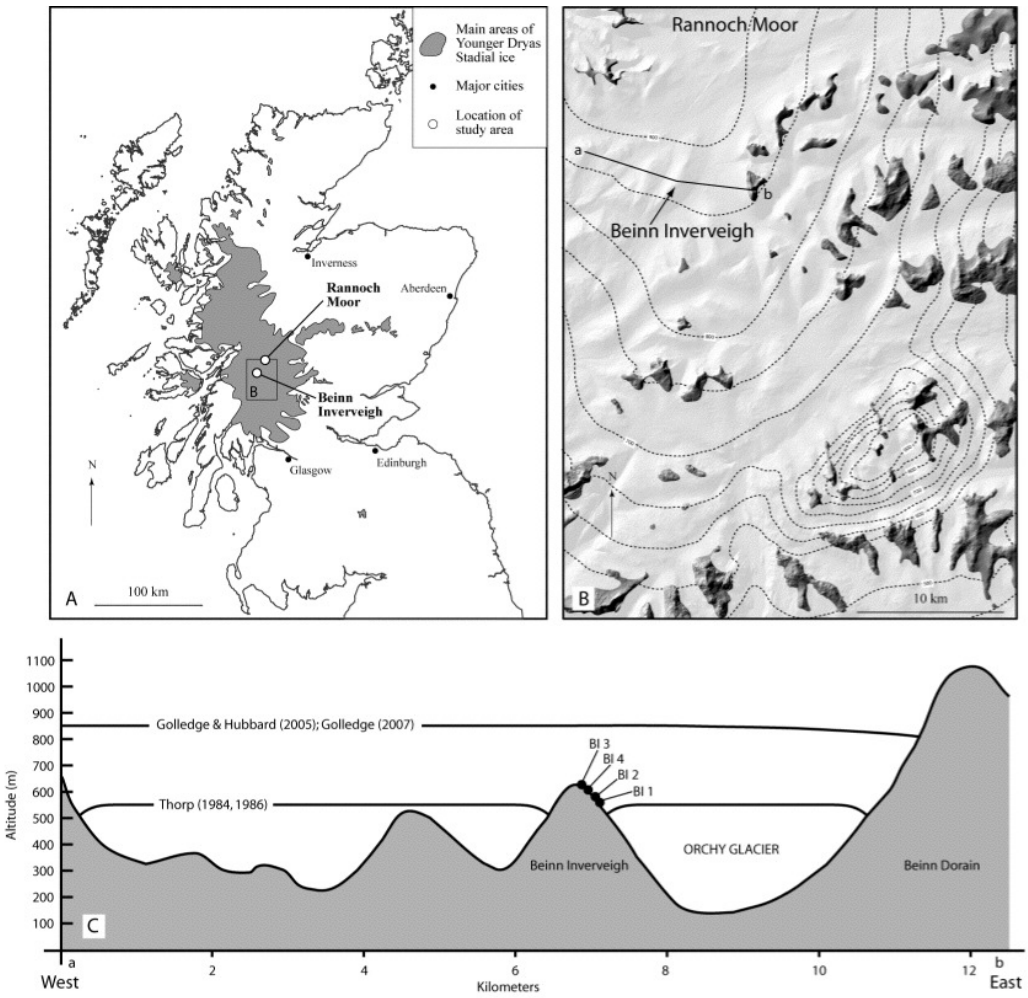

Figure 4.1: A: Location map of the Beinn Inverveigh sample site showing its proximity to Rannoch Moor, and the wider Scottish context. Shaded area indicates generalised extent of Younger Dryas ice cover, redrawn from Ballantyne (1997). Box delimits area shown in B. B: Palaeoglaciological reconstruction of the area surrounding Beinn Inverveigh, after Golledge (2007a). Note complete ice cover over the sample site. Solid line *a*—*b* describes the transect shown in C. C: Schematic west-east cross-section centred on Beinn Inverveigh summit, showing reconstructed ice surfaces from Thorp (1986) and Golledge (2007a), and sample altitudes.

Locality	^{14}C age (ka BP)	Reference	Calib. age (ka BP)
Drymen	11.5–11.9	Sissons (1967b)	13.4–13.7
Mentieth	11.6–12.0	Sissons (1967b)	13.5–13.8
Mollands	10.6–10.8	Lowe (1978)	12.6–12.8
Loch Goil	12.1–12.4	Sutherland (1981)	13.9–14.5
Balloch	10.8–11.1	Browne & Graham (1981)	12.8–13.0
Helensburgh	11.7–11.8	Browne *et al.* (1983)	13.5-13.7
Croftamie	10.4–10.7	Rose *et al.* (1988)	12.3–12.8
Torrie	12.7–12.8	Merritt *et al.* (1990)	14.9–15.2

Table 4.1: Published radiocarbon dates and calibrated equivalents (using Calib v.5.0.2) for the southern part of the western Scottish Highlands. All except Mollands are from overridden material, thus providing maximum ages for Younger Dryas glacial onset. The Mollands date comes from immediately inside a former glacier limit, thus providing a minimum age for marginal recession of this lobe. Errors associated with radiocarbon ages from recently deglaciated terrain, however, require all of these dates to be interpreted with some caution (Lowe & Walker, 1980; Sutherland, 1980).

that aims to, 1) constrain (for the first time) the age of the Younger Dryas ice cap by cosmogenic methods, and 2) quantitatively establish the likely former ice surface height of the Younger Dryas ice cap. In doing so it is hoped that the differences between contrasting palaeoglaciological reconstructions may be resolved.

4.3 Sample site and methods

Beinn Inverveigh (636 m a.s.l.) lies on the northwestern side of Glen Orchy, approximately 20 km southwest of the former Younger Dryas ice cap centre on Rannoch Moor (Fig. 4.1 A & B). Southwestward ice flow from Rannoch Moor towards Beinn Inverveigh is evidenced by ice-flow indicators such as striae, and by the distribution of transported erratics of Rannoch granodiorite (Hinxman *et al.*, 1923; Sissons *et al.*, 1973; Sissons, 1980; Horsfield, 1983; Thorp, 1984, 1986). Horsfield (1983) used this and other evidence derived from aerial photo analysis to infer the former presence of an ice cap in this area whose maximum surface altitude exceeded 1000 m a.s.l. Using primarily field-based interpretations focussed on establishing the altitudes of periglacial trimlines, Thorp (1984) predicted a maximum ice height around Beinn Inverveigh considerably lower than that of Horsfield (1983) at 550–500 m a.s.l. In Thorp's reconstruction, the summit of Beinn Inverveigh formed a nunatak protruding above the surrounding ice surface (Fig. 4.1 C).

Recent numerical models, and empirical reconstructions based on wider field evidence, favour a maximum ice surface height of c. 900 m a.s.l., somewhat higher than that of Thorp (1984, 1986), but slightly lower than the one proposed by Horsfield (1983), (Hubbard, 1999; Golledge & Hubbard, 2005; Golledge, 2007a). These latter models predict Beinn Inverveigh to have been completely over-run by ice during the Younger Dryas.

Samples were taken from the highest parts of three granodiorite boulders on the summit ridge of Beinn Inverveigh at 581 m, 590 m, and 604 m a.s.l. in order to establish whether the mountain top had been exposed since Main Late Devensian deglaciation, as implied by Thorp (1986), or whether it had been ice-covered more recently. In all cases the sampled boulders had open aspects, were exposed on all sides, and ranged in height from 0.8–1.4m (Fig. 4.2

Figure 4.2: Sampling of erratics and bedrock on Beinn Inverveigh, A: BI 1, B: BI 2, C: BI 3, D: BI 4.

A–D). A ground-level quartz vein protruding above the psammite bedrock at 623 m a.s.l. was also sampled. Shielding angles were calculated for 30° sectors, resulting in a horizon correction of <0.5% (shielding correction factor = 1). Sample location data are shown in Table 4.2.

4.3.1 Sample processing and measurement

Samples were sawn to isolate only the uppermost 5cm of rock, which was subsequently crushed and milled, etched with HF, and processed following procedures modified from Kohl & Nishiizumi (1992) and Child *et al.* (2000). $^{10}Be/^{9}Be$ ratios were measured at the Scottish Universities Environmental Research Centre (SUERC) AMS facility, and were corrected by full chemistry procedural blanks that yielded typically <3% of the number of ^{10}Be atoms in the samples. Independent repeat measurements of AMS samples were combined as weighted means with the larger of the total statistical error or mean standard error. Final analytical error in concentrations (atoms g^{-1} quartz) are derived from a quadrature sum of the standard mean error in AMS ratio, 2% for AMS standard reproducibility, and 2% in Be spike assay.

Apparent exposure ages (Table 4.2) were calculated using a ^{10}Be production rate of 5.1 ± 0.3 atoms g^{-1} y^{-1} scaled to site specific altitude and latitude using Stone (2000). Sample thickness correction was calculated using an attenuation coefficient of 150 g cm^{-2} and a rock density of 2.68 g cm^{-3}. Uncertainties in single-nuclide exposure ages represent full propagation of the production rate uncertainty and all concentration errors defined above. The relatively larger uncertainty for BI 4 stems from low AMS counting statistics as a result of a small quartz sample mass (approx. 10 g). Exposure age corrections due to production rate variations as a

Sample	Lithology	Lat. Long. (deg.)	Altitude (m)	Height above surface (m)	Quartz mass (g)	^{10}Be conc.* (x 10^4 atom g^{-1})	Exposure age (ka BP)
BI 1	Granodiorite	56.51N 4.80W	581	1.4	26.90	9.96±0.66	11.6±1.0
BI 2	Granodiorite	56.51N 4.80W	590	0.8	37.93	10.81±0.47	12.5±0.9
BI 3	Vein quartz	56.51N 4.81W	623	0.5	33.33	11.45±0.62	12.9±1.0
BI 4	Granodiorite	56.51N 4.80W	604	1.0	10.05	11.23±1.10	12.9±1.5

*Data relative to NIST SRM 4325 taking ^{10}Be/^{9}Be = 3.06 x 10^{-11} (Middleton *et al.*, 1993) and ^{10}Be half-life of 1.51 Ma (Hofmann *et al.*, 1987). Procedural ^{10}Be blanks < 8 x 10^4 atoms (^{10}Be/^{9}Be < 4 x 10^{-15}). Thickness correction for all samples is 0.957 (see text for details).

Table 4.2: Location and analysis data for the Beinn Inverveigh samples.

function of changes in the palaeo-geomagnetic dipole intensity are not required for latitudes greater than about >55°. Reduction of production rates by intermittent snow cover is unlikely since the samples were collected from the tops of large boulders and an exposed summit where storms would rapidly blow snow off the surfaces. Hence we do not correct for potential snow cover.

As with other Scottish studies (e.g. Phillips, 2001; Everest & Kubik, 2006; Phillips *et al.*, 2006) we make no adjustment for isostasy, since considerable difficulty exists in the precise quantification of the rate and amount of post-Younger Dryas isostatic uplift. This is mainly due to uncertainties surrounding the thickness and extent of the Main Late Devensian ice sheet, the timing, lag, horizontal and vertical magnitude of crustal response, and the extent of Younger Dryas retardation or redepression of the crust (Firth & Stewart, 2000). Based on estimated uplift rates for selected sites in Scotland, however, it is likely that post-Younger Dryas uplift may be of the order of 30–50 m, most of which occurred in the early postglacial period (Firth & Stewart, 2000, Table 1). Uplift of this magnitude would result in < 5% change in the apparent exposure ages.

4.4 Results

The apparent surface exposure ages range from 12.9 ± 1.5 ka to 11.6 ± 1.0 ka (Table 4.2 and Fig. 4.3). These ages assume no inheritance from a previous exposure, and zero erosion, zero shielding, and zero uplift since final deglaciation. Whilst erosion, shielding and uplift might increase the age of the samples, any inheritance would, conversely, make the 'true' sample ages younger. Inherited ^{10}Be is unlikely to affect the three samples from erratics (unless reworked from older moraines), but the bedrock sample may be more susceptible if insufficient subglacial erosion occurred. Despite these uncertainties, the clustering of exposure ages is encouraging.

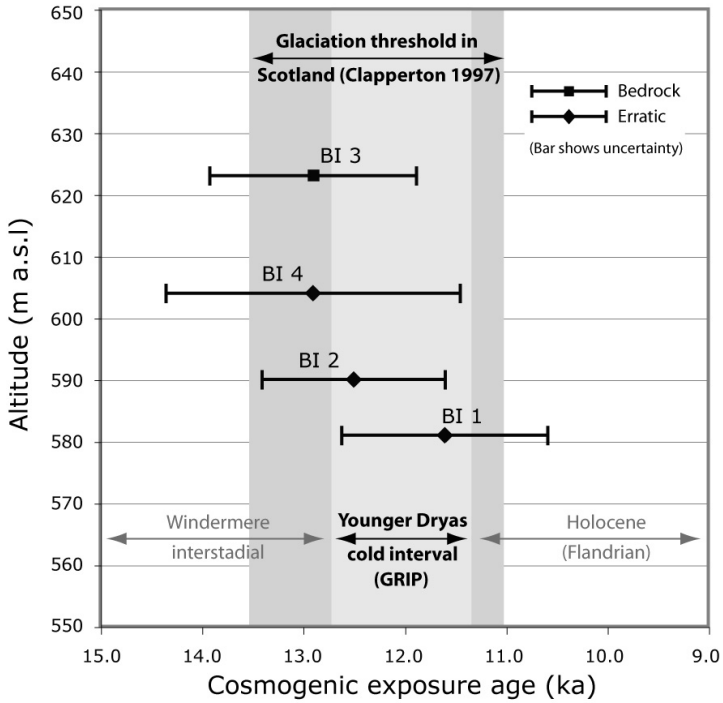

Figure 4.3: Cosmogenic exposure age plotted against sample altitude. Light grey box denotes time period of climatic nadir suggested by isotopic data from Greenland ice cores (Dansgaard *et al.*, 1993; Lowe *et al.*, 2001), dark grey box indicates period when Scotland's climate cooled below the glaciation threshold calculated by Clapperton (1997).

4.5 Discussion

4.5.1 Age and chronology of glaciation

The interpreted exposure ages from samples of granodiorite erratics and vein quartz from metasedimentary bedrock all fall within the temporal range of the Younger Dryas as determined from δ^{18}O ratios in the GISP2 ice core (Fig. 4.4), and are all equivalent to, or younger than, the ^{14}C dates that bracket the maximal extent of outlet glaciers in the western Scottish Highlands (Lowe, 1978; Sutherland, 1984a; Rose *et al.*, 1988; Merritt *et al.*, 1990) (Table 4.1). Consequently, it seems most plausible to interpret the exposure ages presented here as representing bedrock erosion and erratic deposition attributable to ice cover during the Younger Dryas, or Loch Lomond Stadial.

4.5.2 Implications for the timing of renewed glaciation in western Scotland

Because the new data corroborate existing ^{14}C dates that suggest a period of maximal outlet glacier extent after c. 12.8 ka, the combined dataset represents multi-proxy constraint on the timing of the Younger Dryas glaciation in western Scotland. Additionally this ^{10}Be / ^{14}C chronology may hint at a build-up of ice in the western Scottish Highlands that began earlier than the climatic nadir (12.9–11.3 ka) indicated by GRIP and GISP2 ice core data (Dansgaard *et al.*, 1993; Alley, 2000; Lowe *et al.*, 2001). Increasing snow accumulation

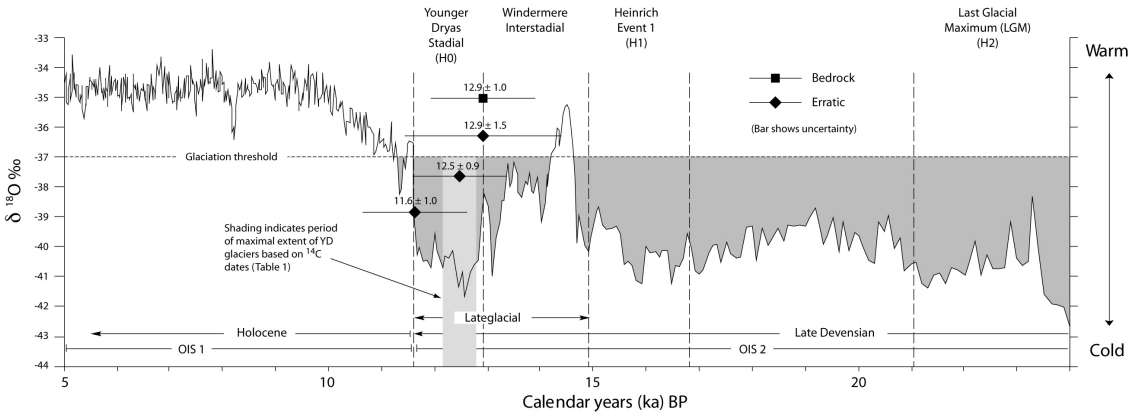

Figure 4.4: GISP2 δ^{18}O curve and the interpreted cosmogenic exposure ages for Beinn Inverveigh. Dates are shown with respect to sample altitude (see Figure 4.3) in the order BI 1 (lowest), BI 2, BI 4, BI 3 (highest). Dark shading denotes periods when Scotland's climate cooled below the glaciation threshold calculated by Clapperton (1997), light grey shading indicates period of maximal glacier extent indicated by ^{14}C data (Sutherland, 1984a; Rose *et al.*, 1988). GISP2 is used in preference to GRIP, following the recommendations of Lowe *et al.* (2001) for comparing ice core years with calibrated ^{14}C dates older than 10.3 ^{14}C ka. Ice core data provided by the National Snow and Ice Data Center, University of Colorado at Boulder, and the WDC for Paleoclimatology, National Geophysical Data Center, Boulder, Colorado. Oxygen Isotope Stages (OIS) from Dawson (1992).

as a result of increased precipitation was triggered by southerly migration of the oceanic polar front during interstadial cooling (Sissons & Sutherland, 1976; Clapperton, 1997). As a result of the greater climatic anomalies typical of the east Atlantic region, compared to the west (Lie & Paasche, 2006), ice build-up in the western Scottish Highlands may have been out of phase with Greenlandic cooling as inferred from ice core data. Indeed, several authors have previously suggested that ice either survived the Windermere Interstadial, or began to accumulate in Scotland prior to the isotopically-inferred climatic minimum (Peacock, 1970; Sutherland, 1984a; Bennett & Glasser, 1991; Clapperton, 1997; Merritt *et al.*, 2004).

Support for the latter scenario may be found in proxy palaeoclimatic data, which suggest that the interstadial was a period of 'marked climatic instability', in which the warm phase was interupted by renewed cooling intially from around 14.5 ka, and irreversibly so from 13.0 ka (Witte *et al.*, 1998; Mayle *et al.*, 1999; Brooks & Birks, 2000). By using palaeoclimatic data pertinent to the Younger Dryas, Clapperton (1997) determined a 'glaciation threshold' of -37‰ δ^{18}O for this period in Scotland, equating to a drop of 3°C in mean July temperature at sea level. Applying this to the GISP2 curve (Fig. 4.4) it is clear that renewed ice accumulation in some of the higher Scottish mountains was indeed possible late in the interstadial, and would have continued throughout the Younger Dryas. Modelled simulations of build-up of the Younger Dryas ice cap suggest that, even from intially ice-free conditions, its maximum extent and thickness may have been reached in less than 550 years (Hubbard, 1999). When the new dates presented here are considered in the context of the palaeoenvironmental proxy data and glaciological model predictions, it therefore seems plausible that renewed glacial accumulation began towards the end of the Windermere Interstadial.

4.5.3 Former ice thickness in the western Highlands

The internal consistency of the results, and the good agreement between bedrock and erratic ages, allows a minimum Younger Dryas ice surface altitude of > 623 m to be defined. Given that bedrock erosion implies the former presence of warm-based ice and a degree of basal sliding (Roberts & Long, 2005), it is reasonable to assume that the ice surface lay somewhat higher than this altitude, perhaps in excess of 700 or even 800 m. Such an inference is clearly at odds with the trimline-based reconstruction of Thorp (1984, 1986), under whose model the sample sites would have been exposed since Main Late Devensian deglaciation, and would thus have been expected to yield ages >15 ka. These results therefore provide new constraint on the minimum altitude of the former Younger Dryas ice cap surface in this area.

4.6 Conclusions

The new cosmogenic exposure ages presented here allow the following conclusions to be drawn:

1. Glacially-eroded bedrock and ice-transported boulders on the summit of Beinn Inverveigh, a mountain close to the centre of the former Younger Dryas ice cap on Rannoch Moor, have yielded internally-consistent ^{10}Be ages ranging from 12.9 $\pm$ 1.5 ka to 11.6 $\pm$ 1.0 ka.

2. All these dates fall within the accepted time period of the Younger Dryas, as indicated by isotopic data from Greenland ice cores, implying complete ice cover of Beinn Inverveigh during this period.

3. Close agreement of these dates with published ^{14}C dates from the margins of outlet glaciers lends veracity to the notion that ice accumulation in the Scottish Highlands was initiated towards the close of the Windermere Interstadial.

4. The dates imply that trimline-based palaeoglaciological reconstructions in this area have underestimated former ice surface altitudes, and consequently also former ice volumes.

5. Further research is required to constrain this chronology over a wider area, and to quantify the upper ice surface altitude of the Younger Dryas ice cap.

Chapter 5

Numerical ice-sheet modelling

5.1 Summary

Geological investigations in formerly glaciated areas can provide a wealth of information about the glacial significance of surviving landforms and sediments, from which inferences can be made about the age, geometry, and dynamics of the ice masses that produced them. These interpretations are invaluable in providing local and specific detail, but may have more limited application beyond the particular study area. In order that the inferences drawn from the local studies presented in the preceding papers can be properly considered in a wider context, however, it is necessary to employ other techniques, such as numerical modelling. A combined numerical and geological approach involves iteration of the model according to inferences drawn from local investigations (e.g. thickness or extent of glaciers), such that the resultant 'best fit' model scenario is empirically grounded as far as possible. In this way, inferences may be made about glacier extent and dynamics in areas where field evidence is either lacking, or ambiguous. Additionally, model simulations allow larger scale spatial variability in climatological and glaciological parameters to be more clearly seen.

In these two papers a high-resolution numerical ice sheet model was used to:

1. simulate the extent of Younger Dryas glaciation in mainland Scotland (the model domain), and to compare this with mapped glacier limits, and
2. use this simulation to infer glaciological conditions of the Younger Dryas ice cap, such as its mass balance regime, mechanisms of flow, and subglacial processes.

The first paper describes a series of experiments attempting to reproduce mapped Younger Dryas glacier extents as closely as possible. Numerical aspects of the model, and the methodology employed in experiment iteration, are described, together with a synthesis of glacial and palaeoclimatic research in Scotland. The article highlights areas where the model accurately replicates mapped glacier limits, as well as those areas where discrepancies occur, and discusses reasons for the mismatches. In the second paper, the focus is more specifically on glaciological aspects of the modelled Younger Dryas ice cap, particularly on the pattern and variability of its velocity and temperature, likely subglacial hydrological organisation, and the capacity of the ice cap to erode its bed. The outputs predicted by the model enable direct comparison of the simulated ice cap with geological field evidence, thereby validating the former and adding greater detail and accuracy to the interpretation of the latter.

Modelling involves simplifying assumptions, which inevitably lead to a degree of inaccuracy. For example, the model experiments presented here do not include lake bathymetry in the topographic input data, and use a simplified climate parameterisation to calculate precipitation and temperature. The model does not predict proglacial or subglacial lakes and so cannot modify glacier behaviour accordingly. These shortcomings are commonly most relevant at the local (valley glacier) scale, but are less of a problem when the ice cap is considered more widely. Nonetheless, future work might focus on these areas as key targets for refinement of the model.

The model was originally coded by Alun Hubbard, but all subsequent experimentation was carried out by myself according to a research design that I had conceived. On many

occassions I required additional functionality from the model, which I requested from Alun. He amended the code accordingly and I continued my experiments. The numerous model iterations undertaken during the early stages were all carried out by me, in isolation, guided by empirical target glacier limits and an evolving understanding of the respective influence of variation in each parameter. The modelling methodology therefore largely consisted of logical and incremental changes applied to a series of controlling variables, with a small component of trial and error. Derivations of model outputs presented in Paper VII were all conceived and implemented by me, mainly through grid calculation techniques in ESRI ArcGIS 9.2, but in some instances were inspired by discussions with either Alun or David Sugden. David's contribution to both of these papers was principally of a supervisory nature. The related modelling experiments described later, in the 'Discussion' chapter, were all conceived and implemented by me, as was the manufacture of the synthetic climate files, and the re-scaling of the GRIP temperature forcing used in the seasonality experiments.

PAPER VI

High-resolution numerical simulation of Younger Dryas glaciation in Scotland

Nicholas R. Golledge[1,2], Alun Hubbard[3] and David E. Sugden[2]
[1]British Geological Survey, Murchison House, West Mains Road, Edinburgh, EH9 3LA*
[2]Institute of Geography, University of Edinburgh, Drummond Street, Edinburgh, EH8 9XP
[3]Institute of Geography & Earth Sciences, The University of Wales, Aberystwyth,
Penglais Campus, Aberystwyth, Ceredigion, SY23 3DB

email n.golledge@bgs.ac.uk, *phone* +44 131 6671000.
ph: +44 131 667 1000, fx: +44 131 668 1535, email: n.golledge@bgs.ac.uk

Abstract

We use a 500 m resolution three-dimensional thermomechanical ice -sheet model forced by a scaled GRIP temperature pattern to retrodict the extent of glaciers during the Younger Dryas episode in Scotland. Using empirical data from sources spanning half a century we systematically perturb temperature depression, precipitation distribution, and the amount of basal sliding to identify the parameter space that most closely reproduces the glacier margins identified from field investigations. Arithmetic comparison of predicted ice cover with empirical glacier extent enables mismatch to be quantified and an 'optimum fit' timeslice to be identified. This 'best-fit' scenario occurs with a maximum mean annual temperature depression from present of 10°C and steep eastward and northward gradients imposed on a modern precipitation distribution, coupled with restricted basal sliding. Even small deviations around these values produce considerably less well-fitting glacier configurations, suggesting that only a narrow range of optimal parameterisation exists. Mismatch between modelled and empirically reconstructed glacier extents occurs as a consequence of local conditions not accommodated by the model, such as wind-blown snow accumulation and lake (loch) bathymetry, and where geological evidence is equivocal. At the domain scale, however, our simulation suggests that inception of Scottish glaciers occurs rapidly, and leads to a coherent ice cap within 400 years of initial climatic cooling. According to our model, the ice cap begins to decay relatively early in the stadial, probably as a result of increasing aridity leading to net thinning and recession of many of its margins, with final and catastrophic collapse of the ice cap occurring largely within a century.

KEYWORDS: Ice-sheet modelling; Younger Dryas; glaciation; Scotland

5.2 Background

Numerical modelling of former ice sheets can be an effective method of inferring palaeoclimate, particularly when constrained by empirical evidence (Plummer & Phillips, 2003; Siegert & Dowdeswell, 2004; Napieralski *et al.*, 2007). Ice sheet simulations thus serve to further understanding of glacial climatic conditions, whilst also providing an independent method by which to appraise glacier reconstructions based on geological or geomorphological field evidence (e.g. Van Tatenhove *et al.*, 1996; Golledge & Hubbard, 2005). This is particularly important in areas where current understanding is an amalgam of reconstructed ice limits published by many different workers over many decades, as is the case in Scotland (Clark *et al.*, 2004). Numerical models allow ice-sheets to be considered in their entireity, and importantly, in all four dimensions (Sugden, 1977; Grigoryan *et al.*, 1985; Clark *et al.*, 1996; Sugden *et al.*, 2002; Hubbard *et al.*, 2005). A numerical model that is validated by empirical data in one area may thus be used to infer glacier dimensions in another, where perhaps field data is equivocal or lacking. Field data commonly reflect either isochronous events such as a stillstand of the glacier terminus, or time-transgressive processes such as streamlining or overprinting of older landforms, but rarely allow detailed insights into the evolution of the glacier through a glacial episode. However, the landform record enables model predictions to be assessed in the field, thus facilitating an iterative process from which an accurate glacier reconstruction may be derived.

The glacial landform assemblage in Scotland has traditionally been interpreted as reflecting two key events - extensive ice-sheet glaciation during the Main Late Devensian (c. 25 - 16 ka BP), and a subsequent, more restricted growth of ice during the Younger Dryas (12.7 - 11.5 ka BP) (Sutherland, 1993). The legacy of this latter episode - the Loch Lomond Readvance (LLR) - is evident primarily in the western Scottish Highlands, where landforms and sediments indicate the former presence of an ice cap centred along the main axis of the mountains and several satellite icefields around its periphery (Thorp, 1986; Bennett & Boulton, 1993a; Ballantyne, 1989, 2002; Golledge, 2007a). Considerable research has been undertaken on both the extent and timing of these glaciers, enabling a reasonably complete picture to emerge (Fig. 5.1). A general consensus exists that the δ^{18}O GRIP and GISP2 ice core records in Greenland indicate a considerable climatic downturn during the Younger Dryas, the pattern of which was closely mirrored in Scotland and which led to the re-establishment of full glacial conditions. Renewed glaciation in western Scotland probably began during the close of the Lateglacial interstadial (Clapperton, 1997; Golledge *et al.*, 2007), and appears to have reached its maximal extent after c. 12.3 - 12.8 ka BP (Rose *et al.*, 1988). Palaeoenvironmental data from numerous Scottish sites broadly constrain the geometry of the renewed ice masses to areas where interstadial deposits are apparently absent (Fig. 5.1).

5.3 Objectives

Several previous attempts have been made at glacier modelling in Scotland, some focussing on the characteristics of the Main Late Devensian ice sheet (Boulton *et al.*, 1977; Gordon, 1979; Glasser, 1995; Hall & Glasser, 2003; Boulton & Hagdorn, 2006), and others specifically

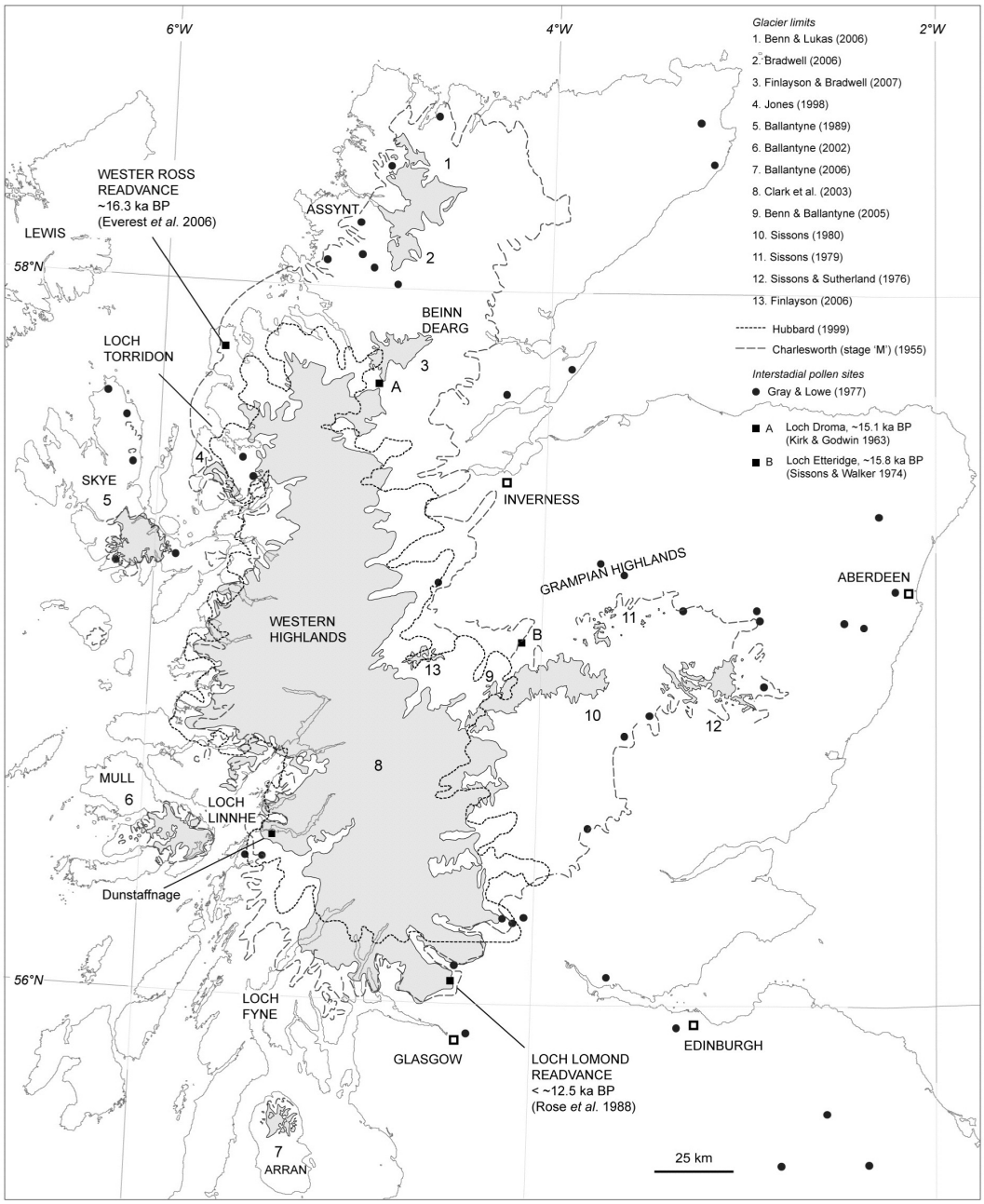

Figure 5.1: The model domain, showing glacier limits from empirical studies published between 1955 and 2007, as well as the 'best-fit' model scenario of Hubbard (1999). Nunataks are not shown. Key dated margins and Lateglacial pollen sites provide important constraints for model experiments.

targetting the Younger Dryas ice cap (Payne & Sugden, 1990; Hubbard, 1997, 1999; Starr, 2001). Of those concerned with the Younger Dryas, model resolution has varied from 1 km - 5 km, primarily governed by a limited availability of high-resolution topographic datasets and the computational resources required to solve complex algorithms over a model domain exceeding 100 000 km^2. In this paper we aim to:

1. Refine the work of Hubbard (1997, 1999) by employing a numerical model with a horizontal grid resolution of 500 m, four times greater than previously possible, to simulate glacier extent in Scotland during the Younger Dryas.

2. Describe the basic characteristics and limitations of the model and the assumptions made in its use.

3. Use empirical palaeoclimatic data to initially force the mass balance component of the model, so as to replicate perceived stadial environmental conditions as closely as possible.

4. Assess the sensitivity of the model to pertubations in the parameters governing ice flow (principally basal sliding and internal deformation) and mass balance (temperature, precipitation volume and distribution).

5. Validate the model by attempting to reconstruct ice masses that honour as many of the maximal limits of LLR glaciers, established from empirical reconstructions, as possible.

6. Describe the palaeoclimatic and glaciodynamic conditions that combine to produce a 'best-fit' model scenario for the model domain during the Younger Dryas.

7. Highlight areas where mismatch occurs between model predictions and the empirical record, and to offer resolutions where possible.

5.4 Methods

The three-dimensional thermomechanical model used for this experiment is modified from the one previously used to model the Younger Dryas ice cap in Scotland (Hubbard, 1997, 1999), the Last Glacial Maximum (LGM) ice cap in Patagonia (Hubbard *et al.*, 2005) and the LGM ice sheet in Iceland (Hubbard *et al.*, 2006). Necessary input data are a) basal topography at 500m resolution derived from NEXTMap digital elevation data and British Geological Survey bathymetric data, b) mean annual air temperature (MAAT), and c) present precipitation pattern. The two climatic components are derived from regression analysis of modern temperature and precipitation patterns within the model domain, based on the United Kingdom Climatic Impacts Programme (UKCIP) baseline climate (Purves & Hulton, 2000b). Mass balance is driven by an elevation-related Positive Degree Day (PDD) scheme based on that of Laumann & Reeh (1993) that derives total melt from integrated positive temperatures. Despite the limitations of such schemes (van der Veen, 2002), their general ability to simulate glacier responses in contemporary environments (e.g. Braithwaite, 1995; Jóhannesson *et al.*, 1995) lends confidence in their use. Precipitation is distributed evenly throughout the model year and daily temperature is calculated from mean annual temperature using a sinusoidal function that determines the standard deviation of mean July temperature. The model is iterated by manually perturbing MAAT with a 20-year GRIP-forced ELA

Table 5.1: Principal parameters used to force the ice sheet model, with their values and units.

Parameter		Value	Units
g	Gravity	9.81	m s^{-2}
ρ	Density of ice	910	kg m^{-3}
ρ_w	Density of sea water	1028	kg m^{-3}
G_value	Geothermal heat flux	55	W m^{-2}
d SL	Sea level (western Scotland)	+ 10	m
A_wert	Weertman sliding parameter	7.50E-14	–
lapse_rate	Temp / elevation relation	-0.00615	°C m^{-1}
dt	Time step	0.02	a
	cell_size	500	m
	x_min	100000	BNG
Domain	x_max	400000	BNG
	y_min	600000	BNG
	y_max	975000	BNG

depression scaled to Scottish palaeotemperatures, and by introducing spatial gradients to the precipitation distribution. Ice flow occurs through internal deformation and Weertman (1964)-type sliding when basal temperatures reach the pressure melting point, and which is adjusted with a dimensionless scaling factor. Longitudinal stresses become increasingly important in high resolution models such as the one used here, and are computed using an empirically validated ice-stretching algorithm (Hubbard, 2000). Calving is accomodated using an empirical function related to water depth (Brown *et al.*, 1982), which although simplistic compared to more complex relationships (e.g. Benn *et al.*, 2007a,b), does at least offer a reasonable approximation of calving loss with minimal computation. Given the limited extent of tidewater margins of the Younger Dryas ice cap, the use of this simple function in preference to the more complex solutions is unlikely to produce significantly different overall results, but may be a possible area for future model refinement. Key variables and their parameterization are described in Table 5.1; other variables governing ice flow and mass balance calculations can be found in Hubbard (2006) (Table 1).

Given the above boundary conditions, distribution grids for ice-surface elevation were calculated by solving at a 0.02 year time step from initial ice-free conditions. The model offers an approximation of reality and necessarily involves simplifying assumptions that are common to most modelling experiments. In particular, the spatial resolution and smoothing of basal topography may produce some inaccuracy, and the lack of terrestrial water bodies (including proglacial lakes) will locally neglect calving-related ablation. The mass balance model used may have a degree of error, and furthermore snow accumulation does not take into account mass redistribution by wind-blow or avalanching. Assuming uniform rheology of the glacier bed may similarly mask complex ice dynamics at a local scale. However, only a very small proporation of the glaciated area is underlain by unconsolidated deposits thicker than a metre or two (mainly near glacier terminii), and at the domain scale these local differences become less critical.

5.5 Model parameterization

Any attempt to realistically model former glaciers must be guided by empirical data as far as possible. To that end, consideration of previous palaeoenvironmental studies is given below, with the aim of establishing plausible ranges for the distributions governing mass balance (temperature, precipitation amount and spatial gradients), as well as other influential factors such as stadial sea level and typical geothermal heat flux.

5.5.1 Palaeoenvironment

The Lateglacial period (c. 11.5 - 15 ka BP) in Britain was one of 'marked climatic instability' (Mayle *et al.*, 1999, p421) characterized by 'abrupt and intense climatic changes' throughout northwestern Europe (Witte *et al.*, 1998, p435). Both ice core data and palaeoecological proxies indicate that only a brief warm period occurred during the interval 14-15 ka BP at the close of the Main Late Devensian, perhaps lasting no more than 500 years, before stepwise cooling ensued during the Older Dryas (c. 13.7 - 14.5 ka BP, Clapperton, 1995). This Bond cycle was temporarily interupted by a warm period from c. 13.1 - 13.7 ka BP prior to the high magnitude thermal decline marking the onset of the Younger Dryas stadial. Cold conditions persisted in Greenland until 11.6 ka BP (Severinghaus *et al.*, 1998; Alley, 2000), after which very rapid warming of 5-10°C took place, perhaps in as little as 1-3 years (Dansgaard *et al.*, 1989; Alley *et al.*, 1993; Alley, 2000). During the 1200-1300 years of full-glacial conditions, the climate throughout the North Atlantic region may have experienced considerably greater seasonality than at present (Denton *et al.*, 2005), most probably related to a reduction in strength of the thermohaline circulation that led to a southward migration of the oceanic polar front to below 50°N (Ruddiman & McIntyre, 1981; Bard *et al.*, 1987; Isarin & Renssen, 1999) and the spread of winter sea ice into lower latitudes (Alley, 2000). Sea-surface temperature and salinty oscillated frequently during this period, however, as a consequence of decadal-scale incursions of warm and relatively saline water from lower latitudes (Kroon *et al.*, 1997). Residual isostatic depression following recession of the Main Late Devensian ice sheet produced stadial sea levels on the west coast of Scotland slightly higher than present at 5 - 11 m above sea level (a.s.l) (Gray, 1974, 1978; Gray & Lowe, 1977; Peacock *et al.*, 1977; Shennan *et al.*, 1999). Geothermal heat flux across the model domain varies little, and for simplicity is kept constant at 55 Wm^{-2} (Rollin *et al.*, 1993).

5.5.2 Scottish palaeoclimate

The calculation of Lateglacial palaeotemperatures through regression analysis has become possible due to the close empirical relationship between the occurrence of individual chironomid taxa and summer surface-water temperature, and use of the mutual climatic range (MCR) method of relating coleopteran assemblages to mean maximum and minimum air temperatures (Atkinson *et al.*, 1987; Brooks & Birks, 2000). Palaeoecological datasets used as UK temperature proxies appear to be in good agreement with climatic patterns identified in the GRIP data (Fig. 5.2) (Atkinson *et al.*, 1987; Mayle *et al.*, 1999; Brooks & Birks, 2000), suggesting that oscillations throughout the North Atlantic were broadly contemporaneous, even if their relative magnitudes may have differed. Such an association is also bourne out by the close

match between the pattern of sea-surface temperature variation west of Scotland, and the Greenland δ^{18}O record (Kroon *et al.*, 1997). Several Lateglacial sites in the UK have yielded important data pertinent to our understanding of climate change through this period, generally indicating a stadial mean July temperature of c. 8-10°C at sea level (Witte *et al.*, 1998; Brooks & Birks, 2000) and winter temperatures no warmer than c. -13.5°C (Witte *et al.*, 1998). A mean annual temperature of -2 or -3°C can thus be approximated, representing a cooling of around 10-14°C on present values. Although some of these proxies tend to overestimate mean temperatures, particularly in the case of the coleoptera, and thus may not entirely reflect the full seasonal range of former climatic conditions (Isarin & Renssen, 1999; Denton *et al.*, 2005), these values are comparable to those calculated by Benn & Ballantyne (2005) based on glacier reconstructions in the West Drumochter hills. Clapperton (1997) used modern climatic data to derive a 'topographic glaciation threshold'. This was calibrated against δ^{18}O data from the GRIP ice core (in which 1‰ change in δ^{18}O represents a temperature drop of about 1.5°C in Scotland) (Fig. 5.2), allowing him to identify periods when conditions were cold enough for glaciers and ice sheets to have formed in the Scottish Highlands. Despite the generalizations implicit in this approach, the implication that much of the interstadial was cold enough for ice to have accumulated is compelling.

5.5.3 Cryospheric response in Scotland

The response of glaciers in Scotland to climate change during the Lateglacial period remains somewhat enigmatic, due partly to a lack of high-resolution dates from relict glacial landforms. Instead, the chronology of Main Late Devensian ice sheet recession and the subsequent Younger Dryas readvance is constrained largely by ^{14}C dates from organic material related to either the Lateglacial interstadial, or early Holocene. These uncertainties aside, numerous attempts have been made to gain palaeoclimatic insights from empirical reconstructions of glaciers ascribed to the YD throughout Scotland, principally through calculations of the Equilibrium Line Altitude (ELA) of former glaciers using the methods of Sissons (1974), Sissons & Sutherland (1976), and Osmaston (2005). These techniques are validated to some extent by their grounding in empirical observations (e.g. Sutherland, 1984b; Ohmura *et al.*, 1992), but the derived ELAs and palaeoclimatic inferences may still be erroneous in areas where either the hypsometry of the glacier is misidentified (cf Rea *et al.*, 1998), or where the margins used for area calculations remain undated. An additional problem with reconstructions based on the Ohmura *et al.* (1992) dataset is that the concept of continentality is ignored; the polynominal relationship linking precipitation and temperature effectively represents an approximation of a global dataset, which includes highly maritime glaciers in New Zealand as well as much more continental glaciers in the Canadian high Arctic. Model experiments demonstrate that, for any given summer temperature, greater seasonal variations result in lower mean annual temperatures and hence a reduced ablation season (Hughes & Braithwaite, 2008). Consequently, accumulation (or precipitation) calculations based on Ohmura *et al.* (1992) will tend to overestimate the volume required to maintain glacier mass balance at the reconstructed ELA, since they erroneously assume greater ablation.

Table 5.2 shows inferred climate data from both palaeoglaciological and palaeoecological

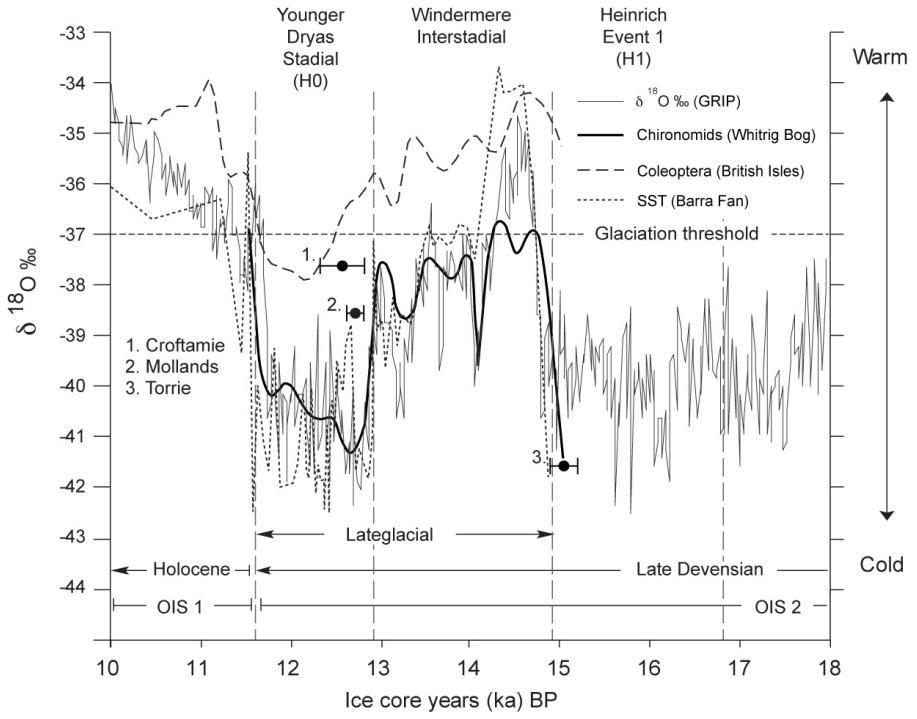

Figure 5.2: Oxygen isotope record (thin line) representing climate change during the last glacial - interglacial transition, from the GRIP ice core in central Greenland (Johnsen *et al.*, 2001). Other lines show the Younger Dryas climate pattern reconstructed from chironomids in southeast Scotland (Brooks & Birks, 2000), coleopteran fauna in the British Isles (Atkinson *et al.*, 1987), and sea-surface temperatures calculated from foraminifera (Kroon *et al.*, 1997) (curves shown for comparison only, and no calibration with GRIP is implied). Calibrated radiocarbon dates (Calib 5.0.2) are shown for Croftamie (overridden deposits), Mollands (postglacial sequence only), and Torrie (outside presumed Callander moraine).

Table 5.2: Modern temperature and precipitation values together with reconstructed values for the Younger Dryas, from a range of empirical studies.

Time	Location	Jan	July	Annual	Precipitation (mm)	Source
Present	Scotland	2.5	13	7.5	1500	Met. Office (1971-2000)
	Dunstaffnage	–	–	9.1	–	
	Model domain	–	–	11	–	
Younger Dryas	Scotland	-25	10	-8 – -17	–	Ballantyne & Harris (1994); Isarin & Renssen (1999)
	NW	–	6 – 7	–	–	Ballantyne (1989); Benn (1997); Ballantyne (2006)
	SW	-7 – -21	5 – 7	-1 – -8	2500–2800*	Gray & Lowe (1977); Sissons (1979b, 1980); Gray & Coxon (1991); Ballantyne (2002)
	SE	–	8	–	–	Brooks & Birks (2000)
	NE	–	6–7	–	500–650	Sissons & Sutherland (1976); Sissons (1980); Sutherland (1984b)

* Corrected to sea level using precipitation gradient from Ballantyne (1983)

studies for areas pertinent to the present study, together with modern reference values. These varied sources demonstrate considerable evidence for climatic cooling during the Younger Dryas, in particular highlighting the bias of cooling in the winter, when estimated palaeotemperatures may have been as low as -20°C . Cooling during the summer months was less severe, but was nonetheless sufficient to produce stadial-averaged mean annual temperatures around 8°C colder than present. Additionally, data from palaeoglaciological reconstructions in eastern parts of Scotland (e.g. Sissons & Sutherland, 1976) indicate that precipitation there was considerably less than at present. The consequently west-skewed precipitation distribution led to a southwest to northeast precipitation reduction of 70-80%. This would have favoured high accumulation rates in western Scotland, closest to the influence of maritime air masses, but led to considerable aridity further east largely as a result of the reduced capacity of cold air masses to hold and transport moisture.

5.6 Model strategy

Whilst a good body of palaeoclimatic data clearly exists, few methods are available with which to appraise its reliability. Numerical modelling offers the opportunity to tackle the inter-relationship between palaeoenvironment and glacier extent and to generate both plausible and implausible glacier configurations through the evolution of the model run. Through systematic perturbation of forcing factors, many different ice sheet configurations can be generated and each assessed for their degree of fit to empirical data. Controlled iteration of the model thus enables continual refinement of the output towards a 'best-fit' scenario. Some modelling studies employ sophisticated methods of margin-matching in order to accurately reproduce mapped glacial limits as closely as possible (e.g. Arthern & Hindmarsh, 2003; Tarasov & Peltier, 2004), but in contrast to our experiments, these other examples start with the *a priori* assumption that the empirical limits are correct. Here, we aim specifically to test the mapped limits, and thus avoid localised 'hand tuning' (Tarasov & Peltier, 2004, : p373). The sensitivity of our model to key parameters is gauged by the relative discrepancy between the results of each incremental parameter change and those of an optimum simulation. In this manner both the reliability and quality of model fit may be inferred, as well as the relative importance of margin mismatches. Above all, the model provides an important connection between theoretical glaciological processes and the nature of the observed landform record.

5.7 Results

5.7.1 Sensitivity tests

Each of the following experiments aimed to reduce the degree of mismatch between the best result of the previous experiment and the empirical record. This involved a considerable number of model runs and parameter iterations, commonly involving very small, incremental changes to individual parameters. Complex feedbacks within the climate system, however, preclude the possibility of completely isolating each parameter in turn, and thus the possibility remains that controlled changes to one variable may also produce unknown changes in another (e.g. changing temperature and its effect on precipitation). Thus, whilst they constitute an essential component of modelling methodology, and indeed, the only pragmatic option from a computational point of view, sensitivity experiments must be interpreted with some caution.

It is neither necessary nor practical to describe every configuration of model parameters that were tried; instead a key selection of the results from each experiment are presented, in order to convey overall patterns and trends. For the step cooling experiments (1 and 2), a model run of 1500 years was chosen, in order to broadly reflect the lifetime of the Younger Dryas. Where a scaled GRIP temperature forcing was employed (experiments 3-5), each model run was 4000 years, from 15 -11 ka (ice-core years) BP.

Experiment 1: Step cooling with present precipitation conditions

A suite of initial model runs aimed to establish the degree of influence exerted by the mass balance parameters on glacier location, volume, and area. In these experiments, a series of

MAAT step coolings of values consistent with those inferred from previous studies (Table 5.2) were applied across the model domain, using a modern precipitation distribution. Figure 5.3A shows ice conditions after 500 years under five different cooling scenarios. Under a 6°C cooling (compared to modern temperatures), the resultant ice masses are disparate and located only over the main mountain massifs, but with an 8°C cooling these ice centres are coalescent and form an extensive ice cap not entirely dissimilar to the 'Highland Readvance' glacier configuration proposed by Charlesworth (1955) ('Stage M', Fig. 5.1). With more severe cooling of 10°C, a considerable ice sheet develops over Scotland. Cooling in excess of 10°C results in complete glaciation of the entire landmass and coastal fringes. Figure 5.4A illustrates the growth trajectories of glacier area, volume, and mean thickness for each temperature scenario for the duration of the model run (1500 years). Under the 6°C cooling, the majority of ice accumulation occurs within the first 200-300 years, after which the glaciers appear to stabilise and continued expansion is very slow. With an 8°C cooling, glaciers expand quickly but continue to thicken when lateral expansion begins to slow, producing ice caps that do not reach equilibrium even after 1500 years. At colder temperatures both glacier area and volume initially increase rapidly but come close to steady state after 800-1000 years.

These results illustrate the sensitivity of the model to a step cooling, principally highlighting the strong influence exerted by topography on ice sheet growth. The results are somewhat at odds with the geometry of reconstructed LLR glaciers, particularly in central and southern areas, and thus require refinement.

Experiment 2: Step cooling with imposed precipitation gradients

In order to more closely replicate the empirical record of glaciation, the distribution of precipitation is modified through the imposition of west to east and south to north gradients. Systematically altering the latitudinal and longitudinal ranges within which these gradients operate provides an important additional control on mass balance forcing, enabling gradual iteration of the mass balance field towards one that produces a better fit (Fig. 5.3B). As with experiment 1, the results show comparatively restricted glacierization with a step cooling of 6°C, but with an 8°C cooling a coherent ice cap develops within 500 years. The impact of the imposed precipitation gradients is clearly apparent in the much altered spatial pattern of accumulation, and the main ice mass more closely resembles the Younger Dryas glacier configuration of the western Highlands (Fig. 5.1). Further cooling of 10-15°C ultimately tends toward complete terrestrial ice cover, with the imposed gradients producing a rather implausible west-skewed dome in an expansive ice sheet. The imposition of gradients with which to control the pattern of accumulation therefore appears to be effective over a range of temperature depressions, but functions most sensibly in these experiments within a narrow range (c. 8-10°C).

When precipitation distribution is controlled by the gradients described above, net ice volume at any given temperature depression is reduced, accumulation occurs at a slightly slower rate, and mean ice thickness also decreases (Fig. 5.4B). The latter becomes more evident at temperature depressions below 10°, due to the skewed volume-to-area distribution that occurs.

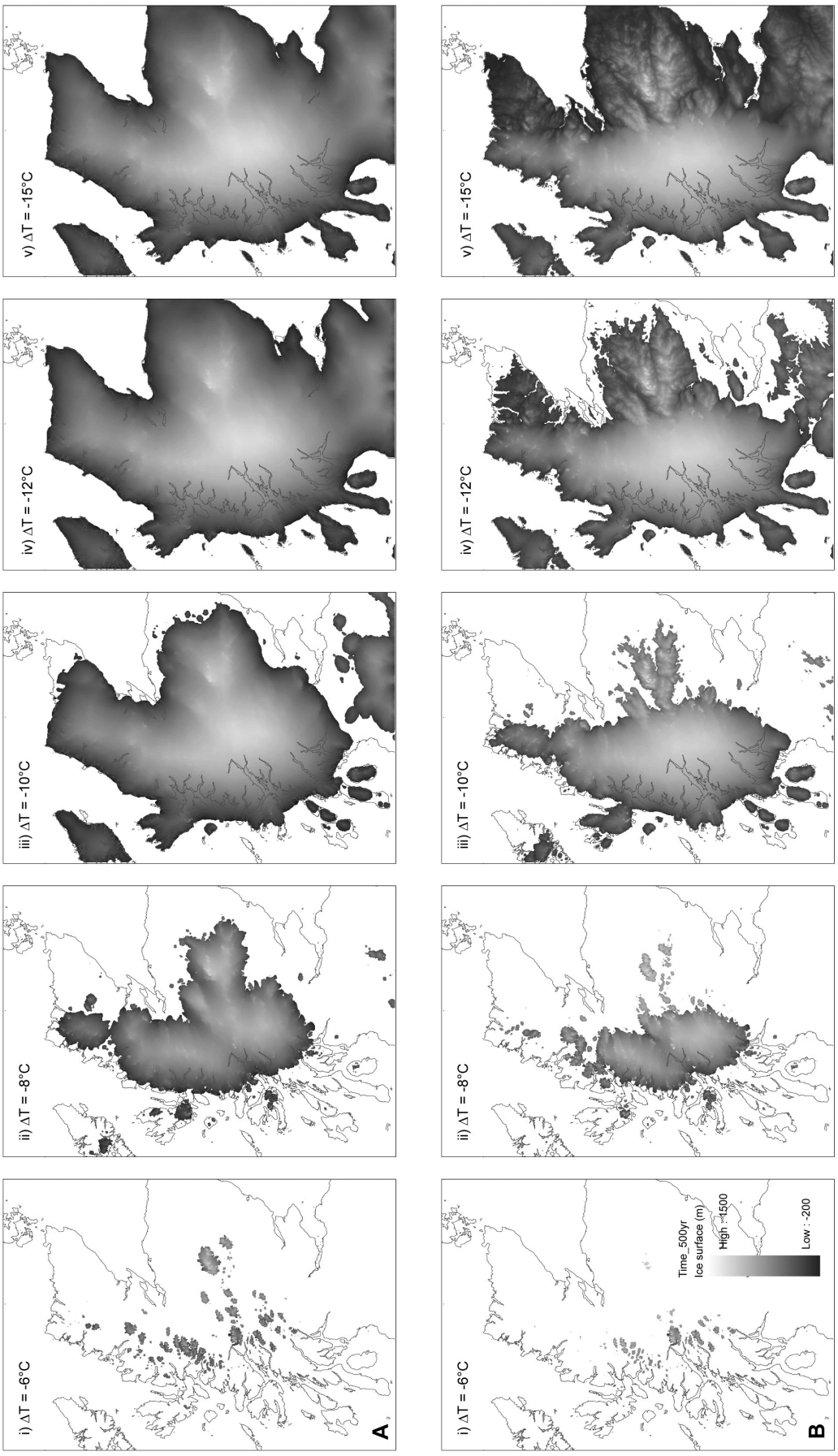

Figure 5.3: A: Ice extents resulting from 146 step coolings of 6 - 15°C under present precipitation conditions, and B: with imposed south-north and west-east precipitation reductions of 60% and 80% respectively, operating north and east of Rannoch Moor.

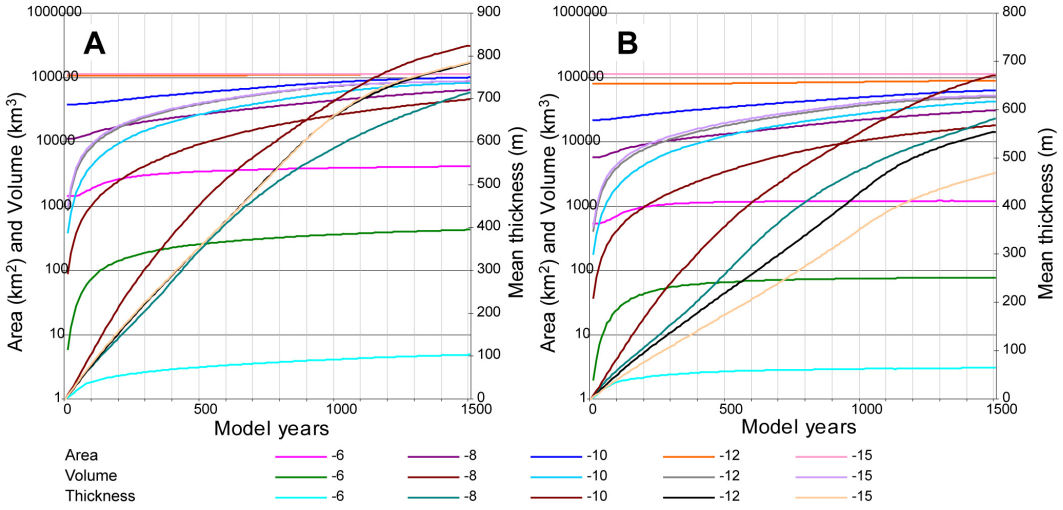

Figure 5.4: A: Ice extents, volumes and thicknesses resulting from step coolings of 6 - 15°C under present precipitation conditions, and B: with imposed south-north and west-east precipitation reductions of 60% and 80% respectively, operating north and east of Rannoch Moor.

Experiment 3: Scaled GRIP temperature depression

Step cooling experiments are useful in identifying the sensitivity of the model to both the amount of precipitation, and its distribution. However, the close correlation between the patterns of palaeoenvironmental changes in Scotland and those reflected in the GRIP ice core suggest that a uniform cooling throughout the Younger Dryas is not realistic. To better reproduce the likely climatic conditions affecting Scotland during the whole of the Lateglacial period, a time-series file representing ELA depression (relative to maximum conditions) was calculated from the 20-year GRIP δ^{18}O data (Johnsen *et al.*, 2001), based on the difference between a present value of -35‰ (Clapperton, 1997) and values in the period 11-15 ka BP. This 20-year temperature pattern was then used to force the model by scaling it according to the range of temperature depressions represented by the MAAT values inferred from the palaeoclimate studies in Table 5.2. The precipitation gradients imposed during Experiment 2 to restrict eastern glacier build-up are again applied in this scenario.

Figure 5.5A illustrates the effect on glacier build-up of GRIP-forced climatic variability scaled to a range of plausible palaeotemperature depressions. The time-slice shown is 2500 model years, broadly equivalent to 12.5 ka BP. Comparing these results with those produced under step-cooling scenarios (Fig. 5.3) it can be seen that temperature drops of 6°C and 8°C give rise to small ice masses located only over the higher hills, and generally only in the west of Scotland as a result of the imposed precipitation gradients. There is a clear difference between the results of 8°C step cooling and the GRIP experiment scaled to 8°C (Figs. 5.3 & 5.5A). This is due to the variability in ELA depression through the Younger Dryas; a climatic minimum was reached early in the stadial but was short-lived, and in fact the majority of the episode was slightly milder (Fig. 5.2). Consequently it is with a scaling factor of 10°C that the most reasonable glacier pattern develops, composed of a western ice cap along the main mountain chains and satellite icefields in Arran, Mull, Skye, Assynt and the central Highlands. Scaling factors greater than 10°C lead to excessive ice build-up at low altitudes and the growth of an

expansive ice cap or ice sheet that greatly exceeds the empirical limits.

Whilst the spatial extents of glaciers shown in Figure 5.5A may resemble those produced under step cooling conditions, Figure 5.6A dramatically illustrates the much more complex process of ice build-up that occurs under the GRIP-forced scenarios. Several trends are apparent in all of the runs:

1. ice accumulation occurs during the transition into the Lateglacial Interstadial from the Main Late Devensian 15 - 14.6 ka BP (0 - 400 model years), and is terminated by abrupt warming.

2. an ice-free period occurs from 14.6 - 14.2 ka BP (400 - 800 model years).

3. regrowth of ice occurs rapidly from 14.2 ka BP (800 model years), marking the beginning of a period of glacier fluctuation that lasts for 1200-1400 years during the latter half of the interstadial.

4. onset of the Younger Dryas at c. 13 ka BP (c. 2000 model years) is characterized by an expansion of ice that began accumulating during the preceding millennium.

5. rapid deglaciation occurs within a period of a few hundred years at the end of the Younger Dryas, leading to ice free conditions by 11.6 - 11.4 ka BP (3400 - 3600 model years) for the milder scenarios, and 11.4 ka BP (3600 model years) or later for more severe conditions.

In addition to these general patterns, the following aspects of glacier evolution can be inferred from Figure 5.6A. Temperature scalings of less than 10°C produce ice masses that seem unable to grow effectively, that is, accumulation during cold spells is quickly matched by ablation during periods of a rising ELA, resulting in little or no net increase in ice mass. Conversely, ice growth under temperature depressions greater than 10°C appears to continue throughout the warmer oscillations of the Younger Dryas, producing steady volumetric increases that are maintained by fluctuations in area and mean thickness. This implies the existence of a threshold in ice geometry, beyond which an ice mass is able to effectively buffer itself from climatic perturbations of the magnitudes occuring through the Younger Dryas. The ability to do this appears to lie in the control exerted by the interaction of topography and climate on the dynamic behaviour of an ice mass, leading to thickening in higher areas due to a greater likelihood of snowfall, whilst receding elsewhere where rainfall dominates. Indeed, the results show that at temperature scalings of less than 10°C , ice extent and volume decline steadily through the milder conditions of the mid – late stadial, whereas ice masses evolving under temperature scalings colder than this maintain considerably more stable extents over the same period.

In summary, the GRIP-forced model scenarios provide considerably more information on the dynamic nature of glacier evolution than the step-cooling experiments. They show a clear bifurcation in glacier behaviour between relatively mild conditions (temperature scaling $\leq$ 8°C) and more severe conditions (scaling $\geq$ 10°C).

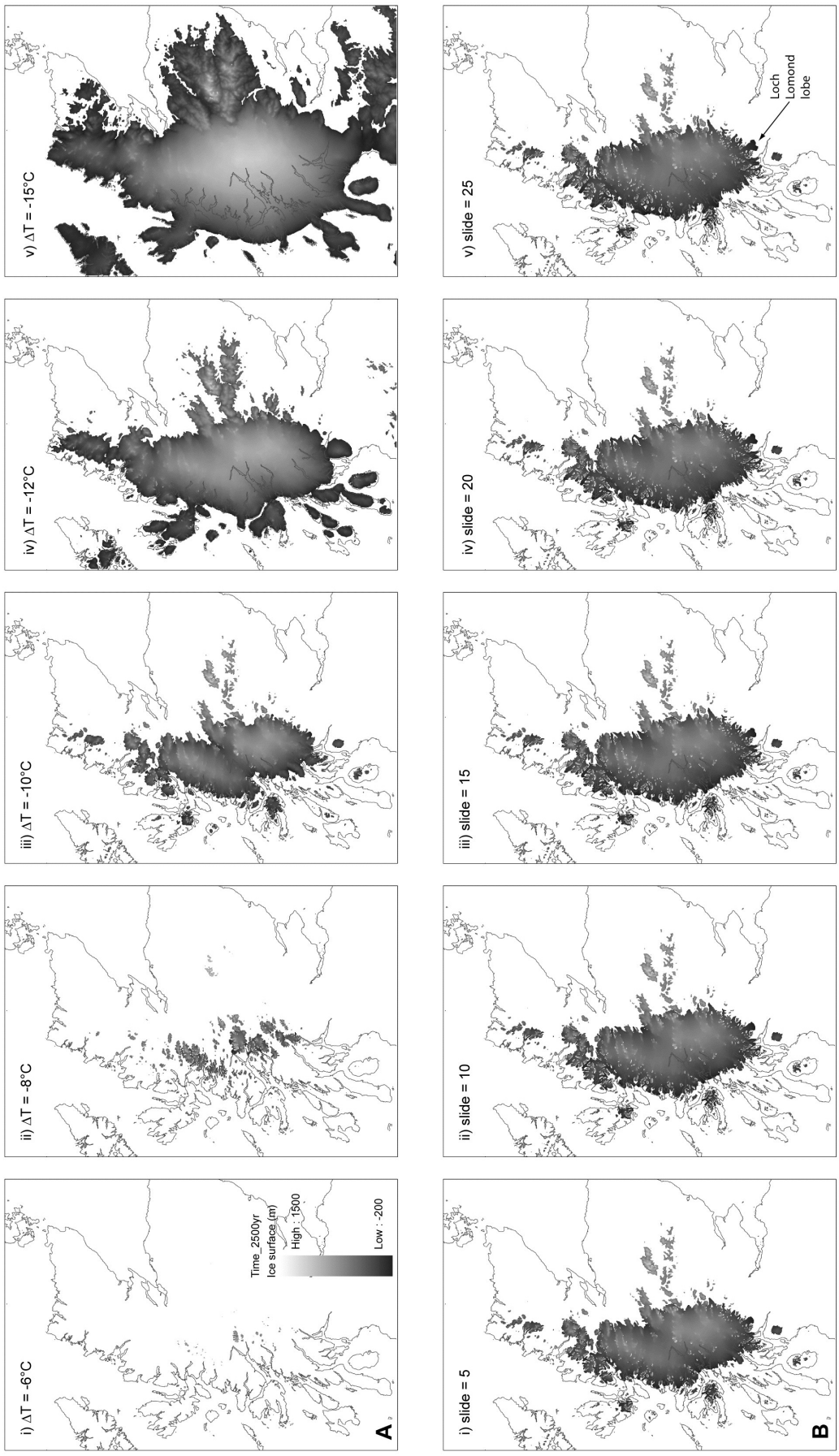

Figure 5.5: A: Ice extents resulting from 149 scaled coolings of 6 - 15°C applied to a 20-year resolution GRIP temperature pattern and using the precipitation reductions from Fig. 5.3B, and B: ice extents for a range of basal sliding conditions under a -10°C scaled GRIP pattern with imposed precipitation reductions.

Experiment 4: The role of basal sliding

Further experiments introduce variability in the sliding factor, (the ability of ice to move at its bed as well as through internal deformation), to determine the sensitivity of the model to glaciodynamic changes. Where basal sliding occurs, its effectiveness is linked to bed roughness, thus the higher the sliding factor, the greater the ease with which ice can flow over obstacles. Figure 5.5B illustrates the effect of a range of sliding factors on the geometry of the ice cap, using the precipitation gradients gleaned from Experiment 2 and the GRIP climate pattern from Experiment 3 at its optimum scaling of -10°C . The differences between runs are more subtle than in previous experiments, but consistent trends are nonetheless evident. Using the results of Experiment 3 (scaling = -10°C , sliding = 0) as a comparator, the scenarios shown in Experiment 4 show that an increase in basal sliding leads to:

1. greater horizontal spreading of the entire ice mass, producing more extensive ice cover of the domain.

2. thinner ice cover, with more nunataks becoming evident within the main ice mass.

3. more expansive outlet glaciers, for example the Loch Lomond glacier in the south of the domain.

4. further advance of terrestrial glaciers into low-lying areas, within the ablation zone.

5. greatly enlarged marine margin along the west coast, with outlet glaciers from the mainland beginning to coalesce with those on Mull.

The changes that occur as a result of enhanced basal sliding are more clearly seen in time-series plots of ice mass geometry (Fig. 5.6B). Through the model run, overall ice extent (shown by the 'area' plots) varies according to temperature depression, as expected. Interestingly, however, the largest differences between scenarios occur during relatively warm periods, when greatest ablation occurs. During cold phases, particularly during the Younger Dryas episode, total ice extent becomes remarkably consistent between all of the sliding scenarios. A similar pattern can be seen in the early phases of the ice volume plots, although differences increase beyond 3000 model years with higher sliding scenarios producing slower increases in total ice volume. Ice thickness data shows the effect of these different responses on ice mass evolution, with the highest sliding values producing the thinnest ice masses overall.

In summary, because ice masses with no basal sliding behave as non-linear viscous bodies deforming at a rate largely governed by their temperature, surface slope, and thickness, any increase in the amount of basal sliding greatly facilitates the lateral expansion of outlet glaciers. Higher sliding values produce greater velocities in outlet glaciers, which in turn steepen ice surface gradients towards accumulation areas and so increase local driving stresses. Consequently, ice flux from the interior is enhanced, leading to a more extensive but generally thinner ice mass than one moving by ice creep alone. Most importantly with respect to our aim of replicating empirical margins, the geometry of the simulated ice masses changes considerably with variation in sliding, most particularly in their overall thickness. In attempting to reproduce a main ice cap whose ice thickness agrees with empirical data, and whose outlet glaciers most closely match moraine limits, it is necessary to impose a sliding factor less than

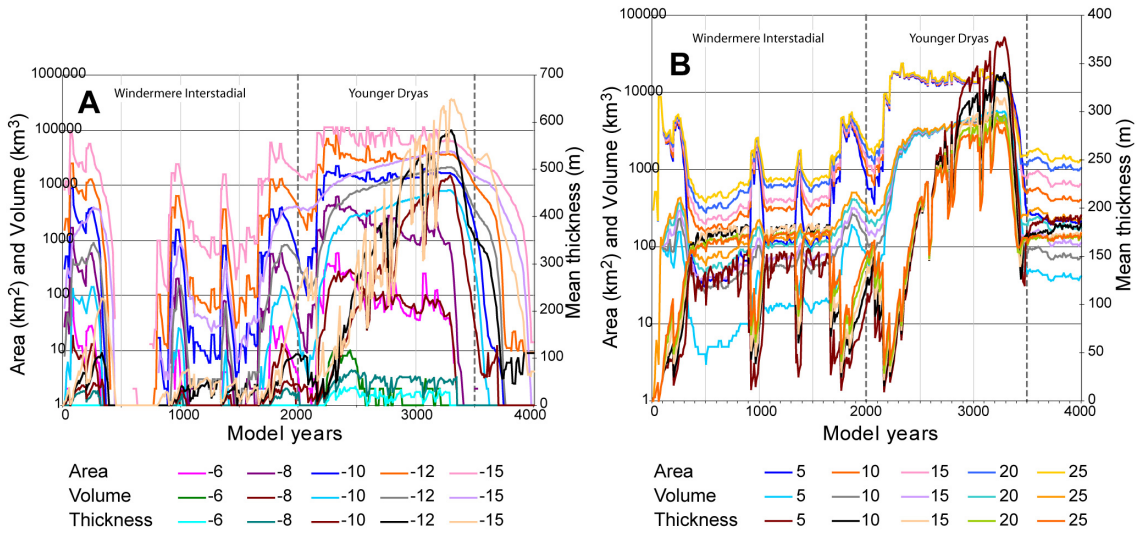

Figure 5.6: A: Ice extents, volumes and thicknesses resulting from scaled coolings of 6 - 15°C applied to a 20-year resolution GRIP temperature pattern and using the precipitation reductions from Fig. 5.3B, and B: ice extents, volumes and thicknesses for a range of basal sliding conditions using a scaled GRIP cooling of 10°C and imposed precipitation reductions.

five (Fig. 5.6B), but greater than zero (Fig. 5.6A).

Experiment 5: Optimum fit scenario

Iteration of the above parameters in a systematic and incremental manner allows the results of numerous experiments to be refined. For example, in Experiment 3, the initial precipitation boundary conditions led to a temperature-specific bifurcation in ice sheet growth. At the 10°C 'optimum' scaling, this bifurcation produces continued expansion of the main ice cap despite the overall warming trend in the scaled GRIP temperature field. The ice cap becomes increasingly focussed around the principal accumulation areas in the southwest of the domain, and begins to exceed the limits indicated by the landform record. Palaeoclimatic studies in Skye have shown that aridity may have played a key role during maximum stadial conditions, not only limiting glacier expansion but actually propagating deglaciation (Benn *et al.*, 1992). Consequently, in order to inhibit uncontrolled glacier expansion in our simulation we impose an additional stepped precipitation reduction for the remainder of the stadial (20% reduction at 2500 model years increasing to 50% reduction by 2700 model years, and returning to normal conditions by the close of the stadial) (Fig. 5.7A).

With the imposition of these final mass balance controls, an 'optimum fit scenario' is achieved in which model output throughout the run replicates as many of the empirical constraints as closely as possible, within the limits of model parameterization. The closeness of fit of the model through its evolution can be measured by grouping empirical reconstructions into broad climatic zones within the model domain, and by comparing these zonal areas with the simulated ice extents (Fig. 5.7B). Zone 1 represents strongly maritime areas, comprising Mull, Skye and Applecross. Zone 2 includes the northern icefields of Assynt and Beinn Dearg, Zone 3 is the main

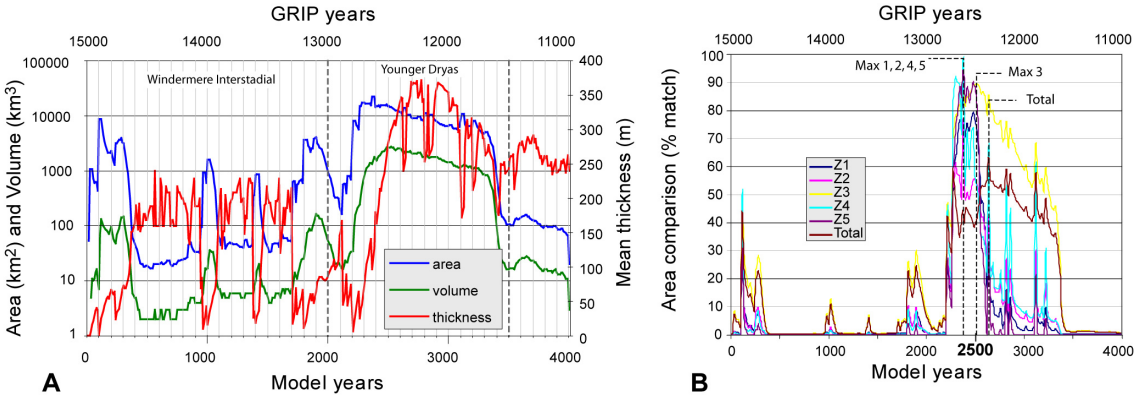

Figure 5.7: A: Ice growth under optimum conditions through the model run. B: Comparison of areal extent of modelled ice cover with empirical reconstructions in different parts of the domain. Note that satellite areas (Z1, 2, 4, 5) reach their best fit coeval with the GRIP climatic minimum c. 2450 model years (Fig. 5.2), whereas the main ice mass (Z3) achieves best fit slightly later, c. 2500 model years. 'Total' represents overall discrepancy between empirical reconstructions and modelled ice extent, across the entire domain. See text for explanation of zones.

ice cap, Zone 4 the more arid glaciers of the Central Highlands, and Zone 5 is the southernmost glacier complex on Arran. This simple technique gives an objective measure of model fit and enables 'best-fit' time slices to be identified (Fig. 5.7B).

Figure 5.8 shows the evolution of the ice cap during the Younger Dryas period (12.9 - 11.5 ka BP) under 'optimum' conditions. Initial ice build-up occurs in many disparate seed areas across the model domain that coalesce into coherent icefields relatively quickly. Away from the main ice centre, west coast icefields in the mountains of Arran, Mull, Skye, and Assynt reach their maximum extents relatively early in the stadial, close to the climatic minimum at around 12.6-12.7 ka BP (2300-2400 model years). Around this time, the icefields of the Western Highlands begin to coalesce and give rise to an ice cap whose geometry becomes increasingly elongate under the influence of the prescribed gradients focussing precipitation over the western Highlands. Continued evolution under the scaled GRIP climate leads to progressive thickening and expansion of the west Highland ice cap, with the majority of outlet glaciers reaching positions close to empirical limits by 12.5 ka BP (2500 model years), when the outlying icefields have already begun to retreat (Fig. 5.8). Since many of the empirical margins along the west coast of Scotland are now matched by the model almost exactly, as well as those in Wester Ross and Beinn Dearg (Fig. 5.9), we consider this the 'optimum fit' timeslice. Thin icefields are predicted over much of the central Highlands, consistent with empirical evidence, but few areas of thick glacier ice occur there.

In our experiments, we have achieved an optimum Younger Dryas simulation using:

1. a GRIP-forced temperature distribution scaled to a maximum mean annual temperature depression of 10°C

2. modern precipitation values for part of the west coast and western Highlands, modified with imposed south-north and west-east precipitation reductions of 60% and 80% respectively, operating north and east of Rannoch Moor

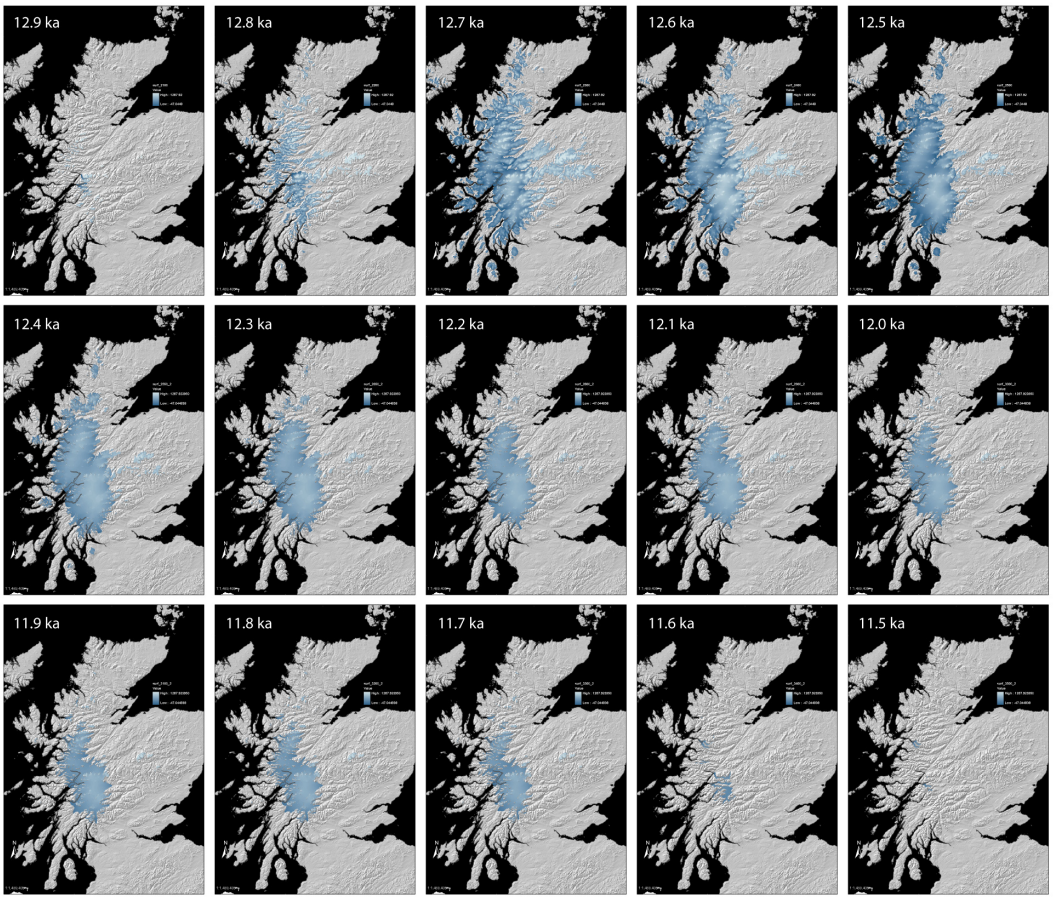

Figure 5.8: Timeslices from the optimum run, showing the build-up and decay of ice across the domain during the Younger Dryas, from 12.9-11.5 ka BP (2100 - 3500 model years). Note how ice build-up is initially characterized by disparate icefields which later coalesce to form a coherent ice cap. Mid-stadial aridity leads to net marginal recession, but with local expansion of some outlet lobes, such as Loch Rannoch. Final deglaciation occurs rapidly after 11.7 ka BP.

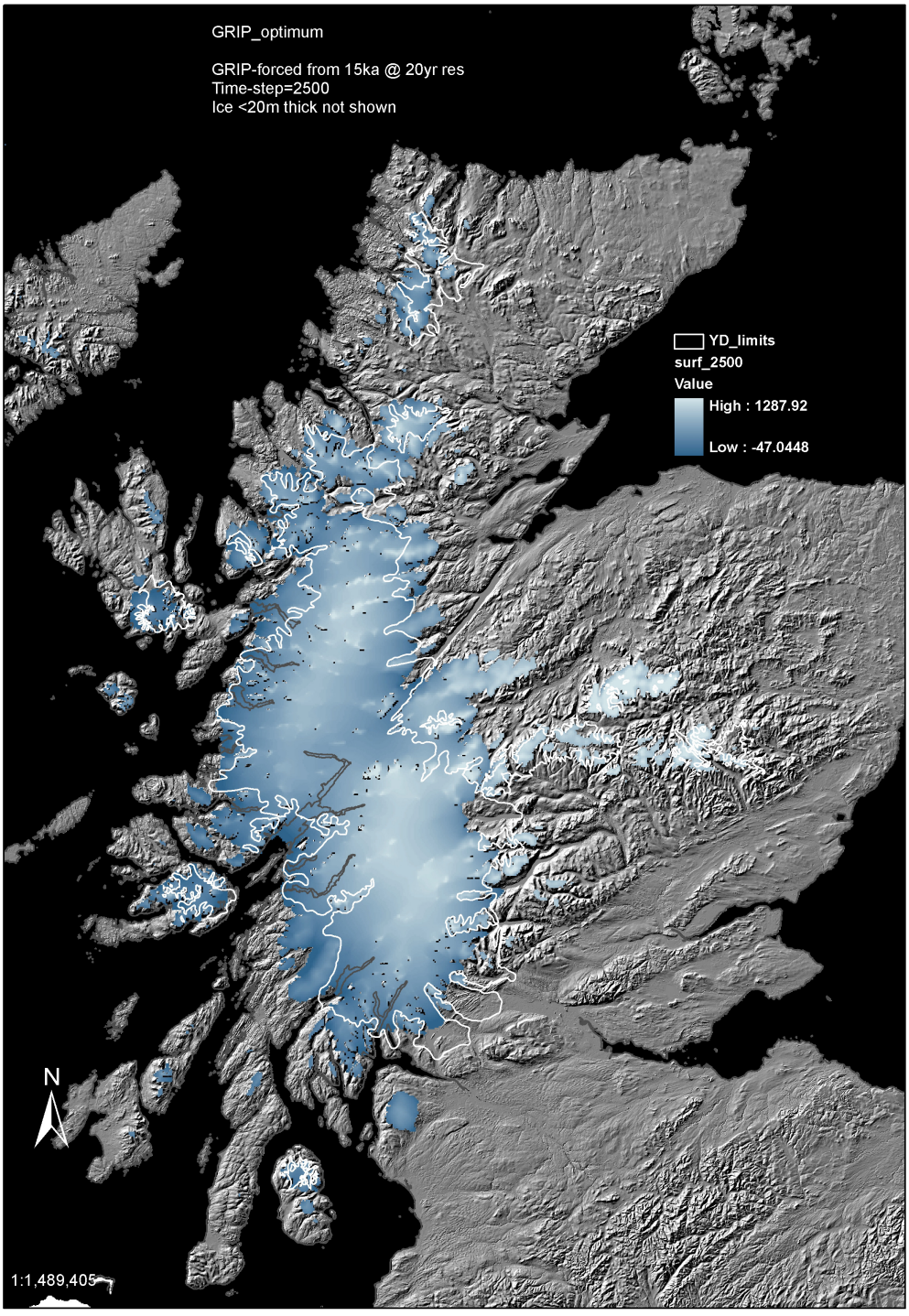

Figure 5.9: Ice extent after 2500 model years - the 'optimum fit' for the majority of Younger Dryas ice masses in the domain. Most satellite icefields are at their maximum extent, and many outlet glaciers of the main ice cap are also close to their empirical terminal limits. Margins in the east and south achieve their maximum configurations somewhat later, prior to rapid deglaciation. Ice surface height values include isostatic depression.

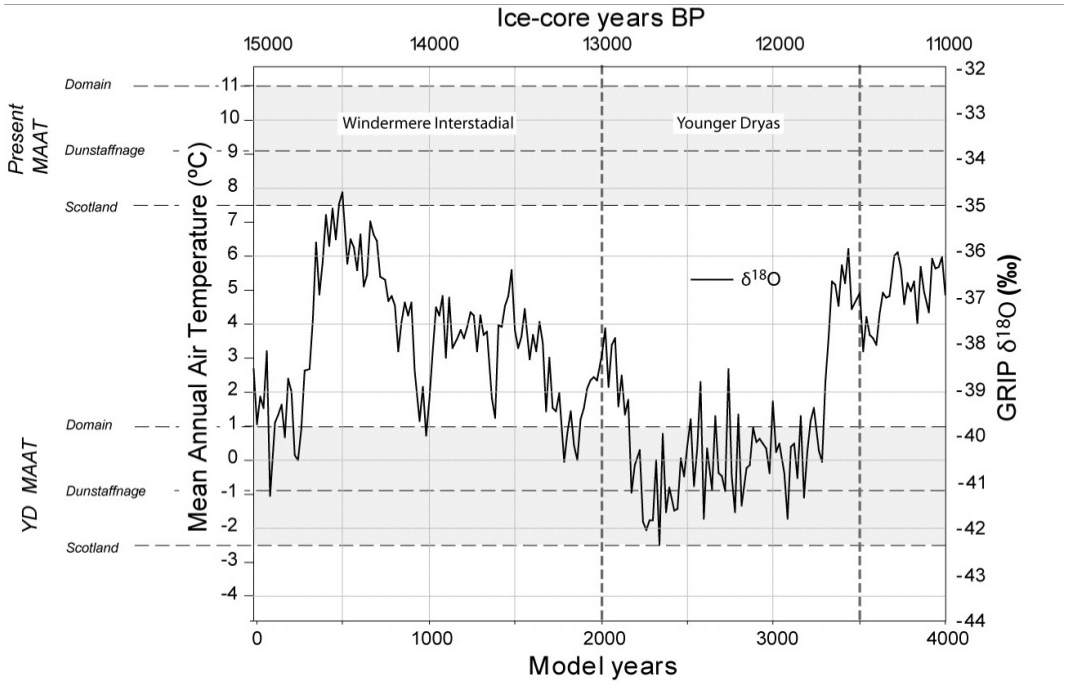

Figure 5.10: Optimum-fit scaled oxygen isotope record showing equivalent mean annual Scottish palaeotemperatures during the period 15 - 11 ka BP (0 - 4000 model years), from the GRIP ice core in central Greenland (from Johnsen *et al.*, 2001).

3. low basal sliding (sliding factor = 2)

4. an additional stepped reduction in precipitation across the domain at the height of the stadial, from 12.5 - 12.0 ka BP, gradually returning to present values by the end of the stadial.

The series of sensitivity tests demonstrate that the region of parameter space within which the 'best-fit' occurs is remarkably small. Experiments 1-3 show that the optimum temperature depression occurs within a range of 1-2°C (approximately the same as the likely error in the PDD mass balance model), optimum precipitation occurs only in a range of ± 5% mean annual volume, and basal sliding is prescribed to between zero and five. The sensitivity experiments show that parameter variability beyond these ranges produces ice masses that compare less well with empirical reconstructions.

Having systematically iterated the model by perturbing mass balance and dynamic parameters we have reproduced a pattern of ice extent that closely reflects empirical limits. The experiments have highlighted the manner in which ice masses evolve differently under different climate scenarios, and have shown the degree of influence that dynamic controls such as basal sliding exert on overall geometry. Despite some areas of local mismatch, the degree of overall fit is encouraging, and lends confidence to palaeoclimatic inferences drawn from the model. In particular, we are now able to retrodict likely mean annual air temperatures for the Lateglacial period, based on the scaling factor we applied to the GRIP δ^{18}O ice core data (Fig. 5.10).

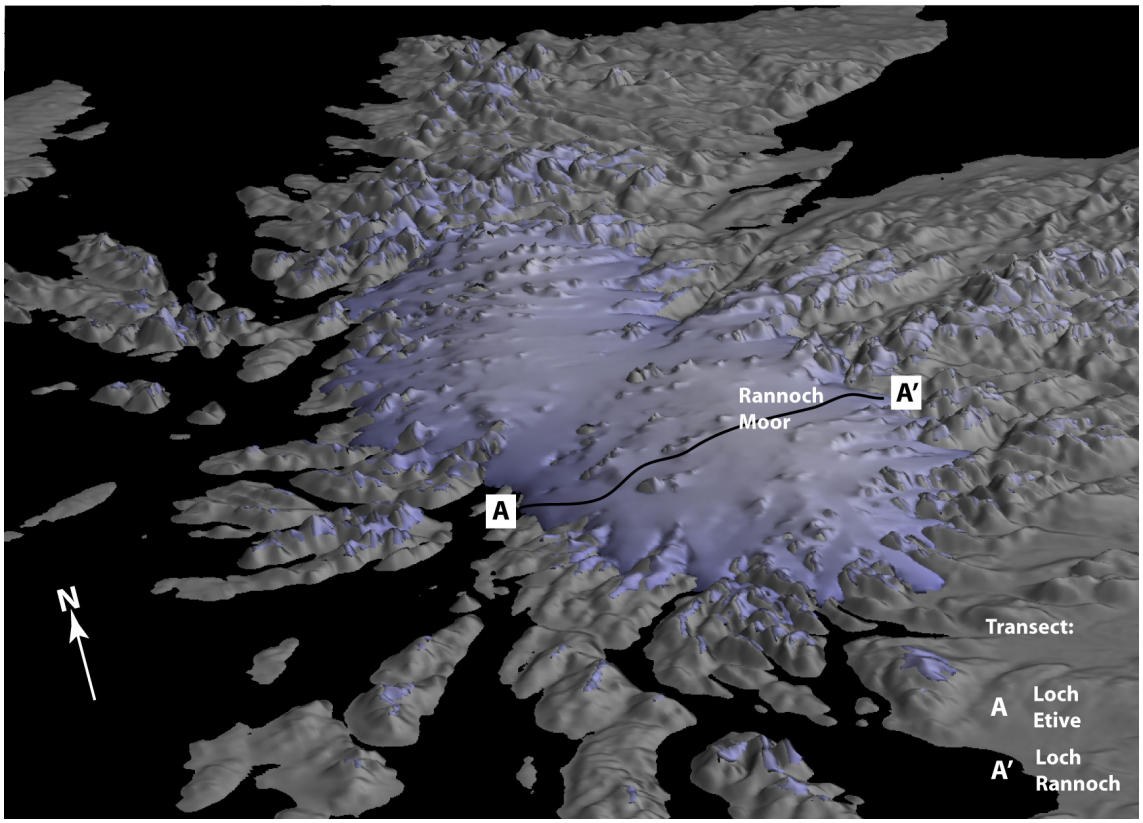

Figure 5.11: Perspective view of the 'optimum fit' scenario ice surface overlain on present topography. Note the low, domed surface of the main ice cap feeding radial outlet glaciers, and the presence of satellite icefields in Mull, Skye and the Northern Highlands. Transect line shows location of Fig. 5.12. Vertical exaggeration x5.

5.8 Discussion

Recent empirical studies have shown that the Younger Dryas ice mass south of Rannoch Moor left a landsystem fingerprint consistent with that of a domed ice cap feeding steep outlet glaciers (Golledge & Hubbard, 2005; Golledge, 2006, 2007a). Such a scenario appears to be consistent with the simulated form of the west Highland ice cap at maximum conditions (Fig. 5.11). A major ice dome over Rannoch Moor is coalescent with a lower ice centre north of the Great Glen, together defining an elongate ice shed along the west Highland mountain chain that dominates the geometry of the ice cap. These central accumulation areas feed outlet glaciers that drain along the main valleys around the periphery of the ice cap, mostly terminating on land but with some tidewater margins along the west coast from Loch Torridon in the north to Loch Fyne in the south. The model predicts total calving losses during the height of the stadial of 1-2 km^3a^{-1}, of which approximately half is generated by the c. 7 km wide calving front in Loch Linnhe. Although our calving function is relatively crude, these results nonetheless demonstrate that this former glacier clearly played a key role in ice discharge from the central area of the main ice cap, and was probably also instrumental in sediment transport to the coast and the generation of ice-rafted debris.

During the stadial, our model predicts that the geometry of the main ice cap evolves in

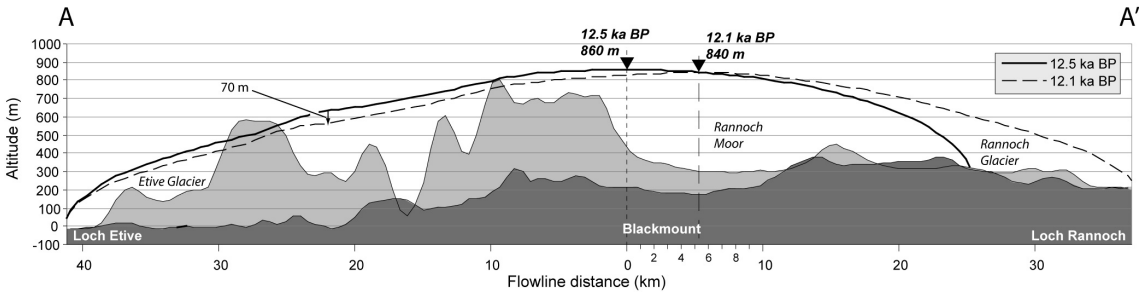

Figure 5.12: Cross-profile through the central portion of the Younger Dryas ice cap along the transect shown in Fig. 5.11. Note the change in geometry between 12.5 and 12.1 ka BP, characterised by an eastward migration of the ice divide, greater extension of the Rannoch Glacier, and a surface lowering of the Etive Glacier. Dark shading illustrates topography along the flowline, light shading indicates surrounding relief.

response to mass balance and glaciodynamic changes. A transect across the ice from west to east shows how the initial asymmetry of the ice cap changes through the stadial, as ice that had accumulated in western mountain areas subsequently converges as it flows eastward, fills Rannoch Moor, and begins to discharge via Loch Rannoch (Fig. 5.12). The Rannoch Glacier reaches its maximum extent around 12.1 ka BP, advancing at a mean rate of 25 ma^{-1} through the preceding 400 years. Significantly, the advance of the Rannoch Glacier occurred mid-stadial, when aridity and gradual temperature rise leads many other margins to recede (Fig. 5.8). Thus its appears that the glacier responded to an internal mass balance forcing that produced climatically asynchronous behaviour. Convergent flow in the catchment of this glacier, together with its dynamic, internally forced, advance, perhaps indicates that the Rannoch Glacier played a similar mass balance role in the Younger Dryas ice cap to that of modern ice streams in contemporary ice sheets. During this advance, the ice divide over Rannoch Moor migrates more than 5 km eastward, leading to 50-70 m surface lowering of the Etive Glacier.

Although many areas of the model domain accurately simulate empirical glacier limits, some areas are less well-matched. Three distinct areas stand out: Kinlochewe and Loch Fannich in the far north, the Monadhliath Mountains to Glean Spean in the central Highlands, and the southeastern limits from Loch Rannoch to Loch Lomond (Fig. 5.13).

Around Kinlochewe and Loch Fannich the optimum model run predicts less ice than the empirical limits would suggest (Fig. 5.13A). Bennett & Boulton (1993a) reconstructed a coherent margin from Achnasheen northward to Loch Droma, implying that ice sourced on the hills north of Loch Fannich was coalescent with that accumulating around Torridon. By contrast, the model shows that ice accumulation on the higher ground is insufficient to infill the wide expanse of low ground that exists in this area, which effectively forms a through-valley from Loch Maree to the Cromarty Firth at Dingwall. Intriguingly the geomorphological evidence presented by Bennett & Boulton (1993a) (p138, Figure 7) shows that evidence for glacier margins is sparse in the low area north of Achnasheen, restricted in fact to a series of moraines west of Loch Fannich with no obvious source area. The survival of moraine and delta complexes around the Achnasheen lobe (Benn, 1996) has been used to constrain the geometry of former glaciers in this area, but since they remain undated it is uncertain as to whether the model is in error in this region or not.

The Monadhliath Mountains form an extensive area of upland plateau between Loch Ness and the Cairngorm Mountains (Fig. 5.13B), but despite the size of the area only a very limited amount of palaeoglaciological work has been undertaken in the area, largely by research students (e.g. Finlayson, 2004, 2006; Gyte, 2004). The model predictions for this area suggest that extensive ice cover of the plateau is likely to have occurred during the Younger Dryas, simply as a function of its high altitude and broad summit area (cf. Manley, 1955). Much of the snow may have been redistributed by wind, and thus it seems plausible that valley glaciers draining the high ground would have been adequately nourished to achieve extents comparable to the model simulation. However, there is considerable evidence for the former existence of glacial lakes in Glen Gloy, Glen Roy, and Glen Spean during the Younger Dryas (Sissons, 1977, 1978, 1979a; Peacock & Cornish, 1989), which our model cannot predict. Thus whilst the possibility exists that there was a greater extent of ice in the area than currently mapped, it was most likely sourced from an icefield on the Monadhliath plateau that was kept separate from the western ice cap by the presence of proglacial or intralobe lakes.

Numerous glaciers drained the southeastern side of the Younger Dryas ice cap, and their limits have been the source of several differing interpretations (Thompson, 1972; Sissons *et al.*, 1973; Horsfield, 1983; Thorp, 1986). Our model shows (above) that the Rannoch Glacier reaches its limit relatively late in the stadial, but modelled glacier configurations show significant shortcomings at Callander, Menteith and Loch Lomond, and an overprediction at Loch Tay (Fig. 5.13C). Limits in Glen Lyon and Balquhidder are fairly close to empirical limits. The glacier occupying Loch Lomond reached its maximal limit south of the loch some time after 12.5 ka BP (Rose *et al.*, 1988), but is underestimated by 10-12 km in our model. Other limits have less temporal constraint, however. In particular, the presumed limit at Callander (Thompson, 1972) is bracketed by dates at Torrie of 15.1 ka BP and at Mollands of 12.7 ka BP (Lowe, 1978; Merritt *et al.*, 1990) (Fig. 5.2), suggesting that ice actually receded *prior* to the Younger Dryas. Although radiocarbon dates in recently deglaciated areas are commonly considered 'too old' due to mineral carbon contamination (Lowe & Walker, 1980; Sutherland, 1980), in other areas they appear to be reliable (Sissons, 1967b; Rose *et al.*, 1988). If the Callander dates are in fact correct, they imply that the limit identified by Thompson (1972) relates to an earlier glacier, and thus the model may indeed be correct.

These three areas of mismatch are persistent features of the model, occurring across a breadth of parameter space far greater than the narrow 'optimum' range identified from the sensitivity tests (e.g Figs. 5.3 & 5.5). We consider several possibilities to explain the discrepancies. Firstly, the lack of fit may be a result of model limitations, such as topographic smoothing, grid resolution, or simplifications of the physics governing ice flow. If this were the case, however, it would seem likely that the model would not achieve the closeness of fit that it does elsewhere. Second, it could be that the model is incorrectly parameterised, but this again seems unlikely given the degree of fit across the majority of the domain. Thirdly, our experiments run from initially ice-free conditions, and so may underestimate ice volumes in areas where large ice masses may have been inherited from deglaciation of the Main Late Devensian ice sheet. However, this would be most likely to occur in highland areas in the north, being colder, and yet the largest mismatches occur mainly in low areas in the south where ice survival is least likely. Another possibility is that local factors (that our model does not accomodate) exert a significant influence on glacier geometry. For example, the local presence of a highly deformable bed or large body of water may greatly reduce basal drag and thus increase sliding

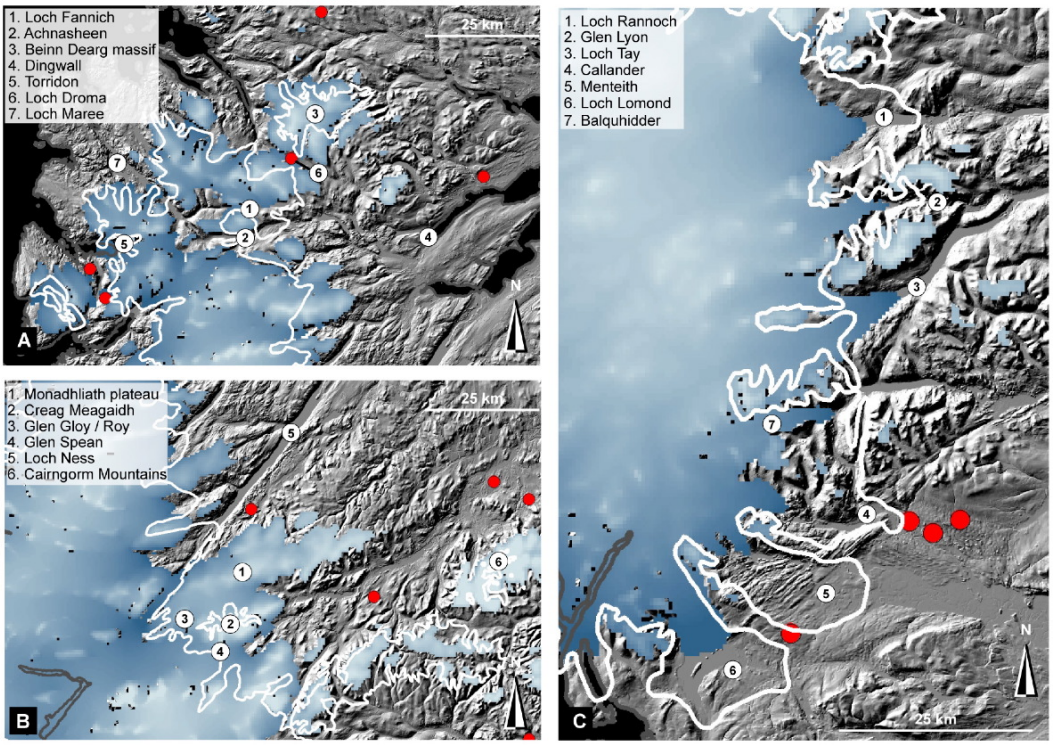

Figure 5.13: A: The area around Loch Fannich, showing model predictions compared with the empirical reconstructions (white line). Time step is 2450 years. B: The Monadhliath mountains in the Central Highlands, showing extensive plateau ice not previously mapped. Time step is 2450 years. C: The southeast sector of the main Younger Dryas ice cap, showing mismatches around the Loch Lomond, Menteith and Callander lobes. Time step is 2650 years.

beyond the value prescribed in the experiments. Our topographic grid does not incorporate loch bathymetry, and with Loch Lomond reaching almost 200 m depth at its deepest, this may be the most likely source of mismatch in this particular area. The former Loch Lomond lobe was, however, relatively thin at its maximal extent, so although the model underpredicts its area, there may be less error in terms of total ice volume. A final consideration is that some of the empirical limits may have been misinterpreted, either in terms of their age, or with respect to the way in which landforms have been used to reconstruct and extrapolate former ice margins. Given the very localised nature of our mismatches with the empirical evidence, we consider a combination of these last two factors most likely.

5.8.1 Synthesis

In attempting to simulate the extent of glaciers during the Younger Dryas stadial we have gained considerable insight into the nature of ice-mass evolution in Scotland during the Lateglacial period, and the likely climatic regime that prevailed. Our model predicts that climatic deterioration during the Older Dryas (c. 14.5-13.7 ka BP) could result in the gradual build-up of ice, but is followed by recession during the initial stages of the Allerød (c. 13.7-13.1 ka BP). Subsequent regrowth of ice leads to widespread glacierization during the Younger Dryas, reaching most empirical limits by c. 12.5 ka BP. Maximum ice volume was achieved early in the stadial, after which increasing aridity leads to gradual thinning and incremental recession of many of the ice cap margins. During this period, however, the eastward-flowing Rannoch Glacier advances at a rate of 25 ma^{-1} and alters the geometry of the ice cap sufficiently to produce a net thinning of westward-flowing glaciers such as the Etive Glacier. Very rapid deglaciation takes place at the end of the stadial, resulting in the loss of approximately 1000 km^3 ice in 100 years from c. 11.7 - 11.6 ka BP, after which only small patches of inactive ice remain. The volume of melt generated during this rapid collapse of the ice cap probably led to significant jökulhlaup activity (cf Russell *et al.*, 2003), considerable glaciofluvial erosion and sediment transport, and could have produced a sustained annual freshwater input to the oceans of around 9 billion litres per year.

Our simulation also presents a testable model for areas where empirical data is either lacking or ambiguous. For example, Fig. 5.9 predicts the existence of numerous satellite icefields and glaciers beyond the margins of the main ice cap, which in areas such as the Monadhliath and Cairngorm Mountains are far more extensive than previously recognised. It is therefore hoped that the 'optimum fit' simulation presented here may stimulate further palaeoglaciological investigations in Scotland, by offering testable glacier limits for areas where empirical data is, at present, limited. Further modelling research may be able to refine the simulation presented here, perhaps by employing a more realistic calving function, incorporating modern lake bathymetry, modelling the growth of proglacial lakes, and by adjusting the degree-day scheme to allow for greater seasonal temperature variation.

5.9 Conclusions

We have used a three-dimensional thermomechanical ice sheet model to simulate the likely glacier configuration of the Younger Dryas episode in Scotland at a higher resolution than previously possible. By systematic perturbation of the parameters governing ice accumulation and subsequent movement we have been able to accurately reproduce many of the glacier limits suggested by empirical reconstructions based on field evidence. The narrow range of parameter values that allow a simulation showing close agreement with empirical limits suggests that the model is sensitive to mass balance and dynamic perturbations. The good degree of overall fit between modelled and mapped ice margins is encouraging. Where areas of significant mismatch have been highlighted, they are most likely attributable to local variables not accomodated by the model, errors in the interpreted age of some moraines, or the presence of pre-existing ice.

These local uncertainties aside, the optimum-fit model simulation predicts that ice accumulation begins during the close of the Lateglacial Interstadial, and accelerates into the Younger Dryas achieving maximal glacier extents in the period 12.6 - 12.4 ka BP. Terminal positions in the north and west are reached earlier than those in the south and east. Basal sliding plays a limited role in Younger Dryas glacier movement in Scotland, but may have been locally enhanced where beds of easily deformable sediments occur, or where bodies of water were present. Our model predicts that mean annual temperatures at the height of the glacial phase were approximately 10°C lower than the Lateglacial interstadial, and precipitation was strongly focussed along the western Highland mountain chain. Modelled aridity is necessary in central and eastern Scotland in order to restrict ice build-up throughout the stadial, whereas the west probably only became influenced by a drier climate after c. 12.5 ka BP.

PAPER VII

Mass balance, flow, and subglacial processes of a modelled Younger Dryas ice cap in Scotland

Nicholas R. Golledge[1,2], Alun Hubbard[3] and David E. Sugden[2]
[1]British Geological Survey, Murchison House, West Mains Road, Edinburgh, EH9 3LA*
[2]Institute of Geography, University of Edinburgh, Drummond Street, Edinburgh, EH8 9XP
[3]Institute of Geography & Earth Sciences, The University of Wales, Aberystwyth, Penglais Campus, Aberystwyth, Ceredigion, SY23 3DB

email n.golledge@bgs.ac.uk, *phone* +44 131 6671000.
ph: +44 131 667 1000, fx: +44 131 668 1535, email: n.golledge@bgs.ac.uk

Abstract

We use an empirically validated high-resolution three-dimensional ice sheet model to investigate the mass balance regime, flow mechanisms, and subglacial characteristics of a simulated Younger Dryas stadial ice cap in Scotland, and compare the resulting model forecasts with geological evidence. Input data for the model are basal topography, a temperature forcing derived from GRIP δ^{18}O fluctuations, and a precipitation distribution interpolated from modern data. The model employs a Positive Degree Day scheme to calculate net mass balance within a domain of 112500 km^2, which under the imposed climate gives rise to an elongate ice cap along the axis of the western Scottish Highlands. At its maximum, the ice cap is dynamically and thermally zoned, reflecting topographic and climatic controls respectively. In order to link these palaeoglaciological conditions to geological interpretations, we calculate the relative balance between sliding and creep within the simulated ice cap; forecast areas of the ice cap with the greatest capacity for basal erosion; and predict the likely pattern of subglacial drainage. We conclude that ice flow in central areas of the ice cap is a largely due to internal deformation, and is associated with geological evidence of landscape preservation. Conversely, the distribution of streamlined landforms is linked to faster-flowing ice whose velocity is predominantly the result of basal sliding. The geometry of the main ice mass focusses subglacial erosion in the mid-sections of topographic troughs, and produces glaciohydraulic gradients that favour subglacial drainage through low-order arterial routes.

5.10 Introduction

The Younger Dryas cold episode (12.7–11.5 ka BP, Alley, 2000) was marked in the Northern Hemisphere by the expansion of the Laurentide and Fennoscandian ice sheets, and by a partial regrowth of the British Ice Sheet (Sutherland, 1984a; Mangerud, 1991; MacAyeal, 1993). Understanding the evolution of these former ice sheets helps appreciation of contemporary ice masses and their likely behavioural response to future climate change scenarios. Attempts to reconstruct former glaciers commonly focus on the identification and interpretation of empirical (geological) data within a relatively small area, and permit only local-scale interpretations of glaciers either at their maximum extent or during their retreat. In Scotland this geological approach is complicated by the variable overprinting, reworking or complete removal of landforms relating to the Main Late Devensian ice sheet by those of the much smaller, later, Younger Dryas ice cap (e.g. Golledge, 2006). Consequently, geological studies are commonly hampered by their limited ability to accurately constrain marginal contemporaneity, and so struggle to evince details of glacier mass balance or flow characteristics. Numerical modelling of glaciers and ice sheets allows insight into these areas, by simulating ice masses and their governing climates and most importantly, by enabling the interpretation of glacier evolution through a glacial episode (e.g. Siegert & Dowdeswell, 2004). This temporal element is of great importance when trying to identify and differentiate dynamically and climatically forced margin oscillations, and promotes a more complete understanding of the surviving geological record.

Despite the clear benefits of a combined geological and modelling analysis, previous attempts at numerical simulations of Younger Dryas glaciers in Scotland are relatively uncommon (e.g. Payne & Sugden, 1990; Hubbard, 1999), and rarely incorporate explicit field data. In order to address such shortcomings, Golledge *et al.* (2008a) presented an empirically validated ice sheet model for Scotland for the Lateglacial period (15-11 ka BP). In this article we aim to:

1. explore the mass balance regime of the modelled ice cap during its evolution
2. calculate the balance between flow by internal deformation and flow resulting from basal sliding, and its spatial variability, during the height of the Stadial
3. calculate the likely pattern of erosion potential of the modelled ice cap and identify areas where greatest basal erosion might occur
4. predict the spatial organisation of subglacial hydrology beneath the ice cap
5. compare these model results with empirical evidence in western Scotland in order to more confidently link geological features with former glaciological conditions

5.11 The Model

The three-dimensional finite-difference ice sheet model uses algorithms developed and validated by Hubbard (1999) and Hubbard *et al.* (2005, 2006). For the experiments presented here, this thermomechanical model uses a domain of 300 x 375 km, with basal topography at 500 m horizontal resolution derived from Intermap's 1.2 m vertical resolution NextMAP terrestrial elevation data and British Geological Survey 10 m vertical resolution marine bathymetric data.

Mean annual air temperature and mean annual precipitation are calculated from the United Kingdom Climatic Impacts Programme (UKCIP) dataset (Perry & Hollis, 2005), which provides 5 km resolution data for the entire United Kingdom (UK), interpolated from a national network of 3500 weather stations. Whilst recognising the benefits of integrating ice sheet models with atmospheric general circulation models (AGCM), we consider this high-resolution, locally derived, UKCIP dataset to be more suitable as input data than climatic parameters derived from the relatively coarse AGCMs, which are more suitable for use in hemispheric-scale ice sheet modelling (e.g. Siegert & Dowdeswell, 2004). Use of linear interpolations of climate trends between individual 'snapshots' has undoubtedly facilitated greater integration of AGCMs with ice sheet models, but in some cases such generalisation completely removes short-lived climatic events such as the Younger Dryas (e.g. interpolation between timeslices at 15 ka and 9 ka BP of Charbit *et al.*, 2002). Use of local-scale data is thus preferable for these experiments, but introduces the possibility that quite different model scenarios may result if other climate forcings are used.

An elevation-related Positive Degree Day (PDD) scheme drives mass balance by calculating annual accumulation and melt through integration of the snow – rainfall ratio, the amount of refreezing, and the net altitude-related snow balance, following Laumann & Reeh (1993). Input temperatures are computed using a sinusoidal annual temperature variation fluctuating within a range, and from a mean annual temperature, derived from the UKCIP dataset. Precipitation is distributed evenly through the year. Use of a PDD scheme such as this, in preference to a full energy-balance algorithm, is the only pragmatic option where palaeo-data for the latter are lacking (e.g. long- and short-wave radiation balance, wind flux, albedo etc). We further modify accumulation and ablation patterns by imposing eastward and northward precipitation reductions away from the main ice mass, of 80% and 60% respectively (Golledge *et al.*, 2008a). Variations in GRIP 20-year resolution δ^{18}O data (Johnsen *et al.*, 2001) are used to define the pattern of temperature fluctuation in the model domain, which is scaled to Scottish palaeotemperatures by analogy with modern isotopic values in Greenland (Clapperton, 1997) (Figure 5.14).

Use of the GRIP temperature pattern as a suitable proxy from Scotland is supported by the close similarity between temperature trends observed in its isotopic variations and those inferred from palaeoecological proxies in the UK (Atkinson *et al.*, 1987; Kroon *et al.*, 1997; Brooks & Birks, 2000). Furthermore, palaeoglaciological studies in Ireland have established that glacier fluctuations there were broadly consistent with isotopic trends evident in the GRIP record during the Younger Dryas, despite being out-of-phase prior to c. 17 ka BP (Knight, 2003). Spatial variability of modelled surface temperatures and precipitation inputs across the domain at the height of the Stadial is shown in Figure 5.15.

Net mass balance (b) is related to the three-dimensional evolution of the ice cap through time (t) through the equation for the conservation of mass, based on the assumption that ice is incompressible:

$$\frac{\partial H}{\partial t} = b - \nabla \cdot (H\bar{u}) \,, \tag{5.1}$$

where H is ice thickness, t is time, $\bar{u}$ is the vertically averaged horizontal velocity, and ∇ in this instance represents the ice flux between adjacent nodes minus surface mass balance. Ice

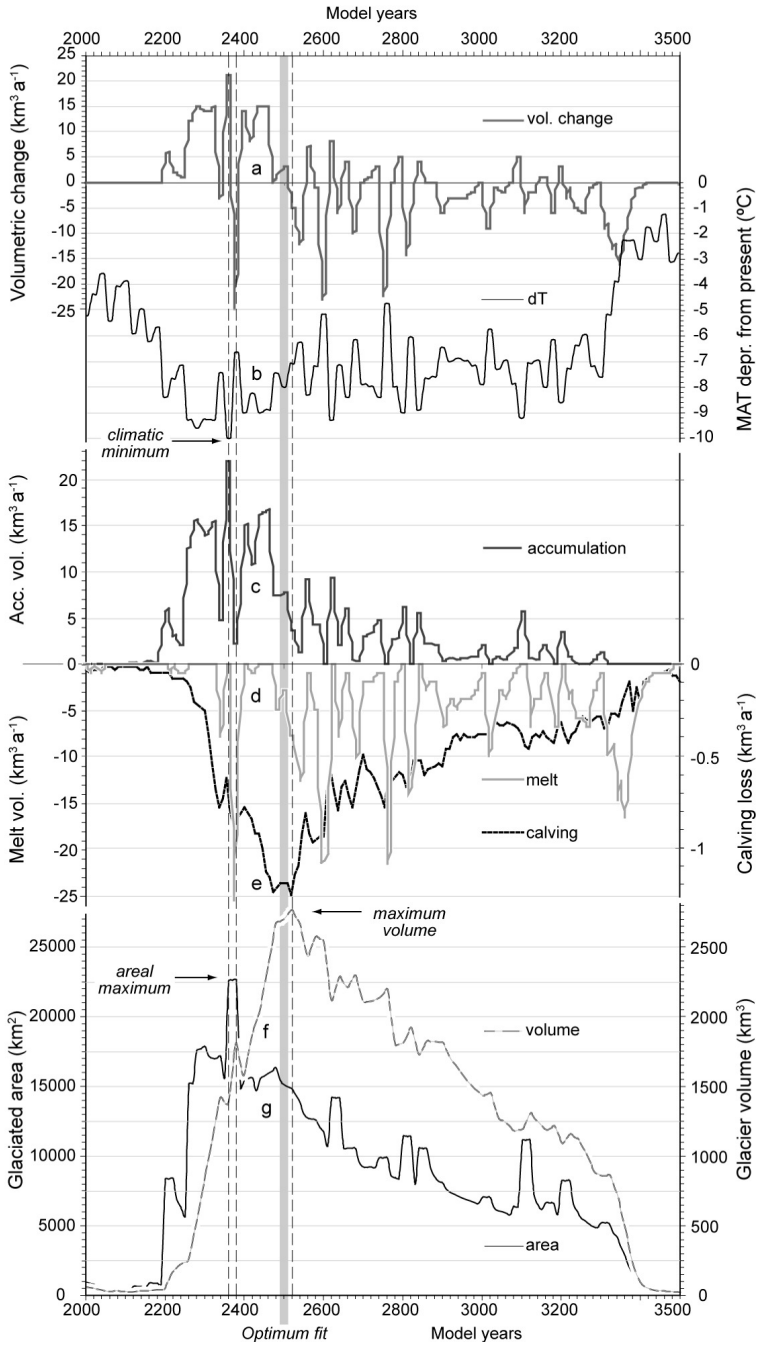

Figure 5.14: Mass balance parameter and forcing temperature variability through the Younger Dryas model run, showing a: fluctuations in rate of annual volumetric change, b: the 20-year resolution temperature pattern used to force the model run, c, d, e: accumulation, annual melt, and annual calving volumes, f, g: changes in net volume and areal extent of ice in the domain. Note lag between climatic minimum and maximum ice volume.

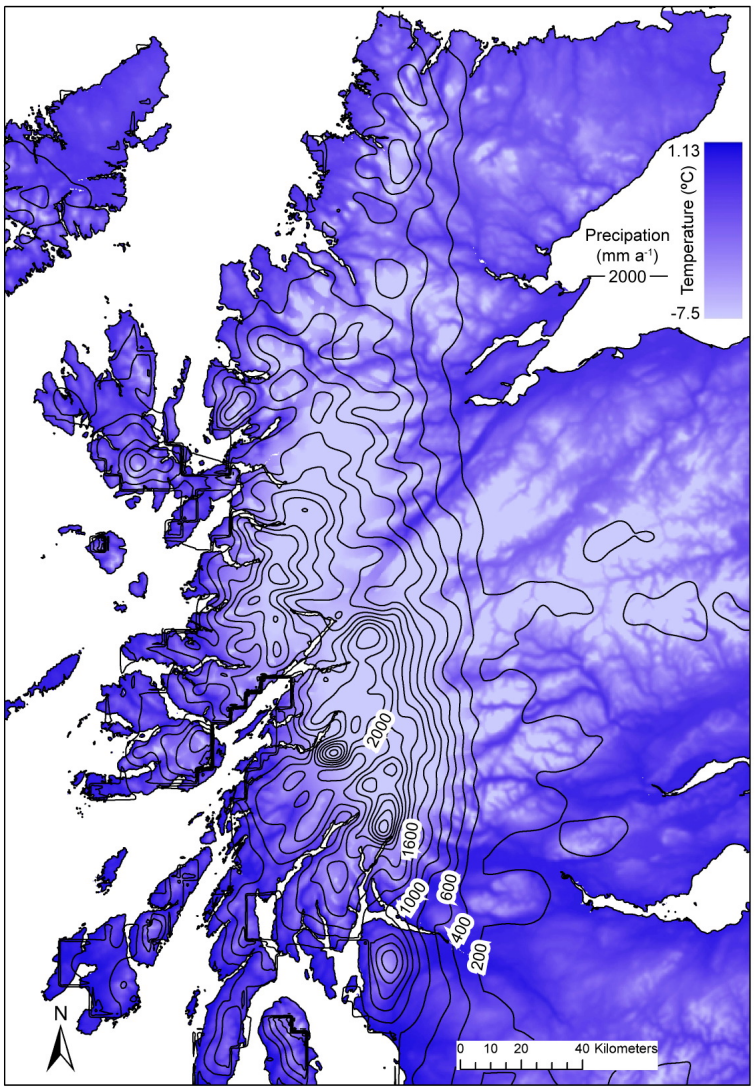

Figure 5.15: Modelled surface temperatures across the domain at 2500 model years, and contoured annual precipitation totals. Temperatures incorporate cooling due to altitude; precipitation pattern reflects imposed eastward and northward reductions simulating aridity away from the main ice mass.

velocity is composed of internal deformation (Glen, 1955), and Weertman-type sliding when basal temperatures are sufficient to generate pressure melting, and is determined through calculation of basal shear stresses corrected by a term for the vertically averaged longitudinal deviatoric stress. The basis and full derivation of this empirically validated ice-stretching algorithm are presented elsewhere (Hubbard, 1999, 2000, 2006), and so are not reiterated here. Many studies have found that water depth exerts the principal control on the rate of calving at water-terminating glacier margins (e.g. Zweck & Huybrechts, 2003). We employ a relatively simple scheme which calculates mass lost due to calving (U_c) as a product of ice thickness, (H), water depth, (W_d), and a calving parameter (A_c) (Brown *et al.*, 1982; van der Veen, 1999) (Equation 5.2):

$$U_c = A_c H W_d \,. \tag{5.2}$$

This crude approximation of calving is clearly less preferable than more complex relationships (e.g. Benn *et al.*, 2007a,b) but is computationally less intensive and is a reasonable solution in our domain, where calving losses are close to zero through much of the model run. Sea level is parameterised at +10 m for the duration of the model run, in accordance with empirical sea level reconstructions for this time period from coastal areas of western Scotland (Peacock *et al.*, 1977; Shennan *et al.*, 1999). Although this parameterisation of calving and sea level altitude has allowed many west coast glacier limits to be faithfully reproduced by the model (Golledge *et al.*, 2008a), we acknowledge that using different functions and parameter values may have a significant effect on overall ice cap geometry by locally altering the ablation component of the ice cap's mass balance. Our domain topography does not include the bathymetry of freshwater bodies, which may also introduce local errors in areas where particularly deep lochs occur (e.g. Loch Lomond).

Thermal evolution of the ice sheet through time ($\partial T/\partial t$) is calculated according to the relationship

$$\frac{\partial T}{\partial t} = \frac{k_{ice}}{\rho_{ice} C_p} \nabla^2 T - \vec{u} \cdot \nabla T + \frac{\Phi}{\rho_{ice} C_p} \,, \tag{5.3}$$

in which k_{ice} and C_p are the temperature dependent parameters of conductivity and specific heat capacity, $\vec{u}$ is the three-dimensional velocity vector and Φ denotes frictional heat resulting from internal strain (Hubbard, 2006).

The model evolves through a 4000 year run from initially ice-free conditions at 15 ka BP to complete deglaciation by 11 ka BP. A 0.02 year time-step is used in order to most effectively balance model stability against computation time. The spin-up period of 2000 model years (15–13 ka BP) prior to the Younger Dryas episode described here (13–11 ka BP) resulted in intermittent ice growth related to fluctuations in the imposed temperature depression, but almost complete loss of ice from the model domain by 1600 model years. Optimal parameterisation was achieved through a series of sensitivity experiments designed to gauge the relative influence of changes in temperature forcing, precipitation distribution, and the amount of basal sliding, which are described in detail elsewhere (Golledge *et al.*, 2008a). The relative closeness of fit of the numerical simulation to empirical reconstructions through the model run is calculated and logged using a grid-comparison algorithm that compares model outputs against empirical reconstructions in five zones (Golledge *et al.*, 2008a). This enabled the 'best-fit' timeslice to be objectively identified where domain mismatch is at its minimum, which was found to occur

between 2400 - 2600 model years. In general, outlying icefields reached their maxima earlier than the outlet glaciers of the main ice cap, which showed greater evidence of lags in the transfer of mass through the glacier system (Golledge *et al.*, 2008a). Reduction of annual precipitation totals *during* the Stadial was necessary in order to control ice sheet mass balance and to prevent a 'run-away' scenario that produced an implausible glacier configuration. Precipitation was reduced by 20% per century from 2500 - 2700 model years, held constant at a 50% reduction from 2700 - 3300 years, and returned to normal conditions by increases of 20% per century from 3300 - 3500. This artificially enforced aridity during the latter stages of the model run is consistent with inferences from palaeoenvironmental proxies in western Scotland that suggest a drier climate during this period (Benn *et al.*, 1992). That the resulting simulation closely approximates the distribution of ice cover during the Younger Dryas glaciation in Scotland is demonstrated by close agreement of modelled maximal ice margins with geologically reconstructed Younger Dryas ice limits (cf. Sissons, 1979b; Ballantyne, 1989, 2002; Clark *et al.*, 2004), and concurrence between spatial variations of modelled ice cap characteristics and interpretations of geological data in the south-east sector of the ice cap (cf. Golledge, 2006, 2007a,b; Golledge & Phillips, 2008).

5.12 Model results

5.12.1 Mass balance

The scaled GRIP-pattern PDD scheme used to drive the mass balance component of the model couples interpolated horizontal changes in precipitation and temperature across the domain with calculated vertical changes resulting from topography. Figures 5.14A-G show aspects of climatic and glacier evolution through the Younger Dryas model run; Table 5.3 describes the variability of mass balance parameters and values at the 'Optimum fit' timeslice of 2500 model years. Annual accumulation peaks at approximately +1 $\mathrm{m\,a^{-1}}$ (Table 5.3) during the coldest part of the stadial, from around 2370 model years, producing a net annual volumetric increase of 21.6 $\mathrm{km^3}$ (Figure 5.14A). Annual ablation rates achieve a maximum of -1.2 $\mathrm{m\,a^{-1}}$ (equivalent to a net decrease in volume of 24.9 $\mathrm{km^3}$) only a decade later, due to an abrupt (but short-lived) warming oscillation in the GRIP-based temperature curve. Although these extreme values are not subsequently repeated, the lesser peaks evident in Figure 5.14A nonetheless illustrate the sensitivity of the mass balance model to transient high-magnitude climate oscillations that occur throughout the stadial (Figure 5.14B). Net accumulation through the Younger Dryas (Figure 5.14C) integrates losses due to melting (Figure 5.14D), and calving (Figure 5.14E). Net accumulation is greatest during the short-lived climatic minimum and decreases subsequently as precipitation is reduced, as melting increases (due to the warming climate), and as the ice mass expands to the west coast and calving losses increase. Calving is, however, negligible throughout much of the stadial, exceeding 1 $\mathrm{km^3\,a^{-1}}$ only between 2460 - 2540 model years when ten west coast glaciers are marine-terminating. Figures 5.14F & G illustrate the integrated consequences of transient mass balance perturbations through the stadial, describing changes in total ice volume and total ice extent respectively. The latter peaks shortly after the lowest temperatures, due to the immediate lowering of the climatic equilibrium line altitude (ELA), whereas ice volume in the domain does not reach its maximum until 2520 model years, 150 years after the thermal nadir. At the 'Optimum fit' timeslice of 2500 model years, the

Table 5.3: Mass balance parameters through the model run.

Parameter (km^3 a^{-1})	Range	Thickness equivalent ($m\,a^{-1}$)	YD Max.	Thickness equivalent ($m\,a^{-1}$)
Accumulation	0 - 22.1	0 - 1.0	7.7	0.5
Melt	0 - –26.8	0 - –1.2	–3.7	–0.2
Calving loss	0 - –1.2	0 - –0.1	–1.2	–0.1
Net vol. change	21.6 - –24.9	0.9 - –1.1	3.3	0.2

Younger Dryas ice cap exhibits relatively low mass-turnover, and a net mean thickening of 0.2 $m\,a^{-1}$ (Table 5.3), comparable with current rates in central-northwest Greenland (Johnsen *et al.*, 1995; Dethloff *et al.*, 2002).

These results highlight considerable high-magnitude short-term variability in the mass balance regime of the ice cap during the Younger Dryas, largely due to transient oscillations in the the imposed temperature forcing. The generally positive bias of the mass balance fluctuations leads to rapid ice cap growth at the onset of the stadial, but following the stadial maximum (2500 model years), the manually imposed enhanced aridity instigates a change to an overall negative mass balance (Figure 5.14A). Final ice cap decay during the closing centuries of the stadial occurs under reduced precipitation conditions and consistent climatic warming. Deglaciation is more-or-less complete by 3300 - 3500 model years (Figure 5.14F & G), due to overwhelmingly negative net mass balance (Figure 5.14A), which results in the loss of c. 1000 km^3 ice in 150 years (Figure 5.14G).

5.12.2 Velocity and flow mechanisms

At the optimum fit timeslice of 2500 model years (12.5 ka BP), surface velocities of modelled glaciers in the domain commonly exceeding 100 $m\,a^{-1}$, with some achieving a maximum of nearly 550 $m\,a^{-1}$ (Table 5.4). Figure 5.16A shows the vertically integrated mean velocity distribution across the ice cap at this time. High velocities in outlet glaciers contrast with much of the interior of the ice cap being relatively static. The maritime icefields on Skye and Mull host zones of relatively fast flow but eastern plateau icefields (Cairngorms, Monadhliath) are largely inactive. Even within the main ice cap, the majority of faster-flowing ice occurs on the west rather than east. This west-east asymmetry is particularly clearly shown in the differences between the Loch Linnhe area glaciers in the west, and those in the east such as the Rannoch glacier (Figure 5.16B & C).

In order to establish such regional contrasts more easily, we calculate catchment-averaged velocities and mean temperatures across the domain (Figure 5.17A & B). These summaries integrate surface and basal values at all points within each glacier catchment, and serve to illustrate the dominance of western glaciers in dynamical aspects of the ice cap, in contrast to eastern areas that are colder and flow more slowly. In particular, Figure 5.17A highlights the importance of Loch Linnhe and Loch Etive as sinks for the largest contiguous area of relatively fast-flowing ice, focussing drainage from mountainous areas both north and south of the Great Glen.

Table 5.4: Parameter ranges, means and variance at optimum fit, 2500 model years.

Parameter	Range	Mean ($\bar{x}$)	Std. Dev. (σ)
Driving stress (k Pa)	0 - 164.9	45.6	21.1
Surface slope (%)	0 - 35.9	4.98	4.5
Surface velocity (m a^{-1})	0 - 547.6	20.6	36.2
Basal velocity (m a^{-1})	0 - 314.9	9.1	18.5
Surface temperature (°C)	1.1 - –7.51	–0.65	1.39
Basal temperature (°C)	0 - –5.91	–0.84	1.26
Total melt (m a^{-1})	0 - 3.7	0.38	0.4

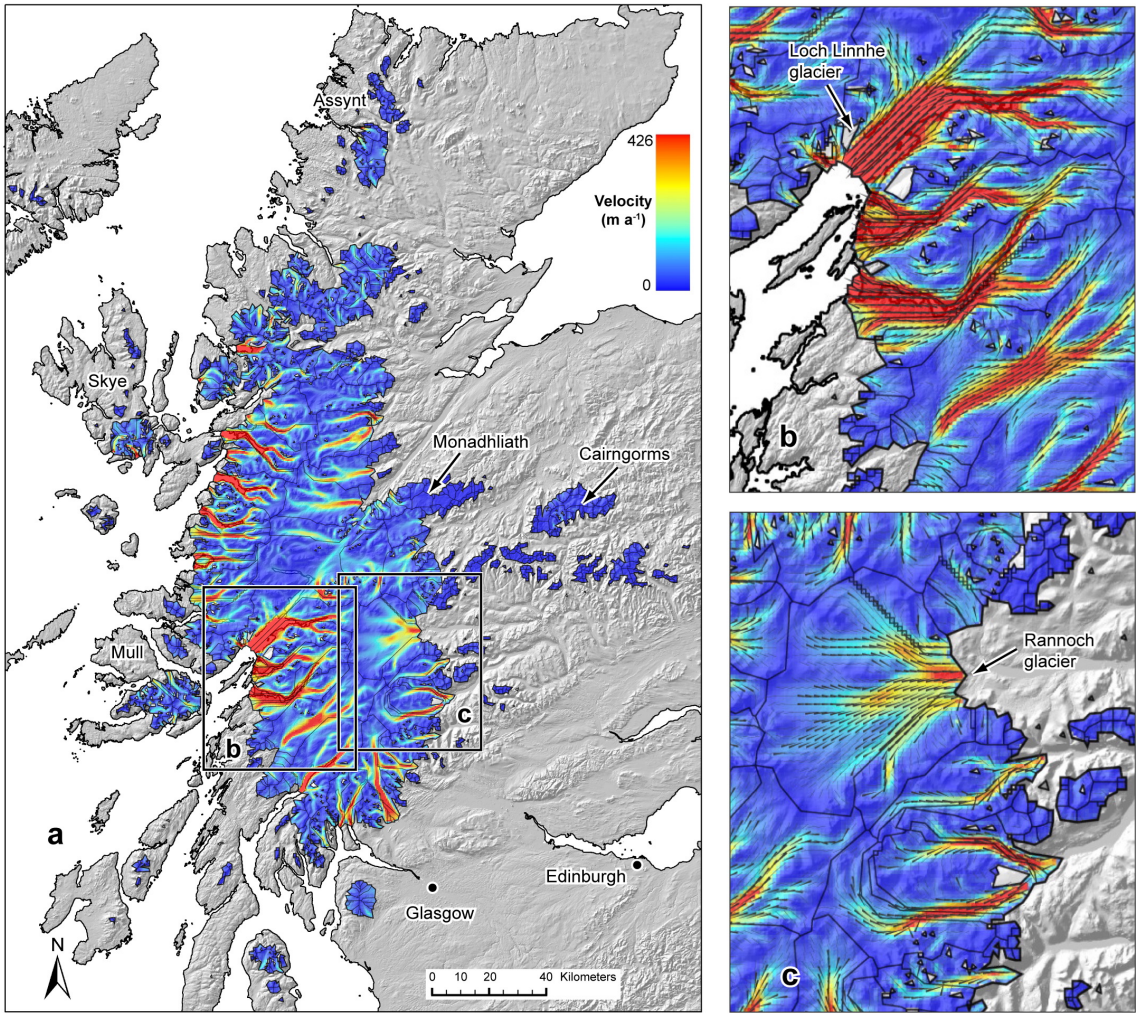

Figure 5.16: a: Mean velocity distribution in the domain at 2500 model years, boxes locate detail areas b & c. b: detail of Loch Linnhe area glaciers, showing flow vectors and glacier catchments, and c: detail of Loch Rannoch area glaciers, showing flow vectors and glacier catchments. Legend for detail areas same as main figure.

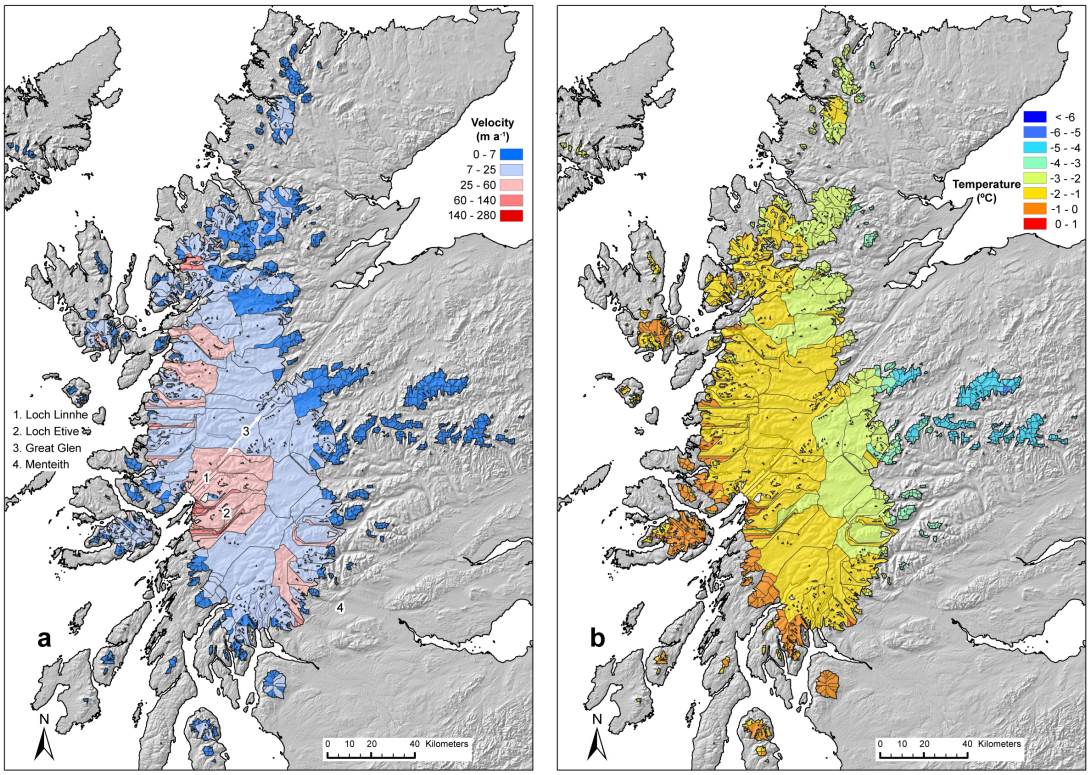

Figure 5.17: Model output at 2500 model years showing a: catchment-averaged velocities across the model domain, and b: catchment-averaged mean temperatures. Note the higher values in western areas in both cases.

From surface and basal ice velocities (V_s and V_b respectively) it is possible to calculate the proportion of glacier flow that results from basal sliding and from internal deformation (creep) of the ice above the glacier bed. Since surface velocity (V_s) also represents total velocity, which is the sum of basal sliding plus internal deformation, we calculate the velocity due to creep from $V_s - V_b$, making the assumption that any deformation of ice at the glacier bed will probably result in pressure melting and facilitate sliding, thereby reducing the creep component of basal motion to close to zero. Using this approach we can calculate the relative proportion of flow occuring as a result of each mechanism, by defining the relationship

$$S = \frac{(V_s - V_b)}{V_s} - \frac{V_b}{V_s}. \tag{5.4}$$

According to this simple relationship, a value of +1 defines areas flowing entirely by creep, and -1 areas whose total velocity is accounted for by basal motion, assumed to be sliding. Figure 5.18 shows the spatial variability of dominant flow mechanisms forecast by the relationship, as well as areas where basal velocities are less than 1 m a^{-1}.

The results show concentric zonation of the ice cap in which creep dominates in the interior of the ice cap, and basal sliding becomes most important nearer the margins. This distribution differs significantly from the pattern of mean velocities shown in Figure 5.16A, in which relatively fast-flowing radial corridors of ice extend considerable distances into glacier

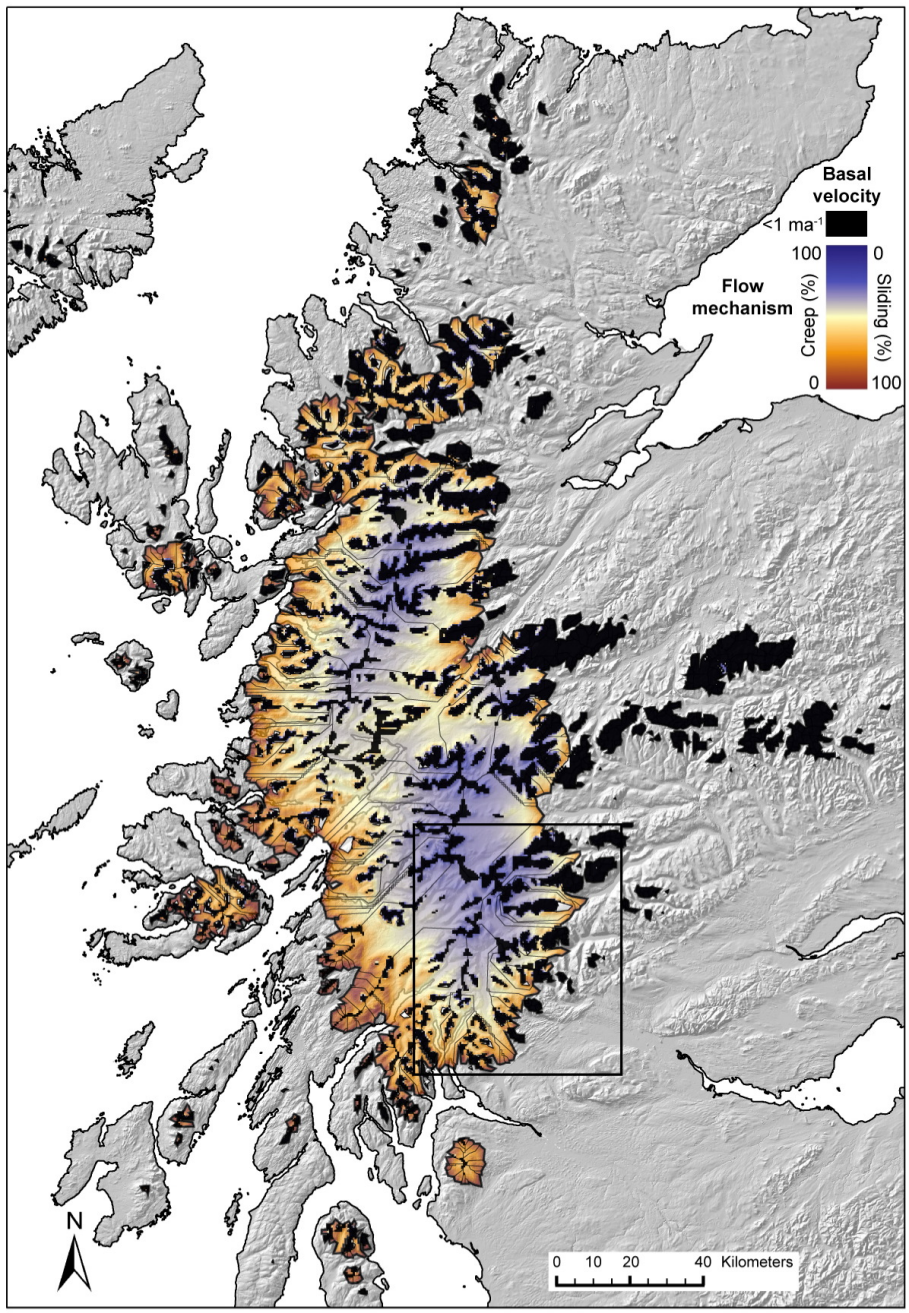

Figure 5.18: Calculated proportions of flow by sliding and by creep, (S), within the Younger Dryas ice cap and its outlying icefields, at 12.5 ka BP, and areas where ice is effectively immobile, with basal velocities < 1 m a^{-1}. Note 1) the dominance of internal deformation in central areas of the ice cap, 2) the asymmetry in the width of the marginal fringe of basal sliding, and 3) the far more extensive areas of non-sliding ice in the east. Box shows area of Figure 5.20.

accumulation areas from their ablation-zone terminii. West-east contrasts are again evident, clearly illustrated by the marked differences between the icefields in Mull, Skye, and Assynt, and in the Cairngorms and Monadhliath, and in the width of the sliding 'fringe' around the main ice cap. Sliding is the dominant mode of flow up to c. 20 km up-glacier from western ice margins and only small areas of immobile ice occur, but in the east, sliding is only dominant in the lower reaches of outlet glaciers, which are separated from one another by extensive areas of immobile ice. This low velocity, non-sliding, ice is mostly associated with ice divides, interfluves and plateaux (Figure 5.18). We do not account for warming of the firn by the release of latent heat from percolation and refreezing of seasonal meltwater, as is reported in many Arctic glaciers (e.g. Trabant & Mayo, 1985; Rabus & Echelmeyer, 1998), but the possibility nonetheless exists that, by ignoring this process, sliding may be under-predicted in these eastern areas.

5.12.3 Basal processes

The relative ability of ice to erode its bed (E) can be approximated from its basal velocity and the overburden pressure resulting from its thickness (H), so that $E = -f \mid V_{\mathrm{b}} \mid H$, where f is a constant representing bedrock erodibility (Jamieson *et al.*, 2007). In order to calculate only the spatial pattern of erosion potential exerted by the ice, rather than the amount of basal substrate eroded, we assume a uniform bed rheology and set $f = 1$. Figure 5.19A shows the areas forecast by this formula to be subjected to greatest potential erosion by the Younger Dryas ice cap. The assumption of a uniform bed hardness probably masks the extent of local variability, but at the domain scale the calculated pattern reflects focussed erosion along major flowlines within the main ice cap. Due to its dependence on ice thickness, erosion potential is considerably less along glacier margins than beneath their trunks. In these mid-sections of glaciers, elongate zones of high erosion potential occur many tens of kilometers up-glacier from glacier terminii (Figure 5.19A). Where ice is thin, such as in many of the outlying icefields, the potential for subglacial erosion is negligible.

Theoretically, where basal ice reaches the pressure melting point, the meltwater produced will either refreeze, permeate into the underlying substrate, or flow along a vector representing the glaciohydraulic gradient. The magnitude of this gradient is largely governed by the thickness of overlying ice and the topography of the glacier bed. Basal meltwater plays a critical role in glacier dynamics, by facilitating sliding where its pressure (P_{w}) exceeds that exerted by the weight of ice overburden (P_{i}). As the difference between these two components (the separation pressure (P_{s})) increases, effective pressure at the ice-bed interface (P_{e}) decreases and basal sliding is enhanced. The magnitude of this enhancement is limited, however, by increasing bed roughness, since higher water pressures are required to overfill the larger bed cavities, according to the relationship

$$P_{\mathrm{s}} = P_{\mathrm{i}} - \frac{\lambda\tau}{a\pi}\,, \tag{5.5}$$

where λ is the wavelength of bedrock bumps, τ is the basal shear stress, and a is the amplitude of bed roughness (Paterson, 1994, p. 149).

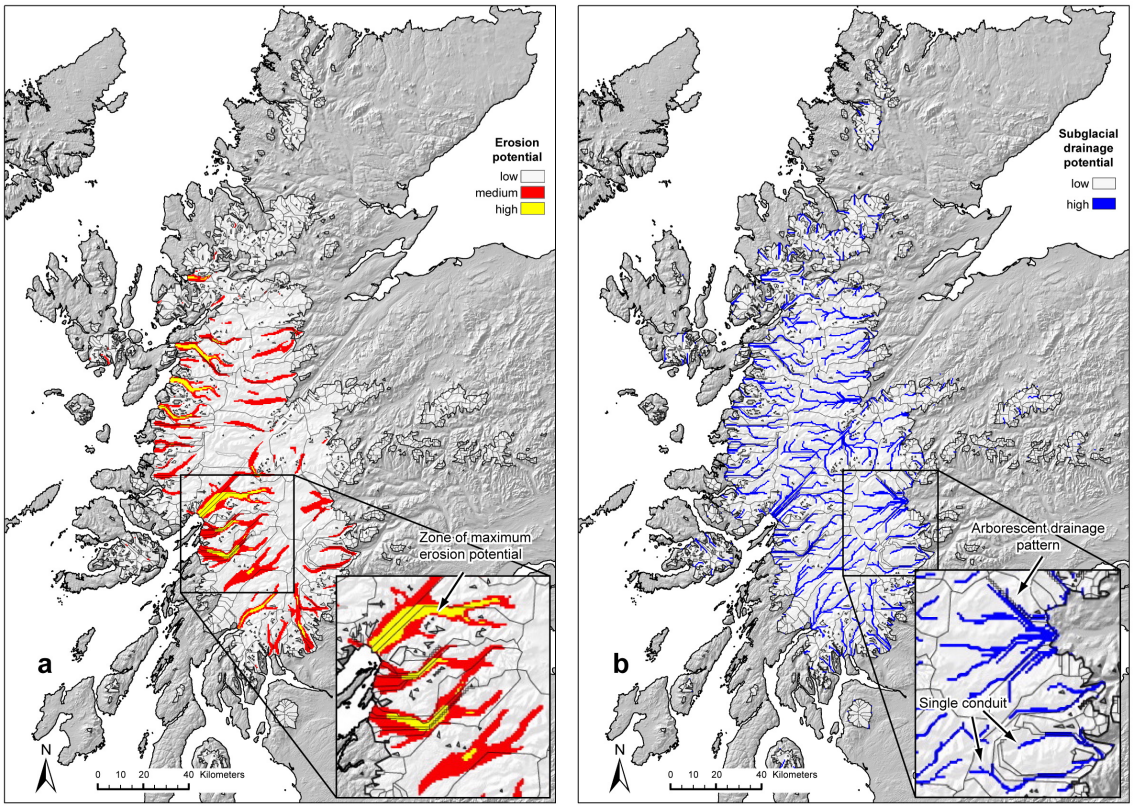

Figure 5.19: a: Areas exposed to greatest subglacial erosion potential, based on ice thickness and velocity; inset shows detail. b: likely subglacial drainage pathways calculated from the glaciohydraulic gradient; inset shows detail. Legend for insets same as main figures.

Since we do not calculate melt volumes here, however, we make the assumption that $P_w = P_i$ and thus that $P_s = 0$. Under such conditions it is possible to use ice thickness and basal topography to calculate glaciohydraulic gradients at the ice-bed interface. We used ESRI ArcGIS 9.2 flow accumulation tools to then identify where meltwater would most likely accumulate and the direction in which it would flow. Figure 5.19B illustrates these potential routeways for basal meltwater drainage, based on accumulation within subglacial catchments. Given the dependence on ice overburden pressure it is not surprising that the principal drainage paths flow approximately radially from the thick ice cap centre to its thinner margins, along the main valleys that also focus the flow of ice. Although weakly developed arborescent drainage networks may occur in some catchment areas beneath the centre of the ice cap, the majority of subglacial meltwater beneath outlet glaciers is predicted to preferentially follow only one dominant path, giving rise to a distribution of low-order subglacial streams (Strahler, 1952) (Figure 5.19B). These hypothetical subglacial streams largely accord with modern drainage networks, due to the high degree of topographic control exerted by the mountainous relief underlying the majority of the ice cap. By simplifying the subglacial hydrology, and by excluding subglacial or ice-marginal lakes, we are able to identify major characteristics of the former ice cap but are unable to provide the spatial detail and accuracy necessary for field comparison. Consequently, this remains a goal for future research.

5.13 Discussion and comparison with geological data

The mass balance data presented here are the first to be calculated for a simulated Younger Dryas ice cap in Scotland at such a high temporal and spatial resolution. Such data are valuable both for local palaeoglaciological studies that seek to infer former glaciological conditions from reconstructed ice margins, as well as for studies of contemporary ice caps such as Austfonna (Svalbard) or Devon Ice Cap (Nunavut, Canada) where only remotely sensed or short-term field records are available (e.g. Bamber *et al.*, 2004; Colgan *et al.*, 2008). Additionally, a consideration of the mass balance of former ice caps may be useful when assessing the current 'health' of glaciers in areas currently experiencing significant changes in their governing climates (Dowdeswell *et al.*, 1997), or in better understanding the role of mass balance in influencing glacier response times (Bahr *et al.*, 1998; Pfeffer *et al.*, 1998). Our results show that glacier inception occurs rapidly under a cooling climate, and that glacierized areas are most widespread more-or-less coincident with the coldest part of the stadial. This close relation between cooling and area of ice cover is not, however, matched by the pattern of volumetric changes. Integrated glacier volume in the domain reaches a maximum c. 150 years after the climatic minimum, representing a lag in mass transfer through the glacier system as the ice cap endeavours to achieve a state of equilibrium under the fluctuating climate. The possibility that this change in volume-area relationship may be partially influenced by the advection of cold ice towards the glacier bed, stiffening basal ice, as inferred recently in Devon Ice Cap (Colgan *et al.*, 2008) is one that may be fruitful to explore in the future. An appreciation of such internally regulated glacier oscillations, representing climatically decoupled thermo-mechanical feedbacks, may be especially pertinent to the way in which glacier limits and the geological record in deglaciated areas such as Scotland are interpreted.

The way in which glaciers flow excites considerable debate (Boulton, 1986; Boulton *et al.*, 2001; Piotrowski *et al.*, 2001, 2002; Kjær *et al.*, 2007), primarily because of the implications associated with the different flow mechanisms. Whereas widespread deformation of unconsolidated basal sediments may play an important role in glacier motion, it is also clear that basal environments are highly complex and vary in both space and time (Piotrowski *et al.*, 2004). Consequently, bed deformation will most likely be accompanied by meltwater-lubricated sliding on rigid beds, as well as flow by the deformation of ice crystals (creep). Whilst our model does not differentiate between basal sliding and deformation of the *bed*, it allows the balance between basal motion and internal deformation of the Scottish Younger Dryas ice cap to be quantified for the first time. Furthermore, it enables the spatial pattern of this variability to be calculated at 500 m resolution. Figure 5.18 highlights how flow mechanics are partitioned into concentric zones within the ice cap, reflecting down-glacier changes in basal conditions. From this it may be inferred that deforming beds will only be generated where ice thicknesses and sliding velocities are high, that is, in topographic troughs beneath the ice cap. Accretion of subglacial sediments will occur downglacier of these areas, where ice is thinner but where it is still sliding and able to transport entrained sediment. Glacier recession would have led to spatial changes in the location of these sediment 'sinks', thus the thickest deformable sequences probably accumulated at maximal margins with thinner sequences laid down nearer the ice cap core. These model inferences also imply that in some central areas, a deforming substrate may have been either completely absent, or patchy, as a result of the very limited sliding that is forecast

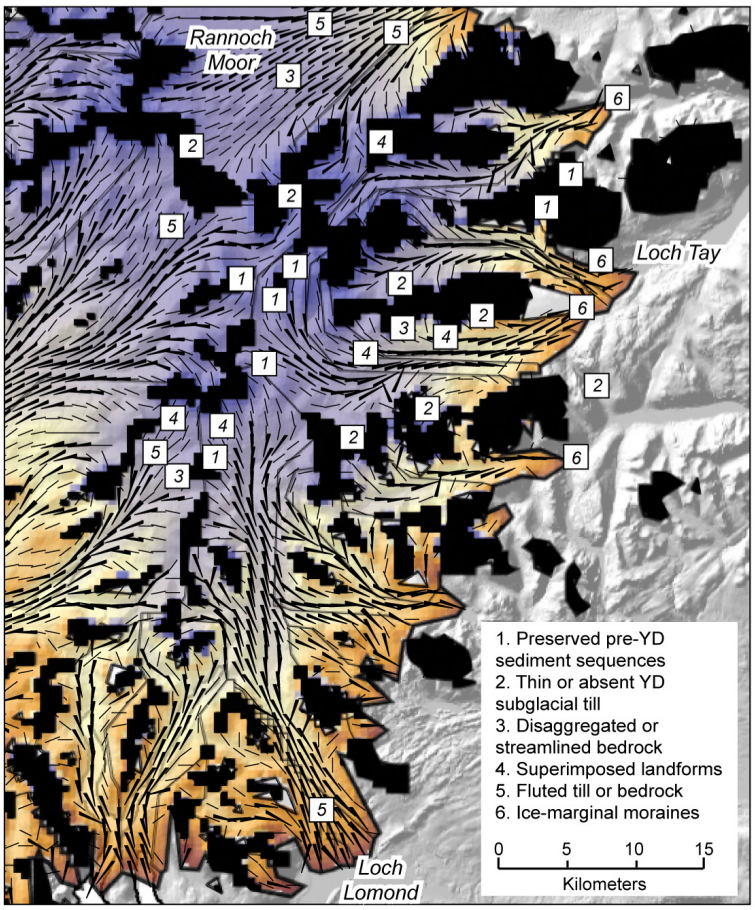

Figure 5.20: The southeast sector of the modelled Younger Dryas ice cap, showing locations of geological features described in the text, in relation to areas of immobile, sliding-dominated and creep-dominated zones as described in Figure 5.18. Glacier flow vectors are also shown.

to have occurred there. Low velocities in the ice cap core would also have favoured the preservation of pre-existing landscape elements. Transitional areas between non-sliding and sliding ice are likely to have a mixed basal signature. Such areas may host pockets of deformable sediments, partially modified (remoulded) landforms, and unmodified relict landscape components.

Geological mapping in the southeast sector of the ice cap has revealed that thick sequences of sediments *pre-dating* the Younger Dryas are only preserved in topographic hollows near the centre of the ice cap (Golledge, 2007a,b), which, according to the modelled flow patterns, coincide with areas of immobile ice on ice divides between divergent glaciers (Figure 5.20, '1'). Modelled ice divides in this area are also associated with mapped areas lacking thick or widespread Younger Dryas subglacial till (Figure 5.20, '2'), presumably due to the limited erosion and transport capacity of basal ice in such locations. Disaggregated or streamlined bedrock characterised by metre-scale displacement of blocks, (Figure 5.20, '3') (Golledge, 2006), occurs in locations where the model forecasts the downglacier transition to sliding-dominated ice-flow, perhaps reflecting limited transport of basal substrate previously frozen to the glacier bed. Superimposed bedforms showing lineations that cross-cut older features (Figure 5.20, '4'), are mapped in areas where the model forecasts either convergent flow or the onset of flow

in tributary glaciers feeding a major outlet, whereas more pervasively streamlined (fluted) bedforms (Figure 5.20, '5') are found where modelled ice-flow is more substantially dominated by basal sliding, rather than creep. Ice-marginal moraines are present throughout the western Highlands, marking successive positions of retreating glaciers. Extensive suites of such moraines thought to represent maximal Younger Dryas glacier limits are shown in Figure 5.20 ('6'), adjacent to the sliding terminii of discrete outlet glaciers draining the eastern margin of the ice cap.

The pattern of greatest erosion potential (Figure 5.19A) shows that the greatest work done by outlet glaciers should be concentrated in narrow zones between the core of the ice cap and its margins. Where these zones of high erosion potential coincide with relatively high proportions of flow by basal sliding (Figure 5.18), the deforming layer is liable to excavation and mobilisation. Fluctuation of glacier margins both through a single glacial episode and over repeated glaciations serves to accentuate these patterns, leading to overdeepened rock basins beneath the mid-sections of outlet glaciers. When the locations of greatest erosion potential forecast by the model (Figure 5.19A) are compared with the pattern of rock basins in Scotland identified by Sissons (1967a), a striking similarity can be seen (Figure 5.21). That these basins extend beyond the modelled Younger Dryas limits, and probably require repeated glacial cycles to develop, may suggest that the ice configuration achieved at the height of the Younger Dryas perhaps represents a stage that has been reached many times during repeated Pleistocene glaciations.

The discharge of meltwater beneath glaciers influences their rate of flow by changing effective pressures and basal thermal conditions, seen most dramatically in surge-type glaciers (Kamb, 1987; Murray *et al.*, 2000). Understanding the mechanisms of subglacial drainage also greatly assists in the interpretation of the glacial sedimentary sequences (Golledge & Phillips, 2008), and may help to identify areas where glaciofluvial erosion and deposition are most likely to have taken place. Modelled potential drainage patterns for the maximum Younger Dryas ice cap show that, if $P_{\mathrm{w}} = P_{\mathrm{i}}$, subglacial meltwater flow may have followed a small number of low-order paths at the beds of individual outlet glaciers. Conduit-type systems are highly effective at discharging meltwater (Kamb, 1987; Paterson, 1994), and, by keeping P_{w} low, maintain high overburden pressures, which to some extent act as a brake on glacier flow. In our simulated ice cap, P_{w} would have most likely been greatest during deglaciation, due to the considerably increased volume of meltwater generated by the warming climate. This may have reduced effective pressure sufficiently to promote accelerated flow, and possibly even surge-type behaviour amongst some of the outlets, as inferred from geological evidence for Younger Dryas glaciers in Loch Lomond (Thorp, 1991b), and the neighbouring outlet in Menteith (Evans & Wilson, 2006). The infuence of a permeable bed on meltwater pressure and drainage pathways is not accounted for by the model, however.

Geological investigations north and west of the ice cap centre have identified landforms indicative of thinner, more dynamic glaciers than those inferred in the south and east (e.g. Thorp, 1986; Bennett & Boulton, 1993a). These studies have focussed on the relative importance of deforming beds to facilitate flow, rather than internal deformation. By identifying the glaciological contrasts evident between different sectors of the ice cap, the model results presented here go some way towards reconciling these apparently opposing views. The

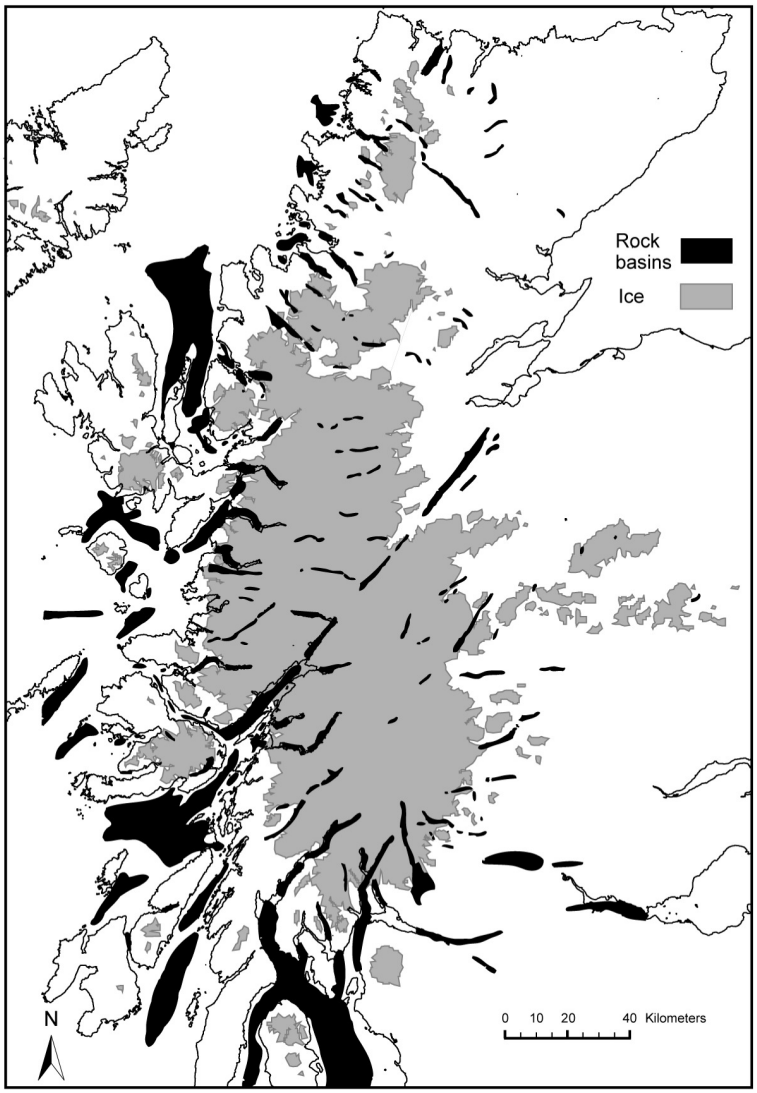

Figure 5.21: Rock basins in Scotland, modified from Sissons (1967a), and their context in relation to the modelled extent of Younger Dryas ice described here. Note the similarity in general distribution to the pattern of erosion predicted in Figure 5.19A

higher velocities, warmer beds, and greater integrated melting ablation occuring in western areas reflect the former presence of high-turnover dynamic corridors within the ice cap that drained the central accumulation areas steeply towards a sea level only slightly higher than present (Shennan *et al.*, 1999). East of the main ice divides, however, topographic slopes are considerably lower, and the palaeoclimate was drier. These less dynamic areas would have experienced less strain heating, raising the effective viscosity of the ice and favouring thicker, more sluggish and probably less erosive glaciers. Whether these thermodynamic contrasts are sufficient to explain the absence of erosional periglacial trimlines in eastern areas, in contrast to their abundance further west, remains an interesting future research avenue (Thorp, 1986; Golledge, 2007a).

5.14 Conclusions

Investigation of the mass balance regime and resultant growth and flow characteristics of numerically simulated Younger Dryas ice masses in Scotland, and their relation to geological evidence, has revealed the following new insights:

1. The modelled ice cap grows rapidly during the onset of the stadial, and is characterised by extensive but relatively thin ice at the stadial climatic minimum. Lags in the glacier system result in thickening of the ice cap to reach a maximum domain-averaged thickness around 2500 model years.

2. The modelled ice cap is significantly influenced by spatial contrasts in the climate that gives rise to it, so that it is dynamically asymmetric at its maximum, with western glaciers generally warmer and faster-flowing that their eastern counterparts.

3. Flow in the core of the Younger Dryas ice cap probably occurred primarily through ice deformation, enabling the preservation of older sediments and landforms.

4. Basal sliding dominated the flow of western outlet glaciers, and led to relatively thick Younger Dryas sediment accumulations at their margins. East of the ice cap centre, the modelled ice cover is colder than that in the west, was not sliding at its bed, and had very low erosion potential.

5. The geometry of the modelled ice cap favours focussed basal erosion in the mid-sections of topographic troughs, and gives rise to a pattern of erosion potential that closely matches many of the locations of mapped rock basins in Scotland.

6. The combined influence of ice thickness variability and bed topography produce glaciohydraulic gradients that would have preferentially facilitated basal meltwater drainage along low-order glaciofluvial systems, focussed into central conduits.

7. Manually enhanced aridity during the latter part of the stadial, coupled with rapidly rising temperatures towards the end of the stadial, lead to negative net mass balance and culminate in complete deglaciation around 3300-3500 model years.

Chapter 6

Synthesis and Discussion

6.1 Synthesis

Papers presented in this thesis address key areas of uncertainty surrounding aspects of the Younger Dryas glaciation in Scotland. Specifically, the research attempts to provide further clarification on i) timing, rate, and location of glacier inception, ii) extent and thickness of component ice masses, iii) the dynamical behaviour of these glaciers, iv) timing and manner of deglaciation, and v) characteristics of the prevailing climate during the stadial. These questions have been investigated using a methodology that combines geological interpretation and numerical simulations. Geological data were collected by field and remote survey, in an area of the western Scottish Highlands that previously hosted the southeastern sector of the Younger Dryas ice cap. The research has described and interpreted the genesis of the glacial sediments mapped, their stratigraphic relationships, landform types present in the area and their connection to former glaciers. Dating of glacially deposited erratics and ice-worn bedrock has provided new data to an existing chronological framework for these landforms and sediments. Interpretations of the geological and geochronological data have been presented here at a range of scales, from local to regional studies. Numerical modelling has subsequently extended the research to a wider context, by simulating glaciers within a model domain of $> 100\ 000\ km^2$, which includes most of mainland Scotland and its proximal outlying islands. Although the focus and scope of each paper has been different, the conclusions that they reach share certain commonalities. Table 6.1 illustrates the principle conclusions of each paper, and their contribution towards answering the initial questions set out in the 'Aims' of Chapter 1. A 'Synthesis' is presented below that discusses the inter-relatedness of each paper in the context of Table 6.1, and highlights areas where data are equivocal or where the evidence is insufficient to provide an adequate answer.

6.1.1 Growth and evolution

Identifying geological evidence that might constrain the pattern of ice build-up and subsequent evolution of the resultant ice cap is hampered by the amalgamation of landforms and sediments into a single archive, where individual events are difficult to separate. Varved sediment sequences deposited in glacial lakes north of Rannoch Moor have been interpreted by others to indicate that at least some Younger Dryas glaciers reached their maximal limits during the mid- to late-stadial, at around 11.8 ka BP (Palmer *et al.*, 2008), whereas calibrated radiocarbon dates from the southern margin of the ice cap constrain the maximal extent to somewhat earlier, around 12.8 – 12.3 ka BP (Rose *et al.*, 1988). The ^{10}Be exposure ages presented here (Paper V) all fall within the Younger Dryas period, and demonstrate that ice cover of Beinn Inverveigh (and by implication the surrounding area) may have been thickest relatively early in the stadial, after which it thinned sufficiently to expose the summit and deposit erratics, the youngest of these yielding an age of 11.6 ± 1.0 ka BP. Despite the apparent correspondence between lower altitudes and younger ages (Fig. 4.3), the dataset is insufficient to draw firm conclusions with respect to rates of glacier thinning. Furthermore, exposure ages such as these may be affected by isotopic inheritance, surface weathering, isostatic uplift, or variation in ^{10}Be production rate since their emplacement. Each of these factors may result in an under- or over-estimate of sample age. Nevertheless, the sample ages from Beinn Inverveigh all fall in the range 12.9 ± 1.5 – 11.6 ± 1.0 ka BP. If these ages are *over*estimates, then they would indicate

	Conclusions	Early maximum	Late maximum	Extensive	Restricted	Thin	Thick	Deforming bed (erosive)	Creep & sliding (non-erosive)	Gradualistic (linear)	Threshold-driven (non-linear)	Stagnation	Active recession	Maritime	Continental
Paper I	Dynamic water-terminating glaciers existed, & actively oscillated during deglaciation							■					■		
Paper II	Thick sedimentary sequences reflect mainly Main Late Devensian (MLD) and older glaciations, not Younger Dryas (YD)								■						
	Minimal basal till deposition by YD glaciers; flow was therefore by sliding not deforming bed								■						
	Landscape preservation probably more widespread than previously assumed								■						
Paper III	Landsystem implies thick central ice cap with steep outlet glaciers, and satellite icefields				■		■								
	Greater net accumulation required means slower flow, or wetter or colder YD climate								■					■	■
Paper IV	Limited deformation of bed, flow more by basal sliding; short basal debris entrainment								■						
	Little net basal erosion, mainly sediment reworking; landscape is partially inherited from MLD								■						
	Glaciers were active during deglaciation, associated with wet ice-marginal forelands												■		
Paper V	YD glaciers thicker than predicted by Thorp (1986); 'trimlines' therfore may not identify maximum ice surface altitude						■								
	Ice build-up may have begun during the Windermere Interstadial (WI)	■													
Paper VI	Modelled ice extent agrees closely with empirical reconstructions (Clark et al. 2004 & Golledge 2007a)				■		■								
	Ice accumulation begins during WI, accelerates early in YD & reaches maximal extents in west and north c. 12.6 ka BP, east and south c. 12.4 ka BP	■									■				
	Limited basal sliding, mainly creep								■						
	Climate governed by steep east and northward precipitation gradients; widespread aridity from c. 12.5 ka BP														■
	Some glaciers advanced during overall ice cap recession										■		■		
Paper VII	Western margins are warmer, wetter, faster-flowing; ice cap core and eastern areas colder, slower creep-dominated flow							■	■				■		
	Subglacial erosion focussed in mid-trough areas, basal meltwater mainly discharged via valley-parallel central conduits														

Table 6.1: Key conclusions from each of the seven papers presented in this thesis (vertical axis), and their contribution towards answering each of the 'Aims' set out in Chapter 1 (horizontal axis).

continued glaciation into a time when climatic warming at the onset of the Holocene had most likely led to the complete disappearance of ice from Scotland. Alternatively, if they represent an *under*estimate of the true exposure age, then they could only realistically be explained if they related to the preceeding glaciation, the Main Late Devensian, which would require exposure ages approximately 2000 years older. Given the uncertainties described above, it is tempting to accept the ages as they are, and to interpret the data as indicating ice cover of the mountain relatively early in the stadial.

Modelling experiments presented in Papers VI and VII demonstrate that the fastest rate of ice accumulation took place within the first centuries of the stadial, when climatic cooling was greatest and precipitation was plentiful. Such simulations accord with empirical reconstructions that infer particularly wet conditions in the early Younger Dryas, as the oceanic polar front migrated southward and led to heavy precipitation under increasingly cold conditions (Ruddiman & McIntyre, 1981; Bard *et al.*, 1987; Isarin & Renssen, 1999). The new modelling data presented here propose most rapid glacial build-up from 12.9 – 12.7 ka, during which time the widest area of the model domain becomes glaciated. Continued accumulation leads to a thickening of the ice cap, which peaks at 12.5 – 12.3 ka BP. As a result of the interaction between changing areal extent and thickness, the maximum total ice volume within the domain occurs from 12.7 – 12.5 ka BP. These timings concur broadly with the ^{10}Be exposure ages from Beinn Inverveigh, and with the calibrated radiocarbon ages from the southern margins of the ice cap (Rose *et al.*, 1988). The apparent inconsistency with varve records north of Rannoch Moor (Palmer *et al.*, 2008), suggesting much later glacial expansion, is explained below (see 'Behaviour'), by considering the mass balance characteristics that controlled ice cap behaviour during the stadial and the influence they exerted on the timing of glacier oscillations.

6.1.2 Extent and thickness

Much of the geological component of this work was undertaken within the central area of the Younger Dryas ice cap, and consequently little field data specifically addressing glacier terminii was collected. Nonetheless, deglacial landforms in glens Lyon, Lochay and Dochart (Figure 1.4) indicate declining ice surface altitudes more consistent with the maximal limits proposed by Sissons *et al.* (1973) and Sissons (1979b), than those predicted by reconstructions of more extensive ice (e.g. Charlesworth, 1955; Horsfield, 1983). That this ice mass was relatively thick, however, is shown by the occurrence of high-level streamlining and dated high-level erratics, which together place the maximum ice surface altitude at around 850 - 900 m in this area south of Rannoch Moor, approximately 100 - 150 m higher than the upper limit proposed by Thorp (1984, 1986). Thus the empirical evidence appears to support the notion of a thick, but restricted ice cap, rather than a thin or extensive one. Modelling simulations presented here specifically attempted to replicate the 'restricted' pattern of ice extent, and in achieving this demonstrate that this ice configuration is at least possible, given the right climatic forcing. Additionally, the model results highlight a complexity of flow pattern in the former ice cap not fully appreciated in the reconstruction based on geological evidence (compare Figs. 3.5 and 5.20).

Uncertainty in ice cap extent is greatest in the east of the study area where glacier limits are least well-defined. Whereas clear terminal limits exist in some areas, for example north of Loch Rannoch, other glens show no such distinctive single moraine. This poses the question of why there is so much ambiguity in the interpretation of surviving landforms in the east - that is - if the Younger Dryas Readvance was such a significant and clearly-defined event, why did it not leave a signature that can be easily distinguished from the substantially older landforms of the retreating Main Late Devensian ice sheet? Whilst dating offers the most promising approach to resolving the problem, since features of Younger Dryas age should be at least 2000 years younger than those relating to the MLD, its application is predecated on the assumption that this intervening period was ice-free. New data from Assynt, north of the study area, show convincingly that glaciers remained active during the Windermere Interstadial, and did not disappear and regrow as previously thought (Bradwell *et al.*, 2008). If this suggestion is correct for other areas of Scotland, several lingering conflicts with respect to the extent and thickness of the Younger Dryas ice cap might be resolved.

6.1.3 Dynamics

The concept of a thin icefield as advocated by Thorp (1984, 1986) requires very low basal shear stresses beneath its glaciers in order that they might reach the mapped terminal limits. Values reconstructed by Thorp (1991b) for the study area described here fall in the range 40 - 60 kPa, and are explained to result from enhanced sliding over easily deformable substrates. This mechanism no doubt facilitated glacier flow through the principal troughs, particularly around the periphery of the ice mass, but the new evidence described here suggests that deformable substrates in the central area of the former ice cap were not as ubiquitous as previously thought. Futhermore, where thick sediments occur, there is rarely evidence for their deformation or progressive removal, but instead considerable evidence for their preservation. Consequently, it is unlikely that glaciers flowed by deformation of their bed to the extent envisaged by Thorp, rather, they most likely moved by meltwater-lubricated sliding over predominantly rigid beds with isolated 'pockets' of softer sediments. Such a scenario is consistent with more recent investigations proposing spatially and temporally variable bed conditions that, at any given moment, may be best represented as a 'mosaic' (Piotrowski *et al.*, 2004). This mosaic reflects changes in basal temperature, meltwater volume and pressure, and substrate lithology, and evolves through the glacial cycle as basal conditions change. Where deforming substrates occurred, they were advected towards glacier margins, as in Glen Chaorach (Paper I), whereas more central areas of the ice cap overrode but did not remove sediments, as in Coire Chailein (Paper II). That glaciers can result in such limited modification of a pre-existing landscape is now becoming widely accepted elsewhere (e.g. Kleman, 1994; Fabel *et al.*, 2002; Hättestrand & Stroeven, 2002; Stroeven *et al.*, 2002b; Fabel *et al.*, 2006), and explains similar observations in other parts of Scotland (Hinxman *et al.*, 1923; Wilson & Evans, 2000; Phillips *et al.*, 2006). The conclusion that much of the Younger Dryas ice cap in the field area did little to modify its bed is further supported by the model simulations. These demonstrate that, during the height of the Younger Dryas, sliding probably only dominated in the lower sectors of outlet glaciers, particularly those in the west and south (Paper VII). The central area of the ice cap

flowed by internal deformation of ice – creep – thereby enabling a thick ice cap to exist, but leave only limited evidence of its passage. During deglaciation, rising temperatures coupled with enhanced basal meltwater flux most probably increased the role of basal motion relative to creep, and may have led to thinner, more dynamic, glaciers with lower basal shear stresses, such as those reconstructed by Thorp (1986).

6.1.4 Behaviour

Since geological evidence typically records the sum of previous glacial activity integrated into suites of inter-related landforms and sediments, it is difficult to make inferences concerning the behaviour of the former ice cap, other than at a local scale. Paper I highlights the importance of active oscillation of retreating ice margins in the genesis of Younger Dryas landforms in the study area, which may have been typical of the ice cap in general. Evidence for dynamic behaviour at the margins of southern outlet glaciers is seemingly abundant (e.g. Phillips *et al.*, 2002; Rose, 2003; Evans & Wilson, 2006), and it is perhaps significant that both Thorp (1991b) and Evans & Wilson (2006) invoke surging glaciers in their theoretical and empirical reconstructions respectively. The possibility that at least some of the Younger Dryas glaciers surged is perhaps one explanation for the apparent mismatches between numerical model simulations (Paper VI) and the accepted maximal limits (e.g. Clark *et al.*, 2004). Comparison with modern analogues (e.g. Figure 6.1) may suggest that these surges were triggered by disruption of the basal meltwater drainage system, together with short-lived and migratory changes in the thermal state of the glacier bed (Murray *et al.*, 2000; Fowler *et al.*, 2001; Smith *et al.*, 2002).

Whatever the genesis of individual landforms, further evidence of dynamic behaviour of the ice cap is inferred from aspects of the modelling experiments. In particular, the advance of the Rannoch Glacier described in Paper VI shows that rapid glacier advances of considerable distance are not only possible, but may not necessarily be synchronous with changes in climate. This decoupling of climate and glacier response reflects longer term mass balance adjustments, in which mass that accumulated during colder and wetter periods is progressively advected through the glacier system, and may explain the apparent conflict between studies claiming early or late glacier maxima (Rose *et al.*, 1988; Palmer *et al.*, 2008), as described above. The unique topography of Rannoch Moor – a relatively high plateau surrounded by high mountains – no doubt conditioned this behaviour, by funnelling large volumes of widely distributed ice through a single dominant outlet route. This modelled advance could only occur, however, if the rate of ice flow from the accumulation areas was sufficiently high to offset melting in the ablation zone. Since nearly all other modelled outlet glaciers show retreat during this period (12.5 - 12.1 ka BP), it seems likely that the ability of a glacier to advance through a period of climatic warming is strongly governed by thresholds in its mass balance regime. That this regime is conditioned and controlled largely by overall climatic trends rather than transitory 'flickers' is further evident in the evolution of volumetric changes through the glacial episode shown in Paper VII. These data show that, despite variability in precipitation supply throughout the model run, and abrupt, decadal-scale, jumps in temperature, net volume of the domain ice masses waxes and wanes gradually, and is little influenced by the highly-variable annual mass balance.

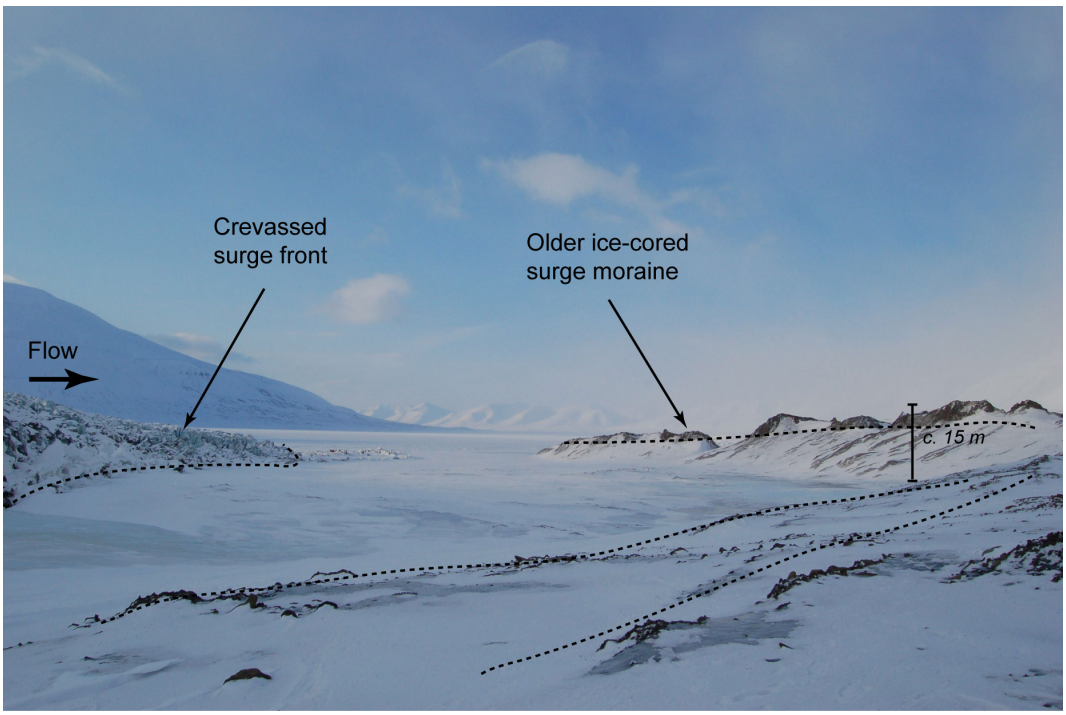

Figure 6.1: Crevassed surge front of Bakaninbreen, Svalbard, and an older ice-cored moraine marking the limit of a previous, more extensive, surge event. The moraine contains imbricated clasts, which may reflect formation by proglacial thrusting.

6.1.5 Deglaciation

Moraines throughout the study area show sedimentological evidence of abrupt changes in sediment supply, changes in depositional environment, and compressive glaciotectonism (Papers I, II, III, and IV). Together, these characteristics reflect oscillations of an adjacent or closely proximal ice-margin. The abundance of such evidence, and the relative absence of features typical of widespread areal stagnation, such as kettled outwash terraces, eskers, kames, and chaotic ice-marginal dump mounds, suggest that deglaciation of the study area proceeded actively, with glaciers that retreated dynamical rather than decayed *in situ*. This scenario agrees with other Younger Dryas glacier reconstructions elsewhere in Scotland, (e.g. Bennett & Boulton, 1993b; Benn, 1997; Lukas, 2005b; Finlayson, 2006). Localised stagnation no doubt occurred where glacier tongues were cut-off from their accumulation areas, but was probably restricted in its spatial extent. Widespread evidence of laminated sediments within moraines, commonly glaciotectonised and interbedded with diamicton units, suggests that glacier forelands were very wet, and were characterised by ephemeral ponds at the margins of still active glaciers. Such conditions are most likely to occur during periods of high precipitation (to maintain mass turnover) combined with relatively rapid climatic warming (to enhance ice-marginal and ice-surface melting). Rapid warming at the end of the Younger Dryas is shown by the GRIP δ^{18}O record to have begun sometime after 11.9 ka BP, and to have continued until 11.5 ka BP.

6.1.6 Climate

Whilst climatic inferences can be drawn from deglacial landforms, as described above, complexity in the climate–glacier system makes it difficult to precisely link glacier geometry with specific climatic conditions, a concept that is explored in more detail below (see 'Discussion', below). Nonetheless, many studies, including Paper III presented here, have attempted to use empirical glacial reconstructions to derive palaeoenvironmental parameter values, principally precipitation or temperature (e.g. Sissons & Sutherland, 1976; Sutherland, 1984b; Ballantyne, 2002; Golledge, 2007a). Despite some variability between studies, most have concluded that Younger Dryas precipitation was more strongly focussed along the western mountains ranges than it is at present, and that consequently, much of central and eastern Scotland was considerably more arid than now. Palaeoenvironmental proxies such as chironomids and coleoptera indicate that annual temperature ranges may have been greater than present, which, coupled with the precipitation pattern, suggests a much more 'continental' climate than present. Geological evidence in the study area indicates a thick ice cap with steep margins (Paper III), which may have resulted from either colder or wetter conditions than previously thought, but which was nonetheless controlled in its eastward extent by steep climatic gradients. Model simulations driven by such a climate successfully replicate this overall ice cap geometry (Paper VI), lending support to its feasibility. Additionally, these experiments also demonstrate that a temperature threshold exists, below which only small icefields develop, and above which an extensive ice cap grows. However, greater cooling leads to a runaway scenario unless precipitation is reduced during the stadial, which probably occurred as a result of the southerly migration of the oceanic polar front and its concomitant impact on the amount of sea ice forming around Scotland (Bard *et al.*, 1987; Denton *et al.*, 2005).

6.2 Discussion: Glacier–climate relationships

The research described and synthesized above employs standard techniques and widely used assumptions regarding the correspondence between climate, topography, and glacier geometry. Such simplifications are necessary, since real-world complexity is too great to either identify in the geological record, or to model in numerical simulations. Consequently, areas of uncertainty remain with respect to the way in which glacier reconstructions can be linked to palaeoclimatic conditions, and, perhaps more importantly, this highlights the difficulty in relating predicted future climate changes to likely glacier and ice sheet responses. Three areas of uncertainty are considered below: empirical mass balance relationships and their use in palaeoglaciological reconstructions; the role of continentality in influencing glacier growth and distribution; and non-linearity in glacial systems.

6.2.1 Mass balance and the Equilibrium Line Altitude

Glaciers achieve steady-state when accumulation and ablation are approximately equal over a number of years. Theoretically, under steady-state conditions, a glacier is more-or-less in harmony with its governing climate, thus any additional accumulation will lead to thickening of the glacier and most probably an advance of the ice front, whereas decreased accumulation or increased ablation will result in thinning and retreat. Whilst 'steady-state' is an important theoretical concept, it is one that, 'is never encountered in practice' (Paterson, 1994, p30), due to lags in the transmission of accumulated mass through the glacier system to its terminus, and the natural variability of climate. The Equilibrium Line Altitude (ELA) is another theoretical concept, identifying the ice surface altitude where net accumulation is zero at the end of a 'balance year', of a glacier flowing in steady-state. Calculation of a former ELA is commonly practised in studies aiming to describe and compare glaciers and their evolution through time. Whilst net mass balance over any particular year may not be a good reflection of the longer-term balance state of a glacier, the ELA concept is nonetheless useful for comparative studies where glaciers are assumed to persist in steady-state, and where the relationship between glacier response and climate is assumed to be linear.

Many palaeoglaciological studies have employed a variety of methods for calculating former glacier ELAs (e.g. Ballantyne, 1989, 2002; Osmaston, 2005; Ballantyne, 2006), and have used empirical relationships from modern glaciers to infer palaeoclimatic conditions from the height of the ELA (Liestøl, 1967; Sutherland, 1984b; Ohmura *et al.*, 1992). Such investigations are extremely effective in allowing precipitation or temperature at the ELA to be calculated, if one or other is known or can be inferred. Since Scottish summer maximum temperatures and annual temperature ranges have been reconstructed from palaeoenvironmental studies in areas that were not glaciated during the Younger Dryas (Atkinson *et al.*, 1987; Brooks & Birks, 2000, 2001), from regional scale modelling experiments (Isarin & Renssen, 1999), and from the distribution and form of periglacial features (Ballantyne & Harris, 1994), these may be used, in combination with calculated ELAs, to derive former precipitation estimates for Younger Dryas glaciers in Scotland. In several instances, the use of these parameters and empirical functions has led to conclusions that the Younger Dryas in Scotland was wetter than present (Ballantyne, 2002; Benn & Lukas, 2006; Ballantyne, 2007). Such studies may be useful, but

appear to conflict both with regional climatic indications that North Atlantic sea ice was considerably more extensive than present during the Younger Dryas, leading to much colder, drier conditions over much of Northwest Europe (Bond *et al.*, 1993; Mayewski *et al.*, 1994; Isarin & Renssen, 1999), and with Scottish modelling experiments indicating lower annual precipitation totals during the stadial (Hubbard, 1999; Golledge *et al.*, 2008a).

This apparent disparity may be resolved in one of two ways. Firstly, it may be that the palaeoenvironmental proxies used to calculate ELA precipitation over-estimate air temperatures at the glacier surface. The second consideration is that of the annual temperature range occurring during the Younger Dryas, and most especially its difference from modern values, and the way in which this is addressed in temperature / precipitation functions.

Climatic and glacier surface air temperature

Methods employed in the reconstruction of absolute air temperatures and ranges from palaeoecological proxies are known to be affected by uncertainties associated either with variability in the climatic tolerances of the indicator species being used, or with the methodological techniques employed in the necessary regression analyses (Walker *et al.*, 1993; Coope *et al.*, 1998; Isarin & Bohncke, 1999). Nonetheless, when collated over a wide area, there is encouraging agreement between inferences from different proxies (Isarin & Renssen, 1999). These authors note, however, that their regional climatic reconstructions tend to overestimate summer temperatures compared to those inferred from former glacier geometries in Scotland by Sissons & Sutherland (1976), Sissons (1979b,c), Sutherland (1984b) and Ballantyne & Harris (1994). Reasons for this may be complex and individually different, but perhaps the simplest explanation is that the palaeoenvironmental proxies used (plants, coleoptera, chironomids) typically occur and are preserved only in ice-free areas, and thus reflect air temperatures unaffected by the cooling effect of glaciers known to influence ice surface air temperatures (Khodakov, 1975; Braithwaite, 1980; Singh *et al.*, 2000; Hughes & Braithwaite, 2008). Katabatic effects and greater albedo serve to lower temperatures in the area immediately adjacent to an ice sheet or glacier, thereby producing effective temperatures at the ice surface somewhat cooler than those of the regional climate in ice-free areas. According to the relationship of Khodakov (1975), calculated from 'data of both ice sheet and mountain glaciers of the world' (p26), this 'temperature leap' may be as much as 1.6–2.0°C for glaciers 10–20 km in length respectively (Fig. 6.2). This lowering of temperatures ultimately results in greater net accumulation. Given these considerations, it may be prudent for studies employing palaeoenvironmental proxy data for temperature reconstructions to treat such values as maxima, and to calculate precipitation values at the ELA using a range of temperatures adjusted for glacier cooling.

Continentality

The ability of water bodies to absorb, store, and release heat means that large oceans exert a moderating influence on the temperature of air masses that pass over them. Conversely, air passing over land (or extensive terrestrial or sea ice) is much more liable to higher magnitude and more rapid changes in temperature. The term 'continentality' therefore describes the degree to which the climate of a region is influenced by its proximity to open oceans, such

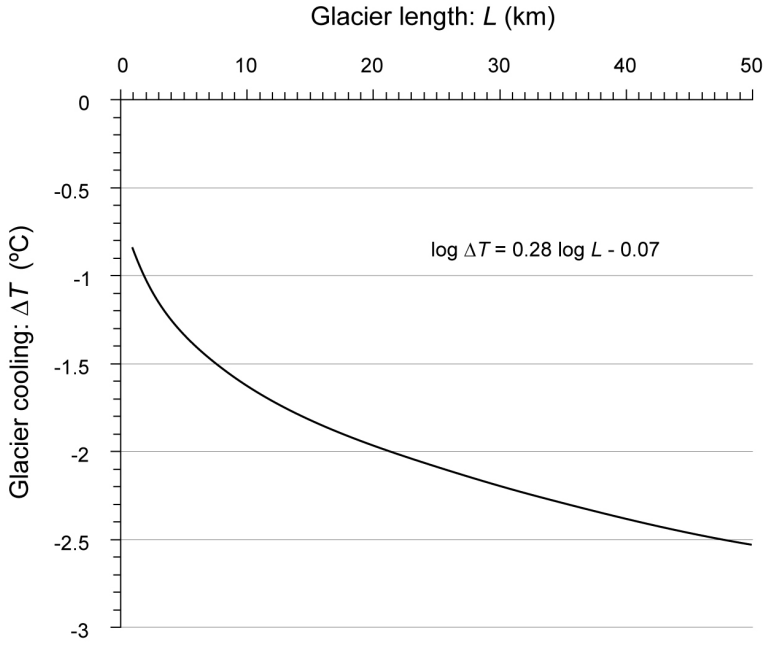

Figure 6.2: The cooling effect exerted by glaciers on their immediate climate, as a function of glacier length, based on global glacier data (Khodakov, 1975).

that areas far from open seas and surrounded mainly by land or ice are 'continental', whereas land close to open water, and affected predominantly by air masses that pass over it, is 'maritime'. Continental climates tend to exhibit greater annual temperature ranges than maritime climates, and are often characterised by hot summers and harsh winters rather than the moderate winters and cooler summers typical of coastal areas. At comparable latitudes, eastern Canada is more continental than the United Kingdom, due to the influence of the Atlantic Ocean on the prevailing southwesterly air masses that affect the latter. The term 'seasonality' refers to the seasonal occurence of particular climate phenomenon, and is often related to precipitation. Thus a highly seasonal rainfall pattern would be one in which a large proportion of the annual total falls in a particular season. The term has also been applied to temperature patterns, where high seasonality of temperature indicates that greater seasonal, or *intra-annual*, differences occur. In this sense, a continental climate may also be loosely referred to as a highly seasonal one, with respect to temperature. The use of 'seasonality' to describe annual temperature range is now commonplace in the literature (e.g. Denton *et al.*, 2005; Hughes & Braithwaite, 2008), and is used here in the same context.

Alley *et al.* (2004) and Denton *et al.* (2005) use a combination of Greenland ice-core palaeothermometry and Greenlandic glacier ELAs to argue that seasonal differences in air temperature were accentuated during the Younger Dryas stadial, with respect to present. These seasonal differences were most evident during winter months, when temperatures plummeted well below present values, whereas summer temperatures were only slighter cooler than today. Such 'switching' of seasonal variability 'during ice-age events' (Alley *et al.*, 2004) resulted from extensive North Atlantic winter sea ice formation akin to that presently evident in Antarctic seas. Sea ice expansion in the North Atlantic was enabled due to the reduced activity of the North Atlantic thermohaline circulation, essential for the transport of heat from

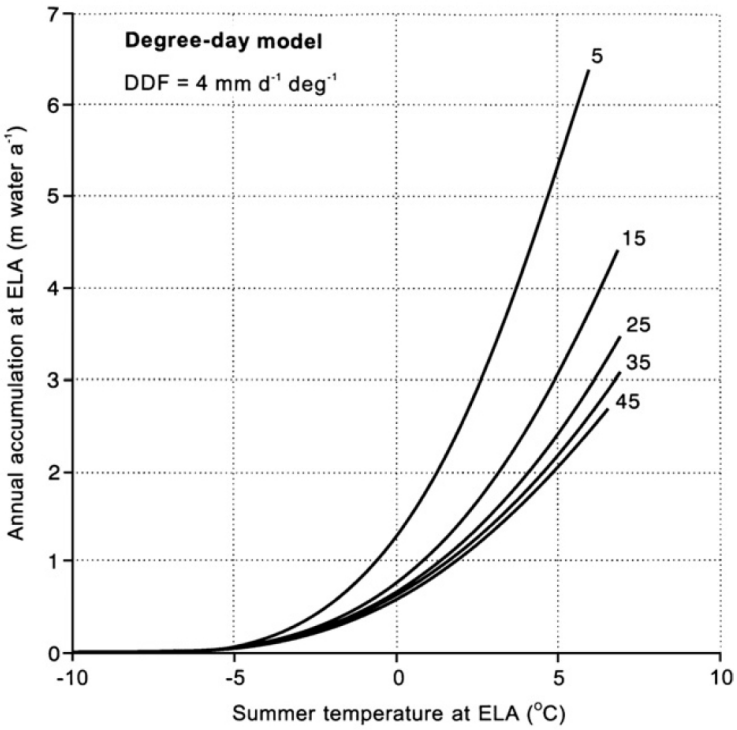

Figure 6.3: A family of curves representing annual accumulation at the ELA for different annual temperature ranges, represented as a function of summer mean temperature (June, July, August), from the degree day model of Hughes & Braithwaite (2008). The model assumes sinusoidal temperature variability throughout the year.

the tropics, and for the supply of high density saline surface water that maintains high-latitude overturning and deep water formation. Denton *et al.* (2005) argued that, due to these effects, a 20°C increase (from present) in the annual temperature range occurred in Greenland during the Younger Dryas. Lie & Paasche (2006) subsequently found that an increase of only 10°C could also satisfactorally explain the available data, but despite this, they concur with Denton *et al.* (2005) that seasonal variability was enhanced during the Younger Dryas, and go on to suggest that this variability was not equal across the North Atlantic region, but was accentuated in the eastern Atlantic region. This scenario supports the 'hinged-door' mode of seasonal polar front migration proposed by COHMAP (1988), in which the 'hinge' lies in the western Atlantic, with greatest seasonal variability occurring around Northwest Europe. Palaeoenvironmental reconstructions for Britain and Northwest Europe support these inferences, suggesting seasonal temperature ranges during the Younger Dryas of 20-30°C (c. 10-20°C greater than present in the UK) (Atkinson *et al.*, 1987; Ballantyne & Harris, 1994; Isarin & Renssen, 1999).

These studies suggest that Scotland experienced a much more continental climate during the Younger Dryas than the maritime regime prevailing today. Hughes & Braithwaite (2008) demonstrated effectively that glacier mass balance relationships are strongly influenced by annual temperature range, and that accurate reconstruction of Pleistocene climates from glacier geometries necessitates the use of a 'family' of temperature / precipitation functions, depending on the seasonal variability of their former climate (Fig. 6.3).

This approach clearly identifies the effect of considering continentality, yet has still to be

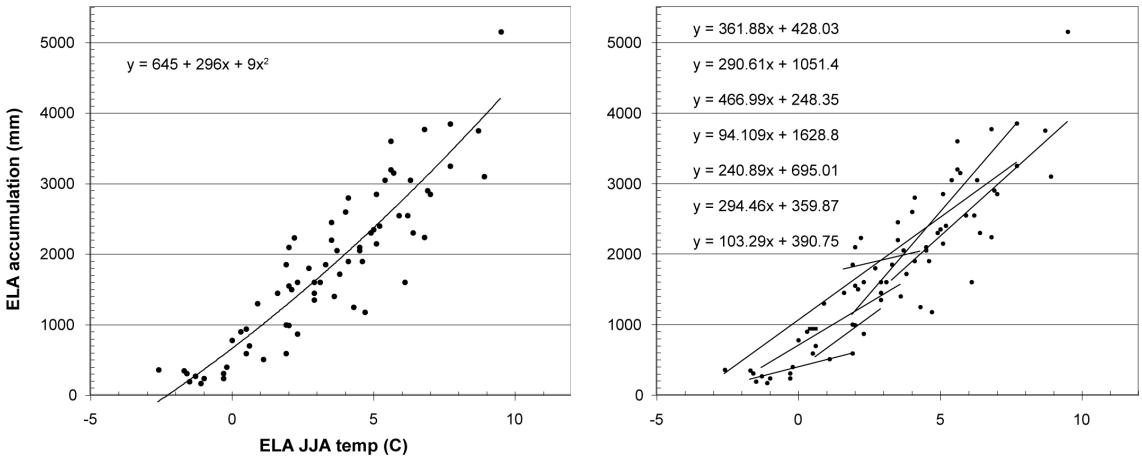

Figure 6.4: The dataset of temperature / precipitation data for 70 globally distributed glaciers presented by Ohmura *et al.* (1992). On the left, the regression line that defines the general relationship, and on the right, the many different regression lines that define each group of glaciers. The highly variable slope and y-intercept values of these lines reflects the variability in the climatic regimes included in the dataset, particularly their degree of continentality and associated annual temperature range.

adopted for Scottish glacier reconstructions. To date, most such studies have employed regression equations based on the datasets of Liestøl (1967) or Ohmura *et al.* (1992), of which the latter is most commonly used (e.g. Ballantyne, 2006; Finlayson, 2006; Golledge, 2007a). The global dataset presented by Ohmura *et al.* (1992) includes glaciers from widely contrasting climatic regimes, from very cold and arid environments in high-Arctic Canada, to very maritime glaciers in western Norway (Fig. 6.4).

It has been suggested that this 'amalgamation' of differing glacier-climate relationships adds strength to the derived temperature / precipitation regression equation, as it 'smoothes out regional variations' (Benn & Ballantyne, 2005, p589). However, as described above, several recent Scottish studies that use this equation have calculated wetter Younger Dryas conditions than is consistent with wider evidence. These differences may be at least partially resolved by using a degree-day approach to calculate ELA accumulation, where intra-annual temperature variability and its role in glacier mass balance is properly considered.

Degree day schemes sum the total number of 'positive degrees' in a year by assuming a sinusoidal temperature variability constrained by summer maximum and winter minimum temperatures (T_{max} and T_{min}), or by T_{max} and inferred annual temperature range, R. Monthly temperatures (T_{month})can be calculated thus:

$$T_{month} = [\sin \pi \cdot (-0.5 + ((M-1) \cdot 0.167)) \cdot (\frac{1}{2}R + (T_{max} - \frac{1}{2}R))] \tag{6.1}$$

where M is number of the month in the year, R is annual temp range, and T_{max} is maximum (July) temperature. Based on this relationship, mean annual air temperature ($\overline{T}$) can be calculated with:

$$\overline{T} = \frac{[\sum_{i=1}^{12}[\sin \pi \cdot (-0.5 + ((M_i - 1) \cdot 0.167)) \cdot (\frac{1}{2}R + (T_{max} - \frac{1}{2}R))]]}{12} \tag{6.2}$$

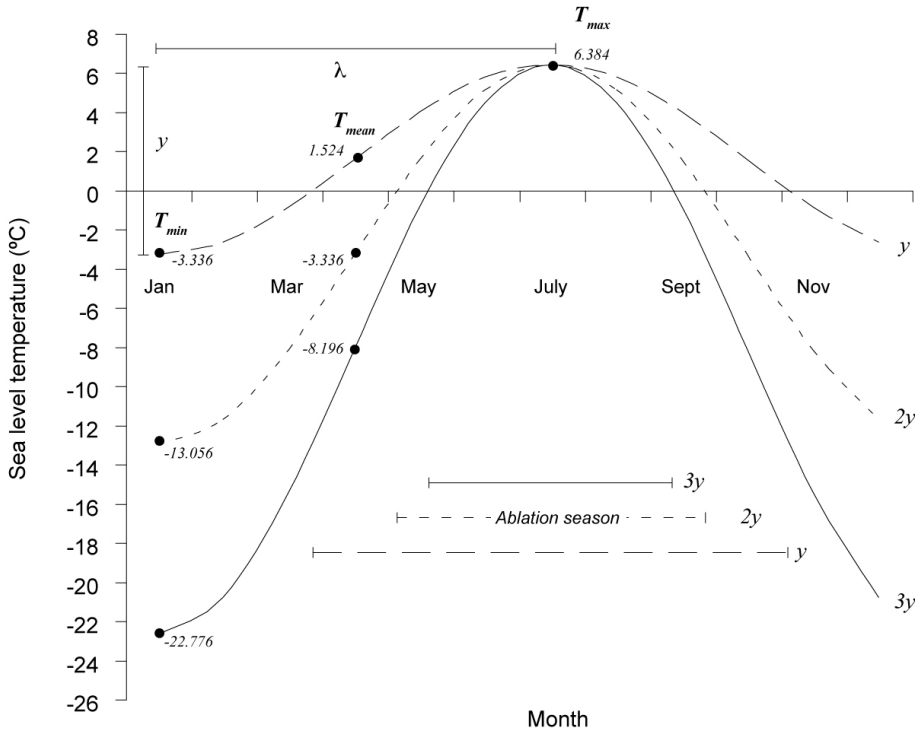

Figure 6.5: The effect of increasing annual temperature range on mean air temperature, showing 10°C , 20°C and 30°C ranges, typical of the Younger Dryas stadial (Denton *et al.*, 2005; Lie & Paasche, 2006). Note also how the length of the ablation season decreases markedly with increased continentality.

which equates to:

$$\frac{T_{max} + T_{min}}{2} \tag{6.3}$$

Using these simple functions it is possible to illustrate how increasing annual temperature range affects both the mean annual temperature, and the length of the ablation season. Figure 6.5 shows these effects with a sea level summer temperature of 6.384°C , as ascertained through the modelling experiments of Paper VI, rather than the 8.25°C , calculated (using a lapse rate of 0.006°C /m) from chironomid-based temperature reconstructions at 125 m above sea level in part of southern Scotland that escaped Younger Dryas glaciation (Brooks & Birks, 2000).

For glaciers in steady state, which is the assumption necessary to any ELA calculation, accumulation at the ELA (b) must equal ablation, itself a function of the number of positive degree days in the year (PDD) and the amount of snow or ice each degree can melt (the degree-day factor - f) (Equation 6.4). Higher reflectance combined with percolation and refreezing mean that snow melts less readily than ice, giving rise to a range of commonly used values from 3 - 8 mm day^{-1} °K^{-1} (Singh *et al.*, 2000; Braithwaite *et al.*, 2006; Hughes & Braithwaite, 2008; Golledge *et al.*, 2008a):

$$b = [\sum [PDD \cdot f]] \tag{6.4}$$

Clearly, the lower mean temperatures and shorter ablation season associated with higher annual temperature ranges results in reduced annual melt, which, for a steady-state glacier,

means that less accumulation is necessary to maintain net mass balance. Thus for any given glacier and a prescribed summer maximum temperature, accumulation at the ELA will be less in a highly continental climate than in a more maritime climate with a lower annual temperature range. Glacier reconstructions that utilise the Ohmura *et al.* (1992) relationship may therefore inadequately represent palaeoprecipitation at the ELA, since the generalised regression equation employed encompasses glaciers with both high and low season temperature ranges. By virtue of its bias towards maritime climates, reconstructed values in similar areas will be reasonably accurate, whereas those in more continental areas will be less so. Without an appreciation of palaeotemperature range, therefore, uncertainty will surround any calculations derived using this method.

By itself, the degree-day model described above (Equation 6.4) remains rather abstract. Incorporated into a thermomechanical ice sheet model, however, such schemes become considerably more useful for reproducing former accumulation / ablation characteristics. The model simulations presented in Papers VI and VII assume a present day annual temperature range (seasonality = 1). In order to assess the influence exerted by greater intra-annual temperature ranges, new experiments were run for the model domain, with the aim of producing a simulated ice cap of comparable extent to the 'optimum fit' result of Paper VI. For these experiments, the GRIP temperature pattern was used again, but adjusted so that Mean Annual Temperature is decreased by an amount that maintains a constant summer temperature depression for each of the three scenarios, and which also accounts for the greater intra-annual range. The magnitude of *inter*-annual changes remains the same, however. The results are shown in Figure 6.6 below. Since increasing temperature ranges result in lower mean temperatures, which favours increased accumulation, it is necessary to reduce total precipitation across the model domain in order to most closely reproduce the target ice extent. In the examples shown here, a doubled intra-annual temperature range requires a domain precipitation reduction of 15%, whereas under trebled seasonality a reduction of 30% is necessary. Initial experiments showed that greater seasonal temperature variability exacerbated west-east and south-north precipitation gradients, leading to much less accumulation in eastern and northern areas than required. In order to maintain the correct volumes in western and southern areas, therefore, the eastward and northward precipitation reductions were relaxed from 80% and 60% to 70% and 60% respectively for double seasonality, and to 65% and 55% for treble seasonality. Thus the impact of altering the annual temperature range is that both precipitation volume and its distribution need to be adjusted. Furthermore, experimentation proved that under the trebled seasonality scenario, ice accumulating in the higher areas of the domain did not flow into the lower valleys as readily as under warmer conditions, and thus many 'optimum fit' outlet glacier limits were not reached. Since this is likely to result from thermomechanical effects – that is, colder ice being less able to flow – the amount of basal sliding prescribed in the model input file was increased by an order of magnitude.

The results (Fig. 6.6) show that, under increased annual temperature ranges, a variety of parameters need to be adjusted to accurately reproduce the 'optimum fit' glacier configuration. Doubling the annual temperature range from 9.72°C to 19.44°C gives rise to a mean annual temperature of -3.336°C and a winter temperature of -13.056°C (Fig. 6.5). The increase in effective accumulation as a result of these lower temperatures means that a precipitation

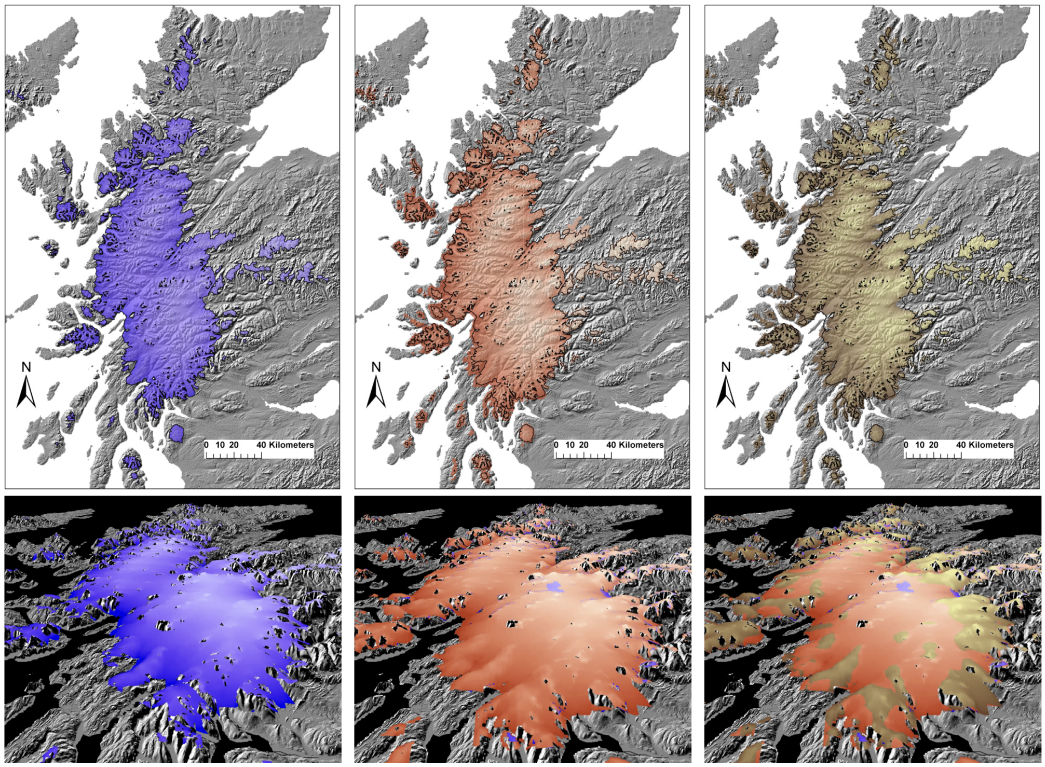

Figure 6.6: Ice extents under a range of annual temperature variability, where T_{max} remains constant. Upper panels show plan view, lower panels show perspective view looking north. Perspective views show successively superimposed surfaces; note how ice under double seasonality is generally thicker than under single, but that ice under treble seasonality is thinner in core areas than under double, due to the necessity to increase basal sliding.

reduction across the domain of 15% is necessary to control ice build-up, but with 10% less aridity in the east. Under these conditions an ice cap is produced that resembles the 'optimum fit' both in horizontal extent and in thickness (Fig. 6.6). Greater overall accumulation is most evident in the higher areas around the periphery of the main ice cap, and some of the outlet glaciers are also slightly more extensive. No increase in sliding is required in this scenario, however. Trebling the annual temperature range to 29.16°C produces an annual mean of -8.196°C and a winter minimum of -22.776°C (Fig. 6.5), which leads to excessive build-up of ice unless precipitation is reduced by 30% across the domain. The amount of additional aridity imposed in the east and north is reduced to 65% and 55% respectively, which enables ice build-up in all the necessary areas of the domain. However, accumulation is focussed on high ground and accumulation in valleys is suppressed, as a result of slower ice flux under the colder conditions. With internal deformation (creep) being controlled so significantly by temperature, flow of ice into lower areas of the domain requires an order of magnitude increase in the basal sliding factor. Under these conditions, the ice mass that evolves reaches most of the target margins (Fig. 6.6), with only slightly greater accumulation in the west and on high plateaux in the east. The ice mass is thicker around its margins than under single or double seasonality, but is thinner in much of its interior (Fig. 6.6, lower right). Outlet glaciers are similar in extent to the other simulations, but the ice mass has a lower overall surface slope.

The model simulations described above illustrate that mild and wet conditions of annual temperature ranges similar to present give rise to an ice cap that is thick in its central area, and slopes relatively steeply towards its margins. By contrast, the ice build-up under more continental scenarios results in a thinner central ice mass with a consequently shallower surface profile. These implications may be significant. If a change in the prevailing climate from low to high continentality took place during a former glacial episode, therefore, it might reasonably be expected to have resulted in a corresponding change in the geometry of extant glaciers. The isotopic record preserved in the GRIP ice core suggests that more highly seasonal climates probably dominated the Heinrich Event (HE) phases of the last glacial cycle, due to the cooling of the North Atlantic, reduction in efficiency of the thermohaline circulation, and consequent expansion of winter sea ice (Denton *et al.*, 2005). The Younger Dryas has previously been associated with 'HE 0' (Kirby, 1998; Rahmstorf, 2002), thus it seems likely that it experienced greater seasonality than the preceding interstadial. New evidence has shown that, during the interstadial, ice survived and oscillated in northwest Scotland (Bradwell *et al.*, 2008), whilst cosmogenic exposure ages from the western Highlands also demonstrate that ice thicknesses may have been greatest early in the Younger Dryas stadial (Golledge *et al.*, 2007), prior to thinning under a drier climate (Benn *et al.*, 1992; Golledge *et al.*, 2008a). Furthermore, the geomorphological evidence indicative of relatively thick ice mapped in southern and eastern areas glaciated during the Younger Dryas (Horsfield, 1983; Golledge, 2007a), is at odds with studies further north and west which use the presence of periglacial trimlines to infer the former presence of low surface gradient glaciers and a relatively thin mountain icefield (Thorp, 1984, 1986). Could it be that the evidence interpreted throughout Scotland as reflecting the expansion and retreat of Younger Dryas glaciers in fact records the transition from a relatively thick ice cap, inherited from the decaying Late Devensian ice sheet during the mild and wet interstadial, into a thinner, less dynamic icefield that regrew and subsequently persisted through the much colder, drier, more highly seasonal stadial? If these ideas are correct, the geomorphological legacy of Scotland may be reinterpreted in a new light. Rather than recording the waxing and waning of glaciers in response to a short-lived, isolated climatic 'hiccup', the surviving landform and sedimentary archive may instead be offering clues as to the timing and style of the climate shift that occurred during the last glacial–interglacial transition, and the way in which the decaying British Ice Sheet adapted.

Calculations of mass balance at the ELA

The model outputs illustrated in Figure 6.6 represent ice extent shortly after the coldest part of the Younger Dyras stadial, when the 'optimum fit' of modelled ice extent to empirical limits occurs (Golledge *et al.*, 2008a). Although variability in imposed GRIP-scaled climate prevents modelled glaciers achieving true 'steady-state' conditions, this time-slice represents the period closest to overall equilibrium. Using precipitation, temperature and mass balance output data from these numerical simulations it is possible to investigate their inter-relationship in a manner similar to that adopted by Ohmura *et al.* (1992). In contrast to the Ohmura dataset, however, the model data provide c. 12500 discrete data points for regression analysis, rather than 70. Additionally, the data is specifically tuned to the topography and inferred climate of Scotland, making insights derived from observed relationships more relevant to local studies.

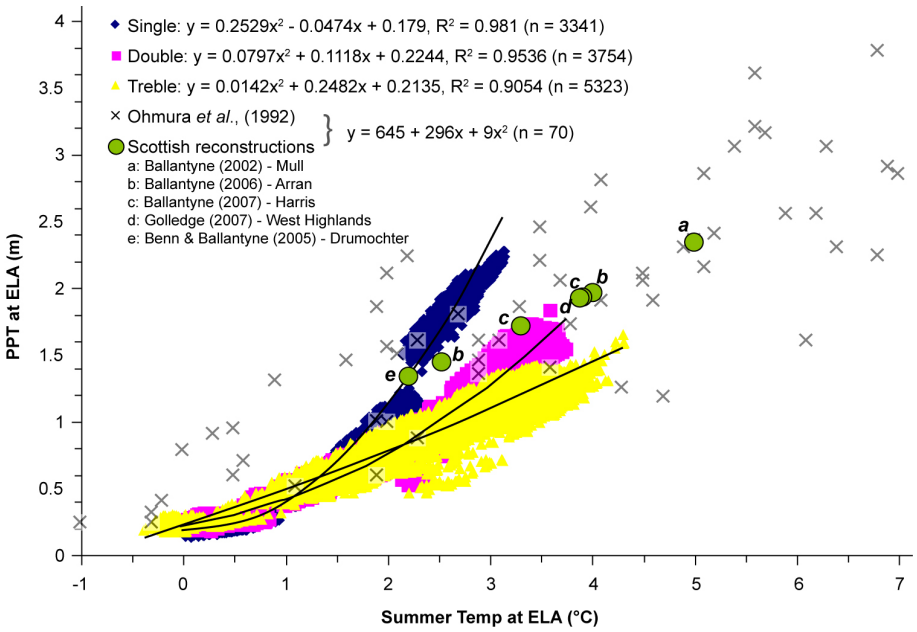

Figure 6.7: Temperature / precipitation data from three model runs simulating present day (single), double, and treble seasonality. Black lines illustrate the regression trends described in the legend. For comparison, data from the glaciers described by Ohmura *et al.* (1992) are shown, representing a wide range of climatic regimes. Seven Scottish palaeoglaciological studies based on the Ohmura temperature / precipitation relationship are also shown, with recalculated values normalised to the lapse rate and sea level July temperature used in the model runs for clearer comparison.

Points were selected where net mass balance (b) = 0 ± 0.05m, and had corresponding precipitation, elevation and temperature data appended, using cell extraction and data sampling techniques in ArcGIS 9.2. These data, for each of the three different intra-annual ranges investigated, are shown in Figure 6.7. Regression curves fitted to these data yield R^2 values of 0.9054 - 0.981, suggesting that there is a very good correspondence between summer temperature at the ELA and precipitation at the ELA in each case. There are notable differences between the populations, however, reflecting the differences in climate and resultant ice distribution produced by increasing annual temperature ranges. Where ELA temperatures are relatively low (-0.5°C – +2.0°C), a similar temperature / precipitation relationship exists for all three regimes. These low ELAs would be most likely encountered in high and arid areas. Where ELAs are lower, and their summer temperatures correspondingly higher, greater divergence occurs between the three scenarios. Under present day seasonality, precipitation at the ELA increases rapidly with warmer ELA summer temperatures, whereas with more seasonal climates, the rise in precipitation is much less steep.

Also shown on Figure 6.7 are data points from Ohmura *et al.* (1992), and seven additional points marking values calculated from reconstructed Scottish glaciers using the Ohmura regression equation. The Scottish examples have been recalculated from their originally published form to standardise lapse rates across the population (0.006°C / m), and to normalise sea level July temperatures to that used in the numerical simulations (6.4°C) to enable direct comparison with model data. Given the spread of climatic regimes represented by the Ohmura

et al. (1992) dataset, it is hardly surprising that the reconstructions based on these data span all three of the modelled temperature / precipitation envelopes. It is interesting to note that glacier calculations from the relatively warm and wet palaeoenvironment of Mull (Fig. 6.7 - 'a') closely match the range of values predicted by the modelled data for such temperatures only under enhanced seasonality scenarios, whereas under the same conditions, the reconstructed values in Drumochter, furthest east, overpredict precipitation at the ELA by up to 500 mm (Fig. 6.7 - 'e'). Geographically between these two extremes are the western Highlands, whose reconstructed values also lie between the two end members (Fig. 6.7 - 'd'). Data for Arran and Harris show less clear relationships for one of each of their reconstructed ELAs, perhaps reflecting the influence of additional local factors at these sites.

What is clear from these data is that the Ohmura dataset adequately reproduces palaeoprecipitation values only where the former climate was relatively warm and wet, that is, essentially maritime. Where the former climate regime was more continental, dominated by aridity and higher, colder, ELAs, the generalised regression based on the global dataset fares less well. By modelling temperature / precipitation relationships using a degree-day scheme incorporated into a validated thermomechanical ice sheet model, it is now possible to define ELA precipitation (y) as a simple function of ELA temperature (x) in a way that is optimised for the Scottish Younger Dryas environment, with a seasonal temperature range three times that of present (Equation 6.5):

$$y = 0.0142x^2 + 0.2482x + 0.2135 \tag{6.5}$$

A new temperature / precipitation curve can now be calculated, based on this function, for the values presented in the Scottish studies shown in Figure 6.7. For comparison, linear regression equations based on data from each of the geographic groups incorporated in the Ohmura dataset are also used to calculate precipitation, over the same range of ELA temperatures (Fig. 6.8). The Ohmura-based individual population curves clearly show the very different temperature / precipitation relationships that characterise modern maritime and continental glaciated environments, whereas the new modelled curve illustrates the relationship that is inferred to have existed during the Younger Dryas in Scotland, when inland glaciers were considerably colder and more arid than their coastal counterparts.

6.2.2 Non-linearity

Thresholds

Climatic relationships such as those shown in Figure 6.7 produce increasingly large differences in predicted values of y for uniform increments of x. This type of *non-linear* response of a dependent variable is typical of many natural systems, and can be identified in the growth patterns and dynamical behaviour of simulated ice sheets. For example, Paper VI highlighted the climatically decoupled response of the modelled Rannoch Glacier, which continued to advance during 400 years of climatic warming and decreased precipitation. The mass balance forcing to which it was reacting, therefore, was one inherited from an earlier stage of the model run representing the Younger Dryas climatic minimum, when accumulation in the glacier source regions was greatest. That the glacier continued to advance during a phase of decreasing mass

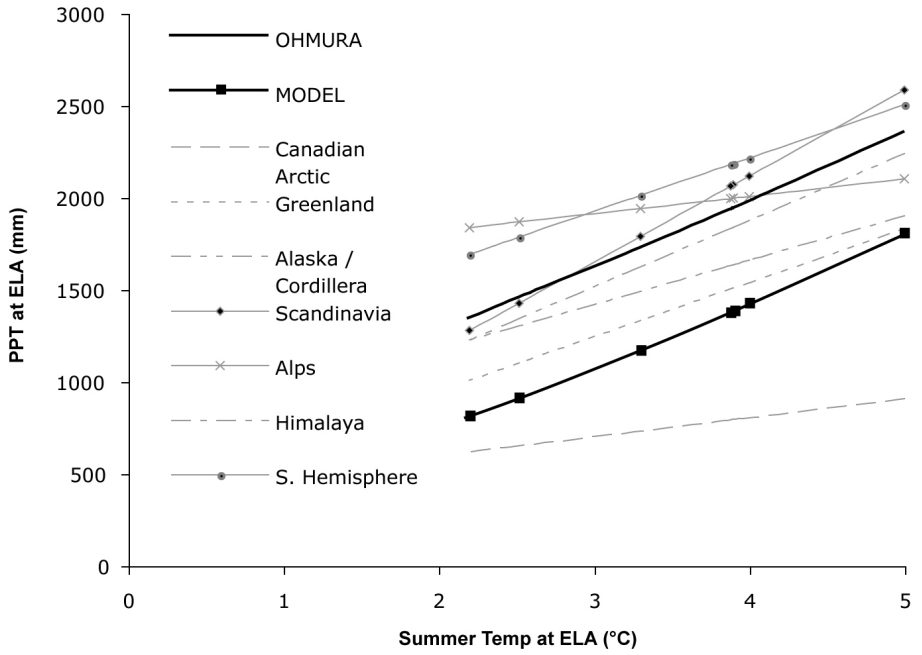

Figure 6.8: ELA temperature / precipitation relationships according to regression equations from component geographic groups of global glaciers presented by Ohmura *et al.* (1992), as well as predictions from the generalised Ohmura function used in most Scottish studies, and the non-linear relationship defined by a positive degree-day driven ice sheet model. Note how the modelled relationship approximates end members of both cold, arid ELA relationships (e.g. Canadian Arctic) as well as more maritime mass balance environments (e.g. Scandinavia).

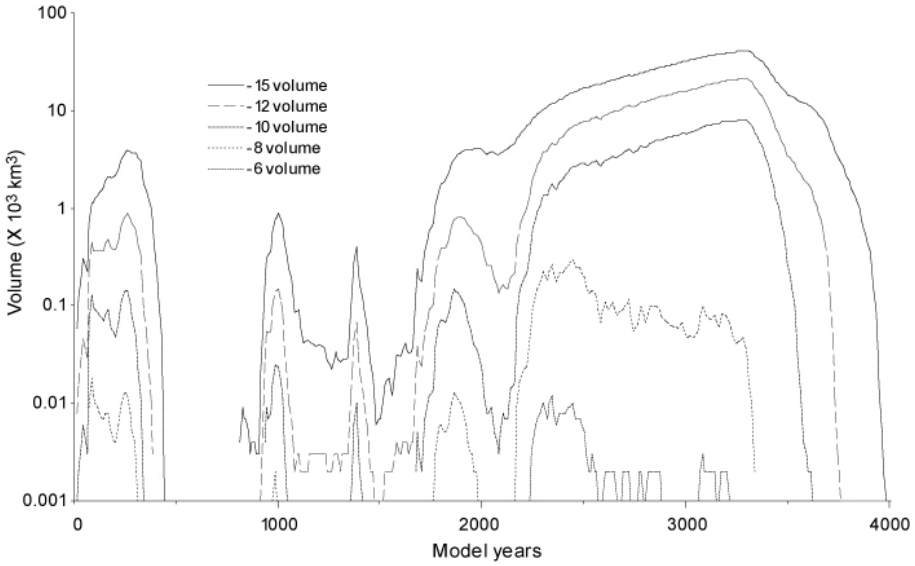

Figure 6.9: Bifurcation of volumetric growth trajectories of modelled ice sheets under different climatic cooling scenarios, based on a 20-year GRIP temperature pattern and modern Scottish topography. Based on data from model runs described in Golledge *et al.* (2008a).

input suggests that sufficient mass already existed in the glacier catchment to ensure overall positive mass balance. This appears to indicate the existence of a critical mass balance threshold, which, in this scenario, promotes a non-linear response when exceeded. This mass balance threshold is also demonstrated by time-series plots of ice sheet volume through the model run (Fig. 6.9). In this example, mass balance is controlled by present precipitation patterns modified with imposed reductions eastward and northward as described in Paper VI, and by various scalings of the GRIP palaeotemperature record. The coldest part of the Younger Dryas occurs at 12.64 ka BP, or 2360 model years in the model run. When scaled to maximum mean annual temperature depressions at this time of 6°C below present, ice volumes peak coincident with maximum cooling; with an 8°C scaling ice volume peaks shortly after the climatic minimum at 12.5 ka BP (2500 model years); both decline thereafter. Temperature depressions greater than this (10°C - 15°C), however, result in sustained volumetric growth throughout much of the rest of the stadial, despite climatic warming (Fig. 6.9). This type of threshold has been noted in similar studies previously, and is likely to occur as a result of topographic influences (Payne & Sugden, 1990; Hulton & Sugden, 1997). This is critical, since climatic scenarios producing accumulation rates only slightly below such thresholds will only give rise to disparate icefields largely controlled by topography, whereas scenarios producing slightly higher accumulation will lead to considerably more extensive ice build up and will ultimately be influenced less by their underlying topography.

Lags

The scenarios described above occur under a climatic forcing pattern defined by empirical data (the GRIP δ^{18}O record). Such records are essential for producing realistic model simulations of past glacial episodes, yet the natural variability in the climate trends may introduce unwanted complexity into more generic considerations of ice sheet–climate linkages. In order that these

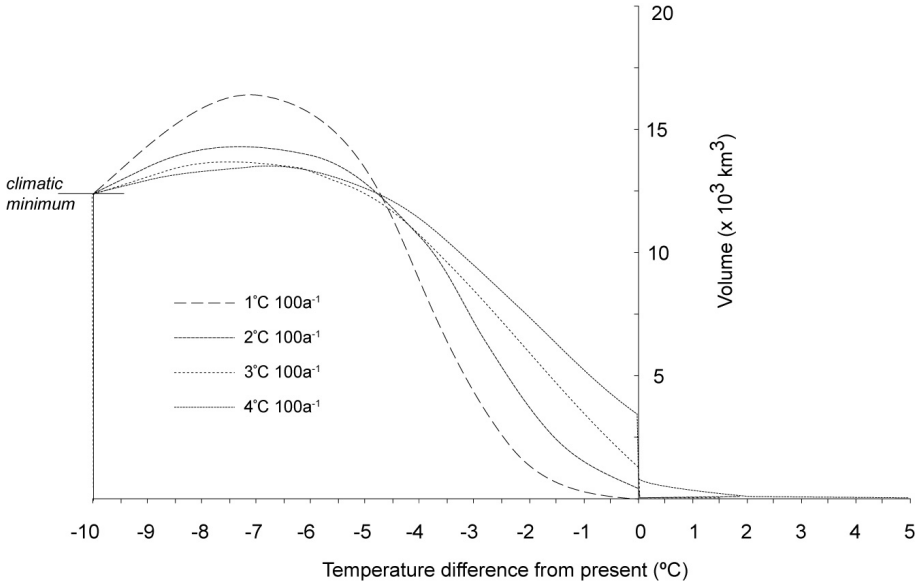

Figure 6.10: Volumetric changes of simulated ice sheets as a function of total temperature depression from present, based on decay under a range of climatic warming scenarios from initially uniform maximum conditions. Note how more gradual warming rates initially allow significant continued growth of the ice sheet, but subsequently undergo greater volumetric decay per degree of climate warming than glaciers exposed to faster climatic changes.

may be studied more clearly, the validated Scottish Younger Dryas ice sheet model can be forced with an artifical climate file. Of particular societal interest at present is the manner in which extant glaciers might respond to rising global temperatures, thus further experiments were carried out to investigate the relative importance of both the amount, and the rate, of warming. The model described in Paper VI reaches near maximum conditions within 500 years, when forced with a 10°C cooling from present. Taking the resultant ice mass from this scenario as a starting point, a series of model runs were carried out in which the simulated ice mass was subjected to climatic warming rates of 0°C - 4°C 100 a^{-1}, based on the likely range of temperatures for modern warming scenarios envisaged by the IPCC 4th Assessment (Solomon *et al.*, 2007): 0.6 - 4.0°C 100 a^{-1}. In all cases except 0°C 100 a^{-1}, model simulations were run for as long as necessary to achieve complete deglaciation in the model domain, thus a longer run was required for the glaciers exposed to slower warming rates, than for the experiments forced with a faster rate of warming. Figure 6.10 shows the results of these experiments, with results of each run plotted according to the magnitude of temperature change, rather than model time elapsed, thereby removing the variable temporal element. Data for the 0°C 100 a^{-1} scenario are omitted, since no warming leads to continued growth, rather than deglaciation.

Figure 6.10 illustrates that with rising temperatures, ice volumes only continue to increase at magnitudes below a certain threshold – between 6 - 8°C lower than present. Within this range, glaciers warming at slower rates accumulate the greatest volume, whilst those warming faster accumulate less. However, despite its greater volume, the simulated ice sheet warming at 1°C 100 a^{-1} subsequently loses greater volume per unit temperature change than those warming more quickly. This may be due to the longer time period involved, enabling transfer of mass through the glacier system and consequently less imbalance in the overall mass budget. More rapidly warming glaciers have less time to adjust and so exist in a state of disequilibrium

with the forcing climate, and will exhibit responses that lag behind the climatic conditions that initially gave rise to them. Interestingly, and perhaps as a consequence of these factors, the synthetic ice sheets forced with 2 - 4°C 100 a^{-1} temperature rises all return to their initial starting temperature with positive mass. In the most extreme case, the simulated ice sheet warming at 4°C 100 a^{-1} requires a further temperature rise of c. 2°C to ensure complete deglaciation. These experiments highlight the importance of considering the *rate*, as well as the *amount*, of warming when assessing likely responses of glaciers to changes in climate. With respect to reconstructive studies, these data suggest that the geometry of an ice mass and its derived ELA, as calculated from surviving landforms, will actually represent the climatic conditions (particularly the temperature / precipitation relationship) that prevailed somewhat earlier in the glacial cycle, rather than the environment at the time of a glaciers maximum extent.

Hysteresis

That many of the experiments described above result in residual mass when runs return to their initial starting temperature illustrates the effect of ice sheet 'hysteresis' (*sensu* Oerlemans, 1982; Huybrechts, 1993; Pollard & DeConto, 2005). Modelling experiments simulating global ice sheets have identified similar scenarios, for example, in Greenland, '... an ice sheet would not reform with present boundary conditions if it were to melt' (Crowley & Baum, 1995, p358), and in Patagonia '...whereas only modest ELA lowering is necessary to grow the ice cap, considerably more of an ELA rise is required to remove it' (Hulton & Sugden, 1997, p89). Using the ice sheet model validated for the Younger Dryas in Scotland, it is possible to run a series of controlled experiments that use the same IPCC-derived rates of climate change as described above, and to inspect the mass balance data for evidence of hysteresis. The previous experiment principally concerned lags evident in ice sheet decay. In this next experiment, both ice sheet growth and decay are forced by the same rate of temperature change, producing a climate file for the length of the model run that is 'symmetrical'. If mass balance is simply governed by the magnitude of temperature change, and if the ice sheet responds to this change rapidly, the resultant growth curve for each model run should also be symmetrical about the axis marking maximum temperature depression. However, Figure 6.11 demonstrates that this does not occur, and that a considerable lag occurs between the timing of coldest conditions and the peak in ice volume. The lags in these simulations range in length from approximately 12.5 - 15% of the total duration of the model runs, or 25 - 30% of the growth period, and result from the continued growth of ice masses beyond climatic minima as described above and in Figure 6.10.

In the model runs described above, each scenario requires a different amount of time to cool to, and warm from, the same maximum depression. Data from simulations with different run lengths can be more easily compared by plotting volume data against area. Where area is high and volume low, the ice sheet is thin, whereas a thicker ice sheet is characterised by higher volume with respect to area. Volume / area relationships have been investigated in many other studies, due to the relative ease of calculation of the latter, and the more difficult estimation of the former (Bahr *et al.*, 1997; Radić *et al.*, 2007), and can be useful in understanding the response times of glaciers in steady state (Bahr *et al.*, 1998; Pfeffer *et al.*, 1998; Harrison *et al.*, 2001). Glaciers in non-steady (transient) state may exhibit quite different volume /

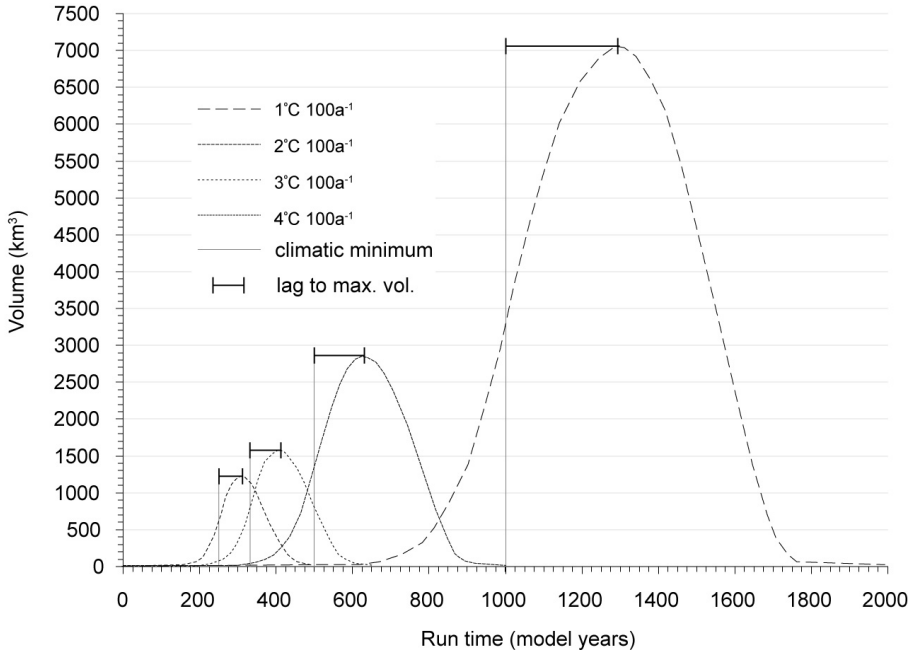

Figure 6.11: Volumetric changes of simulated ice sheets as a function of time, based on a range of symmetrical climatic cooling and warming scenarios. Note the occurence of lags between the timing of maximum climatic cooling, and the maximum volume of the simulated ice sheet, which occurs irrespective of size or model run length.

area relationships, however, such as during growth and decay phases (see below), but these differences are thought to result in only a minimal error in volume predictions over a relatively long time scale (Radić *et al.*, 2007).

Figure 6.12 illustrates the results of model runs forced by a range of climate perturbations during both growth and decay phases, using present Scottish topography and precipation distribution as input data.

During the growth phase (lower limb), each temperature scenario differs slightly from the others in terms of its volume / area relationship, with thickest ice accumulating under the most gradual cooling scenario, and thinnest ice with fastest cooling. Areal expansion is limited in every case by the total ELA depression of -10°C common to all of the model runs, however, volumetric increases take place and continue into the initial stages of the decay curve (upper limb), giving rise to thickening ice sheets in a manner similar to that described in the previous (decay only) experiment. Interestingly, despite volume / area differences during growth, geometric relationships during decay under each of the climatic scenarios converge to almost uniform values. At the point of convergence, decay volumes are approximately an order of magnitude greater than for equivalent areal extent during ice sheet growth. This pattern is maintained, and increases slightly, during the latter stages of decay, resulting in residual mass at the end of the model run in every case.

The reason for this effect most probably lies in the influence of the accumulating ice on the mass balance forcing that produces it. A positive feedback takes place, in which cooling leads to accumulation, which in turn produces thickening and thus further cooling of the ice sheet

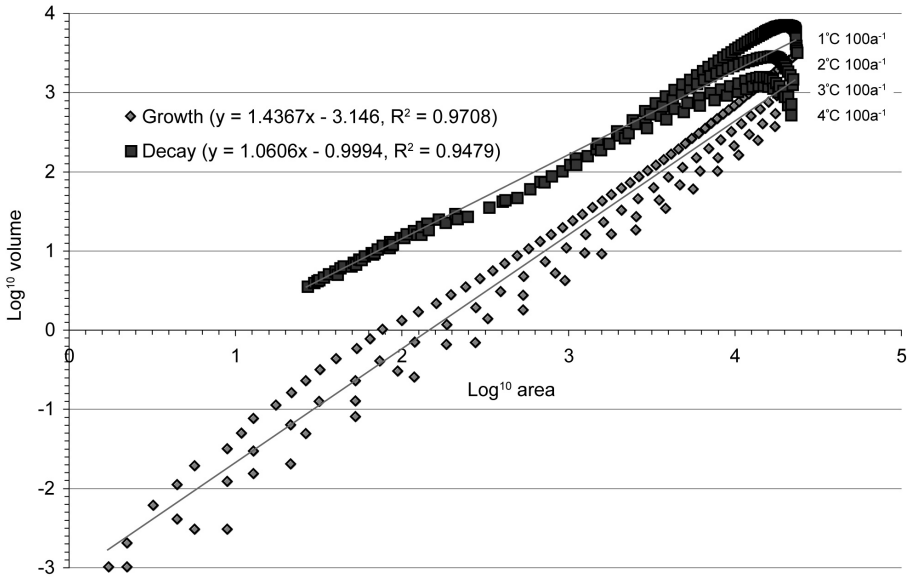

Figure 6.12: Area / volume relationships of modelled ice sheets evolving under a range of synthetic climatic scenarios, where cooling and warming rates are identical, switching from one to the other when a cumulative temperature depression of -10°C is achieved.

surface, at a rate controlled by the environmental lapse rate. For a highly dissected mountain topography such as the one used in these experiments, the infilling of valleys and basins with ice gives rise to a considerably higher mean elevation across the domain than accounted for by topography alone. Consequently, glacier accumulation area is vastly increased and only ice discharged by outlet glaciers enters the ablation zone. Growing an ice sheet to the stage where it can affect its own climate in this way is largely governed by the critical climate–topography threshold described in the bifurcation experiment above, and noted by others (Payne & Sugden, 1990), and thus it is likely that the role played by ice sheet hysteresis will be greatest for ice sheets and ice caps, and least for valley glaciers and relatively thin mountain icefields.

6.3 Summary

From the above Discussion it is clear that the usefulness of glacier reconstructions as tools for inferring palaeoclimatic values is limited by the complexities and uncertainties that surround glacier–climate relationships. Mass balance regimes are strongly governed by seasonal variability; bifurcations in ice sheet growth are largely conditioned by topography; lags between climatic change and ice sheet response occur if the glacier is not in steady-state; and hysteresis effects may lead to different volume / area relationships for any given glacier depending on its stage of evolution and the direction of its evolutionary trend. Consequently, caution must be adopted when interpreting inferences drawn from all empirical studies, unless each of these factors can be justifiably disregarded. Despite these uncertainties, however, the insights gleaned from ice sheet modelling may nonetheless assist with glacier reconstructions, since, by highlighting the complexities, we are more at liberty to entertain hypotheses that may have previously seemed counter-intuitive. Ultimately, this freedom to explore new interpretations may prove fruitful for glaciological studies not just in Scotland, but in all past and presently

glaciated environments.

Chapter 7

Conclusions

7.1 Conclusions

This thesis has combined geological mapping and glaciological modelling to investigate glaciation in western Scotland during the Younger Dryas. In particular, sedimentology, geomorphology, geochronology and numerical simulations have been used to address a series of key questions, in order to clarify:

1. the pattern and rate of ice build-up, and the timing of maximum ice extent and thickness,
2. whether glaciation was extensive or restricted, and composed of relatively thick or thin ice masses,
3. the relative balance between ice flow by bed deformation, basal sliding and creep,
4. whether glacier behaviour was climatically synchronous, and whether or not glaciers retreated actively, and
5. the dominant climate characteristics during the stadial

.

Additionally, the research aimed to establish whether geological evidence is sufficient to enable accurate palaeoglaciological reconstructions; to discover if a numerical model could closely simulate such reconstructed glacier limits; and to ascertain the extent to which a combination of the two could be used to understand wider issues of glacier–climate relationships.

Although the investigations described in each paper of the thesis have enabled insights into different aspects of these questions, their synthesis allows the following conclusions to be drawn. Glaciation in western Scotland during the Younger Dryas was characterised by a main ice cap that was linear in form, and which straddled the north-south mountain chain from the Highland Boundary at Loch Lomond to Wester Ross in the north (Fig. 5.1). Around this ice cap grew independent icefields on isolated massifs. In central and eastern Scotland, glaciation was restricted to small, high-level, plateau icefields. Geomorphological evidence indicates that the ice surface of the main ice mass was at least 800 m above sea level in its central areas (e.g. Rannoch Moor), which, according to modelling and geochronology evidence, may have occurred early in the stadial (i.e. prior to 12.5 ka BP). Whether this ice mass grew from ice that had survived the preceding interstadial (GI-1) is not known, but emerging new data from elsewhere in Scotland (Bradwell *et al.*, 2008) suggest that this may have been the case, at least in some areas. Modelling experiments show that thick ice caps tend to form under relatively warm and wet conditions, whereas thinner icefields tend to result from colder, drier climates. The seemingly contradictory evidence in Scotland indicating both thick ice cap glaciation (Horsfield, 1983; Golledge, 2007a), and thin *icefield* glaciation (Thorp, 1986; Bennett & Boulton, 1993a), may be reconciled if a climate transition – dominated by an increase in seasonality – occurred early in the stadial, leading to geometric readjustments of the ice cap such that the latter part of the stadial was characterised by relatively thin glaciers under a more continental (high-arctic style) climate.

Both geological and numerical evidence points to limited deformation of glacier beds in the central areas of the ice cap during the Younger Dryas, instead, ice flow was accomodated

principally by meltwater-lubricated sliding on rigid beds (mainly bedrock), and by deformation of ice above the bed (creep). This enabled the preservation of pre-existing sediment sequences, and the overprinting or subtle modification of older landforms. Further from the ice cap centre, basal sliding velocities were higher and deforming beds were more widespread, leading to thicker accumulations of Younger Dryas-age subglacial till near to glacier margins. Glaciers expanded according to the major climatic changes that occurred during the transition into the Younger Dryas, but the timing of their maximum extents was affected by lags in the propagation of ice through the glacier system, such that outlets with large catchments and low bed gradients (e.g. Rannoch glacier) reached their most extensive several centuries after the coldest part of the stadial. All glaciers were subject to topographically related thresholds, which required specific climatic conditions to overcome. For example, marginally insufficient cooling would have restricted glacier build-up to high mountain areas, whereas slightly too much cooling would have led to overly extensive glacierization. Modelling experiments have shown that a delicate balance existed between mean annual temperature depression, annual temperature range, precipitation volume, precipitation distribution, and the amount of basal sliding that took place.

Sedimentological data in the main study area south of Rannoch Moor has been interpreted as reflecting very wet conditions during final deglaciation, accompanied by active oscillations of glacier margins. These inferences concur with modelled scenarios in which glacier recession continues during rapid climatic warming at the close of the stadial. Overall, the mean Younger Dryas climate in Scotland was probably c. 10°C cooler than present during the summer months, but perhaps as much as 30°C colder during the winter. The greater annual temperature range occuring during the stadial resulted from more extensive North Atlantic sea ice, which suppressed the moisture-carrying capacity of prevailing south-westerly winds and led to considerably drier conditions across much of the landmass, most especially in areas east of the main ice cap.

These insights into the characteristics of Younger Dryas glaciation and climate demonstrate that geological mapping, combined with glaciological modelling, represents an effective system for palaeoglaciological reconstructions. Geological data alone provide insufficient, and commonly ambiguous, evidence to adequately deduce glaciological or climatological details, but are fundamental for establishing glacier geometry and chronology. Numerical simulations excel at providing much more detailed information on former flow patterns, flow mechanisms, and the governing climate, but require the geological inferences for guidance and validation. The experiments described here demonstrate that it is possible to closely simulate empirical glacier limits using an ice sheet model, but also highlight that recurrent inconsistencies occur. Where such mismatches between numerically simulated and geologically reconstructed glacier limits occur, further research may be necessary to determine whether model input data needs to be refined (for example by the inclusion of freshwater bathymetric data), or whether better geochronological constraint is needed on the features used in the empirical studies. Modelling experiments have also illuminated the complexity of glacier–climate relationships, and the necessary appreciation of non-linear behaviour in such systems. Furthermore, modelling has enabled more detailed insight into mass balance relationships, particularly for Scottish glaciers during the Younger Dryas, and offers a new method for the effective calculation of former temperature / precipitation parameters from geological data.

These conclusions considerably advance current understanding of the Younger Dryas in Scotland, but a key area of uncertainty still persists. Much of the work presented here is predicated on the widely held assumption that Scotland was largely ice-free during the Windermere Interstadial (i.e. GI-1), and that glaciation began afresh at the onset of the stadial (GS-1). These views are based on only a limited number of radiocarbon dates from low altitude sites around the margins of the main ice cap. To-date, no organic deposits firmly dated to the interstadial period have been reported from within the ice cap core area. New evidence is showing that landforms previously thought to be diagnostic of Younger Dryas glaciers may also occur outside stadial limits (Golledge *et al.*, 2008b), that in some areas glaciers retreated actively throughout the interstadial (Bradwell *et al.*, 2008), whilst in other areas there appears to be an almost seamless geomorphological transition between 'old' and 'new' features. Future work should aim to improve our understanding of glacier–climate interactions through the Lateglacial, to quantify the potential role of seasonality shifts in prevailing climate patterns, and to establish more solid boundary conditions for further modelling experiments. Together, these might enable changing glacier configurations during the whole of the last glacial termination to be reproduced with even greater accuracy and validity.

Chapter 8

References

Bibliography

Agassiz, L. 1841. On glaciers, and the evidence of their having once existed in Scotland, Ireland, and England. *Proceedings of the Geoloical Society of London*, **3**, 327–332.

Ahlmann, H.W. 1948. *Glaciological research on the North Atlantic coasts.* Royal Geographical Society Research Series 1. Royal Geographical Society, London.

Alley, R. B. 2000. The Younger Dryas cold interval as viewed from central Greenland. *Quaternary Science Reviews*, **19**, 213–226.

Alley, R. B., & MacAyeal, D. R. 1994. Ice-rafted debris associated with binge purge oscillations of the Laurentide Ice-Sheet. *Paleoceanography*, **9**(4), 503–511.

Alley, R. B., Meese, D. A., Shuman, C. A., Gow, A. J., Taylor, K. C., Grootes, P. M., White, J. W. C., Ram, M., Waddington, E. D., Mayewski, P. A., & Zielinski, G. A. 1993. Abrupt increase in Greenland snow accumulation at the end of the Younger Dryas event. *Nature*, **362**, 527–529.

Alley, R. B., Cuffey, K. M., Evenson, E. B., Strasser, J. C., Lawson, D. E., & Larson, G. J. 1997. How glaciers entrain and transport basal sediment: Physical constraints. *Quaternary Science Reviews*, **16**, 1017–1038.

Alley, R. B., Denton, G. H., Comer, G. C., & Broecker, W. S. 2004. The role of changing seasonality in North Atlantic abrupt climate changes. *Eos Transactions, AGU, Fall Meeting Supplement*, **85**(Abstract number PP13B-01).

Ambrose, K. 2000. *Specifications for the preparation of 1:10 000 scale geological maps.* BGS Research Report RR/00/02. British Geological Survey, Keyworth.

American Geographical Society. 1958. *Geographic study of mountain glaciation in the northern hemisphere. Department of Exploration and Field Research, contract DA19-129-QM-409.* Exploration and Field Research, contract DA19-129-QM-409 Exploration and Field Research, contract DA19-129-QM-409. Part 1. American Geographical Society, New York.

American Geological Institute. 1957. *Glossary of geology and related sciences.* Publication 501. American Geological Institute, Washington D.C.

Anderson, J. B., Shipp, S. S., Lowe, A. L., Wellner, J. S., & Mosola, A. B. 2002. The Antarctic Ice Sheet during the Last Glacial Maximum and its subsequent retreat history: a review. *Quaternary Science Reviews*, **21**, 49–70.

Andrews, J. T, & Smithson, B. B. 1966. Till fabrics of the cross-valley moraines of north-central Baffin Island, Northwest Territories, Canada. *Geological Society of America Bulletin*, **77**, 271–290.

Andrews, J. T., Barry, R. G., & Drapier, L. 1970. An inventory of the present and past glacierization of Home Bay and Okoa Bay, east Baffin Island, N.W.T., Canada, and some climatic and palaeoclimatic considerations. *Journal of Glaciology*, **9**, 337–362.

Andrzejewski, L. 2002. The impact of surges on the ice-marginal landsystem of Tungnaárjókull, Iceland. *Sedimentary Geology*, **149**, 59–72.

Arthern, R., & Hindmarsh, R. C. A. 2003. Optimal estimation of changes in the mass of ice sheets. *Journal of Geophysical Research*, **108**(F1, 6007), doi: 10.1029/2003JF000021.

Atkinson, T. C., Briffa, K. R., & Coope, G. R. 1987. Seasonal temperatures in Britain during the past 22,000 years, reconstructed using beetle remains. *Nature*, **325**, 587–592.

Bahr, D. B., Meier, M. F., & Peckham, S. D. 1997. The physical basis of glacier volume-area scaling. *Journal of Geophysical Research*, **102**(B9), 20355–20362.

Bahr, D. B., Pfeffer, W. T., Sassolas, C., & Meier, M. F. 1998. Response time of glaciers as a function of size and mass balance: 1. Theory. *Journal of Geophysical Research*, **103**(B5), 9777–9782.

Ballantyne, C. K. 1979. A sequence of Lateglacial ice-dammed lakes in East Argyll. *Scottish Journal of Geology*, **15**, 153–160.

Ballantyne, C. K. 1983. Precipitation gradients in Wester Ross, northwest Scotland. *Weather*, **38**, 379–387.

Ballantyne, C. K. 1989. The Loch Lomond Readvance on the Isle of Skye, Scotland: glacier reconstruction and palaeoclimatic implications. *Journal of Quaternary Science*, **4**, 95–108.

Ballantyne, C. K. 1997. The periglacial geomorphology of Scotland. *Pages 166–178 of:* Gordon, J. E. (ed), *Reflections on the Ice Age in Scotland: an Update on Quaternary Studies*. Glasgow: Scottish Association of Geography Teachers and Scottish Natural Heritage.

Ballantyne, C. K. 2002. The Loch Lomond Readvance on the Isle of Mull, Scotland: glacier reconstruction and palaeoclimatic implications. *Journal of Quaternary Science*, **17**, 759–771.

Ballantyne, C. K. 2006. Loch Lomond Stadial Glaciers in the Uig Hills, Western Lewis, Scotland. *Scottish Geographical Journal*, **122**, 256–273.

Ballantyne, C. K. 2007. Loch Lomond Stadial glaciers in North Harris, Outer Hebrides, North-West Scotland: glacier reconstruction and palaeoclimatic implications. *Journal of Quaternary Science*, **26**, 3134–3149.

Ballantyne, C. K., & Harris, C. 1994. *The Periglaciation of Great Britain*. Cambridge: Cambridge University Press.

Ballantyne, C. K., & Stone, J. O. 2004. The Beinn Alligin rock avalanche, NW Scotland: cosmogenic Be-10 dating, interpretation and significance. *Holocene*, **14**(3), 448–453.

Bamber, J. L., Krabill, W. B., Raper, V., & Dowdeswell, J. A. 2004. Anomalous recent growth of part of a large Arctic ice cap: Austfonna, Svalbard. *Geophysical Research Letters*, **31**, doi:10.1029/2004GL019667.

Bard, E., Arnold, M., Maurice, P., Duprat, J., Moyes, J., & Duplessy, J. C. 1987. Retreat velocity of the North Atlantic polar front during the last deglaciation determined by ^{14}C accelerator mass spectrometry. *Nature*, **328**, 791–794.

Barnard, P. L., Owen, L. A., & Finkel, R. C. 2006. Quaternary fans and terraces in the Khumbu Himal south of Mount Everest: their characteristics, age and formation. *Journal of the Geological Society, London*, **163**, 383–399.

Beaudry, L. M., & Prichonnet, G. 1991. Late Glacial De-Geer moraines with glaciofluvial sediment in the Chapais area, Québec (Canada). *Boreas*, **20**, 377–394.

Benn, D. I. 1989. Debris transport by Loch Lomond Readvance glaciers in Northern Scotland: basin form and the within-valley asymmetry of lateral moraines. *Journal of Quaternary Science*, **4**, 243–254.

Benn, D. I. 1992. Scottish Landform Examples - 5 The Achnasheen Terraces. *Scottish Geographical Magazine*, **108**, 128–131.

Benn, D. I. 1994. Fluted moraine formation and till genesis below a temperate valley glacier - Slettmarkbreen, Jotunheimen, southern Norway. *Sedimentology*, **41**(2), 279–292.

Benn, D. I. 1996. Subglacial and subaqueous processes near a glacier grounding line: Sedimentological evidence from a former ice-dammed lake, Achnasheen Scotland. *Boreas*, **25**, 23–36.

Benn, D. I. 1997. Glacier fluctuations in western Scotland. *Quaternary International*, **38-9**, 137–147.

Benn, D. I., & Ballantyne, C. K. 1994. Reconstructing the transport history of glaciogenic sediments - A new approach based on the co-variance of clast form indexes. *Sedimentary Geology*, **91**, 215–227.

Benn, D. I., & Ballantyne, C. K. 2005. Palaeoclimatic reconstruction from Loch Lomond Readvance glaciers in the West Drumochter Hills, Scotland. *Journal of Quaternary Science*, **20**, 577–592.

Benn, D. I., & Evans, D. J. A. 1996. The interpretation and classification of subglacially-deformed materials. *Quaternary Science Reviews*, **15**(1), 23–52.

Benn, D. I., & Evans, D. J. A. 1998. *Glaciers and Glaciation.* London: Arnold.

Benn, D. I., & Lehmkuhl, F. 2000. Mass balance and equilibrium-line altitudes of glaciers in high-mountain environments. *Quaternary International*, **65-6**, 15–29.

Benn, D. I., & Lukas, S. 2006. Younger Dryas glacial landsystems in western Scotland: possible modern analogues and palaeoclimatic implications. *Quaternary Science Reviews*, **25**, 2390–2408.

Benn, D. I., Lowe, J. J., & Walker, M. J. C. 1992. Glacier response to climatic change during the Loch Lomond Stadial and early Flandrian: geomorphological and palynological evidence from the Isle of Skye, Scotland. *Journal of Quaternary Science*, **7**, 125–144.

Benn, D. I., Kirkbride, M. P., Owen, L. A., & Brazier, V. 2003. Glaciated valley landsystems. *Pages 372–406 of:* Evans, D.J.A. (ed), *Glacial Landsystems*. London: Arnold.

Benn, D. I., Hulton, N. R. J., & Mottram, R. H. 2007a. 'Calving laws', 'sliding laws' and the stability of tidewater glaciers. *Annals of Glaciology*, **46**, 123–130.

Benn, D. I., Warren, C. R., & Mottram, R. H. 2007b. Calving processes and the dynamics of calving glaciers. *Earth-Science Reviews*, **82**, 143–179.

Bennett, M. R. 1993. Patterns of deglaciation during the Loch Lomond Stadial; an example from the Northwest Highlands. *Quaternary Newsletter*, **69**, 90.

Bennett, M. R., & Boulton, G. S. 1993a. Deglaciation of the Younger Dryas or Loch Lomond Stadial ice-field in the northern Highlands, Scotland. *Journal of Quaternary Science*, **8**, 133–145.

Bennett, M. R., & Boulton, G. S. 1993b. A reinterpretation of Scottish hummocky moraine and its significance for the deglaciation of the Scottish Highlands during the Younger Dryas or Loch-Lomond Stadial. *Geological Magazine*, **130**, 301–318.

Bennett, M. R., & Glasser, N. F. 1991. The glacial landforms of Glen Geusachan, Cairngorms: a reinterpretation. *Scottish Geographical Magazine*, **107**, 116–123.

Bennett, M. R., Huddart, D., & Thomas, G. S. P. 2002. Facies architecture within a regional glaciolacustrine basin: Copper River, Alaska. *Quaternary Science Reviews*, **21**(20-22), 2237–2279.

Bentley, M. J., Evans, D. J. A., Fogwill, C. J., Hansom, J. D., Sugden, D. E., & Kubik, P. W. 2007. Glacial geomorphology and chronology of deglaciation, South Georgia, sub-Antarctic. *Quaternary Science Reviews*, **26**, 644–677.

Björck, S., Walker, M. J. C., Cwynar, L. C., Johnsen, S., Knudsen, K. L., Lowe, J. J., Wohlfarth, B., & INTIMATE Members. 1998. An event stratigraphy for the Last Termination in the North Atlantic region based on the Greenland ice-core record: a proposal by the INTIMATE group. *Journal of Quaternary Science*, **13**, 283–292.

Blake, K. P. 2000. Common origin for De Geer moraines of variable composition in Raudvassdalen, northern Norway. *Journal of Quaternary Science*, **15**, 633–644.

Blunier, T., & Brook, E. J. 2001. Timing of millennial-scale climate change in Antarctica and Greenland during the last glacial period. *Science*, **291**, 109–112.

Bond, G., Broecker, W., Johnsen, S., McManus, J., Labeyrie, L., Jouzel, J., & Bonani, G. 1993. Correlations between climate records from North Atlantic sediments and Greenland ice. *Nature*, **365**, 143–147.

Borgström, I. 1979. De Geer moraines in a Swedish mountain area? *Geografiska Annaler*, **61**(1-2), 35–42.

Boulton, G. S. 1986. A paradigm shift in glaciology? *Nature*, **322**, 18.

Boulton, G. S. 1996. Theory of glacial erosion, transport and deposition as a consequence of subglacial sediment deformation. *Journal of Glaciology*, **42**, 43–62.

Boulton, G. S., & Hagdorn, M. 2006. Glaciology of the British Isles ice sheet during the last glacial cycle: form, flow, streams and lobes. *Quaternary Science Reviews*, **25**, 3359–3390.

Boulton, G. S., & Hindmarsh, R. C. A. 1987. Sediment deformation beneath glaciers - rheology and geological consequences. *Journal of Geophysical Research-Solid Earth and Planets*, **92**(B9), 9059–9082.

Boulton, G. S., Jones, A. S, Clayton, K. M., & Kenning, M. J. 1977. A British ice-sheet model and patterns of glacial erosion and deposition in Britain. *Pages 231–246 of:* Shotton, F. W. (ed), *British Quaternary Studies: Recent Advances*. Oxford: Clarendon Press.

Boulton, G. S., Dobbie, K. E., & Zatsepin, S. 2001. Sediment deformation beneath glaciers and its coupling to the subglacial hydraulic system. *Quaternary International*, **86**, 3–28.

Bradwell, T. 2006. The Loch Lomond Stadial glaciation in Assynt: a reappraisal. *Scottish Geographical Journal*, **122**, 274–292.

Bradwell, T., Fabel, D., Stoker, M. S., Mathers, H., McHargue, L., & Howe, J. A. 2008. Ice caps existed throughout the Lateglacial Interstadial in northern Scotland. *Journal of Quaternary Science*, **23**, 401–407.

Braithwaite, R. J. 1980. On glacier energy balance, ablation and air temperature. *Journal of Glaciology*, **27**, 381–391.

Braithwaite, R. J. 1995. Positive degree-day factors for ablation on the Greenland Ice Sheet studied by energy-balance modelling. *Journal of Glaciology*, **41**, 153–160.

Braithwaite, R. J., Raper, S. C. B., & Chutko, K. 2006. Accumulation at the equilibrium line altitude of glaciers inferred from a degree-day model and tested against field observations. *Annals of Glaciology*, **43**, 329–334.

Brazier, V., Gordon, J. E., Hubbard, A., & Sugden, D. E. 1996a. The geomorphological evolution of a dynamic landscape: the Cairngorm Mountains, Scotland. *Botanical Journal of Scotland*, **48**, 13–30.

Brazier, V., Gordon, J. E., Kirkbride, M. P., & Sugden, D. E. 1996b. The Late Devensian ice sheet and glaciers in the Cairngorm Mountains. *Pages 28–53 of:* Glasser, N.F., & Bennett, M. R. (eds), *The Quaternary of the Cairngorms: Field Guide*. London: Quaternary Research Association.

Brazier, V., Kirkbride, M. P., & Gordon, J. E. 1998. Active ice-sheet deglaciation and ice-dammed lakes in the northern Cairngorm Mountains, Scotland. *Boreas*, **27**(4), 297–310.

Broecker, W. S. 2003. Does the trigger for abrupt climate change reside in the ocean or in the atmosphere? *Science*, **300**, 1519–1522.

Broecker, W. S. 2006. Was the Younger Dryas triggered by a flood? *Science*, **312**, 1146–1148.

Broecker, W. S., Kennett, J. P., Flower, B. P., Teller, J. T., Trumbore, S., Bonani, G., & Wolfli, W. 1989. Routing of meltwater from the Laurentide Ice-Sheet during the Younger Dryas cold episode. *Nature*, **341**, 318–321.

Brooks, S. J., & Birks, H. J. B. 2000. Chironomid-inferred Late-glacial air temperatures at Whitrig Bog, southeast Scotland. *Journal of Quaternary Science*, **15**, 759–764.

Brooks, S. J., & Birks, H. J. B. 2001. Chironomid-inferred air temperatures from Lateglacial and Holocene sites in north-west Europe: progress and problems. *Quaternary Science Reviews*, **20**(16-17), 1723–1741.

Brown, C., Meier, M., & Post, A. 1982. *Calving speed of Alaskan tidewater glaciers, with application to Columbia Glacier.* Professional Paper 1258-C. USGS, 13pp.

Browne, M. A. E., & Graham, D. K. 1981. Glaciomarine deposits of the Loch Lomond Stade glacier in the Vale of Leven between Dumbarton and Balloch, west-central Scotland. *Quaternary Newsletter*, **34**, 1–7.

Browne, M. A. E., McMillan, A. A., & Hall, I. H. S. 1983. Blocks of marine clay in till near Helensburgh, Strathclyde. *Scottish Journal of Geology*, **19**, 321–325.

Charbit, S., Ritz, C., & Ramstein, G. 2002. Simulations of Northern Hemisphere ice-sheet retreat: sensitivity to physical mechanisms involved during the Last Deglaciation. *Quaternary Science Reviews*, **21**(1-3), 243–265.

Charlesworth, J. K. 1955. Late-glacial history of the Highlands and Islands of Scotland. *Transactions of the Royal Society of Edinburgh*, **62**, 769–928.

Child, D., Elliott, G., Misfud, C., Smith, A. M., & Fink, D. 2000. Sample Processing for Earth Science Studies at ANTARES. *Nuclear Instruments & Methods In Physics Research B*, **17**, 856–860.

Christoffersen, P., & Tulaczyk, S. 2003. Signature of palaeo-ice-stream stagnation: till consolidation induced by basal freeze-on. *Boreas*, **32**(1), 114–129.

Clapperton, C. M. 1993. Glacier readvances in the Andes at 12 500-10 000 yr BP: implications for mechanism of Late-glacial climate change. *Journal of Quaternary Science*, **8**, 197–215.

Clapperton, C. M. 1995. Fluctuations of local glaciers at the termination of the Pleistocene: 18-8 ka BP. *Quaternary International*, **28**, 41–50.

Clapperton, C. M. 1997. Greenland ice cores and North Atlantic sediments: implications for the last glaciation in Scotland. *Pages 45–58 of:* Gordon, J. E. (ed), *Reflections on the ice age in Scotland: an update on Quaternary Studies.* Scottish Association of Geography Teachers and Scottish Natural Heritage.

Clark, C. D. 1993. Mega-scale glacial lineations and cross-cutting ice-flow landforms. *Earth Surface Processes and Landforms*, **18**, 1–29.

Clark, C. D. 1997. Reconstructing the evolutionary dynamics of former ice sheets using multi-temporal evidence, remote sensing and GIS. *Quaternary Science Reviews*, **16**, 1067–1092.

Clark, C. D., & Stokes, C. R. 2003. Palaeo-ice stream landsystem. *Pages 204–227 of:* Evans, D. J. A. (ed), *Glacial Landsystems*. London: Arnold.

Clark, C. D., Evans, D. J. A., Khatwa, A., Bradwell, T., Jordan, C. J., Marsh, S. H., Mitchell, W. A., & Bateman, M. D. 2004. Map and GIS database of glacial landforms and features related to the last British Ice Sheet. *Boreas*, **33**, 359–375.

Clark, P. U., Licciardi, J. M., MacAyeal, D. R., & Jenson, J. W. 1996. Numerical reconstruction of a soft-bedded Laurentide Ice Sheet during the last glacial maximum. *Geology*, **24**(8), 679–682.

Clayton, L., Mickelson, D. M., & Attig, J. W. 1989. Evidence against pervasively deformed bed material beneath rapidly moving lobes of the southern Laurentide Ice-Sheet. *Sedimentary Geology*, **62**(2-4), 203–208.

COHMAP. 1988. Climatic changes of the last 18,000 years - observations and model simulations. *Science*, **241**, 1043–1052.

Colgan, P. M., Mickelson, D. M., & Cutler, P. M. 2003. Ice-marginal terrestrial landsystems: southern Laurentide Ice Sheet margin. *Pages 111–142 of:* Evans, D. J. A. (ed), *Glacial Landsystems*. London: Arnold.

Colgan, W., Davis, J., & Sharp, M. 2008. Is the high-elevation region of Devon Ice Cap thickening? *Journal of Glaciology*, **54**, 428–436.

Coope, G. R., Lemdahl, G., Lowe, J. J., & Walkling, A. 1998. Temperature gradients in North-west Europe during the Last Glacial-Interglacial Transition (14-9 ^{14}C ka BP) interpreted from coleopteran assemblages. *Journal of Quaternary Science*, **13**, 419–433.

Crowley, T. J., & Baum, S. K. 1995. Is the Greenland Ice Sheet bistable? *Paleoceanography*, **10**, 357–363.

Dansgaard, W., White, J. C., & Johnsen, S. J. 1989. The abrupt termination of the Younger Dryas climate event. *Nature*, **339**, 532–534.

Dansgaard, W., Johnsen, S. J., Clausen, H. B., Dahl-Jensen, D., Gundestrup, N. S., Hammer, C. U., Hvidberg, C. S., Steffensen, J. P., Sveinsbjörnsdottir, A. E., Jouzel, J., & Bond, G. 1993. Evidence for general instability of past climate from a 250-kyr ice-core record. *Nature*, **364**, 218–220.

Dawson, A. G. 1992. *Ice Age Earth*. London: Routledge.

De Geer, G. 1889. Ändmoräner i trakten mellan Spånga och Sundbyberg. *Geologiska Föreningens i Stockholm Förhandlingar*, **11**, 395–397.

Denton, G. H., & Hendy, C. H. 1994. Younger Dryas age advance of Franz Josef glacier in the southern Alps of New Zealand. *Science*, **264**, 1434–1437.

Denton, G. H., Alley, R. B., Comer, G. C., & Broecker, W. S. 2005. The role of seasonality in abrupt climate change. *Quaternary Science Reviews*, **24**(10-11), 1159–1182.

Dethloff, K., Schwager, M., Christensen, J. H., Kiilsholm, S., Rinke, A., Dorn, W., Jung-Rothenhäusler, F., Fischer, H., Kipfstuhl, S., & Miller, H. 2002. Recent Greenland accumulation estimated from regional climate model simulations and ice core analysis. *Journal of Climate*, **15**, 2821–2832.

deVernal, A., Hillaire-Marcel, C., & Bilodeau, G. 1996. Reduced meltwater outflow from the Laurentide ice margin during the Younger Dryas. *Nature*, **381**(6585), 774–777.

Dix, J. K., & Duck, R. W. 2000. A high-resolution seismic stratigraphy from a Scottish sea loch and its implications for Loch Lomond Stadial deglaciation. *Journal of Quaternary Science*, **15**(6), 645–656.

Dowdeswell, J. A., Hagen, J. O., Björnsson, H., Glazovsky, A. F., Harrison, W. D., Holmlund, P., Jania, J., Koerner, R. M., Lefauconnier, B., Ommanney, C. S. L., & Thomas, R. H. 1997. The mass balance of circum-Arctic glaciers and recent climate change. *Quaternary Research*, **48**, 1–14.

Dunlop, P., & Clark, C. D. 2006. The morphological characteristics of ribbed moraine. *Quaternary Science Reviews*, **25**, 1668–1691.

Edwards, M. 1986. Glacial Environments. *Pages 445–470 of:* Reading, H.G. (ed), *Sedimentary Environments and Facies*, second edn. Oxford: Blackwell.

EPICA Community Members. 2006. One-to-one coupling of glacial climate variability in Greenland and Antarctica. *Nature*, **444**, 195–197.

Etienne, J. L., Jansson, K. N., Glasser, N. F., Hambrey, M. J., Davies, J. R., Waters, R. A., Maltman, A. J., & Wilby, P. R. 2006. Palaeoenvironmental interpretation of an ice-contact glacial lake succession: and example from the late Devensian of southwest Wales, UK. *Quaternary Science Reviews*, **25**, 739–762.

Evans, D. J. A. 2003a. *Glacial Landsystems*. Arnold.

Evans, D. J. A. 2003b. Ice-marginal terrestrial landsystems: active temperate glacier margins. *Pages 12–43 of:* Evans, D. J. A. (ed), *Glacial Landsystems*. London: Arnold.

Evans, D. J. A. 2003c. Introduction to glacial landsystems. *Pages 1–11 of:* Evans, D. J. A. (ed), *Glacial Landsystems*. London: Arnold.

Evans, D. J. A., & Rose, J. 2003. Croftamie. *Pages 38–39 of: Classic Landforms of the Loch Lomond Area*. Sheffield: Geographical Association.

Evans, D. J. A., & Twigg, D. R. 2002. The active temperate glacial landsystem: a model based on Breidamerkurjökull and Fjallsjökull, Iceland. *Quaternary Science Reviews*, **21**, 2143–2177.

Evans, D. J. A., & Wilson, S. B. 2006. Scottish Landform Example 39: The Lake of Menteith glaciotectonic hill-hole pair. *Scottish Geographical Journal*, **122**, 352–364.

Evans, D. J. A., Clark, C. D., & Mitchell, W. A. 2005. The last British Ice Sheet: A review of the evidence utilised in the compilation of the Glacial Map of Britain. *Earth-Science Reviews*, **70**, 253–312.

Evans, D. J. A., Phillips, E. R., Hiemstra, J. F., & Auton, C. A. 2006. Subglacial till: formation, sedimentary characteristics and classification. *Earth-Science Reviews*, **78**, 115–176.

Everest, J. D. 2003. *The Late Devensian deglaciation in the Cairngorm Mountains, Scotland.* Unpublished Ph.D thesis, University of Edinburgh.

Everest, J. D., & Kubik, P. W. 2006. The deglaciation of eastern Scotland: cosmogenic ^{10}Be evidence for a Lateglacial stillstand. *Journal of Quaternary Science*, **21**, 95–104.

Everest, J. D., Bradwell, T., Fogwill, C. J., & Kubik, P. W. 2006. Cosmogenic ^{10}Be age constraints for the Wester Ross Readvance moraine: insights into British Ice-Sheet behaviour. *Geografiska Annaler*, **88 A**, 9–17.

Eyles, N. 1983. Glacial geology: a landsystems approach. *Pages 1–18 of:* Eyles, N. (ed), *Glacial Geology.* Oxford: Pergamon.

Eyles, N., & Miall, A. D. 1984. Glacial facies. *Pages 15–38 of:* Walker, R. G. (ed), *Facies Models.* Geoscience Canada Reprint Series, no. 1. Geological Association of Canada.

Eyles, N., Miall, A. D., & Eyles, C. H. 1984. Lithofacies types and vertical profile models - an alternative approach to the description and environmental interpretation of glacial diamict and diamictite sequences - Reply. *Sedimentology*, **31**(6), 891–898.

Fabel, D., Stroeven, A. P., Harbor, J., Kleman, J., Elmore, D., & Fink, D. 2002. Landscape preservation under Fennoscandian ice sheets determined from in situ produced Be-10 and Al-26. *Earth and Planetary Science Letters*, **201**, 397–406.

Fabel, D., Fink, D., Fredin, O., Harbor, J., Land, M., & Stroeven, A. P. 2006. Exposure ages from relict lateral moraines overridden by the Fennoscandian ice sheet. *Quaternary Research*, **65**, 136–146.

Fard, A. M. 2001. Morphology of subglacial conduit deposits: control by bedrock topography, discharge flow variation, or both? A cautionary case study: Axelsberg, Nynäshamn, south central Sweden. *Global and Planetary Change*, **28**, 145–161.

Finlayson, A.G. 2004. *The Loch Lomond Readvance in the Creag Meagaidh area: glacier reconstruction and wider implications for the region around Glen Roy.* Unpublished MSc. thesis, Royal Holloway, University of London.

Finlayson, A.G. 2006. Glacial geomorphology of the Creag Meagaidh Massif, western Grampian Highlands: implications for local glaciation and palaeoclimate during the Loch Lomond Stadial. *Scottish Geographical Journal*, **122**, 293–307.

Finlayson, A.G., & Bradwell, T. 2007. Evidence for Younger Dryas ice cap glaciation of the Beinn Dearg massif, northern Scotland. *Quaternary Newsletter*, **113**, 10–17.

Firestone, R. B., West, A., Kennett, J. P., Becker, L., Bunch, T. E., Revay, Z. S., Schultz, P. H., Belgya, T., Kennett, D. J., Erlandson, J. M., Dickenson, O. J., Goodyear, A. C., Harris, R. S., Howard, G. A., Kloosterman, J. B., Lechler, P., Mayewski, P. A., Montgomery, J., Poreda, R., Darrah, T., Hee, S. S. Que, Smith, A. R., Stich, A., Topping, W., Wittke, J. H., & Wolbach, W. S. 2007. Evidence for an extraterrestrial impact 12,900 years ago that

contributed to the megafaunal extinctions and the Younger Dryas cooling. *Proceedings of the National Academy of Sciences*, **104**, 16016–16021.

Firth, C. R., & Stewart, I. S. 2000. Postglacial tectonics of the Scottish glacio-isostatic uplift centre. *Quaternary Science Reviews*, **19**, 1469–1493.

Fisher, T. G., & Smith, D. G. 1994. Glacial Lake Agassiz - its northwest maximum extent and outlet in Saskatchewan (Emerson Phase). *Quaternary Science Reviews*, **13**(9-10), 845–858.

Fitzsimons, S. J. 2003. Ice-marginal terrestrial landsystems: polar-continental glacier margins. *Pages 89–110 of:* Evans, D. J. A. (ed), *Glacial Landsystems*. London: Arnold.

Fogwill, C. J., & Kubik, P. W. 2005. A glacial stage spanning the Antarctic Cold Reversal in Torres Del Paine (51°S), Chile, based on preliminary cosmogenic exposure ages. *Geografiska Annaler*, **87A**, 403–408.

Fountain, A. G., & Walder, J. S. 1998. Water flow through temperate glaciers. *Reviews of Geophysics*, **36**(3), 299–328.

Fowler, A. C., Murray, T., & Ng, F. S. L. 2001. Thermally controlled glacier surging. *Journal of Glaciology*, **47**(159), 527–538.

Geikie, A. 1863. On the glacial drift of Scotland. *Transactions of the Geological Society of Glasgow*, **1**, 1–190.

Glasser, N. F. 1995. Modeling the effect of topography on ice-sheet erosion, Scotland. *Geografiska Annaler*, **77A**(1-2), 67–82.

Glasser, N. F. 1997. The origin and significance of sheet joints in the Cairngorm granite. *Scottish Journal of Geology*, **33**, 125–131.

Glasser, N. F. 2002. The large roches moutonnées of Upper Deeside. *Scottish Geographical Journal*, **118**(2), 129–138.

Glasser, N. F., & Bennett, M. R. 2004. Glacial erosional landforms: origins and significance for palaeoglaciology. *Progress in Physical Geography*, **28**(1), 43–75.

Glasser, N. F., & Siegert, M. J. 2002. Calculating basal temperatures in ice sheets: an Excel spreadsheet method. *Earth Surface Processes and Landforms*, **27**, 673–680.

Glasser, N. F., Hambrey, M. J., Etienne, J. L., Jansson, P., & Pettersson, R. 2003. The origin and significance of debris-charged ridges at the surface of Storglaciaren, northern Sweden. *Geografiska Annaler*, **85A**(2), 127–147.

Glasser, N. F., Jansson, K. N., Harrison, S., & Rivera, A. 2005. Geomorphological evidence for variations of the North Patagonian Icefield during the Holocene. *Geomorphology*, **71**(3-4), 263–277.

Glen, J. W. 1955. The creep of polycrystalline ice. *Proceedings of the Royal Society of London, Series A*, **228**, 519–538.

Golledge, N. R. 2002. Glaci-tectonic deformation of proglacial lake sediments in the Cairngorm Mountains. *Scottish Journal of Geology*, **38**, 127–136.

Golledge, N. R. 2004. The geomorphology and Quaternary geology of the upper Feshie and northern Gaick. *Pages 144–148 of:* S., Lukas, W., Merritt J., & A., Mitchell W. (eds), *The Quaternary of the central Grampian Highlands: Field Guide*. London: Quaternary Research Association.

Golledge, N. R. 2006. The Loch Lomond Stadial glaciation south of Rannoch Moor: new evidence and palaeoglaciological insights. *Scottish Geographical Journal*, **122**, 326–343.

Golledge, N. R. 2007a. An ice cap landsystem for palaeoglaciological reconstructions: characterizing the Younger Dryas in western Scotland. *Quaternary Science Reviews*, **26**, 213–229.

Golledge, N. R. 2007b. Sedimentology, stratigraphy, and glacier dynamics, western Scottish Highlands. *Quaternary Research*, **68**, 79–95.

Golledge, N. R., & Hubbard, A. 2005. Evaluating Younger Dryas glacier reconstructions in part of the western Scottish Highlands: a combined empirical and theoretical approach. *Boreas*, **34**, 274–286.

Golledge, N. R., & Phillips, E. R. 2008. Sedimentology and architecture of De Geer moraines in the western Scottish Highlands, and implications for grounding-line glacier dynamics. *Sedimentary Geology*, **208**, 1–14.

Golledge, N. R., & Robinson, R.A. J. 2007. OSL dating of glaciotectonised sand deposits from Coire Chailein: evidence of multiple glacial episodes preserved in an ice sheet core area. *Page 29 of: The Growth, Maximum Extent and Decay of the Last British and Irish Ice Sheets: Abstracts volume*. Quaternary Research Association Annual Discussion Meeting, St. Andrews.

Golledge, N. R., Fabel, D., Everest, J. D., Freeman, S., & Binnie, S. 2007. First cosmogenic ^{10}Be age constraint on the timing of Younger Dryas glaciation and ice cap thickness, western Scottish Highlands. *Journal of Quaternary Science*, **22**, 785–791.

Golledge, N. R., Hubbard, A., & Sugden, D. E. 2008a. High-resolution numerical simulation of Younger Dryas glaciation in Scotland. *Quaternary Science Reviews*, **27**, 888–904.

Golledge, N. R., Finlayson, A. G., Bradwell, T., & Everest, J. D. 2008b. The last glaciation of Shetland, North Atlantic. *Geografiska Annaler*, **90A**, 37–53.

Golledge, N. R., Hubbard, A. L., & Sugden, D. E. in press. Mass balance, flow, and subglacial processes of a modelled Younger Dryas ice cap in Scotland. *Journal of Glaciology*.

Gordon, J. E. 1979. Reconstructed Pleistocene ice-sheet temperatures and glacial erosion in northern Scotland. *Journal of Glaciology*, **22**, 331–344.

Graham, D. 1999. The Loch Lomond Stadial (Younger Dryas) moraines of western Britain: genesis and significance. *Quaternary Newsletter*, **88**, 42–44.

Gray, J. M. 1974. Lateglacial and postglacial shorelines in western Scotland. *Boreas*, **3**, 129–138.

Gray, J. M. 1978. Low-level shore platforms in the south-west Scottish Highlands: altitude, age and correlation. *Transactions of the Institute of British Geographers*, **3**, 151–164.

Gray, J. M., & Coxon, P. 1991. The Loch Lomond Stadial glaciation in Britain and Ireland. *Pages 89–105 of:* Ehlers, J., Gibbard, P. L., & Rose, J. (eds), *Glacial Deposits in Great Britain and Ireland*. Balkema.

Gray, J. M., & Lowe, J. J. 1977. The Scottish Lateglacial environment: a synthesis. *Pages 163–181 of:* Gray, J. M., & Lowe, J. J. (eds), *Studies in the Scottish Lateglacial Environment*. Oxford: Pergamon.

Grigoryan, S. S., Buyanov, S. A., Krass, M. S., & Shumskiy, P. A. 1985. The mathematical-model of ice sheets and the calculation of the evolution of the Greenland Ice-Sheet. *Journal Of Glaciology*, **31**(109), 281–292.

Gyte, N. J. 2004. *Late glacial landforms and climate change in the Monadhliath Mountains, Scotland*. Unpublished BSc. thesis, University of Edinburgh.

Hall, A. M., & Glasser, N. F. 2003. Reconstructing the basal thermal regime of an ice stream in a landscape of selective linear erosion: Glen Avon, Cairngorm Mountains, Scotland. *Boreas*, **32**(1), 191–207.

Harrison, W. D., Elsberg, D. H., Echelmeyer, K. A., & Krimmel, R. M. 2001. On the characterization of glacier response by a single time-scale. *Journal of Glaciology*, **47**, 659–664.

Hättestrand, C. 1997. Ribbed moraines in Sweden - distribution pattern and palaeoglaciological implications. *Sedimentary Geology*, **111**(1-4), 41–56.

Hättestrand, C., & Stroeven, A. J. 2002. A relict landscape in the centre of Fennoscandian glaciation: Geomorphological evidence of minimal Quaternary glacial erosion. *Geomorphology*, **44**, 127–143.

Hendry, M. J., McCready, R. G. L., & Gould, W. D. 1984. Distribution, source and evolution of nitrate in a glacial till of southern Alberta, Canada. *Journal of Hydrology*, **70**, 177–198.

Heyman, J., & Hättestrand, C. 2006. Morphology, distribution and formation of relict marginal moraines in the Swedish Mountains. *Geografiska Annaler*, **88A**, 253–265.

Hinxman, L. W., Carruther, R. G., & MacGregor, M. 1923. *The Geology of Corrour and the Moor of Rannoch.* Memoir of the Geological Survey of Great Britain. Edinburgh: HMSO.

Hodgkins, R. 1997. Glacier hydrology in Svalbard, Norwegian High Arctic. *Quaternary Science Reviews*, **16**, 957–973.

Hofmann, H. J., Beer, J., Bonani, G., Gunten, H. R. Von, Raman, S., Suter, M., Walker, R. L., Wölfli, W., & Zimmermann, D. 1987. ^{10}Be: Half-life and AMS-standards. *Nuclear Instruments & Methods In Physics Research B*, **29**, 32–36.

Hoppe, G. 1959. Glacial morphology and inland ice recession in northern Sweden. *Geografiska Annaler*, **41**, 193–212.

Horsfield, B. R. 1983. *The deglaciation pattern of the Western Grampians of Scotland*. Unpublished Ph.D thesis, University of East Anglia.

Hubbard, A. 1997. *High-resolution modeling of glaciers*. Unpublished Ph.D thesis, University of Edinburgh.

Hubbard, A. 1999. High-resolution modeling of the advance of the Younger Dryas ice sheet and its climate in Scotland. *Quaternary Research*, **52**, 27–43.

Hubbard, A. 2000. The verification and significance of three approaches to longitudinal stresses in high-resolution models of glacier flow. *Geografiska Annaler*, **82**, 471–487.

Hubbard, A. 2006. The validation and sensitivity of a model of the Icelandic ice sheet. *Quaternary Science Reviews*, **25**, 2297–2313.

Hubbard, A., Hein, A. S., Kaplan, M. R., Hulton, N. R. J., & Glasser, N. 2005. A modelling reconstruction of the last glacial maximum ice sheet and its deglaciation in the vicinity of the Northern Patagonian Icefield, South America. *Geografiska Annaler*, **87A**, 375–391.

Hubbard, A., Sugden, D. E., Dugmore, A. J., Norddahl, H., & Pétursson, H. G. 2006. A modelling insight into the Icelandic Last Glacial Maximum ice sheet. *Quaternary Science Reviews*, **25**, 2283–2296.

Hughes, P. D., & Braithwaite, R. J. 2008. Application of a degree-day model to reconstruct Pleistocene glacial climates. *Quaternary Research*, **69**, 110–116.

Hulton, N., & Sugden, D.E. 1997. Dynamics of mountain ice caps during glacial cycles: the case of Patagonia. *Annals of Glaciology*, **24**, 81–89.

Hutter, K., & Olunloyo, V. O. S. 1981. Basal stress concentrations due to abrupt changes in boundary conditions: a cause for high till concentration at the bottom of a glacier. *Annals of Glaciology*, **2**, 29–33.

Huybrechts, P. 1993. Glaciological modelling of the Late Cenozoic East Antarctic ice sheet: stability or dynamism? *Geografiska Annaler*, **75A**, 221–238.

Imbrie, J., Hays, J. D., Martinson, D. G., McIntyre, A., Mix, A. C., Morley, R. J., Pisias, N. G., Prell, W. L., & Shackleton, N. J. 1984. The orbital theory of Pleistocene climate: Support from a revised chronology of the marine δ^{18}O record. *Pages 269–305 of:* Berger, A. et al. (ed), *Milankovitch and Climate*, vol. Series C, 126. NATO ASI.

Isarin, R. F. B., & Bohncke, S. J. P. 1999. Mean July temperatures during the Younger Dryas in northwestern and central Europe as inferred from climate indicator species. *Quaternary Research*, **51**, 158–173.

Isarin, R. F. B., & Renssen, H. 1999. Reconstructing and modelling Late Weichselian climates: the Younger Dryas in Europe as a case study. *Earth-Science Reviews*, **48**, 1–38.

Ives, J. D., Andrews, J. T., & Barry, R. G. 1975. Growth and decay of the Laurentide Ice Sheet and comparisons with Fenno-Scandinavia. *Naturwissenschaften*, **62**, 118–125.

Jamieson, S. S. R., Hulton, N. R. J., & Hagdorn, M. 2007. Modelling landscape evolution under ice sheets. *Geomorphology*, **92**, 91–108.

Jansson, P., Hock, R., & Schneider, T. 2003. The concept of glacier storage: a review. *Journal of Hydrology*, **282**(1-4), 116–129.

Jóhannesson, T., Sigurdsson, O., Laumann, T., & Kennett, M. 1995. Degree-day glacier mass-balance modelling with applications to glaciers in Iceland, Norway and Greenland. *Journal of Glaciology*, **41**, 345–358.

Johnsen, S. J., Dahl-Jensen, D., Dansgaard, W., & Gundestrup, N. S. 1995. Greenland palaeotemperatures derived from GRIP bore hole temperature and ice core isotope profiles. *Tellus*, **47**, 624–629.

Johnsen, S. J., Dahl-Jensen, D., Gundestrup, N. S., Steffensen, J. P., Clausen, H. B., Miller, H., Masson-Delmotte, V., Sveinsbjörnsdottir, A. E., & White, J. 2001. Oxygen isotope and palaeotemperature records from six Greenland ice-core stations: Camp Century, Dye-3, GRIP, GISP2, Renland and NorthGRIP. *Journal of Quaternary Science*, **16**, 299–307.

Jones, T. 1998. Empirical testing of Loch Lomond Stadial glacier limits derived from a glaciological model for the Applecross Peninsula, Wester Ross, Scotland. *Scottish Geographical Magazine*, **114**(3), 164–171.

Kamb, B. 1987. Glacier surge mechanism based on linked cavity configuration of the basal water conduit system. *Journal of Geophysical Research*, **92**(B9), 9083–9100.

Kerr, A. 1993. Topography, climate and ice masses: a review. *Terra Nova*, **5**, 332–342.

Khodakov, V. G. 1975. Glaciers as water resource indicators of the glacial areas of the USSR. *Pages 22–29 of: Proceedings of the Moscow Snow and Ice Symposium, August 1971.* IAHS Publication.

Kirby, M. E. 1998. Heinrich event-0 (DC-0) in sediment cores from the northwest Labrador Sea: recording events in Cumberland Sound? *Canadian Journal of Earth Sciences*, **35**, 510–519.

Kjær, K. H., Larsen, E., van der Meer, J. J. M., Ingólfsson, O., Krüger, J., Benediktsson, I. O., Knudsen, C. G., & Schomacker, A. 2007. Subglacial decoupling at the sediment/bedrock interface: a new mechanism for rapid flowing ice. *Quaternary Science Reviews*, **25**, 2704–2712.

Kleman, J. 1994. Preservation of landforms under ice sheets and ice caps. *Geomorphology*, **9**, 19–32.

Kleman, J., & Borgstrom, I. 1994. Glacial landforms indicative of a partly frozen bed. *Journal of Glaciology*, **40**(135), 255–264.

Kleman, J., & Hättestrand, C. 1999. Frozen-bed Fennoscandian and Laurentide ice sheets during the Last Glacial Maximum. *Nature*, **402**(6757), 63–66.

Knight, J. 2003. Evaluating controls on ice dynamics in the north-east Atlantic using an event stratigraphy approach. *Quaternary International*, **99-100**, 45–57.

Kohl, C. P., & Nishiizumi, K. 1992. Chemical isolation of quartz for measurement of in situ-produced cosmogenic nuclides. *Geochimica et Cosmochimica Acta*, **56**, 3586–3587.

Kovanen, D. J., & Slaymaker, O. 2004. Glacial imprints of the Okanogan Lobe, southern margin of the Cordilleran Ice Sheet. *Journal of Quaternary Science*, **19**, 547–565.

Kroon, D., Austin, W. E. N., Chapman, M. R., & Ganssen, G. M. 1997. Deglacial surface circulation changes in the northeastern Atlantic: Temperature and salinity records off NW Scotland on a century scale. *Paleoceanography*, **12**, 755–763.

Krüger, J. 1996. Moraine ridges formed from subglacial frozen-on sediment slabs and their differentiation from push moraines. *Boreas*, **25**, 57–63.

Krüger, J., & Kjær, K. H. 1999. A data chart for field description and genetic interpretation of glacial diamicts and associated sediments – with examples from Greenland, Iceland, and Denmark. *Boreas*, **28**, 386–402.

Lagerbäck, R. 1992. Dating of Late Quaternary faulting in northern Sweden. *Journal of the Geological Society, London*, **149**, 285–291.

Larsen, E., Longva, O., & Follestad, B. A. 1991. Formation of De Geer moraines and implications for deglaciation dynamics. *Journal of Quaternary Science*, **6**, 263–277.

Laumann, T., & Reeh, N. 1993. Sensitivity to climate change of the mass balance of glaciers in southern Norway. *Journal of Glaciology*, **39**, 656–663.

Lee, H. A. 1959. *Surficial geology of southern District of Keewatin and the Keewatin ice divide, Northwest Territories*. Vol. 51. Bulletin of the Canadian Geological Survey.

Lie, O., & Paasche, O. 2006. How extreme was northern hemisphere seasonality during the Younger Dryas? *Quaternary Science Reviews*, **25**, 404–407.

Liestøl, O. 1967. Storbreen Glacier in Jotunheimen, Norway. *Norsk Polarinstitutt Skrifter*, **141**, 1–63.

Lindén, M., & Möller, P. 2005. Marginal formation of De Geer moraines and their implications to the dynamics of grounding-line recession. *Journal of Quaternary Science*, **20**, 113–133.

Linton, D. L., & Moisley, H. A. 1960. The origin of Loch Lomond. *Scottish Geographical Magazine*, **76**, 26–37.

Lønne, I. 1993. Physical signatures of ice advance in a Younger Dryas ice-contact delta, Troms, northern Norway: implications for glacier-terminus history. *Boreas*, **22**, 59–70.

Lønne, I. 1995. Sedimentary facies and depositional architecture of ice-contact glaciomarine systems. *Sedimentary Geology*, **98**, 13–43.

Lowe, A. L., & Anderson, J. B. 2003. Evidence for abundant subglacial meltwater beneath the paleo-ice sheet in Pine Island Bay, Antarctica. *Journal of Glaciology*, **49**, 125–138.

Lowe, D. R. 1982. Sediment gravity flows: II. Depositional models with special reference to the deposits of high-density turbidity currents. *Journal of Sedimentary Research*, **52**, 279–297.

Lowe, J. J. 1978. Radiocarbon-dated Lateglacial and early Flandrian pollen profiles from the Teith Valley, Perthshire, Scotland. *Pollen Spores*, **20**, 367–397.

Lowe, J. J., & Walker, M. J. C. 1976. Radiocarbon-dates and deglaciation of Rannoch Moor, Scotland. *Nature*, **264**, 632–633.

Lowe, J. J., & Walker, M. J. C. 1980. Problems associated with radiocarbon dating the close of the Lateglacial Period in the Rannoch Moor area, Scotland. *Pages 123–137 of:* Lowe, J. J., Gray, J. M., & Robinson, J. E. (eds), *Studies in the Lateglacial of North-west Europe*. Oxford: Pergamon.

Lowe, J. J., Ammann, B., Birks, H. H., Björck, S., Coope, G. R., Cwynar, L., De Beaulieu, J. L., Mott, R. J., Peteet, D. M., & Walker, M. J. C. 1994. Climate changes in areas adjacent to the North Atlantic during the Last Glacial-Interglacial transition (14-9 ka BP): a contribution to IGCP-253. *Journal of Quaternary Science*, **9**, 185–198.

Lowe, J. J., Hoek, W. Z., & INTIMATE group. 2001. Inter-regional correlation of palaeoclimatic records for the Last Glacial–Interglacial Transition: a protocol for improved precision recommended by the INTIMATE project group. *Quaternary Science Reviews*, **20**, 1175–1187.

Lowe, J. J., Rasmussen, S. O., Björck, S., Hoek, W. Z., Steffensen, J. P., Walker, M. J. C., Yu, Z., & INTIMATE group. 2008. Precise dating and correlation of events in the North Atlantic region during the Last Termination: a revised protocol recommended by the INTIMATE group. *Quaternary Science Reviews*, **27**, 6–17.

Lowell, T. V., Fisher, T. G., Comer, G. C., Hajdas, I., Waterson, N., Glover, K., Loope, H. M., Schaefer, J. M., Rinterknecht, V. R., Broecker, W. S., Denton, G. H., & Teller, J. T. 2005. Testing the Lake Agassiz meltwater trigger for the Younger Dryas. *Eos*, **86**, 365, 372.

Lukas, S. 2005a. A test of the englacial thrusting hypothesis of 'hummocky' moraine formation: case studies from the northwest Highlands, Scotland. *Boreas*, **34**, 287–307.

Lukas, S. 2005b. *Younger Dryas moraines in the NW Highlands of Scotland: genesis, significance and potential modern analogues*. Unpublished Ph.D thesis, University of St. Andrews.

Lukas, S., Spencer, J. Q. G., Robinson, R. A. J., & Benn, D. I. 2007. Problems associated with luminescence dating of Late Quaternary glacial sediments in the NW Scottish Highlands. *Quaternary Geochronology*, **2**, 243–248.

MacAyeal, D. R. 1993. Binge/purge oscillations of the Laurentide Ice-Sheet as a cause of the North-Atlantics Heinrich Events. *Paleoceanography*, **8**, 775–784.

Madgett, P. A. 1975. Re-interpretation of Devensian Till stratigraphy of eastern England. *Nature*, **253**, 105–107.

Madgett, P. A., & Catt, J. A. 1978. Petrography, stratigraphy and weathering of Late Pleistocene tills in East Yorkshire, Lincolnshire and North Norfolk. *Proceedings of the Yorkshire Geological Society*, **42**, 55–108.

Manabe, S., & Stouffer, R. J. 2000. Study of abrupt climate change by a coupled ocean-atmosphere model. *Quaternary Science Reviews*, **19**, 285–299.

Mangerud, J. 1991. The last interglacial/glacial cycle in Northern Europe. *Pages 38–75 of:* Shane, L. C. K., & Cushing, E. J. (eds), *Quaternary Landscapes*. University of Minnesota Press.

Mangerud, J., Andersen, S. T., Berglund, B. E., & Donner, J. J. 1974. Quaternary stratigraphy of Norden, a proposal for terminology and classification. *Boreas*, **3**, 109–128.

Manley, G. 1955. On the occurence of ice domes and permanently snow-covered summits. *Journal of Glaciology*, **2**, 453–456.

Maslin, M., Shackleton, N. J., & Pflaumann, U. 1995. Surface water temperature, salinity, and density changes in the northeast Atlantic during the last 45,000 years: Heinrich events, deep water formation, and climatic rebounds. *Paleoceanography*, **10**, 527–544.

Mawdsley, J. B. 1936. Wash-board moraines of the Opawica-Chibougamau area, Quebec. *Transactions of the Royal Society of Canada*, **30**, 9–12.

Mayewski, P. A., Meeker, L. D., Whitlow, S., Twickler, M. S., Morrison, M. C., Bloomfield, P., Bond, G. C., Alley, R. B., Gow, A. J., Meese, D. A., Grootes, P. M., Ram, M., Taylor, K. C., & Wumkes, W. 1994. Changes in atmospheric circulation and ocean ice cover over the North Atlantic during the last 41,000 years. *Science*, **263**, 1747–1751.

Mayle, F. E., Bell, M., Birks, H. H., Brooks, S. J., Coope, G. R., Lowe, J. J., Sheldrick, C., Shijie, L., Turney, C. S. M., & Walker, M. J. C. 1999. Climate variations in Britain during the last Glacial-Holocene transition (15.0-11.5 cal ka BP): comparison with the GRIP ice-core record. *Journal of the Geological Society*, **156**, 411–423.

Menzies, J. 1989. Subglacial hydraulic conditions and their possible impact upon subglacial bed formation. *Sedimentary Geology*, **62**(2-4), 125–150.

Menzies, J. 2000. Micromorphological analyses of microfabrics and microstructures indicative of deformation processes in glacial sediments. *Pages 245–257 of:* Maltman, A. J., Hubbard, B., & Hambrey, M. J. (eds), *Deformation of Glacial Materials*. London: The Geological Society.

Menzies, J., van der Meer, J. J. M., & Rose, J. 2006. Till – as a glacial "tectomict", its internal architecture, and the development of a "typing" method for till differentiation. *Geomorphology*, **75**, 172–200.

Merritt, J. W., Coope, G. R., Taylor, B. J., & Walker, M. J. C. 1990. Late Devensian organic deposits beneath till in the Teith Valley, Perthshire. *Scottish Journal of Geology*, **26**, 15–24.

Merritt, J. W., Auton, C. A., & Firth, C. R. 1995. Ice-proximal glaciomarine sedimentation and sea-level change in the Inverness area, Scotland - a review of the deglaciation of a major ice stream of the British Late Devensian Ice-Sheet. *Quaternary Science Reviews*, **14**(3), 289–329.

Merritt, J. W., Lukas, S., & Mitchell, W.A. 2004. The age of the landforms in the central Grampian Highlands – a synthesis. *Pages 85–91 of:* Lukas, S., Merritt, J. W., & Mitchell, W.A. (eds), *The Quaternary of the central Grampian Highlands: Field Guide*. London: Quaternary Research Association.

Middleton, R., Brown, L., Dezfouly-Arjomandy, B., & Klein, J. 1993. On ^{10}Be standards and the half-life of ^{10}Be. *Nuclear Instruments & Methods In Physics Research B*, **82**, 399–403.

Mitchell, W. A. 1994. Drumlins in ice sheet reconstructions, with reference to the western Pennines, northern England. *Sedimentary Geology*, **91**, 313–331.

Murray, T., Stuart, G. W., Miller, P. J., Woodward, J., Smith, A. M., Porter, P. R., & Jiskoot, H. 2000. Glacier surge propagation by thermal evolution at the bed. *Journal of Geophysical Research*, **105**(B6), 13491–13507.

Muscheler, R., Kromer, B., Björck, S., Svensson, A., Friedrich, M., Kaiser, K. F., & Southon, J. 2008. Tree rings and ice cores reveal ^{14}C calibration uncertainties during the Younger Dryas. *Nature Geoscience*, **1**, 263–267.

Napieralski, J., Hubbard, A., Li, Y., Harbor, J., Stroeven, A. P., Kleman, J., Alm, G., & Jansson, K. N. 2007. Towards a GIS assessment of numerical ice-sheet model performance using geomorphological data. *Journal of Glaciology*, **53**, 71–83.

Nemec, W., Lønne, I., & Blikra, L. H. 1999. The Kregnes moraine in Gauldalen, west-central Norway: anatomy of a Younger Dryas proglacial delta in a palaeofjord basin. *Boreas*, **28**, 454–476.

Nye, J.F. 1952. The mechanics of glacier flow. *Journal of Glaciology*, **2**, 82–93.

Ó Cofaigh, C., Evans, D. J. A., & England, J. 2003. Ice-marginal terrestrial landsystems: sub-polar glacier margins of the Canadian and Greenland high Arctic. *Pages 44–64 of:* Evans, D. J. A. (ed), *Glacial Landsystems*. London: Arnold.

Oerlemans, J. 1982. A model of the Antarctic ice sheet. *Nature*, **297**, 550–553.

Ohmura, A., Kasser, P., & Funk, M. 1992. Climate at the equilibrium line of glaciers. *Journal of Glaciology*, **38**, 397–411.

Osmaston, H. A. 2005. Estimates of glacier equilibrium line altitudes by the Area x Altitude, the Area x Altitude Balance Ratio and the Area x Altitude Balance Index methods and their validation. *Quaternary International*, **138-139**, 22–31.

Palmer, A., MacLeod, A., Lowe, J., & Rose, J. 2008. Climate forcing of glaciolacustrine sedimentation in Scotland during GS-1. *Pages EGU2008–A–12157 of: Geophysical Research Abstracts*, vol. 10. EGU General Assembly 2008.

Paterson, W.S.B. 1994. *The Physics of Glaciers*. 3rd edn. Oxford: Pergamon.

Paterson, W.S.B. 2000. *The Physics of Glaciers*. 3rd (reprinted) edn. Oxford: Pergamon.

Payne, A., & Sugden, D.E. 1990. Topography and ice sheet growth. *Earth Surface Processes and Landforms*, **15**, 625–639.

Peacock, J. D. 1970. Some aspects of the glacial geology of west Inverness-shire. *Geological Survey of Great Britain Bulletin*, **33**, 43–56.

Peacock, J. D., & Cornish, R. 1989. *Glen Roy Area: Field Guide*. Cambridge: Quaternary Research Association.

Peacock, J. D., Graham, D. K., Robinson, J. E., & Wilkinson, I. P. 1977. Evolution and chronology of Lateglacial marine environments at Lochgilphead, Scotland. *Pages 89–100 of:* Gray, J. M., & Lowe, J. J. (eds), *Studies in the Scottish Lateglacial Environment*. Pergamon.

Peck, V. L., Hall, I. R., Zahn, R., Grousset, F., Hemming, S. R., & Scourse, J. D. 2007. The relationship of Heinrich events and their European precursors over the past 60 ka BP: a multi-proxy ice-rafted debris provenance study in the North East Atlantic. *Quaternary Science Reviews*, **26**, 862–875.

Perry, M., & Hollis, D. 2005. The generation of monthly gridded datasets for a range of climatic variables over the United Kingdom. *International Journal of Climatology*, **25**, 1041–1054.

Pfeffer, W. T., Sassolas, C., Bahr, D. B., & Meier, M.F. 1998. Response time of glaciers as a function of size and mass balance: 2. Numerical experiments. *Journal of Geophysical Research*, **103**(B5), 9783–9789.

Phillips, E. R., Evans, D. J. A., & Auton, C. A. 2002. Polyphase deformation at an oscillating ice margin following the Loch Lomond Readvance, central Scotland, UK. *Sedimentary Geology*, **149**, 157–182.

Phillips, W. M. 2001. A review of cosmogenic nuclide surface exposure dating: New challenges for Scottish geomorphology. *Scottish Geographical Journal*, **117**(1), 1–15.

Phillips, W. M., Hall, A. M., Mottram, R., Fifield, L. K., & Sugden, D. E. 2006. Cosmogenic ^{10}Be and ^{26}Al exposure ages of tors and erratics, Cairngorm Mountains, Scotland: Timescales for the development of a classic landscape of selective linear glacial erosion. *Geomorphology*, **73**, 222–245.

Piotrowski, J. A., & Tulaczyk, S. 1999. Subglacial conditions under the last ice sheet in northwest Germany: ice-bed separation and enhanced basal sliding? *Quaternary Science Reviews*, **18**, 737–751.

Piotrowski, J. A., Mickelson, D. M., Tulaczyk, S., Krzyszkowski, D., & Junge, F. W. 2001. Were deforming subglacial beds beneath past ice sheets really widespread? *Quaternary International*, **86**, 139–150.

Piotrowski, J. A., Mickelson, D. M., Tulaczyk, S., Krzyszkowski, D., & Junge, F. W. 2002. Reply to the comments by G. S. Boulton, K. E. Dobbie, S. Zatsepin on: Deforming soft beds under ice sheets: how extensive were they? *Quaternary International*, **97-8**, 173–177.

Piotrowski, J. A., Larsen, N. K., & Junge, F. W. 2004. Reflections on soft subglacial beds as a mosaic of deforming and stable spots. *Quaternary Science Reviews*, **23**, 993–1000.

Plummer, M. A., & Phillips, F. M. 2003. A 2-D numerical model of snow/ice energy balance and ice flow for paleoclimatic interpretation of glacial geomorphic features. *Quaternary Science Reviews*, **22**, 1389–1406.

Pollard, D., & DeConto, R. M. 2005. Hysteresis in Cenozoic Antarctic ice-sheet variations. *Global and Planetary Change*, **45**, 9–21.

Porter, S. C. 2001. Snowline depression in the tropics during the Last Glaciation. *Quaternary Science Reviews*, **20**, 1067–1091.

Purves, R., & Hulton, N. J. 2000a. Experiments in linking regional climate, ice-sheet models and topography. *Journal of Quaternary Science*, **15**, 369–375.

Purves, R. S., & Hulton, N. R. J. 2000b. A climatic-scale precipitation model compared with the UKCIP baseline climate. *International Journal of Climatology*, **20**(14), 1809–1821.

Purves, R. S., Mackaness, W. A., & Sugden, D. E. 1999. An approach to modelling the impact of snow drift on glaciation in the Cairngorm Mountains, Scotland. *Journal of Quaternary Science*, **14**(4), 313–321.

Rabus, B., & Echelmeyer, K. 1998. The mass balance of McCall Glacier, Brooks Range, Alaska, U.S.A.; its regional relevance and implications for climate change in the Arctic. *Journal of Glaciology*, **44**, 333–351.

Radić, V., Hock, R., & Oerlemans, J. 2007. Volume-area scaling vs flowline modelling in glacier volume projections. *Annals of Glaciology*, **46**, 234–240.

Rahmstorf, S. 2002. Ocean circulation and climate during the past 120,000 years. *Nature*, **419**, 207–214.

Rasmussen, S. O., Andersen, K. K., Svensson, A. M., Steffensen, J. P., Vinther, B. M., Clausen, H. B., Siggaard-Andersen, M. L., Johnsen, S. J., Larsen, L. B., Dahl-Jensen, D., Bigler, M., Röthlisberger, R., Fischer, H., Goto-Azuma, K., Hansson, M. E., & Ruth, U. 2006. A new Greenland ice core chronology for the last glacial termination. *Journal of Geophysical Research*, **111**(D06102), doi:10.1029/2005JD006079.

Rasmussen, S. O., Seierstad, I. K., Andersen, K. K., Bigler, M., Dahl-Jensen, D., & Johnsen, S. J. 2008. Synchronization of the NGRIP, GRIP, and GISP2 ice cores across MIS 2 and palaeoclimatic implications. *Quaternary Science Reviews*, **27**, 18–28.

Rattas, M., & Kalm, V. 2001. Lithostratigraphy and distribution of tills in the Saadjärve drumlin field, east-central Estonia. *Proceedings of the Estonian Academy of Sciences, Geology*, **50**, 24–42.

Rea, B. R., & Evans, D. J. A. 2003. Plateau icefield landsystems. *Pages 407–431 of:* Evans, D. J. A. (ed), *Glacial Landsystems*. London: Arnold.

Rea, B. R., Whalley, W. B., Evans, D. J. A., Gordon, J. E., & McDougall, D. A. 1998. Plateau icefields: geomorphology and dynamics. *Pages 35–54 of:* Owen, L. A. (ed), *Mountain Glaciation*. Quaternary Proceedings, vol. 6. Chichester: Wiley.

Reeh, N. 1968. On the calving of ice from floating glaciers and ice shelves. *Journal of Glaciology*, **7**, 215–232.

Rignot, E., & Kanagaratnam, P. 2006. Changes in the velocity structure of the Greenland Ice Sheet. *Science*, **311**, 986–990.

Roberts, D. H., & Long, A. J. 2005. Streamlined bedrock terrain and fast ice flow, Jakobshavns Isbrae, West Greenland: implications for ice stream and ice sheet dynamics. *Boreas*, **34**(1), 25–42.

Rollin, K. E., Kirby, G. A., Rowley, W. J., & Buckley, D. K. 1993. *Atlas of Geothermal Resources in Europe: UK Revision*. British Geological Survey Technical Report WK/95/07. British Geological Survey, Nottingham.

Rose, J. 2003. Gartness: the stratigraphy of the Loch Lomond Readvance moraine ridge. *Pages 111–116 of:* Evans, D. J. A. (ed), *The Quaternary of the Western Highland Boundary – Field Guide*. Quaternary Research Association.

Rose, J., & Letzer, J. M. 1977. Superimposed drumlins. *Journal of Glaciology*, **18**, 471–480.

Rose, J., Lowe, J. J., & Switsur, R. 1988. A radiocarbon date on plant detritus beneath till from the type area of the Loch Lomond Readvance. *Scottish Journal of Geology*, **24**, 113–124.

Ruddiman, W. F., & McIntyre, A. 1981. The North Atlantic during the last deglaciation. *Palaeogeography, Palaeoclimatology, Palaeoecology*, **35**, 145–214.

Russell, A. J., Tweed, F. S., & Harris, T. 2003. High-energy sedimentation, Creag Aoil, Spean Bridge, Scotland: implications for meltwater movement and storage during Loch Lomond Stadial (Younger Dryas) ice retreat. *Journal of Quaternary Science*, **18**, 415–430.

Salt, K. E., & Evans, D. J. A. 2004. Superimposed subglacially streamlined landforms of southwest Scotland. *Scottish Geographical Journal*, **120**(1-2), 133–147.

Schytt, V. 1967. A study of 'ablation gradient'. *Geografiska Annaler*, **49A**, 327–332.

Seager, R., & Battisti, D.S. 2005. Challenges to our understanding of the general circulation: Abrupt climate change. *In:* Schneider, T., & Sobel, A.S. (eds), *The General Circulation of the Atmosphere*. Princeton University Press.

Severinghaus, J. P., Sowers, T., Brook, E. J., Alley, R. B., & Bender, M. L. 1998. Timing of abrupt climate change at the end of the Younger Dryas interval from thermally fractionated gases in polar ice. *Nature*, **391**, 141–146.

Shennan, I., Tooley, M. J., Green, F., Innes, J., Kennington, K., Lloyd, J., & Rutherford, M. 1999. Sea level, climate change and coastal evolution in Morar, northwest Scotland. *Geologie en Mijnbouw*, **77**, 247–262.

Siegert, M. J., & Dowdeswell, J. A. 2004. Numerical reconstructions of the Eurasian Ice Sheet and climate during the Late Weichselian. *Quaternary Science Reviews*, **23**, 1273–1283.

Singh, P., Kumar, N., & Arora, M. 2000. Degree–day factors for snow and ice for Dokriani Glacier, Garhwal Himalayas. *Journal of Hydrology*, **235**, 1–11.

Sissons, J. B. 1965. Quaternary of Scotland. *Pages 467–503 of:* Craig, G. Y. (ed), *The Geology of Scotland*. Edinburgh: Oliver & Boyd.

Sissons, J. B. 1967a. *The Evolution of Scotland's Scenery*. Edinburgh: Oliver & Boyd.

Sissons, J. B. 1967b. Glacial stages and radiocarbon dates in Scotland. *Scottish Journal of Geology*, **3**, 375–381.

Sissons, J. B. 1974. Late-Glacial ice cap in central Grampians, Scotland. *Transactions of the Institute of British Geographers*, **62**, 95–114.

Sissons, J. B. 1977. *The Parallel Roads of Glen Roy*. London: Nature Conservancy Council.

Sissons, J. B. 1978. The Parallel Roads of Glen Roy and adjacent glens, Scotland. *Boreas*, **7**, 229–244.

Sissons, J. B. 1979a. The limit of the Loch Lomond Advance in Glen Roy and vicinity. *Scottish Journal of Geology*, **15**, 31–42.

Sissons, J. B. 1979b. The Loch Lomond Stadial in the British Isles. *Nature*, **280**, 199–203.

Sissons, J. B. 1979c. Palaeoclimatic inferences from former glaciers in Scotland and the Lake District. *Nature*, **278**, 518–521.

Sissons, J. B. 1980. Palaeoclimatic inferences from Loch Lomond Advance glaciers. *Pages 31–43 of:* Lowe, J. J., Gray, J. M., & Robinson, J. E. (eds), *Studies in the Lateglacial of North-west Europe*. Oxford: Pergamon.

Sissons, J. B., & Sutherland, D. G. 1976. Climatic inferences from former glaciers in the south-east Grampian Highlands, Scotland. *Journal of Glaciology*, **17**, 325–346.

Sissons, J. B., Lowe, J. J., Thompson, K. S. R., & Walker, M. J. C. 1973. Loch Lomond Readvance in the Grampian Highlands of Scotland. *Nature*, **244**, 75–77.

Smith, A. M., Murray, T., Davison, B. M., Clough, A. F., Woodward, J., & Jiskoot, H. 2002. Late surge glacial conditions on Bakaninbreen, Svalbard, and implications for surge termination. *Journal of Geophysical Research-Solid Earth*, **107**(B8). 2152.

Smith, G. W. 1982. End moraines and the pattern of last retreat from central and south coastal Maine. *Pages 195–209 of:* Larson, G. J., & Stone, B.D. (eds), *Late Wisconsinan Glaciation of New England*. Dubuque, Iowa: Kendall-Hunt.

Sollid, J. L. 1989. Comments on the genesis of De Geer moraines. *Norsk Geografisk Tidsskrift*, **43**, 45–47.

Solomon, S., Qin, D., Manning, M., Alley, R. B., Berntsen, T., Bindoff, N. L., Chen, Z., Chidthaisong, A., Gregory, J. M., Hegerl, G. C., Heimann, M., Hewitson, B., Hoskins, B. J., Joos, F., Jouzel, J., Kattsov, V., Lohmann, U., Matsuno, T., Molina, M., Nicholls, N., Overpeck, J., Raga, G., Ramaswamy, V., Ren, J., Rusticucci, M., Somerville, R., Stocker, T. F., Whetton, P., Wood, R. A., & Wratt, D. 2007. Technical Summary. *In:* Solomon, S., Qin, D., Manning, M., Chen, Z., Marquis, M., Averyt, K. B., Tignor, M., & Miller, H. L. (eds), *Climate Change 2007: The Physical Science Basis. Contribution of Working Group I to the Fourth Assessment Report of the Intergovernmental Panel on Climate Change*. Cambridge, UK, and New York, USA: Cambridge University Press.

Starr, A. J. 2001. *Numerical modelling of ice sheets using adaptive grids*. Unpublished Ph.D thesis, University of Wales, Aberystwyth.

Stoker, M., & Bradwell, T. 2005. The Minch palaeo-ice stream, NW sector of the British-Irish Ice Sheet. *Journal Of The Geological Society*, **162**, 425–428.

Stokes, C. R., & Clark, C. D. 1999. Geomorphological criteria for identifying Pleistocene ice streams. *Annals of Glaciology*, **28**, 67–74.

Stone, J. O. 2000. Air pressure and cosmogenic isotope production. *Journal of Geophysical Research*, **105**, 23753–23759.

Stone, J. O., & Ballantyne, C. K. 2006. Dimensions and deglacial chronology of the Outer Hebrides Ice Cap, northwest Scotland:implications of cosmic ray exposure dating. *Journal of Quaternary Science*, **21**, 75–84.

Stone, J. O., Ballantyne, C. K., & Fifield, L. K. 1998. Exposure dating and validation of periglacial weathering limits, northwest Scotland. *Geology*, **26**(7), 587–590.

Strahler, A. N. 1952. Dynamic basis of geomorphology. *Geological Society of America Bulletin*, **63**, 923 – 938.

Stroeven, A. P., Fabel, D., Hättestrand, C., & Harbor, J. 2002b. A relict landscape in the centre of Fennoscandian glaciation: cosmogenic radionuclide evidence of tors preserved through multiple glacial cycles. *Geomorphology*, **44**, 145–154.

Stuiver, M., Grootes, P. M., & Brazunias, T. F. 1995. The GISP2 δ^{18}O climate record of the past 16,500 years and the role of the sun, ocean, and volcanoes. *Quaternary Research*, **44**, 341–354.

Sugden, D. E. 1977. Reconstruction of the morphology, dynamics, and thermal characteristics of the Laurentide Ice Sheet at its maximum. *Arctic And Alpine Research*, **9**(1), 21–47.

Sugden, D. E., & John, B. 1976. *Glaciers and Landscape*. London: Arnold.

Sugden, D. E., Hulton, N. R. J., & Purves, R. S. 2002. Modelling the inception of the Patagonian icesheet. *Quaternary International*, **95-96**, 55–64.

Sugden, D. E., Bentley, M. J., Fogwill, C. J., Hulton, N. R. J., McCulloch, R. D., & Purves, R. S. 2005. Late-glacial glacier events in southernmost South America: A blend of 'northern' and 'southern' hemispheric climatic signals? *Geografiska Annaler*, **87A**, 273–288.

Sutherland, D. G. 1980. Problems of radiocarbon dating deposits from newly deglaciated terrain: examples from the Scottish Lateglacial. *Pages 139–149 of:* Lowe, J. J., Gray, J. M., & Robinson, J. E. (eds), *Studies in the Lateglacial of North-west Europe*. Oxford: Pergamon.

Sutherland, D. G. 1981. *The raised shorelines and deglaciation of the Loch Long / Loch Fyne area, western Scotland*. Unpublished Ph.D thesis, University of Edinburgh.

Sutherland, D. G. 1984a. The Quaternary deposits and landforms of Scotland and the neighboring shelves - a review. *Quaternary Science Reviews*, **3**, 157–254.

Sutherland, D. G. 1993. South-west Highlands: Introduction. *Pages 307 – 310 of:* E., Gordon J., & Sutherland, D. G. (eds), *Quaternary of Scotland*. Geological Conservation Review, vol. 6. Scottish Natural Heritage.

Sutherland, D.G. 1984b. Modern glacier characteristics as a basis for inferring former climates with particular reference to the Loch Lomond Stadial. *Quaternary Science Reviews*, **3**, 291–309.

Tarasov, L., & Peltier, W. R. 2004. A geophysically constrained large ensemble analysis of the deglacial history of the North American ice-sheet complex. *Quaternary Science Reviews*, **23**(3-4), 359–388.

Tarasov, L., & Peltier, W. R. 2005. Arctic freshwater forcing of the Younger Dryas cold reversal. *Nature*, **435**, 662–665.

Teller, J. T. 1990. Volume and routing of Late-Glacial runoff from the southern Laurentide Ice-Sheet. *Quaternary Research*, **34**, 12–23.

Teller, J. T. 2003. Subaquatic landsystems: large proglacial lakes. *Pages 348–371 of:* Evans, D. J. A. (ed), *Glacial Landsystems*. London: Arnold.

Teller, J. T., Leverington, D. W., & Mann, J. D. 2002. Freshwater outbursts to the oceans from glacial Lake Agassiz and their role in climate change during the last deglaciation. *Quaternary Science Reviews*, **21**, 879–887.

Teller, J. T., Boyd, M., Yang, Z. R., Kor, P. S. G., & Fard, A. M. 2005. Alternative routing of Lake Agassiz overflow during the Younger Dryas: new dates, paleotopography, and a re-evaluation. *Quaternary Science Reviews*, **24**, 1890–1905.

Thomas, G. S. P., & Chiverrell, R. C. 2006. A model of subaquaeous sedimentation at the margin of the Late Midlandian Irish Ice Sheet, Connemara, Ireland, and its implications for regionally high isostatic sea-levels. *Quaternary Science Reviews*, **25**, 2868–2893.

Thompson, K. S. R. 1972. *The last glaciers of Western Perthshire*. Unpublished Ph.D thesis, University of Edinburgh.

Thompson, L. G., Davis, M. E., Mosley-Thompson, E., Sowers, T. A., Henderson, K. A., Zagorodnov, V. S., Lin, P. N, Mikhalenko, V. N., Campen, R. K., Bolzan, J. F., Cole-Dai, J., & Francou, B. 1998. A 25,000-year tropical climate history from Bolivian ice cores. *Science*, **282**, 1858–1864.

Thompson, L. G., Mosley-Thompson, E., Davis, M. E., Henderson, K. A., Brecher, H. H., Zagorodnov, V. S., Mashiotta, T. A., Lin, P. N, Mikhalenko, V. N., Hardy, D. R., & Beer, J. 2002. Kilimanjaro ice core records: evidence of Holocene climate change in tropical Africa. *Science*, **298**, 589–593.

Thorp, P. W. 1981. A trimline method for defining the upper limit of Loch Lomond Advance glaciers: examples from the Loch Leven and Glen Coe areas. *Scottish Journal of Geology*, **17**, 49–64.

Thorp, P. W. 1984. *The glacial geomorphology of part of the western Grampians of Scotland with especial reference to the limits of the Loch Lomond Advance*. Unpublished Ph.D thesis, City of London Polytechnic.

Thorp, P. W. 1986. A mountain icefield of Loch Lomond Stadial age, western Grampians, Scotland. *Boreas*, **15**, 83–97.

Thorp, P. W. 1987. Late Devensian ice sheet in the western Grampians, Scotland. *Journal of Quaternary Science*, **2**, 103–112.

Thorp, P. W. 1991a. The glaciation and glacial deposits of the western Grampians. *Pages 137–149 of:* Ehlers, J., Gibbard, P. L., & Rose, J. (eds), *Glacial Deposits in Great Britain and Ireland*. Rotterdam: Balkema.

Thorp, P. W. 1991b. Surface profiles and basal shear stresses of outlet glaciers from a Late-glacial mountain ice field in western Scotland. *Journal of Glaciology*, **37**, 77–88.

Trabant, D., & Mayo, L. 1985. Estimation and effects of internal accumulation on five glaciers in Alaska. *Annals of Glaciology*, **6**, 113–117.

van der Meer, J. J. M., Kjær, K. H., & Krüger, J. 1999. Subglacial water-escape structures and till structures, Sléttjökull, Iceland. *Journal of Quaternary Science*, **14**, 191–205.

van der Veen, C. J. 1996. Tidewater calving. *Journal of Glaciology*, **42**, 375–385.

van der Veen, C. J. 1999. *Fundamentals of glacier dynamics*. Rotterdam: Balkema.

van der Veen, C. J. 2002. Polar ice sheets and global sea level: how well can we predict the future? *Global and Planetary Change*, **32**, 165–194.

van der Wateren, F. M. 2003. Ice-marginal terrestrial landsystems: Southern Scandinavian Ice Sheet Margin. *Pages 166–203 of:* Evans, D. J. A. (ed), *Glacial Landsystems*. London: Arnold.

Van Tatenhove, F. G. M., Fabre, A., Greve, R., & Huybrechts, P. 1996. Modelled ice-sheet margins of three Greenland ice-sheet models compared with a geological record from ice-marginal deposits in central West Greenland. *Annals of Glaciology*, **23**, 52–58.

Virkkala, K. 1963. On ice-marginal features in southwestern Finland. *Bulletin de la Commission géologique de Finlande*, **210**, 1–76.

Walker, M. J. C., Coope, G. R., & Lowe, J. J. 1993. The Devensian (Weichselian) Lateglacial palaeoenvironmental record from Gransmoor, East Yorkshire, England. *Quaternary Science Reviews*, **12**, 659–680.

Walker, R. G. 1990. Facies modelling and sequence stratigraphy. *Journal of Sedimentary Research*, **60**, 777–786.

Weertman, J. 1964. The theory of glacier sliding. *Journal of Glaciology*, **5**, 287–303.

Weertman, J. 1973. Creep of ice. *Pages 320–337 of:* Whalley, E., Jones, S.J., & Gold, L.W. (eds), *Physics and chemistry of ice*. Ottawa: Royal Society of Canada.

Wilson, S. B., & Evans, D. J. A. 2000. Coire a' Cheud-chnoic, the 'hummocky moraine' of Glen Torridon. *Scottish Geographical Journal*, **116**(2), 149–158.

Winsemann, J., Asprion, U., & Meyer, T. 2004. Sequence analysis of early Saalian glacial lake deposits (NW Germany): evidence of local ice margin retreat and associated calving processes. *Sedimentary Geology*, **165**, 223–251.

Witte, H. J. L., Coope, G. R., Lemdahl, G., & Lowe, J. J. 1998. Regression coefficients of thermal gradients in northwestern Europe during the last glacial-Holocene transition using beetle MCR data. *Journal of Quaternary Science*, **13**, 435–445.

Zielinski, T., & van Loon, A. J. 1996. Characteristics and genesis of moraine-derived flowtill varieties. *Sedimentary Geology*, **101**, 119–143.

Zilliacus, H. 1989. Genesis of De Geer moraines in Finland. *Sedimentary Geology*, **62**, 309–317.

Zweck, C., & Huybrechts, P. 2003. Modeling the marine extent of Northern Hemisphere ice sheets during the last glacial cycle. *Annals of Glaciology*, **37**, 173–180.